Structure and function studies on the GLUT1 glucose transporter

Edwards, Lee

Award date:
1999

Awarding institution:
University of Bath

Structure and Function Studies on the GLUT1 Glucose Transporter

Submitted by: Lee Edwards

For the degree of Ph.D

of the University of Bath

1999

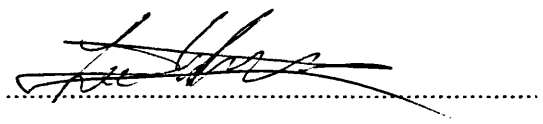

ProQuest LLC
789 East Eisenhower Parkway
P.O. Box 1346
Ann Arbor, MI 48106-1346

Acknowledgements

I would like to thank Prof. Geoff Holman and all the members of the glucose transport lab for their help and support throughout my Ph.D. I would especially like to thank Alison Gillingham and Aliki Kana for their help and support.

Abstract

The baculovirus expression system has been used to express four rabbit glucose transporter constructs. The constructs consist of: 1) a full length glucose transporter, 2) a full length glucose transporter with an N-terminal polyhistidine tag, 3) a construct expressing only the C-terminal half of the glucose transporter and 4) a construct expressing only the C-terminal half of the glucose transporter with an N-terminal polyhistidine tag. Protein expression levels were determined by immunoblot assay. The ability of expressed protein to bind ligand, at both the external and internal glucose transporter sites, was tested by photolabelling.

All four constructs were found to be adequately expressed using the baculovirus system. Photolabelling demonstrated measurable levels of ligand binding activity in three of the four constructs. Ligand binding activity in the polyhistidine tagged C-terminal construct was found to be different to previous results using a non-polyhistidine tagged construct (Cope *et al.*, (1994)).

Cellular targeting of the constructs was observed by scanning confocal microscopy. Confocal microscopy demonstrated that both full length constructs were targeted to the plasma membrane. However, both C-terminal half constructs were observed to be aberrantly targeted throughout intracellular membranes.

Purification trials were carried out in order to test the affinity of the polyhistidine tagged proteins towards a chelating nickel Sepharose column. The level of purification was assessed by polyacrylamide gel electrophoresis, followed by silver staining. The full length polyhistidine tagged glucose transporter proved difficult to purify to homogeneity. This was because it was found to have a low affinity towards the chelating nickel Sepharose column. The column also bound some native insect cell proteins. The yield from the column was calculated to be 379 μg of HIS-GLUT1 / 500 ml of culture, this represented a 20% recovery of polyhistidine tagged protein from the original culture. The polyhistidine tagged C-terminal half construct displayed almost no affinity towards the column.

In related experiments, C-terminally mutated human GLUT1 constructs were expressed in CHO cells. The point mutations were made in order to further study the role of the C-terminal tail on glucose transporter function.

Contents

Introduction

2.0 Materials and Methods

Results

Abbreviations

AcMNPV	*Autographa californica* multiple nuclear polyhedrosis virus
ASA-BMPA	2-*N*-(4-azidosalicoyl)-1,3-bis(D-mannos-4'-yl-oxy)[2-^{3}H] propyl-2-amine
ATB-[2-^{3}H]BMPA	2-*N*-4-(1-azi-2,2,2-trifluoroethyl)benzoyl-1,3-[^{3}H]bis-(D-mannos-4-yloxy)-2-propylamine
ATP	Adenosine triphosphate
BSA	Bovine serum albumin
cDNA	Complementary deoxyribonucleic acid
CHO	Chinese hamster ovary cells
C-TERM	C-terminal portion of the glucose transporter; transmembrane regions 7 - 12 according to the model proposed by Mueckler *et al.*, (1985)
dATP	Deoxy adenosine triphosphate
dCTP	Deoxy cytidine triphosphate
dGTP	Deoxy guanosine triphosphate
dTTP`	Deoxy thymidine triphosphate
ddATP	Dideoxy adenosine triphosphate
ddCTP	Dideoxy cytidine triphosphate
ddGTP	Dideoxy guanosine triphosphate
ddTTP	Dideoxy thymidine triphosphate
DMF	Dimethylformamide
DOPE	dioleoyl phosphatidylethanolamine
DOSPA	2,3-dioleyloxy-N-[2(Sperminecarboxamido)ethyl]-N,N-dimethyl-1-propanaminium trifluoroacetate
DTT	Dithiothreitol
EDTA	Ethylenediaminetetraacetic acid
E. coli	*Escherichia coli*
ER	Endoplasmic reticulum
FCS	Foetal calf serum (Foetal bovine serum)

G-HIS-LUT1	Full length glucose transporter construct containing a polyhistidine tag in the first extracellular loop between helices 1 and 2 according to the model proposed by Mueckler *et al.*, (1985).
GLUT1	Glucose transporter, isoform 1
GLUT2	Glucose transporter, isoform 2
GLUT3	Glucose transporter, isoform 3
GLUT4	Glucose transporter, isoform 4
GLUT5	Glucose transporter, isoform 5
GLUT6	Glucose transporter, isoform 6
GLUT7	Glucose transporter, isoform 7
HepG2	Hepatoma G2
Highfive	*Trichoplusia ni* egg cells (insect cells)
HIS-C-TERM	C-terminal portion of the glucose transporter with an N-terminal polyhistidine tag
HIS-GLUT1	Full length glucose transporter construct with an N-terminal polyhistidine tag
Kd	Dissociation constant
moi	Multiplicity of infection
mRNA	Messenger ribonucleic acid
OG	Octyl glucoside
PAGE	Polyacrylamide gel electrophoresis
PBS	Phosphate buffered saline
pfu	Plaque forming units
SDS	Sodium dodecylsulphate
Sf9	*Spodoptera frugiperda* ovarian cells (insect cells)
TCA	Trichloroacetic acid
TEMED	N,N,N',N'-tetramethylethylenediamine
TES	Tris / EDTA / sucrose buffer
Thesit	Nonaocta (ethylene glycol) dodecyl ether, $C_{12}E_9$
Tris	Tris-(hydroxymethyl)-methylamine
Tween-20	Polyoxylethylenesorbitan monolaurate

UV	Ultraviolet
Vmax	Maximal velocity
X-gal	5-bromo-4-chloroindol-3-yl β-D-galactoside

Introduction

1.0 Glucose Transport

1.1 Introduction

Glucose transport is a fundamental mechanism for all forms of life. The glucose transporter supplies the cell with glucose, which is necessary to sustain cell function. In the absence of a glucose transporter, passage of the polar glucose molecule across the cell membrane would be exceptionally slow.

Within the mammalian system several different forms of the glucose transporter exist; these are functionally identical and are termed isoforms. Glucose transporter isoforms possess different kinetic properties. Their cellular locations and functions are listed below (table 1.1).

Isoform / Principal location	Tissue
GLUT1 / erythrocyte	Primary glucose transporter of foetal tissues, Placenta, Brain, Blood/tissue barrier, erythrocyte membranes.
GLUT2 / liver	High capacity, low affinity glucose transporter present in liver, pancreatic β-cells, small intestine and kidney.
GLUT3 / brain	Primary glucose transporter of neurons and nerve cells also expressed in placenta, kidney, liver and testes.
GLUT4 / muscle	Muscle, heart and adipose tissue, insulin regulated.
GLUT5 - Fructose Transporter	Small intestine, brain, muscle and adipose tissue (muscle and brain low levels).
GLUT6	Non-functional pseudogene whose sequence is most closely related to that of -GLUT3, identified only in humans.
GLUT7	Hepatic microsomal glucose transporter (Liver).

Table 1.1, The table describes the cellular location and function of all 6 reported glucose transporter sequences. Adapted from Bell *et al.*, (1993).

The glucose transporter functions in a bi-directional, passive manner, carrying glucose down its concentration gradient. Glucose transporter, isoform 1, (GLUT1) is probably the best studied of all the glucose transporters. GLUT1 is abundant in brain tissue, transporting glucose as an energy source across the blood brain barrier. GLUT1 is also present in many other cell types. Baldwin *et al.*, (1982) first isolated GLUT1 protein from erythrocyte membranes, which contained 3 - 5% GLUT1. Erythrocyte membranes therefore provide a rich source of the GLUT1 protein for study. The cDNA

encoding the GLUT1 isoform was isolated in 1985 by Mueckler *et al.*. Isolation of the cDNA was followed by the expression of this glucose transporter isoform in non-native expression systems. For example: Sarkar *et al.*, (1988) expressed GLUT1 in *Escherichia coli* (Bacteria), Yi *et al.*, (1992) expressed GLUT1 in *Spodoptera frugiperda* cells (insect cells) and Kasahara and Kasahara, (1996) expressed GLUT1 in *Saccharomyces cerevisiae* (yeast).

Hiraki *et al.*, (1989) showed that transformation of cultured cells can lead to an increased level of GLUT1 expression; GLUT1 expression is also increased during starvation, Haspel *et al.*, (1986). This is advantageous because the transporter is kinetically asymmetric. The binding of intracellular peptides and metabolites appear to allosterically regulate GLUT1. Shi *et al.*, (1995) have identified two specific cytoplasmic proteins of 28 and 70 kDa, which are capable of reducing substrate binding to the internal GLUT1 site. Furthermore, Carruthers and Helgerson, (1989) and Hebert and Carruthers, (1986) have found that ATP can have an inhibitory effect on glucose transport, converting the GLUT1 protein to a low capacity glucose transporter.

Gould *et al.*, (1991) have found that GLUT2 functions as a high capacity transporter with a much higher Km of 15 - 30 mM. Following the consumption of food, GLUT2 acts to lower elevated glucose concentrations rapidly, when other glucose transporters are saturated. GLUT2 is capable of transporting fructose with a Km of 67 mM and is thought to be responsible for the influx of fructose into the liver. Burant *et al.*, (1992) showed that GLUT5 is a specific fructose transporter and although not found in the liver is responsible for the influx of fructose through the small intestine. It has a Km for fructose of 6 mM. GLUT3 is found in abundance in tissues which require a high glucose demand, such as the tissues of the central nervous system. The GLUT3 isoform may well have evolved in tandem with the GLUT1 protein, Gould *et al.*, (1991) demonstrated that GLUT3 has a low Km for glucose enabling the transporter to utilise low concentrations of blood glucose in hypoglycaemic conditions. Keller *et al.*, (1989) showed that GLUT4 has a relatively low Km for glucose of 2 - 5 mM, this ensures that it functions close to its Vmax over the normal range of blood glucose concentrations. In the absence of insulin GLUT4 becomes localised within intracellular vesicles, this leads to the regulation of glucose uptake in cells expressing GLUT4. Following a meal, the

release of insulin into the blood stream causes GLUT4 recruitment to the plasma membrane which allows for the rapid uptake of glucose into these cells.

This thesis is primarily concerned with the glucose transporter isoform one (GLUT1). It is the aim of this thesis to provide a better understanding of the glucose transporter (GLUT1) structure. This has been achieved by mutational analysis and by providing the foundations for starting crystallographic analysis (2-dimensional electron diffraction crystallography or 3-dimensional X-ray crystallography). The thesis begins by examining point mutations made in the human GLUT1 protein, expressed in Chinese hamster ovary (CHO) cells. The thesis then examines four GLUT1 constructs expressed in insect cells. Two of the constructs have been modified to express six contiguous histidine residues (termed a polyhistidine tag) on the N-terminal end of the protein. The aim of this approach was to allow for the attempted purification of the GLUT1 protein on an immobilised nickel column, to which the polyhistidine tag has an affinity. This approach was considered to be a prerequisite for the undertaking of crystallisation and then crystallographic analysis.

1.2 The Origin of the Glucose Transporter

Maiden *et al.*, (1987) have studied the sequences of the arabinose-H^+ symporter and the xylose-H^+ symporter of *E. coli*. The two proteins were found to be homologous to each other and also with the rat brain glucose transporter. On consideration of conservative substitutions between the sequences nearly 40% of the residues were found to be homologous. Furthermore, all three proteins lack an N-terminal signal sequence. Maiden *et al.*, (1987) consider the similarities to be too great to have originated from convergent evolution and postulate that they may have originated from an ancient sugar transporter, which existed before the divergence of organisms to prokaryotes and eukaryotes. Maiden *et al.*, (1987) also propose that the genes of the common ancestor arose from a gene duplication event. The first piece of evidence for this theory comes from hydropathy plot analysis. The hydropathy plot analysis of the human GLUT1 glucose transporter is displayed in figure 1.1.

Szkutnicka *et al.*, (1989) have considered the evidence put forward by Maiden *et al.*, (1987) and have studied 11 transporters; the yeast galactose, glucose, maltose and

lactose transporters; the *E. coli* xylose and arabinose transporters; the human foetal muscle and erythrocyte glucose transporters and the rat brain and adipocyte glucose transporters. Amino acid identity between members of the group was found to be between 20 and 30% after alignment. The identity is even greater if conservative replacements are considered. This homologous group of transporters was termed the HGT superfamily and many sequence motifs are conserved between them. Interestingly though the lengths of the N and C-terminal tails differ significantly between transporters within the HGT superfamily. Szkutnicka *et al.*, (1989) have also presented further evidence to corroborate the gene duplication theory. The GLUT1 glucose transporter is known to be glycosylated on the first extracellular loop. The yeast glucose transporter has been observed to carry an N-linked glycosylation motif in helix 7 in a position analogous to the GLUT1 protein, only contained in the second set of six transmembrane helices. All transporters in the HGT superfamily are observed to lack a cleavable N-terminal signal sequence and insert into the membrane after translation of the mRNA. On considering all of the evidence, ie. sequence homology, similarity of size, distribution of hydrophilic loops and the presence of repeated motifs in corresponding positions it was concluded by Szkutnicka *et al.*, (1989) that members of the HGT superfamily have a common ancestry as proposed by Maiden *et al.*, (1987).

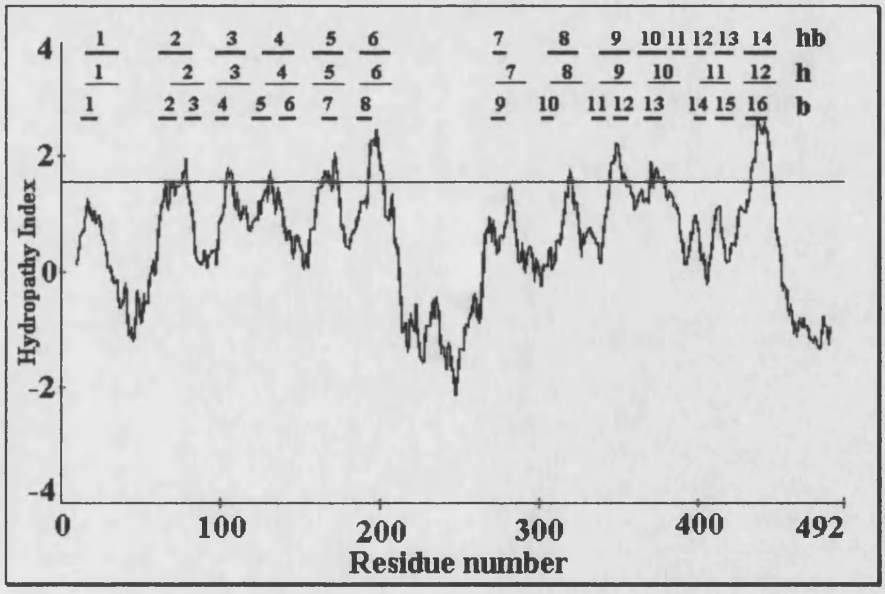

Figure 1.1, Hydropathy plot of the human GLUT1 glucose transporter. The hydropathy plot demonstrates repetition about a large central hydrophilic loop. There are several proposed models that predicted the transmembrane regions of the glucose transporter and are marked on the diagram, the letters hb represent the model proposed by Ducarme *et al.*, (1996), h represents the model proposed by Mueckler *et al.*, (1985) and b represents the model proposed by Fischbarg *et al.*, (1993).

The two halves of the glucose transporter appear to be symmetrical about a large, hydrophilic, cytoplasmic loop. The C-terminal amino acids (amino acids 480 - 492) are observed to be highly hydrophilic, whereas the N-terminal amino acids (amino acids 1 - 20) are not. The observed symmetry, displayed in the hydropathy plot, suggests that a gene duplication event may have occurred in the evolutionary history of the gene.

However, one of the strongest pieces of evidence for a gene duplication event having occurred is the duplication of protein motifs between the N-terminal and C-terminal halves. This is displayed in figure 1.2.

```
1    MEPSSKKVTG  RLMLAVGGAV  LGSLQFGYNT  GVINAPQKVI  EEFYNQTWIH
51   RYGERILPTT  LTTLWSLSVA  IFSVGGMIGS  FSVGLFVNRF  GRRNSMLMMN
101  LLAFVSAVLM  GFSKLAKSFE  MLILGRFIIG  VYCGLTTGFV  PMYVGEVSPT
151  ALRGALGTLH  QLGIVVGILI  AQVFGLDSIM  GNEDLWPLLL  SVIFVPALLQ
201  CIVLPLCPES  PRFLLINRNE  ENRAKSVLKK  LRGNADVTRD  LQEMKEESRQ

251  MMREKKVTIL  ELFRSPAYRQ  PILSAVVLQL  SQQLSGINAV  FYYSTSIFEK
301  AGVQQPVYAT  IGSGIVNTAF  TVVSLFVVER  AGRRTLHLIG  LAGMAACAVL
351  MTIALALLEQ  LPWMSYLSIV  AIFGFVAFFE  VGPGPIPWFI  VAELFSQGPR
401  PAAVAVAGFS  NWTSNFIVGM  CFQYVEQLCG  PYVFIIFTVL  LVLFFIFTYF
451  KVPETKGRTF  DEIASGFRQG  GASQSDKTPE  ELFHPLGADS  QV*
```

Figure 1.2 The Rabbit GLUT1 glucose transporter protein sequence. The above sequence displays the duplicated motifs. Matching motifs have been marked in the same colour. In this figure the glucose transporter has been split in two at amino acid 251.

The matching sequence and structural motifs above have been highlighted in the same colour, motifs such as these occur throughout the glucose transporter superfamily. Apart from the motifs repeating, they occur at the same relative positions in the two halves of the glucose transporter. Since the genes of the mammalian glucose transporters contain introns, which are missing in the yeast and bacterial genes, Szkutnicka *et al.*, (1989) proposed that the duplication event which created the glucose transporter occurred very early in the evolution of the gene; either before yeast and bacteria eliminated introns or before eukaryotic cells acquired them. The human and rat glucose transporters are the only experimentally determined membrane proteins known to insert

into membranes after translation, making it possible to functionally insert these eukaryotic transport proteins into the bacterial plasma membrane.

1.3 The Structure of the Glucose Transporter

Several putative structures have been proposed for the glucose transporter. The first, based on hydropathy profile analysis, was from Mueckler *et al.,* (1985). The GLUT1 sequence was analysed according to the algorithm of Eisenberg *et al.* (1984). This predicted transmembrane spanning segments from 21 non-overlapping amino acid residues with an average hydropathy index value of > 0.42. Mueckler *et al.,* (1985) proposed a structure comprising of 12 transmembrane spanning α–helices, with the hydrophilic amino terminus, carboxy terminus and large central loop remaining within the cytoplasm of the cell. Mueckler *et al.,* (1985) have suggested that the moderately amphipathic helices 3, 5, 7, 8 and 11 cluster to form an aqueous cleft through which glucose can traverse the lipid bilayer. The two dimensional representation of the model proposed by Mueckler *et al.,* (1985) is displayed in figure 1.3 (on the following page).

Hresko *et al.,* (1994) carried out a series of experiments using scanning glycosylation mutagenesis which supported the model proposed by Mueckler *et al.,* (1985). This work involved the insertion of the glycosylated exofacial domain of GLUT4 into each of the putative hydrophilic soluble domains of an aglyco-GLUT1 construct. The constructs were expressed in *Xenopus* oocytes and the cytoplasmic or exofacial orientation of each soluble domain was inferred from its glycosylation state. In brief, insertion of the glycosylation signal into the predicted extracellular loops resulted in their glycosylation when expressed in *Xenopus* oocytes. However, insertion of the glycosylation signal into the predicted cytoplasmic loops did not result in glycosylation. These results were consistent with the model proposed by Mueckler *et al.* (1985).

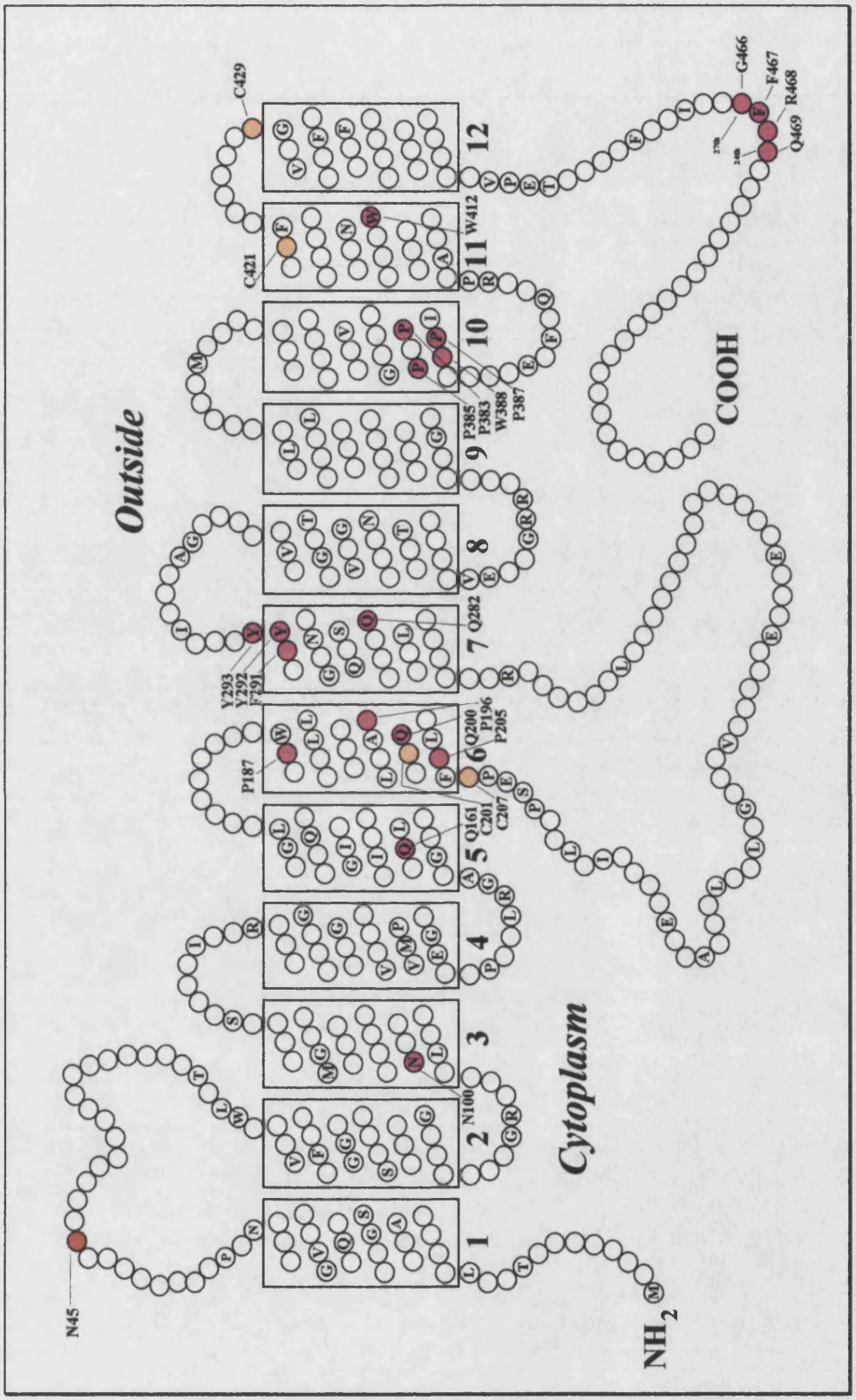

Figure 1.3, The 2-Dimensional theoretical structure of the glucose transporter (modified from Bell *et al.*, (1993)). The above theoretical structure of the glucose transporter was originally proposed by Mueckler *et al.*, (1985). Conserved residues are denoted by the single letter amino acid abbreviation. Coloured residues indicate residues discussed within the text.

It is thought that the glucose transporter has a bilobal structure. Evidence for this comes from photolabelling studies carried out by Cope *et al.*, (1994 (discussed later in this thesis)) and from the observation by Li and Tooth, (1987) using electron microscopy, that the structurally related *Escherichia coli* (*E. coli*) lactose permease appeared to form a bilobal structure.

Throughout this thesis the N-terminal half will refer to helices 1 - 6 and the C-terminal half will refer to helices 7 - 12, of the model proposed by Mueckler *et al.*, (1985).

Alternative GLUT1 structural models have been proposed. The first of the alternative models was that of Fischbarg *et al.*, (1993). The model was based on antibody binding studies. Fischbarg *et al.*, (1993) generated an antibody to the highly conserved sequence Ile 386 - Ala 405 which, according to Mueckler *et al.*, (1985), should lie on the endofacial surface of GLUT1. Fischbarg *et al.*, (1993) suggested that the antibody had a specific affinity towards the exofacial surface of the glucose transporter since it acted to accelerate 2-deoxy-D-glucose uptake. The increase in 2-deoxy-D-glucose uptake was only observed when the antibody was added to the extracellular surface of *Xenopus* oocytes expressing GLUT1. Fischbarg *et al.*, (1993) then proposed a model based on an arrangement of 16 antiparallel β-strands, forming a β-barrel (a porin like structure).

However, the glycosylation studies carried out by Hresko *et al.*, (1994) contradict the model proposed by Fischbarg *et al.*, (1993), in this model, glycosylated domains are predicted to lie on the cytoplasmic side of the membrane. Moreover, the β-barrel model cannot account for the high α-helical content of the protein as predicted by Alvarez *et al.*, (1987) and Chin *et al.*, (1987). These two groups performed, respectively, fourier transform infrared spectroscopy (FTIR) and circular dichroism analysis on the purified erythrocyte transporter. These experiments, discussed in detail below, indicate the structure to be largely α-helical with the helices, on average, aligned perpendicular to the plane of the lipid bilayer. For these reasons, the model by Fischbarg *et al.*, (1993) has been largely rejected from further serious consideration.

Alvarez *et al.*, (1987) have also predicted by FTIR analysis a significant amount of β-strand and random coil conformation. It was not possible in their study to determine whether β-turns were present. Alvarez *et al.*, (1987) suggested that the

12 transmembrane α-helical structure proposed by Mueckler *et al.*, (1985) should be refined to include more β-structure.

Alvarez *et al.*, (1987) noted that other proteins, with similarities to the glucose transporter have also been determined to contain significant levels of β-structure. For example, the *E. coli* lactose permease has an approximate α-helical content of 70% and a β-structure content of 25%. Proton exchange experiments carried out by Alvarez *et al.*, (1987) demonstrated that 80% of the glucose transporter exchanges protons within the first 1h of the experiment. This demonstrates that the majority of the protein is freely accessible to water and would be consistent with the presence of an aqueous water channel within the protein. Other transmembrane proteins, such as rhodopsin, bacteriorhodopsin and the calcium ATPase have been found to exchange protons much more slowly than the GLUT1 protein.

Chin *et al.*, (1987) have performed circular dichroism analysis on the GLUT1 protein and have made slightly different predictions for the structure of GLUT1 than Alvarez *et al.*, (1987). Circular dichroism analysis predicts that the GLUT1 protein is composed of approximately 82% α-helices, 10% β-turns and 8% other random structure, with no β-strands. The high percentage of α-helix suggests that non-transmembrane hydrophilic segments also form α-helical structure. This is because the 82% of α–helix cannot be accounted for by the 12 transmembrane α-helices alone.

In the presence of excess D-glucose the helical content was found to decrease, resulting in a corresponding increase in random coil and β-turn content. The binding of the endofacial ligand cytochalasin B also resulted in a decrease in the helical content. Although the above studies differ slightly on the exact β-structure composition, they do agree on there being a β-structure content.

Ducarme *et al.*, (1996) have developed an α/β-structure model which proposes 10 transmembrane spanning α-helices and 4 transmembrane spanning β-strands. Ducarme *et al.*, (1996) proposed that the GLUT1 protein could form two channels, of which one channel would be responsible for glucose transport. This model is consistent with fourier transform infrared spectroscopy satisfying both the α-helix and β-strand content with the α-helices being perpendicular to the lipid bilayer. The model is less consistent with circular dichroism results, as circular dichroism did not predict the

presence of β-strands. If the two large extra-membrane loops, the carboxy and the amino termini, are α-helical then the α-helical structure in this model is approximately 65% and the transmembrane proportion of β-strands is approximately 8%.

The primary protein sequence was re-analysed by Ducarme *et al.,* (1996) using the methods of Eisenberg *et al.,* (1984) and Jähnig, (1990). Predicted transmembrane regions were determined to be α-helical or β-stranded. The proposed model is displayed in figure 1.4.

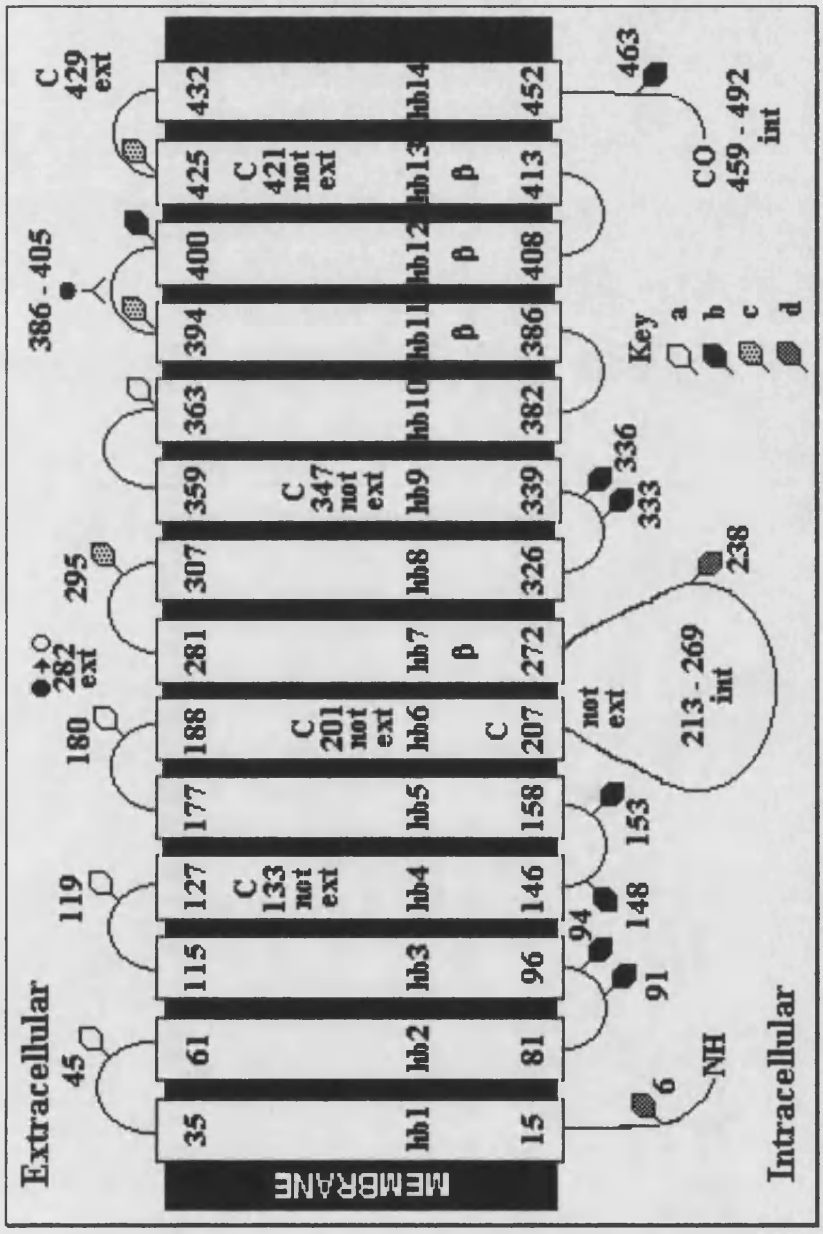

Figure 1.4, The glucose transporter modelled as a 14 transmembrane protein containing β-structure. Taken from Ducarme *et al.,* (1996) the key describes glycosylation studies by Hresko *et al.,* (1994). GLUT1 was mutated to contain glycosylation consensus sequences within each of the predicted extramembrane loops. The key is interpreted as follows: a: the protein becomes glycosylated and is functional; b: the protein is not glycosylated and is non-functional; c: the protein becomes glycosylated and is non-functional; d: the protein is not glycosylated and is functional. Glycosylation will only occur at the extracellular surface of the protein. The letter C displays the results of cysteine analysis and the glutamine 282 mutation is marked. The model contains 14 transmembrane regions, 4 of which are predicted to consist of β-structure.

The model proposed by Ducarme *et al.,* (1996) is consistent with the scanning glycosylation mutagenesis experiments performed by Hresko *et al.*, (1994). It is also consistent with antibody analysis carried out by Fischbarg *et al.,* (1993), the sequence Ile 386 - Ala 405 being accessible to antibody on the extracellular side.

Ducarme *et al.,* (1996) have proposed that the C-terminal half forms a channel capable of transporting glucose and that the N-terminal half forms an independent channel, incapable of transporting glucose. Ducarme *et al.,* (1996) have suggested that the N-terminal channel acts as a water channel; the large extra-membrane loop functioning as a steric or electrical gate, preventing small ions from passing through the channel. In the model proposed by Ducarme *et al.,* (1996), the external loops are too short to form a gate for a single channelled protein, because the channel diameter would be too large. However, a two channelled protein would form a C-terminal channel (Ile 272 - Val 492) of just the right diameter to accommodate the glucose molecule and may sterically or electrically restrict the flow of small ions. This is consistent with the experimental data derived from analysing point mutations, the majority of which that affect glucose transport being mapped to the C-terminal portion of the protein.

A two-channelled glucose transporter is consistent with the observed symmetry of GLUT1 hydropathy plots and current theories of the origin of the glucose transporter from a gene duplication event. Ducarme *et al.,* (1996) suggests that the glucose transporter could be a degenerate form of a co-transport channel, with the N-terminal half still interacting with the C-terminal half of the molecule, but no longer capable of co-substrate transport.

Further evidence, supporting the theory that the glucose transporter evolved from a co-transporter system arises from the observed similarity between the GLUT1 protein and proton linked sugar transporters found in the bacterium *E.* coli. Baldwin, (1993) reports that these proton symporters, which include the D-xylose / H^+ symporter, 27% identical, L-arabinose / H^+ symporter, 23% identical and galactose / H^+ symporter, 26% identical. Both the galactose and arabinose symporters bind and are photolabelled by the fungal toxin cytochalasin B. In conclusion, it is suggested that the glucose transporter may be a redundant proton symporter, the N-terminal region having co-transported protons linked to the uptake of sugar molecules. The redundant proton channel may now function simply as a water channel.

Ducarme *et al.,* (1996) have not predicted a 3-dimensional topographical model of the GLUT1 protein as no transmembrane α/β structure has yet been identified by X-ray crystallography. However, both theoretical and experimental analysis suggests that such a structure does exist in the acetylcholine receptor (Ortells and Lunt, (1996)). The acetylcholine receptor may eventually provide a topographical model on which to model α/β structure within the glucose transporter, should the 3-dimensional structure of the acetylcholine receptor be successfully determined.

Hodgson *et al.,* (1992) have developed a model which is similar to that proposed by Ducarme *et al.,* (1996) as it predicts a transporter consisting of two channels, one to transport substrate and the other a redundant co-transport channel. The model has a similar secondary structure to that proposed by Mueckler *et al.,* (1985), however it predicts that helices 1 - 6 form the first channel and helices 7 - 12 form the second channel, helices 7 - 12 being involved in substrate translocation. Furthermore, the model predicts that more of the primary sequence is involved in α-helical structure than the model proposed by Mueckler *et al.,* (1985). In accordance with Chin *et al.,* (1987) the model does not predict any β-strands.

Widdas and Baker, (1991a) have proposed a model based on the secondary structure suggested by Mueckler *et al.,* (1985). The model is based on a central core of 6 helices (helices 1, 11, 8, 3, 5, and 6), which are structurally supported by the remaining helices (helices 12, 2, 4, 10, 7 and 9), figure 1.5.

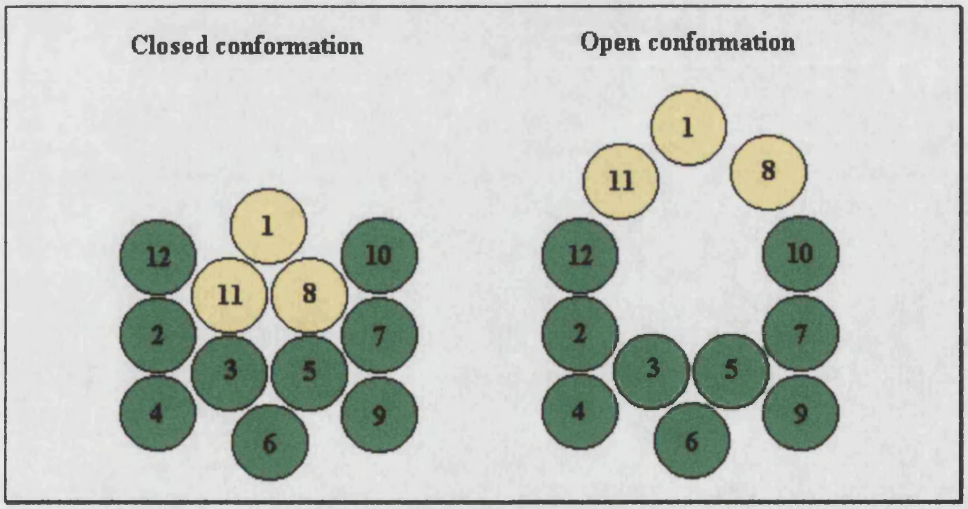

Figure 1.5, Proposed model by Widdas and Baker, (1991a). The diagram, replicated from Widdas and Baker, (1991a) depicts both the open and closed conformation of the glucose transporter. The green coloured helices constitute both the rest of the binding site and supportive structure.

Widdas and Baker, (1991a) proposed that the helices were capable of rocking about a central pivot. On one side of the membrane the helices would adopt the closed conformation and on the opposite side they would adopt the open conformation. Helices 1, 8 and 11 would move away from the rest of the structure to expose the glucose transport channel. It was suggested that the energy for this movement was derived from the surface energy of water, as conformational changes of the magnitude envisaged were too large to be attributed only to thermal agitation of the protein. Widdas and Baker, (1991a) have carried out experiments that support this hypothesis. Alcohols, such as methanol and ethanol were used to lower the surface tension of the aqueous medium. Assays were carried out to measure glucose exit rates in whole erythrocytes suspended in the aqueous medium. It was shown that glucose exit rates were decreased on the reduction of surface tension. It was predicted that at 65% of normal surface tension the glucose transporter would cease to function.

Widdas and Baker, (1991b&c) have further suggested a mechanism by which the glucose transporter prevents the loss of potassium ions from within the erythrocyte. It was observed that several arginine residues were situated on the cytoplasmic surface of the glucose transporter. Due to arginine's high pK value of 12.4, arginine is always positively charged at physiological pH. This would allow the arginine residue to form a positively charged shield which would repel potassium ions. It was noted that the shielding effect would depend on the radius of the ring surrounding the transport channel. Too large a radius would lead to an ineffective barrier. Baker *et al.,* (1998) have presented experimental evidence which supports the hypothesised shielding effect of the arginine residues. Baker *et al.,* (1998) demonstrated that exposure of the glucose transporter to the reagent 1,2-cyclohexanedione, which forms covalent bonds with arginine, resulted in a steady leakage of potassium ions from the erythrocyte.

The model proposed by Widdas and Baker, (1991a) suggests a possible energy source for the glucose transporter and a possible mechanism for excluding positive ions from entering the transport channel. However, analytical evidence for the structure of the glucose transporter seems in many cases to be contradictory and confusing. For example, the amount of helical structure present appears to depend on the method used to determine it. At present the model proposed by Mueckler *et al.,* (1985) is a useful starting point for determining the structure of the glucose transporter.

1.4 Independent Expression of the C-Terminal and N-Terminal GLUT1 Domains in Sf9 Cells

Cope *et al.*, (1994) expressed the two halves of the glucose transporter independently from one another in *Spodoptera frugiperda* cells (Sf9, Insect Cells). Independent expression of the two domains demonstrated the protein halves to be stable in the membrane, but incapable of cytochalasin B binding. However, concurrent expression of the two protein halves in the same cell resulted in a protein capable of cytochalasin B binding. The halves remained separate when subjected to electrophoretic analysis and were not covalently bound. This lead to the idea that the N-terminal domain of the protein could provide a packing surface for the C-terminal domain to rest against. Thus, allowing the C-terminal domain to take on its correct conformational state and form the ligand binding site essential for correct function.

Wu *et al.*, (1996) have carried out a similar study to Cope *et al.*, (1994) using the *E. coli* lactose permease proton symporter. The lactose permease has 12 hydrophobic transmembrane spanning α-helices. As with the glucose transporter both the N and C termini are on the cytosolic side of the membrane. The lactose permease was expressed in two halves in an *E. coli* expression system. The first construct expressed the 6 N-terminal transmembrane helices and the second construct expressed the 6 C-terminal transmembrane helices. When the constructs were expressed individually both constructs were found to be unstable and did not catalyse active transport. However, cells expressing both constructs catalysed active lactose transport. Wu *et al.*, (1996) discovered that the addition of five amino acid residues (Met-Thr-Met-Ile-Thr) to the N-terminal end of the C-terminal construct allowed for a stable C-terminal construct to be expressed independently of the N-terminal construct. Furthermore, this construct was able to catalyse down hill lactose transport. From these results it seems likely that the 6 C-terminal transmembrane helices are responsible for lactose transport and the 6 N-terminal transmembrane helices are responsible for proton translocation. A similar study was undertaken in this thesis which suggested that the C-terminal half of the glucose transporter was capable of ligand binding when polyhistidine tagged. Evidence suggested that glucose transport is mediated exclusively by the C-terminal half of the glucose transporter.

Evidence presented by Cope *et al.*, (1994) appears to be inconsistent with the 3-dimensional arrangement of the helices presented by Fischbarg *et al.*, (1993), Widdas and Baker, (1991a) and Mueckler *et al.*, (1985). The model proposed by Fischbarg *et al.*, (1993) is inconsistent because the whole of the protein is involved in the transmembrane channel as is the model proposed by Widdas and Baker, (1991a). The model proposed by Mueckler *et al.*, (1985) is inconsistent because the transmembrane channel is composed of helices in both the first and second halves of the molecule (helices 3, 5, 7, 8 and 11). The study undertaken by Cope *et al.*, (1994) strongly suggests that both halves of the glucose transporter interact to facilitate ligand binding. This would suggest that the functions of the two halves are likely to be coupled.

1.5 Point Mutational Analysis of the GLUT1 Glucose Transporter

In an attempt to assign a function to specific amino acids, extensive point mutation analysis has been carried out on the GLUT1 glucose transporter. The following studies describe mutations made to the glucose transporter. This work has increased our knowledge of the glucose transporter and has generated mutations, which may be useful for future crystallisation attempts.

1.6 Glutamine 161 Mutational Analysis - N-Terminal Control of Transport

A glutamine 161 mutation was made and studied by Mueckler *et al.*, (1994). Five transmembrane amino acids were chosen for scrutiny based upon their ability to hydrogen bond to the substrate, glucose and because of their complete conservation from GLUT1 through to GLUT5. The results of the study are displayed in table 1.2.

Mutation	2-Deoxyglucose uptake (pmoles / oocyte / 30 min)	Transporter expression (arbitrary units)
Wild-type	42.4 ± 2.0	1.0
N 100 I	38.7 ± 6.3	1.1 ± 0.3
N 100 S	37.9 ± 5.1	0.8 ± 0.2
Q 161 L	**1.1 ± 0.5**	**1.5 ± 0.5**
Q 161 N	**4.1 ± 1.2**	**2.1 ± 0.7**
Q 200 L	32.8 ± 3.5	1.8 ± 0.5
Y 292 F	30.4 ± 2.6	1.7 ± 0.3
Y 293 F	37.6 ± 6.7	1.3 ± 0.2

Table 1.2, Results of point mutation work, taken from Mueckler *et al.*, (1994). Point mutational analysis demonstrates that Q 161 L is expressed above wild-type levels, yet, almost incapable of 2-Deoxyglucose transport.

Table 1.2 shows that the only significant reduction in 2-Deoxyglucose uptake results from the mutation of glutamine 161. In this study the mutation of tyrosine 293 to phenylalanine had very little effect on transporter function. However, the mutation of tyrosine 293 to isoleucine has a profound effect on transporter function (section 1.7).

The non-conservative substitution of glutamine 161, for leucine, reduced transporter activity by 50 fold and the conservative substitution of glutamine 161, for asparagine, reduced transporter activity by 10 fold. The difference between the amino acids glutamine and asparagine is a single methylene group. From the experimental evidence, Mueckler *et al.*, (1994) concluded that glutamine 161 must be involved in the exofacial binding site. It was argued that the conservative substitution of glutamine 161, anywhere other than in the exofacial binding site, would be unlikely to cause a massive change in tertiary structure which would be likely to affect substrate transport.

However, the reduced transport activity was not found to be due to a decreased substrate affinity, since there was no significant difference in the Km for the substrate. Therefore, it was hypothesised that the mutation must also affect a transport mechanism, such as conformational change, subsequent to substrate binding. This is consistent with the observation that the binding of glucose to erythrocyte GLUT1 is much faster than the rate of conformational change which leads to transport (ie. glucose binding is not the rate limiting step). The importance of glutamine 161 is highlighted by its high degree of conservation within the hexose transporter superfamily.

Mueckler *et al.*, (1985) have mapped glutamine 161 to helix 5 in the N-terminal half of the glucose transporter. Mueckler *et al.*, (1994) conclude that glutamine 161 and therefore helix 5 constitute part of the substrate binding site, the site being otherwise composed of helices in the C-terminal half of the transporter.

Ducarme *et al.*, (1996) have also mapped glutamine 161 to the N-terminal half of the glucose transporter. However, Ducarme *et al.*, (1996) propose that the N-terminal half is intimately coupled to the transport activity of the C-terminal half, which could also explain the observed effects on transport activity. Alternatively, it is possible that the mutation of glutamine 161 is simply causing protein mis-folding which would interfere with conformational change but not glucose binding.

1.7 Tyrosine 292 and 293 Mutational Analysis - A Hydrophobic Patch

Mori *et al.*, (1994) have analysed several tyrosine mutations. The mutations made were Y 292 I, Y 292 F, Y 293 I and Y 293 F. Table 1.3 summarises the results of the point mutations studied.

Mutation	Transport nmol/min/mg	ATB-BMPA labelling % of wild-type	Cyt B labelling % of wild-type	Transporter expression % of wild-type
CHO-K1	7.1	16.2 ± 5.3	18.2 ± 2.3	14.4 ± 2.2
Wild-type	74.9 ± 18.2	100	100	100
Y 292 F	72.7 ± 23.6	147.6 ± 60.7	103.5 ± 8.6	100.3 ± 29.7
Y 292 I	75.1 ± 19.2	118.7 ± 15.8	53.8 ± 7.3	129.0 ± 35.3
Y 293 F	83.5 ± 11.7	105.8 ± 27.1	107.3 ± 8.1	97.4 ± 8.9
Y 293 I	10.3 ± 2.8	126.2 ± 34.9	4.5 ± 2.1	134.8 ± 3.4

Table 1.3, Results of point mutation work, taken from Mori *et al.*, (1994). The mutation Y 293 I generates the most significant response. This mutation locks the transporter into an outward facing conformation, as demonstrated by ATB-BMPA and cytochalasin B binding. Mutating Y 292 I has a less pronounced effect, but still results in reduced cytochalasin B labelling at the internal site.

The results demonstrate that the tyrosine 293 to isoleucine mutation generates a stable form of the glucose transporter, which is locked in an outward facing conformation. This can be concluded because of the marked reduction in cytochalasin B (endofacial ligand) labelling accompanied by nearly normal ATB-BMPA (exofacial

ligand) labelling. The tyrosine 292 to isoleucine mutation demonstrates a 2-fold reduction in cytochalasin B binding to the internal site.

Previous work by Barnett *et al.*, (1973a&b), Barnett *et al.*, (1975) and Holman and Rees, (1982) demonstrated that bulky alkyl groups substituted at the carbon 1 position of D-glucose markedly reduce the binding of these glucose analogues to the glucose transporter. However, analogues with hydrophobic alkyl substitutions at the carbon 4 and carbon 6 positions of D-glucose were found to have a high affinity towards the glucose transporter; sometimes exceeding that of D-glucose. These studies suggested that the binding of D-glucose to the exofacial binding site of the glucose transporter resulted in carbon 6 being in close contact with a hydrophobic patch on the surface of the protein. Mori *et al.*, (1994) have therefore postulated that the hydrophobic patch may be composed of phenylalanine 291, tyrosine 292 and tyrosine 293. It was further suggested that the hydrophobic patch closes behind the bound substrate and triggers the conformational change necessary for glucose transport. Although isoleucine is hydrophobic in nature, the residue is thought to be too small to form the correct conformation at this critical site. Disruption of the patch, as seen in the above data, results in a glucose transporter becoming locked in an outward facing conformation. The transporter is then left unable to close the external site and undergo conformational change. Study of tyrosine 293 has placed it in a theoretical location in, or near, the glucose binding site; the preceding amino acids to tyrosine 293 (Q 282 QLSGINAVFYY 293) are thought to form hydrogen bonds with the substrate. This mutation would provide a useful construct for the study of the glucose transporter by X-ray crystallography, producing a transporter locked in a single conformation.

Both Mueckler *et al.*, (1985) and Ducarme *et al.*, (1996) have proposed models which are compatible with the above tyrosine mutations. Both models place the hydrophobic patch at the extracellular surface. Although there is variation in the exact position of the tyrosine residues, both models could fit the results as described above.

1.8 Proline 385 Mutational Analysis - A Helical Hinge

The sequence F 378 FEVGPGPIPW 388 is conserved in GLUT's 1, 2, 3, 4 and 7. Proline 385 is therefore in a proline rich region of the glucose transporter. In an

α-helix the presence of the imino acid proline has the effect of breaking the hydrogen bonding pattern, so disrupting the helix. This is a useful property, enabling the helix to form flexible kinks.

Tamori *et al.*, (1994) substituted proline 385 with either glycine or isoleucine. As a result of the isoleucine substitution a marked reduction in transport activity was observed. Both mutants were capable of binding cytochalasin B with similar activities to the wild-type transporter. However, the binding of ATB-BMPA was perturbed in both mutants, the glycine mutant resulting in a 2-fold reduction in ATB-BMPA binding and the isoleucine mutant resulting in a complete abolition of ATB-BMPA binding. These data indicated that the mutated glucose transporter was locked in an inward-facing conformation.

Wellner *et al.*, (1995a) extended the work of Tamori *et al.*, (1994) by studying mutations made to proline residues in putative transmembrane helices 6 and 10 (according to the model proposed by Mueckler *et al.*, (1985). It was observed that by individually point mutating six proline residues within helices 6 and 10 to alanine (P 187, P 196, P 205, P 383, P 385 and P 387) that there was no detrimental effect on glucose transporter activity. The study of a double mutant, mutating both P 383 and P 385 to alanine, also had no effect on glucose transport activity. However, by creating a triple mutant in which the three proline residues P 383, P 385 and P 387 were mutated to the polar amino acid, glutamine, 2-deoxy-D-glucose uptake was almost abolished. It is thought that this mutation may hinder the conformational flexibility of the glucose transporter, disrupting the helix at the hinge region, therefore reducing transport activity. The isoleucine mutation studied by Tamori *et al.*, (1994) may also have a similar affect in disrupting the hinge region. Studies carried out by Wellner *et al.*, (1995a) suggest that the glucose transporter can compensate for individual mutations of the 6 proline residues with a small hydrophobic residue, alanine. However, the larger amino acid glutamine clearly disrupts the function of helix 10. When Tamori *et al.*, (1994) substituted proline 385 with glycine a reduction in ATB-BMPA binding was observed. Glycine may not have abolished binding as this small residue also confers flexibility to the peptide chain.

1.9 Glutamine 282 Mutational Analysis - The External Binding Site

Hashiramoto *et al.*, (1992) have identified glutamine 282 as being important in exofacial ligand binding. By mutating glutamine 282 to leucine, the group produced a glucose transporter with a reduced affinity to ligand at the exofacial site. Labelling of the mutated glucose transporter with the exofacial ligand ATB-BMPA was reduced by 95% in comparison to the wild-type glucose transporter. However, the mutated glucose transporter was still capable of binding the endofacial ligand cytochalasin B to wild-type levels.

Mueckler *et al.*, (1985) mapped glutamine 282 to the centre of helix 7, Ducarme *et al.*, (1996) mapped glutamine 282 to the exofacial surface of helix 7. Both models place the amino acid in a region where it is capable of binding to ligand. Hashiramoto *et al.*, (1992) postulate that according to the model by Mueckler *et al.*, (1985) the binding of glutamine 282 to the substrate must cause a massive conformational change, lifting the centre of helix 7 out of the membrane towards the surface. Proteolysis evidence is available which appears to support a large conformational change during ligand binding. Holman and Rees, (1987) demonstrated this by subjecting erythrocyte membranes to thermolysin treatment in the presence of both ASA-BMPA and cytochalasin B, which bind to the exofacial and endofacial sites respectively. In the presence of ASA-BMPA at the external binding site there was very little cleavage of the transporter. However, in the presence of cytochalasin B at the internal binding site the transporter was cleaved to produce smaller protein fragments. Thermolysin appeared to cleave the transporter on the internal surface as there was virtually no thermolysin cleavage observed in resealed erythrocyte ghosts. It was concluded from this work that the binding of ASA-BMPA at the external site must have caused a major conformational change which protected the internal thermolysin cleavage site within the transporter structure. Similar results were obtained by Clark and Holman, (1990) using the exofacial ligand ATB-BMPA and trypsin. Clark and Holman, (1990) observed that the exofacial ligand ATB-BMPA protected the erythrocyte glucose transporter from trypsin cleavage. It was hypothesised that this was due to the adoption of an outward facing conformation by the glucose transporter therefore protecting the trypsin site.

Hashiramoto *et al.,* (1992) suggest that the alternation of the glucose transporter between two conformations, an outward and inward facing conformation, involves the upward and downward movements of helixes 7 and 12. This would act to relay the substrate between the external and internal sites.

1.10 Tryptophan 388 and 412 Mutational Analysis - The Internal Binding Site

Inukai *et al.,* (1994) have focused on residues involved at the internal binding site of the glucose transporter. It has been observed that when photolabelling the glucose transporter with the endofacial ligand, cytochalasin B, the wavelength required for photoactivation is 280 nm. This is the wavelength required to activate an aromatic tryptophan residue, rather than the cytochalasin B molecule itself. Two tryptophan residues exist within helices 10 and 11, tryptophan 388 and tryptophan 412, respectively. Inukai *et al.,* (1994) mutated tryptophan 388 and tryptophan 412 to leucine residues, both individually and as a pair. Cytochalasin B binding was reduced but not completely abolished by the individual point mutation of the tryptophan residues. However, analysis of the double mutant indicated that cytochalasin B binding was 30% of the wild-type level and cytochalasin B photolabelling was completely eliminated. Furthermore, the ability of the double mutant to transport glucose was reduced by 70% in comparison to the wild-type. These results suggest that the tryptophan residues are necessary in maintaining a high affinity towards cytochalasin B. Furthermore, the results suggest that the tryptophan residues lie in close proximity to the cytochalasin B binding site. Both Mueckler *et al.,* (1985) and Ducarme *et al.,* (1996) map these tryptophan residues towards the cytoplasmic surface of the glucose transporter.

1.11 Cysteine Residue Mutational Analysis

Wellner *et al.,* (1992) have studied the effect of p-chloromercuribenzene sulfonic acid (a sulfhydryl reactive agent) interaction with cysteine 421 and cysteine 429. Experiments with the impermeant sulfhydryl reagent p-chloromercuribenzene sulfonic acid demonstrated that cysteine 429 is exposed to the external surface of the glucose

transporter, whereas cysteine 421 is protected by the plasma membrane. These findings are consistent with both of the models proposed by Mueckler *et al.,* (1985) and Ducarme *et al.,* (1996). Wellner *et al.,* (1994) studied the effect of point mutating each of the six cysteine residues in the glucose transporter and found that no individual cysteine residue was essential for glucose transporter activity. Even the double mutation C 201 G and C 207 S had no effect on transport activity. Wellner *et al.,* (1994) concluded that the cysteine residues do not have an essential function in maintaining the glucose transporter tertiary structure.

1.12 Antibody Analysis

Davies *et al.,* (1990) have carried out an extensive study using antibodies to map specific regions of the glucose transporter. Antibodies were raised towards regions of the glucose transporter determined by Mueckler *et al.,* (1985) to be extramembranous. Seventeen of the nineteen antibodies raised against peptides recognised the denatured protein by immunoblotting. However, only six antibodies recognised the native membrane bound protein, even after deglycosylation. Four of these antibodies mapped to the large intracellular cytoplasmic loop and the other two antibodies were to the cytoplasmic C-terminal tail. Previous studies by Davies *et al.,* (1987a&b) have demonstrated the C-terminal tail to be cytoplasmic. Binding to the N-terminal tail in the native state was not achieved in either study. This may be due to the N-terminal tail being buried in, or associated with the membrane. It was not possible to determine why the antibodies did not recognise other extracellular regions of the glucose transporter and several possibilities exist, including: a) The extracellular regions are not as predicted and b) The extracellular regions form a complex structure not allowing antibody recognition.

Point mutation analysis has examined the function of individual amino acids. However, several experiments have been performed in order to determine the function of large areas of amino acid sequence. These have included the deletion of the C-terminal amino acids and the construction of chimeric proteins.

1.13 C-Terminal Deletion Analysis of GLUT1

The C-terminal tail of the glucose transporter has been demonstrated to be essential for glucose transport. This has been tested by several groups, who have performed C-terminal deletion analysis on the final 43 amino acids of the glucose transporter. Deletions made are displayed in figure 1.6 and are discussed in the following text.

The smallest C-terminal deletion was made by Lin *et al.*, (1992). Lin *et al.*, (1992) introduced a stop codon at amino acid 480, which was found to have no effect on glucose transport activity. The introduction of a stop codon at 470 and 469 by Due *et al.*, (1995) and Muraoka *et al.*, (1995) respectively, also had no effect on the function of the glucose transporter. However, the progressive deletion of the C-terminal tail by the introduction of stop codons at residues 468, 467 and 466 by Muraoka *et al.*, (1995) resulted in the reduction of glucose transport activity. Indeed, transport activity is greatly reduced by the introduction of a stop codon at residue 468 (deleting 25 C-terminal amino acids) and almost completely abolished by the introduction of a stop codon at residue 467 (deleting 26 C-terminal amino acids). Binding of the exofacial ligand ATB-BMPA to the two mutants with 25 and 26 C-terminal amino acids deleted was perturbed. However, it was still possible for cytochalasin B to bind to the internal binding site with near to wild-type activity.

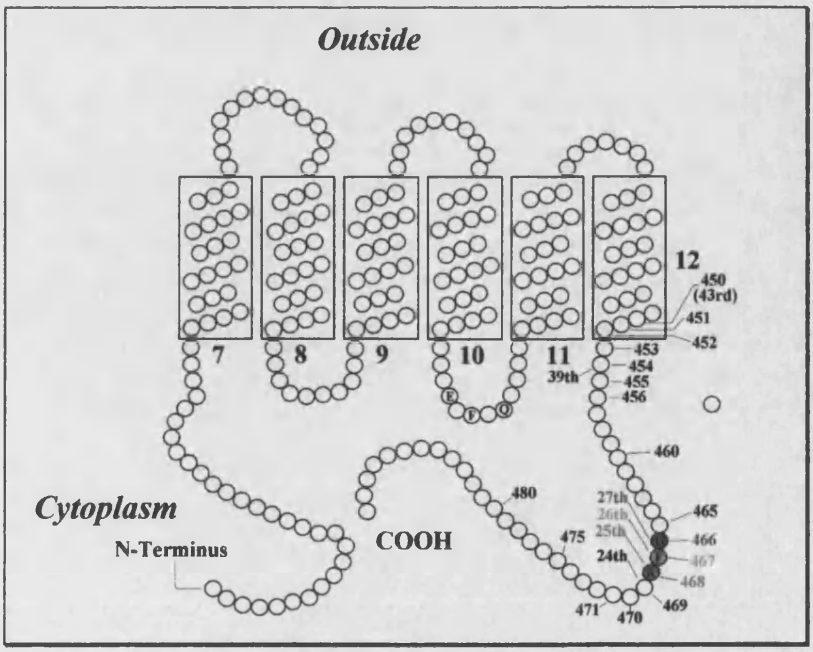

Figure 1.6, The C-terminal portion of the glucose transporter. Modified from the picture of Bell *et al.*, (1993) displaying the last 6 transmembrane α-helices and the C-terminal tail. Residues at which stop codons were introduced into the corresponding DNA are marked.

Amino Acids From N-Terminus	Amino Acids From C-Terminus	Effect of Deletion on Transport Activity
492	1	
480	13	Wild-type
470	23	Wild-type
469	24	Wild-type
468	25	Decreased activity
467	26	Decreased activity
466	27	Decreased activity
454	39	Decreased activity
451	42	Decreased activity
450	43	

Table 1.4, GLUT1 C-terminal amino acid deletions. C-terminal amino acid deletions summarised from the text.

The introduction of stop codons at residues 454 and 451 by Oka *et al.*, (1990) and Due *et al.*, (1995), respectively, produce data consistent with the results of Muraoka *et al.*, (1995). In conclusion, deletion of the C-terminal amino acids may result in a significant conformational change within the protein, giving rise to a glucose transporter locked in an inward facing conformation.

Furthermore, Due *et al.*, (1995) have examined the effect of adding 31 amino acids to the C-terminus of the glucose transporter. These amino acids were derived from the human insulin C-peptide protein. Due *et al.*, (1995) reasoned that if the C-terminal tail is important for conformational change of the protein, the addition of extra amino acids to the C-terminal tail might impair the ability of the glucose transporter to undergo conformational change. Due *et al.*, (1995) found that the addition of the C-peptide protein had no effect on glucose transporter activity, in GLUT1 mutants expressed in *Xenopus* oocytes.

1.14 Chimeric Protein Analysis

Katagiri *et al.*, (1992) reported that the substitution of 39 C-terminal GLUT1 amino acids, with those of GLUT2, result in a chimeric protein with transport kinetics resembling those of GLUT2. The substituted amino acids are displayed in figure 1.7.

```
                    454 39          468
Rabbit GLUT1;   FKVPE/TKGRTFDEIASGFR//QGG
Human GLUT2;    ...../...KS.E...AE.Q//KKS
```

Figure 1.7, A GLUT1 / GLUT2 chimera. The final 39 amino acids of GLUT1 were substituted with the corresponding amino acids of GLUT2. Amino acid E454 corresponds to the 40th residue from the C-terminus. Identical residues are represented by a dot, residues that vary are displayed as the single letter amino acid code.

Due *et al.*, (1995) created a GLUT1 / GLUT4 chimera, composed of GLUT1 amino acids 1 - 463 and then GLUT4 amino acids 480 - 509. The resulting chimera had the same kinetics as the GLUT4 protein. This suggests that the C-terminal tail is capable of regulating the kinetic properties of the glucose transporter and could therefore be responsible for the functional differences between the different isoforms. Dauterive *et al.*, (1996) have studied similar chimeric constructs and have assigned further functions to the C-terminal tail of the glucose transporter.

Dauterive *et al.*, (1996) emphasise that GLUT1 is capable of a unique kinetic property termed 'accelerated exchange'. When the Vmax for uptake is measured with internal and external glucose concentrations in equilibrium, the Vmax is found to be much higher than when uptake is measured in the absence of internal glucose (zero trans entry).

Dauterive *et al.*, (1996) created two chimeric proteins. The first protein was a GLUT1 / GLUT4 chimera composed of GLUT1 amino acids 1 - 444 and then GLUT4 amino acids 461 - 509. The second protein was a GLUT4 / GLUT1 chimera composed of GLUT4 amino acids 1 - 460 and then GLUT1 amino acids 445 - 492. Table 1.5 displays the kinetic data obtained from the chimeric constructs.

mRNA Injected	Vmax (Zero trans) pmol/min/oocyte	Km mM	Equ. Exc. $Vmax_{(ee)}$ pmol/min/oocyte	$Km_{(ee)}$ mM
GLUT1	575 ± 88	10.7 ± 2.0	1450 ± 373	43.9 ± 6.5
GLUT1 cterm 4	296 ± 45	8.0 ± 0.6	302 ± 45	16.7 ± 3.5
GLUT4 cterm 1	480 ± 69	9.5 ± 3.3	461 ± 25	23.3 ± 3.4
GLUT4	76 ± 7.5	8.8 ± 2.1	124 ± 25	19.1 ± 3.3

Table 1.5, Kinetic data from GLUT1 / GLUT4 chimeras. The first two columns display the Vmax and Km in the absence of intracellular glucose and the final two columns display the Vmax and Km in equilibrium conditions. GLUT1 can be seen to lose the property of equilibrium exchange when its C-terminal region is replaced with that of GLUT4.

When the GLUT1 protein is made chimeric with the GLUT4 C-terminus the property of accelerated exchange is lost and the Vmax reduced. When the GLUT4 protein is made chimeric with the GLUT1 C-terminus (GLUT4 1 - 460, GLUT1 445 - 492) the Vmax is raised to GLUT1 levels but the property of accelerated exchange is not conferred upon the GLUT4 protein. Although, it appears that the C-terminal tail has some importance in controlling transporter kinetics, for accelerated exchange to occur the GLUT1 C-terminal domain must interact with other specific sequences not present within the GLUT4 protein.

1.15 Mechanisms of Glucose Transport

It is thought that the glucose transporter oscillates between two conformations, an inward facing and an outward facing conformation. This is proposed to occur both in the presence and absence of substrate, although the latter case is difficult to confirm experimentally. Two possible mechanisms of transport have been considered by Helgerson and Carruthers, (1989). These are the one site (simple) carrier and the two site (fixed site) carrier. The simple carrier describes a transporter mechanism, where sugar influx and sugar efflux binding sites are mutually exclusive, the sites being exposed in an alternating fashion. The fixed site carrier describes a transport mechanism in which sugar influx and sugar efflux binding sites can exist simultaneously. Helgerson and Carruthers, (1989) found that in rat erythrocytes the mechanism of transport is a

better, but not perfect fit to the fixed, two site carrier mechanism. Their results have lead them to reject the simple, one site carrier model.

Zottola *et al.,* (1995) have proposed a transport mechanism consistent with past and current experimental evidence. The model is based on the oligomeric structure of the glucose transporter. Jung *et al.,* (1980) suggested that the human erythrocyte glucose transporter adopts a tetrameric form in the native state. Further to the study carried out by Jung *et al.,* (1980) Hebert and Carruthers, (1992) have suggested that the GLUT1 glucose transporter functions as a complex of four GLUT1 protein monomer units, whose substrate binding properties are linked by reductant-sensitive noncovalent subunit interactions. Zottola *et al.,* (1995) have now proposed a new mechanism based on the GLUT1 homotetramer and propose that a carrier can be thought to comprise of one or more members of an 'E1·E2' catalytic subunit, figure 1.8, cycling between two conformational states. The 'E1' state exposes the substrate export site and the 'E2' state exposes the substrate import site. No single subunit can exist in both E1 and E2 states simultaneously, ie. a simple carrier mechanism. Their view is that current evidence rules against the possibility of the glucose transporter existing as a simple carrier type transporter. The proposed E1·E2 catalytic subunit is displayed in figure 1.8.

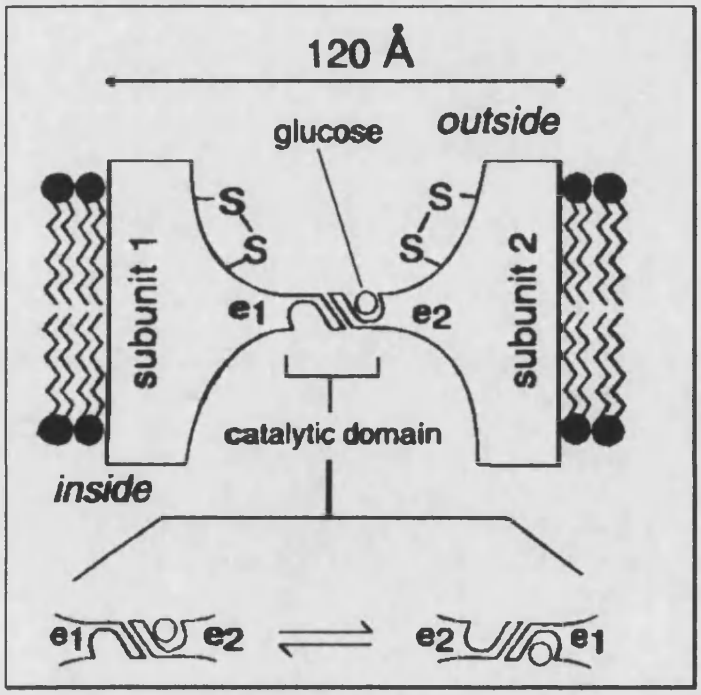

Figure 1.8, An E1 E2 catalytic subunit (taken from Zottola *et al.*, (1995). The diagram shows a section across two of the four subunits that form the hypothetical glucose transporter homotetramer. The E1 E2 catalytic subunit is formed by two associated glucose transporters. Two E1 E2 subunits may then associate to form a homotetramer. In the homotetramer form the transporter acts as a fixed site carrier and in the monomeric form as a simple carrier.

Zottola *et al.*, (1995) suggest that the transporter exposes its E1·E2 sites simultaneously (fixed site carrier) and not sequentially (simple carrier) existing as a homotetramer. When one subunit exists in the E1 state the adjacent subunit must adopt the E2 state, thus the transporter would contain two E1 conformers and two E2 conformers at all times. If the E2 site binds substrate then the adjacent E1 site must undergo the antiparallel conformational change, regardless of the occupancy state. The linked glucose transporter units now act as simple carriers when in the monomeric form. However, when the transporter is in the tetrameric form the whole unit acts as a fixed site carrier, presenting both import and export sites simultaneously. They conclude that the tetrameric form of the transporter satisfies all of the currently available experimental evidence. The units appear to act allosterically, as they suggest the dimeric form of the transporter is some 10 fold less active than the tetrameric form. This is possible because in the tetrameric form the transporter could bypass slow relaxation steps, acting as a simultaneous carrier, where sugar import is coupled with the regeneration of other sugar import sites in one step. The subunits are thought to be connected by noncovalent interactions promoted or stabilised by intramolecular disulfide bridges. On exposure to reductant the tetramer breaks up into dimers, demonstrating the disulfide bridge to be essential for oligomerization.

Zottola *et al.*, (1995) have further shown that *Xenopus* oocyte expressed GLUT1 is not affected by dithiothreitol, suggesting that oocyte GLUT1 is in the dimeric, rather than a tetrameric form. This would explain why *Xenopus* oocyte expressed GLUT1 binds glucose with a 10 fold lower affinity than erythrocyte GLUT1 or CHO cell expressed GLUT1.

Wellner *et al.*, (1995b) disagree with Zottola *et al.*, (1995) and have carried out experiments to disprove the homotetramer theory. They have demonstrated that the individual replacement of cysteine residues has no effect on transporter kinetics when measured in *Xenopus oocytes*. They conclude that individual disulfide bonds do not appear to be essential to catalytic activity. The simultaneous change of three cysteine residues in the N-terminal half to either serine or glycine residues had no effect on 2-deoxy-D-glucose uptake. However, it could not be excluded that multimeric assembly could take place by a different mechanism. The substitution of three cysteine residues within the C-terminal half for serine residues, or the substitution of all six cysteine

residues throughout the transporter resulted in only a slight decrease in catalytic activity. Wellner *et al.*, (1995b) concluded that if oligomerization occurs by disulfide bridges within the membrane, they contribute little towards the intrinsic catalytic activity of GLUT1.

1.16 Regulation of the Glucose Transporter - Cytosolic

Carruthers and Helgerson, (1989) and Hebert and Carruthers, (1986) have demonstrated that the ATP is capable of binding to an intracellular site on the human erythrocyte glucose transporter. Furthermore, the binding of ATP appears to be stereoselective and to act in modifying the function of the glucose transporter. It appears that in the presence of ATP, GLUT1 is converted into a low capacity glucose transporter and in the absence of ATP, GLUT1 is converted into a high capacity glucose transporter. The nucleotides AMP, ADP, UTP, ITP and GTP were unable to mimic the action of ATP. However, the nucleotides AMP and ADP were capable of acting as competitive inhibitors of ATP binding. The glucose transporter lacks any detectable ATPase activity and is not phosphorylated by ATP. These authors suggest that ATP may modify the function of the glucose transporter by allosteric interaction. Studies undertaken using C-terminal peptide antisera indicate that ATP binding either causes subtle changes in carrier structure, or that bound ATP directly interferes with IgG binding. Partial enzymatic digestion of azido-ATP photolabelled GLUT1 protein localises the cytoplasmic ATP binding site to the same domain responsible for the cytoplasmic binding of cytochalasin B and the same extracellular domain responsible for the binding of ATB-BMPA (residues 270 - 456). Three ATP binding domain consensus sequences have been identified within the glucose transporter and are located between residues 111 - 117, 225 - 229 and 332 - 338. The proposed mechanism is summarised in figure 1.9.

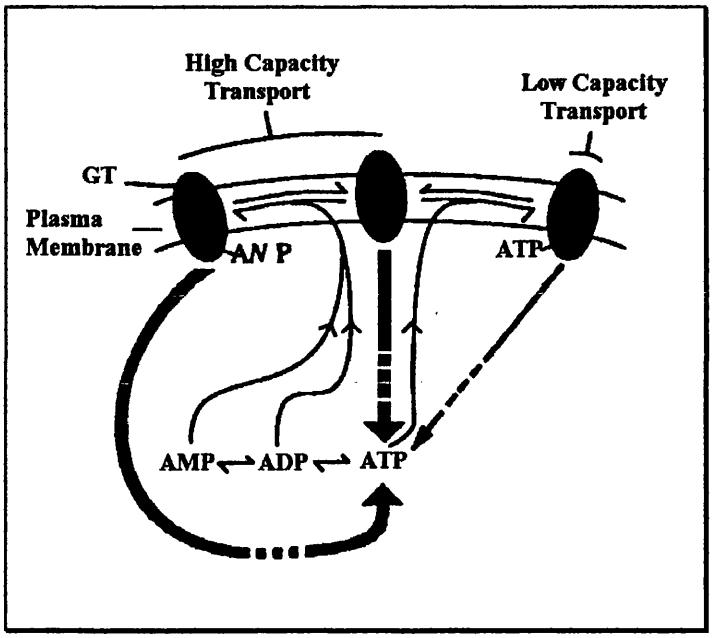

Figure 1.9, ATP can complex with the erythrocyte glucose transporter to alter the function of the protein (taken from Carruthers and Helgerson, (1989). The GLUT1 protein (GT) can exist either dissociated or complexed with ATP, ADP or AMP. When ATP is complexed with the carrier, a low capacity transporter exists. In all other situations a high capacity transporter prevails. High level production of ATP therefore favours low capacity glucose transport.

Shi *et al.*, (1995) have further investigated the effects of exposing Clone 9 cells (a non-transformed rat liver cell line) to inhibitors of oxidative phosphorylation. Chemicals such as azide or cyanide result in an increase in glucose uptake. This increase is observed after exposure of clone 9 cells to azide for a period of 1 - 2 h. The increase in glucose transport activity is not associated with any other glucose transporter isoform, as Clone 9 cells are known to exclusively express GLUT1. Neither is the increase in activity linked to an increase in cellular or plasma membrane levels of GLUT1. However, longer exposure times of up to 24 h result in an increase in GLUT1 mRNA levels. Shi *et al.*, (1995) monitored the increase in glucose transporter activity by cytochalasin B binding. Clone 9 cells possess 3 classes of binding sites; a D-glucose / cytochalasin B sensitive site (site I), a cytochalasin E sensitive site (site II) and a site which is insensitive to cytochalasin E (site III).

Shi *et al.*, (1995) observed that exposure of Clone 9 cells to azide resulted in an increased Vmax for glucose while the Km for glucose remained unaltered. Azide treatment resulted in an increased binding of cytochalasin B at site III. The evidence suggested that site III is an altered form of GLUT1, inactivated by molecular association with a cytoskeletal component. Shi *et al.*, (1995) proposed that the GLUT1 glucose transporter in Clone 9 cells is deactivated in the normal state by a protein with an affinity towards the cytosolic carboxy terminus of GLUT1. In the presence of azide the

regulatory protein would become disassociated from the glucose transporter, allowing the glucose transporter to become functional.

Shi *et al.,* (1995) have identified three proteins with apparent molecular weights of 28, 70 and 85 kDa in Clone 9 cell cytosol. These proteins have been found to specifically bind to the cytoplasmic, carboxy terminal domain, of the glucose transporter. The 85 kDa protein was found to be a phosphoprotein which bound only to GLUT4. Both the 28 and 70 kDa proteins bound to GLUT1, although the 70 kDa protein bound with a higher affinity to GLUT4 than GLUT1. The function of these proteins in Clone 9 cells is at present unclear.

1.17 Regulation of the GLUT1 Glucose Transporter - Hormonal

The GLUT1 glucose transporter is the most widely distributed glucose transporter isoform and is not often thought of as being under hormonal control. However, it has long been known that cultured mammalian cells expressing only GLUT1 can produce relatively fast, profound changes, in glucose transport activity. Such increases in transport activity can be accounted for by translocation of GLUT1 from an intracellular pool to the plasma membrane. Baldwin *et al.,* (1994) has described some of these control mechanisms which affect the GLUT1 glucose transporter.

The GLUT1 glucose transporter is known to be abundant in the plasma membrane of secretory epithelial cells from the mammary glands of lactating rats. No other glucose transporter isoforms are present within these cells. Levels of GLUT1 glucose transporter remain low during pregnancy but increase rapidly with the onset of lactation. Removal of the litter, from the mother, results in a rapid loss of glucose transporter levels, which return to pre-birth levels 24 h later. These changes are not associated with changes in the level of GLUT1 mRNA, hence the control appeared to be post-transcriptional. Cells cultured with the hormone prolactin demonstrated a 5 fold increase in GLUT1 protein over a 2 day period but the hormones cortisol and insulin had no effect. These data demonstrated that prolactin was required for the initiation of GLUT1 expression in lactogenesis.

Confocal microscopy performed on haemopoietic cells demonstrated the presence of an intracellular pool of GLUT1. The intracellular GLUT1 pool could be

translocated to the plasma membrane under the influence of the hormone interleukin 3. GLUT1 translocation was also found to be affected by certain oncogenes (ie. v-*abl*). GLUT1 translocation appears to be an important step in preventing the cell from undergoing apoptosis.

1.18 Glycosylation of Human GLUT1

The human erythrocyte glucose transporter (GLUT1) is glycosylated on asparagine 45 (Asn 45, the N-linked consensus recognition site is Asp - X - Ser / Thr) which is located in the first extracellular loop (figure 1.3). Asano *et al.*, (1991) Asano *et al.*, (1993) and Feugeas *et al.*, (1990) have suggested that GLUT1 glycosylation plays an important role in GLUT1 function and should therefore be taken into consideration when expressing GLUT1 in non-native expression systems. Studies have shown that there is only one glycosylation site on the GLUT1 protein, this glycosylation site is thought to increase the affinity for glucose and therefore increase the rate of glucose transport. Asano *et al.*, (1993) further investigated the role of glycosylation in protein targeting and protein stability. Asano *et al.*, (1993) observed that the majority of glycosylation deficient GLUT1 was located in intracellular vesicles and was not targeted to the plasma membrane. Furthermore, deglycosylation resulted in GLUT1 protein with a reduced stability. Wild-type, glycosylated GLUT1, was observed to have a half-life of 25 - 28 h, while de-glycosylated GLUT1 had a half-life of 16 - 18 h. In conclusion, glycosylation has been shown to affect transporter location and stability, these factors may in turn modify the transporter activity.

1.19 Glycosylation in the *Spodoptera frugiperda* Expression System

This thesis examines GLUT1 expression in *Spodoptera frugiperda* cells (Sf9 cells). Since the glycosylation state of the glucose transporter affects its activity some aspects of glycosylation patterns observed in Sf9 cells are considered.

N-Linked glycosylation is known to occur in the endoplasmic reticulum of insect cells and has been thoroughly studied (King and Possee, (1992)). In both mammalian cells and insect cells, protein glycosylation is inhibited by the presence of tunicamycin.

It is known that mammalian cells carry out extensive modifications to the oligosaccharide moiety. This typically includes the addition of fucose and sialic acid residues, forming complex branched oligosaccharides. Insect cells lack the ability to extensively process the oligosaccharide moiety, and have only very low levels of fucose, galactose and sialic acid transferases. Glycoproteins, expressed in insect cells, typically contain a high proportion of mannose residues in the oligosaccharide moiety. Recombinant glycoproteins expressed in the insect cell system are sensitive to the enzymes endoglycosidase H, N-glycosidase F and N-glycanase which remove immature, high mannose type, oligosaccharides. Because glycosylation is less extensive in insect cells those recombinant proteins which are extensively glycosylated in the native system, exhibit a lower apparent molecular weight when expressed in insect cells.

1.20 Expression of the Mammalian GLUT1 Glucose Transporter

The mammalian GLUT1 glucose transporter has been expressed in a number of systems including: Bacterial (*E. coli*), Yeast (*Saccharomyces cerevisiae*), Insect (*Spodoptera frugiperda*), Amphibian (*Xenopus* oocytes) and non-native Mammalian (Chinese Hamster Ovary (CHO)) cell systems. The latter two examples, *Xenopus* oocytes and CHO cell systems are often used for point mutational analysis of the glucose transporter. This is because these cell systems extensively glycosylate the glucose transporter. The former cell systems are better suited to over-expression of the glucose transporter as they are capable of producing higher yields of the expressed protein. Unfortunately, as described in the previous section, these systems do not undertake extensive post translational modifications, such as glycosylation.

Several membrane glycoproteins have been previously expressed in the insect cell system. These include the following: a) The rabies virus glycoprotein G (a transmembrane glycoprotein expressed in *Spodoptera frugiperda* cells) has been demonstrated to be fully antigenically reactive (Préhaud *et al.*, (1989)) and b) The influenza virus haemagglutinin (an integral membrane protein expressed in *Spodoptera frugiperda* cells) was found to have a fully cleaved signal peptide and N-linked glycosidic modification (Kuroda *et al.*, (1986)). This result demonstrates that insect cell

expressed glycoproteins can be fully functional and can be translocated correctly to the plasma membrane and even undergoing signal peptide cleavage.

1.21 Expression of GLUT1 in the Insect Cell, *Spodoptera frugiperda*

Yi *et al.*, (1992) have demonstrated that the human erythrocyte GLUT1 protein can be over expressed in the insect cell system using *Spodoptera frugiperda* (Sf9) cells. Sf9 cells were infected with the baculovirus, *Autographa californica nuclear polyhedrosis virus* (AcNPV). This was genetically altered to express the human GLUT1 protein instead of the viral coat protein. Infected cells were observed by confocal immunofluorescent microscopy using an anti-GLUT1 FITC conjugated antibody. Fluorescence was observed after just two days of infection. The glucose transporter protein was observed to be located at the plasma membrane, and within intracellular membrane structures. There was no GLUT1 protein observed within the nucleus. Immunoblot analysis confirmed the presence of GLUT1 and demonstrated that all of the GLUT1 protein was associated with cellular membranes (GLUT1 was completely absent from the soluble fractions). Insect cell expressed human GLUT1 had an apparent molecular weight of 45 kDa, which was only slightly reduced with endoglycosidase F treatment. This indicates that only restricted glycosylation of GLUT1 had occurred in insect cells. After a four day infection period, the glucose transporter was found to constitute 8% (1.44 nmol / mg membrane protein) of the total membrane protein, as determined by immunoblot analysis. The protein was stable and found to accumulate until cell lysis. The level of expression achieved by Yi *et al.*, (1992) was comparable with other membrane glycoproteins expressed in the insect cell system.

A precise measurement of glucose transport activity was not possible because insect cells underwent cell lysis during the viral infection cycle and an endogenous glucose transporter was present. Fortunately though, the endogenous Sf9 glucose transporter does not cross react with the anti C-terminal GLUT1 antibody or bind cytochalasin B (Yi *et al.*, (1992)). The Kd for the binding of cytochalasin B to Sf9 cell membranes expressing human glucose transporter was 284 nM. This was almost identical to the Kd observed for cytochalasin B binding to human erythrocyte ghosts (282 nM Yi *et al.*, (1992)). Binding was inhibited by the addition of D-glucose but not

L-glucose, demonstrating that the glucose transporter was still capable of stereoselectivity and that the transporter was likely to adopt its native conformation. The amount of biologically active protein, as determined by cytochalasin B assay, was less than 20% of the total protein determined by immunoblot assay. However, the insect cell expression system still provides sufficient active protein for further biological experimentation.

1.22 Expression of GLUT1 in the Bacterium, *E. coli*

In comparison with the Sf9 baculovirus expression system, the *E. coli* expression system is capable of producing large quantities of protein rapidly and economically. Unfortunately, *E. coli* undertakes very little post-translational modification and the expressed glucose transporter is not glycosylated in this system. Glucose transporter protein expression in the bacterium *E. coli* has been investigated by Sarkar *et al.*, (1988).

Sarkar *et al.*, (1988) have expressed the human erythrocyte glucose transporter, GLUT1, in a strain of *E. coli* (SR425) deficient in all known pathways of glucose transport. Transport studies revealed that the transformed cells were capable of transporting 2-deoxy-D-glucose and D-glucose 4 - 5 times faster than control cells. Unlabelled D-glucose, cytochalasin B and mercuric chloride inhibited uptake of radiolabelled substrate. Uptake of radiolabelled substrate was not inhibited by L-glucose. The expressed glucose transporter was detected by immunoblotting with an anti C-terminal antibody and an antibody directed against amino acids 225 - 238, in the cytoplasmic loop. The apparent molecular weight of the expressed protein was determined to be 34 kDa, a molecular weight similar to de-glycosylated human erythrocyte glucose transporter. This demonstrates that the human erythrocyte glucose transporter can be inserted into the *E. coli* cell membrane in a de-glycosylated functional state.

1.23 Expression of GLUT1 in the Yeast, *Saccharomyces cerevisiae*

The use of a yeast expression system for the expression of the GLUT1 protein has been investigated by Kasahara and Kasahara, (1996). This is a useful expression system as it again offers the advantages of rapid economical protein expression.

Kasahara and Kasahara, (1996) have successfully expressed the rat GLUT1 glucose transporter in the yeast *Saccharomyces cerevisiae*. Observation by confocal immunofluorescence microscopy revealed that the majority of the GLUT1 protein was located within intracellular structures. Very little glucose transport activity was observed in intact cells. However, glucose transport activity was observed in a reconstituted system, resulting in Vmax and Km values similar to those measured in human erythrocytes. Incubation of yeast expressed GLUT1 with N-glycosidase F did not affect the apparent molecular weight of 40 kDa, indicating there to be little or no glycosylation. In comparison, incubation of human erythrocyte GLUT1 with N-glycosidase F reduced the apparent molecular weight of the native protein to 40 kDa. In conclusion, the yeast expression system fails to target the GLUT1 glucose transporter correctly or to glycosylate the protein. Otherwise, the glucose transporter protein appears to be a fully functional, unglycosylated, glucose transporter. Different cells appear to target the glucose transporter in different ways, it appears that protein targeting is very much cell dependent. Simons *et al.,* (1997) are continuing this work, attempting to perfect the expression of GLUT1 in yeast by exploring a range of yeast expression vectors and yeast host strains. Simons *et al.*, (1997) have also modified the GLUT1 protein to express a C-terminal polyhistidine tag. The aim is to utilise the polyhistidine tag in the purification of the glucose transporter, to enable crystallisation studies.

1.24 Affinity Purification of Proteins using a Polyhistidine Tag

Many proteins have now been purified using the approach of immobilised metal ion affinity chromatography (IMAC). To achieve this a polyhistidine tag is genetically engineered into the protein; the modified protein is then expressed in the chosen expression system. The protein is usually engineered to express a sequence of six contiguous histidine residues at either the N-terminal or C-terminal end of the protein. Carlsson *et al.,* (1996) have determined that proteins carrying as few as four or five contiguous histidine residues can be purified using this technique. Carlsson *et al.,* (1996) observed that although longer histidine tails often reduced the level of gene expression, they do increase the level of binding between the polyhistidine residues and the chelated metal ions. In most circumstances the use of four or more histidine residues will assure a strong metal / protein interaction.

Waeber *et al.,* (1993) were the first group to purify a membrane bound protein using nickel chelate affinity chromatography, the protein was the *E. coli* glucose transporter. The *E. coli* glucose transporter combines vectorial transport with the phosphorylation of the translocated substrate. Waeber *et al.,* (1993) modified the membrane bound glucose transporter of *E. coli* by the addition of 10 amino acids to the C-terminus, these ten residues contained six contiguous histidine residues. The addition of ten amino acids to the C-terminus was found to have no effect on either protein stability or activity. In practice slightly more modified protein was expressed in comparison with the control. Following the addition of the polyhistidine tag there was a slight increase in the apparent molecular weight. About 90% of the glucose phosphotransferase activity could be solubilized at pH 8.9 using 2% Triton. Virtually pure glucose transporter protein was eluted from an immobilised metal ion column at pH 5.0. A minor contaminating protein with an apparent molecular weight of 67 kDa was removed by gel filtration chromatography. Following purification, 70% of the glucose transporter's phosphotransferase activity was retained. The high affinity of this polyhistidine tagged glucose transporter to the chelated nickel column indicates that the hydrophilic C-terminus of the *E. coli* glucose transporter is accessible to the external medium.

Waeber *et al.,* (1993) have also attempted to purify the *E. coli* phosphotransferase transporter for mannose. Polyhistidine tags were placed at the N-terminus and C-terminus of the IID^{Man} subunit and the N-terminus of the IIC^{Man} subunit. The constructs demonstrated the importance of correctly positioning the tag for optimum surface exposure. Although all of the constructs were fully active, only the construct with the polyhistidine tag at the most hydrophilic end was capable of being successfully purified on an immobilised nickel column. Polyhistidine tags placed too close to transmembrane regions may become sequestered in the detergent micelle, becoming inaccessible to the immobilised nickel ions.

Pourcher *et al.,* (1995) have expressed, solubilized and purified the *E. coli* melibiose permease. They engineered six contiguous histidine residues onto the C-terminal end. The construct was over-expressed in *E. coli* and the membranes were solubilized in the presence of a novel detergent, 3-(laurylamido)-N,N'-dimethylaminopropylamine oxide (LAPAO), derived from the commercially available detergent SB12. The modified melibiose permease was purified to > 90% purity on an immobilised nickel ion column. During purification the detergent system was changed for n-dodecyl β-D-maltoside in order to maintain the activity of the permease. The permease was then purified to homogeneity on a Macro-Prep Q anion exchange resin. The results showed that the permease was more than 80% functional and that the addition of the C-terminal polyhistidine tag had no effect on the function of the protein.

Loddenkötter *et al.,* (1993) have purified the mature chloroplast triose phosphate-phosphate translocator in a functional state. The chloroplast triose phosphate-phosphate translocator was expressed in a yeast system. The protein was originally derived from spinach. Its function is to export triose phosphates across the chloroplast membrane into the cytosol. It has an apparent molecular weight of 29 kDa, which increased to 30 kDa on the addition of the six contiguous histidine residues on the C-terminal end of the protein. The translocator was localised to the rough endoplasmic reticulum and mitochondrial membrane when expressed in yeast and was solubilized by n-dodecyl maltoside in the presence of high concentrations of inorganic phosphate. The addition of inorganic phosphate helped to preserve functional transport activity during purification. The polyhistidine tagged protein was finally eluted from the column using

100 mM imidazole, resulting in a protein > 95% pure. The transport characteristics of the polyhistidine tagged translocator were similar to that of the wild-type protein.

Weinglass and Baldwin, (1996) have studied the purification of polyhistidine tagged GLUT1 expressed in insect cells. Site directed mutagenesis was used to insert six contiguous histidine residues onto the C-terminal end of human GLUT1 cDNA. The mobility of the histidine tagged construct on a polyacrylamide gel was reported to be reduced. The functional activity, assessed by cytochalasin B binding, was determined to be the same as the wild-type protein. The histidine tagged protein was efficiently solubilized in the detergent octyl glucoside. The solubilized fraction was loaded onto a chelating nickel column, which resulted in the retention of most of the recombinant protein. Analysis of the eluted material by polyacrylamide gel electrophoresis demonstrated the protein to be more than 90% pure.

In many of the above examples 100% purity was not obtained using metal ion affinity chromatography and the use of a second column was required to achieve protein homogeneity. However, the use of metal ion chromatography in membrane protein purification has proved to be a useful technique.

1.25 Membrane lipids

Solubilization and purification of integral membrane proteins by liquid chromatography results in the membrane proteins becoming delipidated. This will be an important consideration when purifying the glucose transporter because membrane proteins depend on a lipid environment to maintain their own structure; a lipid presence should be maintained throughout the purification procedure. The composition of the lipid used for reconstitution into a lipid bilayer can have a marked effect on the catalytic activity of the membrane bound transporter. For example, Tefft *et al.,* (1986) have determined that the activity of the glucose transporter was affected greatly by the lipid bilayer head group composition. Furthermore, Connolly *et al.,* (1985a&b) have studied the effect of cholesterol content in a lipid bilayer. High levels of cholesterol were found to be inhibitory to glucose transport.

Ambudkar and Maloney, (1986) have demonstrated that during the solubilization of the bacterial anion exchange transporter, it was necessary to maintain a lipid

environment to prevent the inactivation of the transporter protein. Ambudkar and Maloney, (1986) also observed that the addition of 10 - 20% glycerol during purification improved the activity of the anion exchange transporter. These are important factors to consider for the purification of the glucose transporter to ensure that a fully functional transporter is obtained. Evidence suggests that a balanced mixture of lipids should allow for the protection and reconstitution of the glucose transporter, during and following purification.

1.26 Determined Crystal Structures for Membrane Bound Proteins

To date, very few integral membrane proteins have been crystallised and subjected to 3-dimensional analysis, such as X-ray crystallography. This is due to the difficulties involved in obtaining pure integral membrane proteins which will form high quality crystals composed of molecules orientated in the same direction. The very first integral membrane protein to be analysed by X-ray diffraction crystallography was bacteriorhodopsin, isolated from the purple membrane of the bacterium *Halobacterium halobium*.

Blaurock, (1982) has reviewed the initial work carried out on the bacteriorhodopsin structure. Bacteriorhodopsin is a light driven proton pump. Its function is to convert the light energy captured into a transmembrane proton gradient. The transmembrane proton gradient can then be used to generate ATP. Bacteriorhodopsin can be isolated from *Halobacterium halobium* purple membranes as a more or less pure protein, contained in flat sheets of membrane as opposed to closed vesicles. Two properties aid further study of the protein: a) Bacteriorhodopsin retains its structure while under vacuum and during desiccation and b) Bacteriorhodopsin forms a crystalline array extending into the plane of the membrane. Therefore, bacteriorhodopsin almost satisfies the basic requirements for X-ray crystallographic analysis and is almost a pure crystalline protein in the natural state. The problem is to obtain crystalline arrays where all of the bacteriorhodopsin molecules within the membrane fragments are in alignment. Desiccation of natural membranes results in crystalline arrays which are not in alignment. Therefore, methods of producing crystals other than by uncontrolled

desiccation were investigated. Several methods were tried including a method employing a limited and gradual dehydration process.

Despite the initial success of isolating and growing crystals of bacteriorhodopsin, it proved difficult to obtain high resolution crystallographic information as the crystals were shown to have a disordered structure. From the initial analysis of bacteriorhodopsin it was determined that the protein contained a high level of α-helical structure which was more or less perpendicular to the plane of the membrane.

Henderson and Unwin, (1975) originally used electron microscopy to determine the position of the helices in bacteriorhodopsin to a resolution of 7 Å. This was later refined by Baldwin *et al.,* (1988) to 2.8 Å using the technique of cryo-electron microscopy.

Bacteriorhodopsin was finally crystallised by Schertler *et al.,* (1993) and formed ordered orthorhombic crystals. The crystals were nucleated on benzamidine and diffracted to a resolution of 3.6 Å. However, the crystallographic data has yet to be analysed. Schertler *et al.,* (1993) took the isolated purple membranes and solubilized them in 1% Triton X-100 for 14 h, at 34°C, in the dark. The debris was removed by centrifugation and the detergent exchanged for 0.5% octyl glucoside on a DEAE Sephacel column. The protein was concentrated and 4% benzamidine hydrochloride added. Crystals were obtained by vapour diffusion at 4°C, for 40 - 60 days. The benzamidine provided a surface for the initiation of bacteriorhodopsin crystallisation in the orthorhombic form; this had proved difficult to obtain as bacteriorhodopsin persistently formed pseudohexagonal crystals. The pseudohexagonal crystals were found to form disordered crystalline arrays resulting in poor diffraction data. The formation of orthorhombic crystals provided high resolution diffraction data.

Following work on bacteriorhodopsin Michel, (1982) crystallised the photosynthetic reaction centre from the bacterium *Rhodopseudomonas viridis*. Bacterial membranes were broken up by sonification and subjected to a sucrose density gradient. The photosynthetic membranes formed a broad band at approximately 35% sucrose. The membranes were then solubilized in the detergent *N,N*-dodecyldimethylamine *N*-oxide and pure reaction centres were obtained in a single step purification, using molecular sieve chromatography. Crystals were obtained by vapour diffusion under high salt conditions and grew to an appropriate size within three weeks. The crystals were found

to diffract X-rays to beyond 2.5 Å resolution. The crystallised reaction centres were demonstrated to be photochemically active by Zinth *et al.,* (1983). The X-ray diffraction data was finally solved and the reaction centre structure was determined by Deisenhofer *et al.,* (1984, 1985) to a resolution of 3 Å. The high quality of the electron density map allowed for the unambiguous chain tracing, even in the absence of amino acid information. This study demonstrated that at least one membrane protein could be crystallised and its 3-dimensional structure solved.

A novel method of crystallisation was conceived by Ostermeier *et al.,* (1997) to overcome the difficulties in crystallising a hydrophobic transmembrane protein. The protein used was Cytochrome C oxidase sourced from the soil bacterium *Paracoccus denitrificans.* Cytochrome C oxidase is a transmembrane helical protein which catalyses the final electron transfer step to molecular oxygen, while translocating protons across the membrane. Ostermeier *et al.,* (1997) generated anti-cytochrome c oxidase monoclonal antibodies. The monoclonal antibodies were over-expressed in the bacterium *E. coli,* allowing for the addition of a biotin tag to the protein sequence. Following purification of the Cytochrome C oxidase the monoclonal antibodies were used to promote crystallisation of the protein. The monoclonal antibody Fv fragments were thought to increase the size of the polar surface of the protein, thereby increasing the chances of obtaining highly ordered crystals (crystallisation was thought to have initiated from the polar region). Iwata *et al.,* (1995) originally diffracted a crystal of the four subunits of cytochrome c oxidase to a resolution of 2.8 Å. In an attempt to refine the crystal information further Ostermeier *et al.,* (1997) diffracted a crystal of cytochrome c oxidase, subunits I and II to a resolution of 2.5 Å. It seems likely that this technique could also be used to crystallise other membrane bound proteins such as the glucose transporter.

Walz *et al.,* (1994) have purified the membrane protein aquaporin 1 which is a specialised water pore found in the plasma membrane of human erythrocytes. Human erythrocytes were alkali stripped and solubilized in Triton X-100. Following filtration, samples were loaded onto a POROS Q/F column. Samples were eluted with a sodium chloride gradient in the presence of 0.1% Triton X-100. Octyl glucopyranoside and purified *E. coli* lipids were then added to the peak elution fraction, which corresponded to pure aquaporin. 2-dimensional crystals of aquaporin were produced and subjected to

cryo-electron microscopy (the microscope stage being liquid helium cooled to 4.2 K). Walz *et al.,* (1997) have calculated the structure of the 2-dimensional crystals to a resolution of 6 Å. From sequence analysis the aquaporin molecule was predicted to contain six transmembrane helices. This was borne out during analysis and fitted all the obtained data, which determined the structure to contain six tilted helices with a right-handed twist. The right-handed twist is a feature commonly observed in soluble proteins. Aquaporin was known to form a homotetramer when reconstituted into lipid vesicles, the cytoplasmic side of the tetramer was found to protrude further from the membrane in comparison to the extracellular side. The C-terminus has been identified as the most prominent cytosolic protrusion. Furthermore, near and far ultraviolet circular dichroism analysis of a homologous protein to aquaporin, the MIP26 protein, predicts that 20% of the protein is β-structure. However, higher resolution information is required to determine the precise structure of the transmembrane spanning helices. Higher resolution information will aid in an understanding of the mechanism by which the aquaporin molecule is capable of selectively transporting water across the human erythrocyte membrane.

Polyhistidine tags have also been used successfully with soluble proteins to purify and produce high quality crystals for X-ray diffraction studies. Narayana *et al.,* (1997) attached six contiguous histidine residues at the N-terminal end of the mouse cAMP-dependent protein kinase (cAPK) catalytic subunit. The protein was purified on an immobilised nickel column and separate isoforms of the recombinant catalytic subunit were isolated on a Mono-S column. Isoform II, phosphorylated at three sites was taken for crystallisation, which took 6 weeks at 4°C. The crystals diffracted to a resolution of 2.2 Å, allowing the complete determination of the protein structure.

Experiments have shown that membrane proteins can be purified and then crystallised. X-ray crystallographic studies on the GLUT1 protein should therefore be possible. Boulter and Wang, (personal communication, 1997) are close to starting studies for possible crystallisation conditions of human erythrocyte GLUT1. Boulter and Wang, (personal communication, 1997) have managed to purify GLUT1 in a stable monodisperse, detergent solubilized form, which exhibits cytochalasin B binding in solution. The GLUT1 protein was solubilized in a maltoside detergent over a period of five weeks. Co-purifying lipids and enzymic deglycosylation of GLUT1 have been

examined and crystallisation experiments are now in progress. However, because this method utilises native GLUT1 protein, mutations within the protein cannot be introduced. This may hinder the progress of crystallisation studies and will prevent the investigation of mutational effects.

1.27 Aims of the Project

- An Investigation of Glucose Transporter Structure and Function

At the onset of this project in 1994 no other group had attempted to express a polyhistidine tag on the N-terminal end of the GLUT1 glucose transporter with the intention of purifying the protein on a chelating nickel Sepharose column. At that time the technique of metal chelate chromatography on recombinant membrane bound proteins was in its infancy and only a few groups had used the technique for this purpose. One such group was Waeber *et al.,* (1993). They successfully purified the *E. coli* glucose transporter by expressing a polyhistidine tag on the C-terminus of the protein. Waeber *et al.,* (1993) have also had success in purifying the *E. coli* mannose transporter using a polyhistidine tag. Furthermore, Loddenkötter *et al.,* (1993) have polyhistidine tagged the chloroplast triose phosphate-phosphate translocator and purified it using an immobilised metal ion liquid chromatography system. The evidence suggests that it is possible to purify membrane bound proteins using a polyhistidine tag purification system.

By 1994, the expression of human and rabbit GLUT1 protein in *Spodoptera frugiperda* cells had been characterised by Yi *et al.,* (1992) and Cope *et al.,* (1994), respectively. The expression of human GLUT1 in *E. coli* had been examined by Sarkar *et al.,* (1988) and Kasahara and Kasahara, (1996) were soon to look at the expression of rat GLUT1 in *Saccharomyces cerevisiae*. However, following the observations made by Asano *et al.,* (1993) of glycosylation deficient GLUT1 it was decided that a system expressing glycosylated protein was required. The current project was initiated to investigate the expression and properties of two novel glucose transporter constructs in *Spodoptera frugiperda* cells. The constructs expressed an N-terminal polyhistidine tag on: a) The rabbit GLUT1 glucose transporter and b) A C-terminal half construct of the Rabbit GLUT1 glucose transporter (transmembrane regions 7 - 12 according to the

model proposed by Mueckler *et al.,* (1985)). Protein purification was undertaken using the technique of immobilised metal ion affinity chromatography. During purification a lipid presence was maintained as it was reported by Ambudkar and Maloney, (1996) that complete delipidation of the anion exchange transporter deactivated the protein. Following studies by Tefft *et al.,* (1986) and Connolly *et al.,* (1985a&b) a balanced lipid composition was chosen as it had been determined to be important for transporter function.

During the course of the present study Weinglass and Baldwin, (1996) published a short report on the attempted purification of a C-terminally polyhistidine tagged human GLUT1 construct. The construct had been expressed in insect cells. Further reference to the similarities and differences of the work carried out by Weinglass and Baldwin, (1996) will be made in the final discussion.

C-terminal half constructs of the GLUT1 glucose transporter were studied for glucose analogue binding activity with and without the addition of a polyhistidine tag. It was theorised that a smaller construct may be more suitable for crystallisation and X-ray crystallographic analysis, forming a more compact simpler crystal structure. The properties of these mutants were also considered to be important. Photolabelling studies on the C-terminal half constructs were carried out in an attempt to determine the conformation of the constructs. Wu *et al.,* (1996) have studied C-terminal constructs of the lactose permease proton symporter. The lactose permease is a very similar protein to the glucose transporter, it has 12 transmembrane helices with both the N and C-terminal ends on the cytosolic side of the membrane. Wu *et al.,* (1996) have observed that a C-terminal construct, with an additional 5 amino acids, was capable of ligand binding. The glucose transporter C-terminal construct was examined to determine if it had similar properties to the lactose permease C-terminal construct.

Mori *et al.,* (1994) studied a tyrosine 293 to isoleucine mutation. This mutation caused the construct to become locked in an outward facing conformation. A construct which was conformationally locked in either an inward or outward conformation may be more suitable for structure determination by crystallography. A locked transporter would not undergo continuous conformational change and may make the formation of an ordered crystal structure more likely. If the deletion of the N-terminal portion of the

glucose transporter caused the glucose transporter to become locked in one conformation then this would also be a useful construct to purify.

The thesis also investigates the effect of a novel set of GLUT1 point mutations. The point mutations were made in the C-terminal tail of human GLUT1. The mutated GLUT1 cDNA was expressed and tested in CHO-K1 cells. This follows on from work undertaken by Katagiri *et al.,* (1992) and Muraoka *et al.,* (1995), where both groups undertook deletion analysis studies on the C-terminal tail of GLUT1. These studies indicated that the C-terminal tail was important for the correct function of the glucose transporter. Both Carruthers and Helgerson, (1989) and Shi *et al.,* (1995) have carried out studies that suggest the function of the glucose transporter can be modified by the binding of intracellular molecules to the C-terminal region, possibly the C-terminal tail. These studies also suggest that this region is important in controlling the function of the glucose transporter.

Targeting of the expressed constructs was examined using the technique of confocal microscopy. Experiments were undertaken to determine if there were any differences on the addition of a polyhistidine tag.

It is hoped that this thesis will provide information on purified GLUT1 stability and its properties in detergent that will be important to consider for future 3-dimensional crystallographic analysis of the GLUT1 glucose transporter.

Methods

2.0 Materials and Methods

Materials

2.1 General Laboratory Chemicals

Unless otherwise indicated, general laboratory chemicals and solvents were obtained from the Sigma-Aldrich Company Ltd. (Poole, Dorset), Bio-Rad Laboratories Ltd. (Hemel Hempstead, Hertfordshire), Fisons Scientific UK Ltd. (Loughborough, Leics.), or BDH Laboratory Supplies (Merck Ltd., Poole, Dorset). Radiolabelled 2-Deoxyglucose (40 Ci / mmol), ^{35}S-dATP (1000 Ci / mmol), γ-^{32}P ATP (3000 Ci / mmol) and Cytochalasin B (18.1 Ci / mmol) were supplied by Amersham International plc (Little Chalfont, Buckinghamshire). The photolabel 2-*N*-4-(1-azi-2,2,2-trifluoroethyl)benzoyl-1,3-[^{3}H]bis-(D-mannos-4-yloxy)-2-propylamine (ATB-[2-^{3}H]BMPA) (~10 Ci / mmol) was synthesised by Prof. Geoffrey Holman (University of Bath, Bath) (Clark and Holman, 1990). Optiphase Safe™ scintillation fluid was from Fisons chemicals (Loughborough, Leics.). Thesit® ($C_{12}E_9$) and Zwittergent® 3-12 (SB12) were supplied by Boehringer Mannheim UK Ltd. (Lewes, East Sussex) and Octyl-β-D-glucopyranoside (Octyl glucoside) was from Alexis Corporation (Bingham, Nottingham). The protease inhibitor 4-(2-aminoethyl)benzenesulfonylfluoride (AEBSF) was supplied by Calbiochem-Novabiochem (UK) Ltd. (Nottingham). X-ray film was supplied by Fuji Photo Film Co. Ltd. (Japan).

2.2 CHO-K1 Cell Culture

Chinese hamster ovary (CHO-K1) clones expressing mutated GLUT1 were kindly provided by Muraoka (Kobe University, Japan). Cryogenic vials (2.0 ml) were from Corning Costar Corporation (Cambridge, MA). Hams F12 culture medium was from ICN Biomedicals Ltd. (Thame, Oxfordshire). Foetal Bovine Serum (FBS), Geneticin® (G418 Sulphate), DMSO, 1× Trypsin (0.25% (1:250), prepared in GIBCO solution A), Nunclon™ cell culture flasks and culture dishes were supplied by

GibcoBRL Life Technologies Ltd. (Paisley, Renfrewshire). Phosphate Buffered Saline (PBS) (Dulbecco 'A') was supplied by Oxoid (Unipath Ltd., Basingstoke, Hampshire). All other materials were supplied by Sigma.

2.3 Insect Cell Culture

Spodoptera frugiperda ovarian cells (Sf9 cells) and *Trichoplusia ni* egg cells (Highfive™ Cells) were kindly provided by Dr Adrian Wolstenholme (University of Bath, Bath, UK). TC100 insect cell medium was from the Sigma-Aldrich Company Ltd. (Poole, Dorset). Culture flasks and Foetal Bovine Serum (FBS) were supplied by GibcoBRL Life Technologies Ltd. (Paisley, Renfrewshire). Cryogenic vials (2.0 ml) were from Corning Costar Corporation (Cambridge, MA). All other materials were from Sigma.

2.4 Molecular Biology Materials and Chemicals

T4 DNA Ligase, calf intestinal phosphatase (CIP) and all restriction enzymes were supplied by New England Biolabs (Hitchin, Hertfordshire). Baculovirus expression vectors and linearised AcMNPV DNA were from Invitrogen® Corporation (Leek, The Netherlands). DNA binding columns for plasmid purification were supplied by Qiagen Ltd. (Crawley, West Sussex). Agar was supplied by Difco Labs (Detroit, Michigan, USA) and LB Broth base, (Luria broth base (10 g / l enzymatic casein digest, 5 g / l yeast extract and 5 g / l of NaCl)) was from the Sigma-Aldrich Company Ltd. (Poole, Dorset). 5-bromo-4-chloro-3-indolyl-β-D-thiogalactoside (X-gal) was supplied by Calbiochem-Novabiochem (UK) Ltd. (Nottingham). 1 Kb DNA ladder, Agarose and low melting point agarose was obtained from GibcoBRL Life Technologies Ltd. (Paisley, Renfrewshire). γ-^{32}P ATP was supplied by Amersham International Plc., all other materials were supplied by Sigma.

2.5 Bacterial strains

Two bacterial strains were used, Epicurian Coli® SURE®, from Stratagene Ltd. and TOP10 from Invitrogen® Corporation (Leek, The Netherlands). The bacterial phenotypes are listed below:

Epicurian Coli® SURE®: E14-(*mcr*A), D(*mcr*CB-*hsd*SMR-*mrr*)*171*, *end*A1, *sup*E44, *thi*-1, *gyr*A96, *rel*A1, *lac*, *rec*B, *rec*J, *sbc*C, *umu*C::*Tn5* (kan^r), *uvr*C, [F' *pro*AB, *lac*I^q ZDM15, Tn10, (tet^r)].

TOP10: F' *mcr*A (*lac*I^q, Tn10(Tet^r)) *mcr*A D(*mrr-hsd*RMS-*mcr*BC) f80*lac*ZDM15 D*lac*X74, *deo*R, *rec*A1, *ara*D139, D(*ara-leu*)7697, *gal*U, *gal*K, *rps*L, *end*A1, *nup*G.

2.6 cDNA and Baculoviruses

Rabbit GLUT1 cDNA was kindly provided by Dr Yoshitomo Oka (Tokyo, Japan). Baculoviruses expressing GLUT1 and C-TERM were kindly provided by Dr Diane Cope (University of Glasgow, Glasgow), as was the HIS-C-TERM DNA.

2.7 Antibodies

GLUT1 rabbit antiserum used for immunoblot analysis was obtained from East Acres Biologicals (Southbridge, Ma, USA). The antibody was raised against a peptide within the carboxy terminus of the rat brain glucose transporter. The antibody was used at a final dilution of 1:4000 in TBS Tween containing 1% BSA.

GLUT1 rabbit antiserum used for immunoprecipitation was kindly provided by Dr Samuel Cushman (National Institutes of Health, Bethesda, USA). The antiserum was raised against a synthetic peptide corresponding to residues 480 - 492 in the C-terminal portion of the molecule.

2.8 Protease Inhibitors

Antipain, aprotinin, pepstatin A and leupeptin (from Sigma) were made as a 500 µg / ml stock and added to a final concentration of 1 µg / ml.

AEBSF (from Calbiochem) was made as a 100 mM stock and used at a final concentration of 100 µM.

Throughout this thesis, the phrase 'protease inhibitors' is defined as the addition of antipain, aprotinin, pepstatin A, leupeptin and AEBSF (at the above final concentrations) to the required buffer.

Photolabelling was carried out using a Rayonett RPR-100 photoreactor containing RPR-3000 lamps. Electrophoresis was performed using either the Protean® II xi slab cell Bio-Rad system or the Mini Atto System (Atto Corporation). Protein transfer was performed using the Multiphor II Nova Blot electrophoretic transfer unit (Pharmacia Biotech).

2.9 General Buffers and Solutions

All buffers were made up using either double distilled or distilled water and are listed at their final concentrations.

Krebs Ringer Hepes

10 mM Hepes
4.7 mM KCl
1.25 mM $CaCl_2$
1.25 mM $MgSO_4$
136 mM NaCl
pH 7.4

TES

10 mM Tris
5 mM EDTA
250 mM Sucrose
pH 7.2

Tris buffered saline (TBS)

10 mM Tris

154 mM NaCl

pH 7.4

Sodium phosphate buffer

5 mM Na_2HPO_4

pH 7.4

Phosphate buffered saline (PBS)

12.5 mM $Na_2HPO_4 \cdot 12H_2O$

154 mM NaCl

pH 7.2

Electrophoresis Buffers:

Resolving buffer

1.5 M Tris

0.4% (w/v) SDS

pH 8.8

Stacking buffer

0.5 M Tris

0.4% (w/v) SDS

pH 6.8

Sample buffer

115 mM Tris

10% (v/v) Glycerol

2% (w/v) SDS

5% (v/v) β–Mercaptoethanol

4 μg / ml (w/v) Bromophenol Blue

pH 6.8

Running buffer

25 mM Tris

192 mM Glycine

0.1% (w/v) SDS

pH 8.3

BCA (Bichinchoninic acid) Protein Assay

Reagent A

1% (w/v) bicinchoninic acid

2% (w/v) sodium carbonate

0.16% (w/v) sodium tartrate

0.4% (w/v) sodium hydroxide

0.95% (w/v) sodium bicarbonate

Reagent B

4% (w/v) copper sulphate

HiTrap and DEAE Cellulose Column Buffers and Solutions

IMAC 0

10 mM Tris
0.5 M NaCl
10% (v/v) Glycerol

1 µg / ml Protease inhibitors
pH 7.4

IMAC 200

10 mM Tris
0.5 M NaCl
10% (v/v) Glycerol
200 mM Imidazole

1 µg / ml Protease inhibitors
pH 7.4

Solubilization buffer

10 mM Hepes
20% (v/v) Glycerol
250 mM Sodium Chloride
1.5 mg / ml Lipids
1.5% (w/v) Octyl glucoside
20 mM Imidazole

1 µg / ml Protease inhibitors
pH 7.9

Wash buffer

10 mM Hepes
20% (v/v) Glycerol
250 mM Sodium Chloride
1.5 mg / ml Lipids
1% (w/v) Octyl glucoside
20 mM Imidazole

1 µg / ml Protease inhibitors
pH 7.9

Elution buffer

10 mM Hepes
20% Glycerol
250 mM Sodium Chloride
1.5 mg / ml Lipids
1% (w/v) Octyl glucoside
300 mM Imidazole

1 µg / ml Protease inhibitors
pH 7.9

Dialysis buffer

100 mM Sodium Chloride
1 mM EDTA
50 mM Tris
pH 7.4

Nickel sulphate

0.1 M Nickel Sulphate

Molecular Biology Solutions

TBE
2 mM EDTA
100 mM Tris
83 mM Boric acid

Agarose gel loading buffer
5% (v/v) Glycerol
10 mM EDTA
0.01% (w/v) Bromophenol blue

Hybridisation buffer
10 mM Tris
100 mM NaCl
5 mM EDTA
pH 7.5

TE Buffer
10 mM Tris
1 mM EDTA
pH 8.0

Miniprep solutions:

Plasmid Prep Mix
25 mM Tris pH 8.0
10 mM EDTA
15% (w/v) sucrose
2 mg / ml Lysozyme

Lysis buffer
0.2 M NaOH
1% (w/v) SDS

Antibiotics

Ampicillin was used in liquid culture at 100 μg / ml. In order to reduce satellite formation on agar plates, ampicillin was used in conjunction with methicillin at the following concentrations: Ampicillin 20 μg / ml, Methicillin 80 μg / ml.

Ethidium bromide

A 10 mg / ml ethidium bromide solution was made in double distilled water and filter sterilised using a Sartorius Minisart 0.2 μM filter (Sartorius, Göttingen, Germany). Ethidium bromide was stored in a foil wrapped bottle at room temperature.

Methods

2.10 Chinese Hamster Ovary (CHO-K1) Cell Culture

Cell Culture

Chinese Hamster ovary cells were routinely cultured in Hams f12 medium, supplemented with 10% (v/v) foetal bovine serum (Myoclone Super Plus), 1% (v/v) L-glutamine (200 mM in tissue culture grade water) and 2% (v/v) penicillin / streptomycin solution (5000 units penicillin and 5 mg streptomycin per ml in 0.9% (w/v) NaCl). Geneticin (G418) sulphate was included in the culture medium at a concentration of 150 mg / 500 ml, to select for growth of transfected cells. Foetal bovine serum was heat inactivated by incubation at 56°C for 30 minutes prior to use. CHO-K1 cells were maintained at 37°C in a 5% CO_2 humidified atmosphere.

Passaging Cells

Cells were passaged on reaching confluence (approximately every 3-4 days, depending of seeding density). Media and PBS were pre-warmed to 37°C before use. Cells were first washed using 3 ml of sterile PBS and then freed from the dish matrix by the addition of 1 ml of trypsin (2.5 g / litre of trypsin in GIBCO solution A) and 1 ml of PBS. Cells were trypsinated for 5 minutes followed by the addition of 10 ml of culture medium. Cells were pelleted at 350 g in a bench top centrifuge and resuspended in culture medium. Cells were counted and seeded at 100,000 cells per 100 mm dish.

Cryogenic storage

Confluent cells were washed, trypsin treated and suspended in culture medium. Cells were centrifuged at 350 g in a bench top centrifuge and resuspended in cryogenic storage medium (10% (v/v) dimethyl sulfoxide (DMSO) in foetal bovine serum). Aliquots of 2 ml were taken, placed in to cryogenic vials, and the cryogenic vials placed in a liquid nitrogen vapour phase cooler for 24 h. Cells were then fully immersed in liquid nitrogen for long term storage.

2.11 CHO-K1 Cell Glucose Transport Assay

Cells were grown to confluence in 35 mm dishes and then harvested for use in a 2-deoxyglucose transport assay. The culture medium was aspirated (into 10% (v/v) bleach) and the cells washed three times with 2 ml of Kreb-Ringer Hepes buffer at 37°C (136 mM NaCl, 4.7 mM KCl, 1.25 mM $CaCl_2$, 1.25 mM $MgSO_4$, 10 mM Hepes buffer, pH 7.4). The cells were incubated in 450 µl of Kreb-Ringer Hepes buffer at 37°C until assayed.

Assays were performed by the addition of 50 µl Kreb-Ringer Hepes buffer containing 0.3 µCi 2-deoxy-D-[2,6-^{3}H]glucose and 2-deoxy-D-glucose, to a final concentration of between 0.05 and 10 mM. Cells were assayed for 1 minute at 37°C and the assay terminated by washing four times with ice cold phosphate buffered saline (PBS (12.5 mM $Na_2HPO_4 \cdot 12H_2O$, 154 mM NaCl, pH 7.2)). The cells were removed from the assay dish by the addition of 500 µl of 0.1 M NaOH and mixed with 7 ml of scintillant (Optiphase Safe™). The samples were then counted in a Packard 1500 TRI-CARB liquid scintillation counter. The data obtained was fitted to the equation $Y = Vmax \times X / (Km + X)$ using GraphPad PRISM™ for the PC; Vmax represents the maximum rate of transport and Km represents the concentration of ligand required to reach half maximal binding.

2.12 Insect Cell Culture

Cell Culture

Spodoptera frugiperda ovarian cells (Sf9 cells) and *Trichoplusia ni* egg cells (Highfive™ Cells) were routinely cultured in TC100 medium, supplemented with 10% (v/v) foetal bovine serum and 2% (v/v) penicillin / streptomycin solution (5000 units penicillin and 5 mg streptomycin per ml in 0.9% (w/v) NaCl). Foetal bovine serum was heat inactivated by incubation at 56°C for 30 minutes prior to use. Insect cells were incubated at 28°C, in both monolayer cultures and suspension cultures. Stock cultures were typically maintained in 75 cm^2 flasks as monolayers.

Passaging Cells

Cells were passaged on reaching confluence (approximately every 4-5 days, depending of cell type and seeding density. Highfive™ cells were observed to have a slower growth rate than Sf9 cells). TC100 Media was pre-warmed to 28°C before use. Cells were first examined to ensure they were healthy and uncontaminated. Monolayer cells, were washed using 10 ml of supplemented TC100 medium and then suspended in 20 ml of supplemented TC100 medium. Cells were freed of the supporting matrix by washing the cell monolayer with medium and were seeded in fresh 75 cm^2 flasks at 500,000 - 1,000,000 cells / flask.

Cryogenic storage

Near confluent cells were washed and suspended in supplemented TC100 medium. Cells were checked for density and high viability (about 90% viable). Cells were centrifuged at 350 g in a bench top centrifuge and resuspended in cryogenic storage medium (TC100, 10% foetal bovine serum, 10% (v/v) DMSO at 4°C) at a density of 1.5 x 10^6 cells / ml. Aliquots of 2 ml were taken and placed in to cryogenic vials, which were then placed in a liquid nitrogen vapour phase cooler for 24 h. Cells intended for long term storage were immersed in liquid nitrogen.

2.13 Molecular Biology Methods

Many of the techniques described can be found in the laboratory manual: 'Molecular Cloning, A Laboratory Manual' (Sambrook *et al.* 2nd Edition, Cold Spring Harbor Laboratory Press, 1989), unless otherwise stated.

2.13 Growth and Maintenance of Bacterial Cultures

Short term storage of bacterial strains was at 4°C on Lennox L agar. Long term storage was at -80°C, in liquid culture, containing 40% (v/v) glycerol. Ampicillin resistant colonies were selected using 20 µg of ampicillin / ml and 80 µg of methicillin / ml.

2.14 Ethanol Precipitation

Ref: Sambrook *et al.*, (1989).

0.1 volumes (ie. to 1 ml add 100 µl) of 3 M sodium acetate, pH 5.2 and 2 volumes of 100% ethanol at -20°C were added to the DNA solution and mixed thoroughly. The mixture was incubated for 20 minutes, at -20°C and centrifuged for 20 minutes at 13,400 g in a bench top microcentrifuge (Micro Centaur). The supernatant was discarded and the pellet washed in 70% ethanol (-20°C). Following removal of the 70% ethanol the pellet was air dried at room temperature and resuspended in double distilled water. For the precipitation of small amounts of DNA, 1 µl of 20 mg / ml glycogen was added, as a carrier, at the start of the protocol.

2.15 Ammonium Acetate / Iso-propanol DNA Precipitation

Ref: Sambrook *et al.*, (1989).

Sufficient EDTA was added to the DNA solution to chelate any divalent cations present. 1µl of 20 mg / ml glycogen (Boehringer Mannheim, special quality for molecular biology) was added as a carrier, followed by 0.4 volumes of 5M ammonium acetate. Two volumes of propan-2-ol were added to the DNA solution and mixed thoroughly. The mixture was incubated at room temperature for 10 minutes and the DNA pelleted in a microcentrifuge at 13,400 g for 10 minutes. The supernatant was discarded and the pellet washed in 70% ethanol (at -20°C). Following removal of the 70% ethanol the pellet was air dried at room temperature and resuspended in double distilled water.

2.16 Small Scale (Miniature) Plasmid DNA Preparations (Plasmid Miniprep)

Ref: Sambrook *et al.*, (1989). Adapted from the method of Birnboim and Doly, (1979).

10 ml of L-broth with ampicillin (100 µg / ml) were inoculated from a single bacterial colony. The inoculum was incubated at 37°C for 16 h at 200 rpm on a rotary shaker. Following incubation, 2 ml of culture were transferred to a microcentrifuge tube and pelleted by centrifugation at 13,400 g for 5 minutes. The supernatant was discarded

and the pellet resuspended in 40 µl of ice cold plasmid prep mix (25 mM Tris, 10 mM EDTA, 15% (w/v) sucrose, 2 mg / ml lysozyme, pH 8.0). Following a 5 minute incubation on ice, 80 µl of 0.2 M NaOH and 1% (w/v) SDS were added , mixed and left on ice for 5 minutes. 40 µl of 3 M potassium acetate was added, gently mixed and incubated on ice for 5 minutes. The mixture was centrifuged for 5 minutes at 13,400 g and the supernatant removed to a clean microcentrifuge tube containing 300 µl of 100% ethanol at -20°C. The supernatant was thoroughly mixed by tube inversion and placed at -20°C for 20 minutes. The mixture was centrifuged at 13,400 g for 10 minutes and the supernatant discarded. The pellet was washed in 200 µl of 70% ethanol (-20°C) and allowed to air dry at room temperature. The pellet was resuspended in 30 µl of TE buffer, pH 8.0, followed by the addition of 10 µl of 8 M LiCl. The mixture was left on ice for 1 h and then pelleted in a microcentrifuge for 5 minutes at 13,400 g. The supernatant was transferred to a clean microcentrifuge tube containing 60 µl of TE buffer, pH 8.0. 200 µl of 100% ethanol (-20°C) was added to the supernatant, mixed by tube inversion and incubated at -20°C for 20 minutes. The mixture was centrifuged at 13,400 g for 10 minutes and the supernatant discarded. The pellet was washed in 200 µl of 70% ethanol (-20°C) and allowed to air dry at room temperature. Finally the resulting plasmid DNA was resuspended in 25 µl of distilled water.

2.17 Small Scale Plasmid DNA Preparations Qiagen

Ref: Qiagen Plasmid Handbook.

Qiagen miniprep spin columns were used to prepare high quality plasmid DNA for sequencing. Plasmid DNA was prepared as described in the manufacturer's protocol (Qiagen Ltd. UK, catalogue number 27104). 10 ml of L-broth with ampicillin (100 µg / ml) were inoculated from a single bacterial colony. The inoculum was incubated at 37°C for 16 h at 200 rpm on a rotary shaker. Following incubation, 2 ml of the culture was transferred to a microcentrifuge tube and pelleted by centrifugation at 13,400 g for 5 minutes. The bacterial pellet was resuspended in 250 µl of buffer P1 (100 µg / ml RNase A, 50 mM Tris-HCl, 10 mM EDTA, pH 8.0 at 4°C). 250 µl of buffer P2 (200 mM NaOH, 1% SDS at room temperature) were added and the mixture was incubated on ice for 5 minutes. 350 µl of buffer N3 at 4°C was added, incubated on ice for 5 minutes and

centrifuged for 10 minutes at 13,400 g. The supernatant was taken and applied to a 2 ml Qiaprep mini spin column. The spin column was centrifuged for 1 minute at 13,400 g and the flow-through discarded. The column was then washed with 750 µl of buffer PB and centrifuged for 1 minute at 13,400 g and the flow-through discarded. A second column wash was performed using 750 µl of buffer PE, the column was then centrifuged for 1 minute at 13,400 g and the flow-through discarded. Plasmid DNA was finally eluted from the column with 100 µl of double distilled water.

2.18 Large Scale Plasmid DNA Preparations Qiagen

Ref: Qiagen Plasmid Handbook.

Large scale preparations (500 µg) of plasmid DNA were produced using a Qiagen Maxi DNA binding column as described in the manufacturer's protocol (Qiagen Ltd. UK, catalogue number 12162). 250 ml of culture media was inoculated with the appropriate bacterial colony and incubated for 16 h at 37°C on a rotary shaker (200 rpm). Bacterial cells were pelleted by centrifugation at 4°C for 15 minutes at 6,000 g using a Sorvall high speed centrifuge. The bacterial pellet was resuspended in 10 ml of buffer P1 (100 µg / ml RNase A, 50 mM Tris-HCl, 10 mM EDTA, pH 8.0 at 4°C) and mixed with 10 ml of buffer P2 (200 mM NaOH, 1% SDS at room temperature). The mixture was incubated at room temperature for 5 minutes. 10 ml of buffer P3 (3 M potassium acetate, pH 5.5 at 4°C) was added to the mixture and incubated on ice for 20 minutes. The cell lysate was then centrifuged at 4°C for 30 minutes at 30,000 g and the supernatant removed. A Qiagen maxi column was equilibrated with 10 ml of buffer QBT (750 mM NaCl, 50 mM Mops, 15% ethanol, 0.15% Triton X-100, pH 7.0) at room temperature and the (cell lysate) supernatant applied to the column. The column was then washed twice with 30 ml of buffer QC (1.0 M NaCl, 50 mM Mops, 15% ethanol, pH 7.0 at room temperature) and eluted with 15 ml of buffer QF (1.25 M NaCl, 50 mM Tris-HCl, 15% ethanol, pH 8.5 at room temperature). The DNA was precipitated using 0.7 volumes of iso-propanol (at room temperature) and centrifuged at 15,000 g for 30 minutes at 4°C. The supernatant was carefully removed and the pellet washed in 15 ml of 70% ethanol (at -20°C). The pellet was air dried and resuspended in 500 µl of double distilled water.

2.19 Restriction Endonuclease Digestion of DNA

Ref: Fuchs, R. and Blakeskey, R. (1983). Up-to-date information was taken from the New England Biolabs catalogue.

Restriction digests were carried out according to the manufacturer's recommended reaction conditions. Typically this was incubation at 37°C for 90 minutes in the appropriate reaction buffer. Digestion was confirmed by running a sample on an 0.8% TBE buffered agarose gel. Restriction enzymes were removed from the digested DNA using ammonium acetate / iso-propanol precipitation.

2.20 Agarose Gel Electrophoresis

Plasmid DNA was electrophoresed in 0.8% agarose gels. Gels were made and run in Tris-borate (TBE) buffer (100 mM Tris, 100 mM boric acid, 2 mM EDTA, pH 8.3) containing ethidium bromide at 1 μg / ml. Samples were mixed with loading buffer (final concentration, 5% (v/v) glycerol, 10 mM EDTA, 0.01% (w/v) Bromophenol blue), loaded and electrophoresed at 50 V / cm (50 mA). Bands were visualised under an ultraviolet transilluminator, and images captured using a Polaroid instant camera. Gel background was reduced by soaking the gel in TBE buffer for 4 h at room temperature.

2.21 DNA Extraction from Agarose Gels

Ref: Sambrook *et al.*, (1989).

DNA for gel purification was restriction digested and electrophoresed on a 0.5% low melting point agarose gel. The agarose gel was made in TBE buffer, loaded and electrophoresed at 4°C and at 25 V / cm. The agarose gel was run until the appropriate band was separated from any other contaminating bands. The band was visualised under UV light and identified using molecular weight markers. The appropriate band was then excised from the gel using a fresh scalpel blade.

The agarose containing the required band was cut, crushed and soaked on ice for 20 minutes in 15 ml of TE buffer (10 mM Tris-HCl, 1 mM EDTA, pH 8.0). The gel

matrix was removed by centrifugation through a glass fibre filter. The sample volume was reduced by butan-1-ol extraction. An equal volume of butan-1-ol was added to the sample, mixed, allowed to phase separate and the organic (top) phase was removed and discarded. This procedure was repeated until a sample volume of about 500 µl was obtained. The sample was phenol extracted by the addition of an equal volume of phenol / chloroform, vortexed and phase separated by centrifugation for 2 minutes at 6,700 g. The upper, aqueous phase was then removed to a clean microcentrifuge tube and the DNA was ethanol precipitated. Finally, the DNA fragment was analysed on an agarose gel.

2.22 Ligation

Ref: Sambrook *et al.*, (1989).

Vector DNA was treated with calf intestinal phosphatase (CIP) to prevent religation of the vector without insert. CIP buffer (50 mM NaCl, 10 mM Tris-HCl, 10 mM $MgCl_2$, 1 mM dithiothreitol, pH 7.9) was added to the vector DNA and an appropriate amount of CIP added (1 unit CIP per pmol DNA ends). The mixture was incubated for 60 minutes at 37°C. CIP was inactivated by incubation at 75°C for 10 minutes and removed by ammonium acetate / iso-propanol precipitation.

Vector and insert DNA were mixed (molar ration of 1:3) and T4 DNA ligase buffer added (50 mM Tris-HCl, 10 mM $MgCl_2$, 10 mM dithiothreitol, 1 mM ATP, 25 µg / ml BSA, pH 7.5). The mixture was incubated at 16°C for 16 h. The ligated DNA was either stored at -20°C or used immediately for bacterial transformation.

2.23 Oligonucleotide End Labelling

Ref: Sambrook *et al.*, (1989).

The length of manufactured oligonucleotides were compared by radiolabelling the oligonucleotide with γ-^{32}P ATP using T4 polynucleotide kinase. The radiolabelled material was analysed on a 15% polyacrylamide gel.

1 µg of oligonucleotide was mixed with 10 units of T4 polynucleotide kinase, 1 µCi γ-^{32}P ATP (3000 Ci / mmol) in T4 polynucleotide kinase buffer (70 mM Tris-HCl, 10 mM $MgCl_2$, 5 mM dithiothreitol, pH 7.6). The mixture was incubated for 30 minutes at 37°C. A 15% polyacrylamide sequencing gel was prepared, the samples loaded and run for 2 h at 1500 V, 40 mA. The gel was visualised by autoradiography.

2.24 Oligonucleotide Mutagenesis

Ref: Sambrook *et al.*, (1989).

Oligonucleotides were manufactured by Seven Biotech Ltd. (Kidderminster, Worcestershire, UK.) and VHBio (Gosforth, Newcastle-upon-Tyne). To anneal complementary oligonucleotides, equal amounts were mixed in hybridisation buffer (10 mM Tris, 100 mM NaCl, 5 mM EDTA, pH 7.5) The melting temperatures of the oligonucleotides were calculated according to the following equation:

Melting temperature in °C = 4°C x G / C + 2°C x A / T

Where G = Guanine, C = Cytosine, A = Adenine, T = Thymine.

The oligonucleotide mixture was heated to the melting temperature and allowed to cool slowly, final cooling was performed on ice. Unphosphorylated linkers were used in excess during ligation, in order to increase the probability of obtaining mutated host DNA.

2.25 Preparation and Transformation of Bacterial Cells

1 ml of an overnight 10 ml L-broth culture of *E.* coli TOP10 cells were diluted into 100 ml of L-broth with 10 mM $MgSO_4$. The culture was grown with good aeration at 37°C, 200 rpm on a rotary shaker, until the optical density was equal to 0.2 - 0.4

absorbance units, measured at 600 nm. The cells were pelleted by centrifugation at 3,000 g for 5 minutes at 4°C. The supernatant was discarded and the cells resuspended in 50 ml of 0.1 M $CaCl_2$ at 4°C and then incubated on ice for 30 minutes. Cells were re-pelleted by centrifugation at 3,000 g for 5 minutes at 4°C. The supernatant was discarded and the cells resuspended in 1 ml of 0.1 M $CaCl_2$. Cells were incubated on ice until they were transformed (according to the following protocol).

10 - 100 ng of DNA were added to 200 µl of competent cells and incubated on ice for 1 h. The cells were heat shocked at 42°C for 3 minutes and added to 2 ml of L-broth. The cells were then incubated for 1 h at 37°C and 100 - 200 µl aliquots were plated on selective medium. Plates were incubated at 37°C for 24 - 36 h.

When only small amounts of DNA were available for transformation Epicurian Coli® SURE® competent cells (Stratagene, La Jolla, California) were used according to the manufacturer's instructions. 100 µl of Epicurian Coli® SURE® competent cells was mixed with 1.7 µl of 1.42 M β-mercaptoethanol and incubated on ice for 10 minutes. Between 0.1 and 50 ng of DNA were added to the competent cells and the mixture was incubated on ice for 30 minutes. Cells were then heat shocked at 42°C for 45 seconds and incubated on ice for 2 minutes. The transformed cells were added to 900 µl of L-broth and incubated at 37°C for 1 h on a rotary shaker at 200 rpm. 100 - 200 µl aliquots (of cells) were plated on selective medium and incubated at 37°C for 24 - 36 h.

2.26 Double Stranded DNA Sequencing using Sequenase Version 2.0

Ref: Sanger and Coulson (1975) and Sanger *et al.* (1977).

Sequencing was essentially performed as described by Sanger *et al.* (1977), with some modifications. The sequenase™ version 2.0 DNA sequencing kit was manufactured by United States Biochemicals (Cleveland, Ohio) and supplied through Amersham International plc (Little Chalfont, Buckinghamshire).

Sequencing plates were washed in 70% ethanol and the front plate coated with 10 ml of dimethyldisaline and allowed to dry. The back plate was coated with 30 ml of binding solution (30 ml of 100% ethanol, 1.2 ml of 10% acetic acid and 200 µl of

silane). Plates were washed in water and then 70% ethanol. A 6% polyacrylamide / urea sequencing gel was prepared.

10 µl (1 µg) of Qiagen mini prep DNA was taken and denatured in 200 mM NaOH, 0.2 mM EDTA for 5 minutes at room temperature. The denatured DNA was ethanol precipitated and resuspended in 7 µl of double distilled. This DNA (the template) was annealed to 100 ng (1 µl) of primer in sequenase reaction buffer (40 mM Tris-HCl, 20 mM $MgCl_2$, 62.5 mM NaCl, pH 7.5). The mixture was then heated to 95°C for 1 minute and immediately placed at 37°C for 15 minutes. The annealed template and primer were labelled by the addition of 1 µl of 0.1 M DTT, 2 µl of diluted labelling mix (dGTP, dCTP, dTTP), 0.5 µl (5 µCi) ^{35}S-dATP (1000 Ci / mmol) and 2 µl of diluted sequenase enzyme followed by a 5 minute incubation at room temperature. 3.5 µl aliquots of labelling mix were added to 2.5 µl of termination mix, ddGTP (ie. 80 µM dGTP, 80 µM dCTP, 80 µM dTTP, 80 µM dATP, 8 µM ddGTP, 50 mM NaCl), ddATP, ddTTP and ddCTP and incubated at 37°C for 5 minutes. The reaction was arrested using 4 µl of stop buffer (95% Formamide, 20 mM EDTA, 0.05% Bromophenol Blue, 0.05% Xylene cyanol FF).

Samples were heated to 80°C for 5 minutes, quenched on ice and loaded on a pre-warmed sequencing gel. The gel was electrophoresed for approximately 2 h (depending on the length of sequence) at 1500 V, 30 mA, 40 W. The gel was then fixed in a 10% (v/v) methanol, 10% (v/v) acetic acid solution for 20 minutes, washed in distilled water for 20 minutes and oven dried at 80°C. The dried gel was then exposed to Kodak photographic film overnight (Kodak Scientific Imaging Film (18 x 43 cm), Eastman Kodak Company, USA).

2.27 Baculovirus Methods

2.27 Co-transfection of Viral DNA and Transfer Vector

Ref: The baculovirus expression system, King and Possee, (1992).

1 µg of recombinant transfer vector was mixed with 200 ng linearised AcMNPV DNA (supplied by Invitrogen®) in a polystyrene universal sterilin sample tube. LipofectAMINE™ (a 3:1 (w/w) liposome mixture of the polycationic lipid DOSPA

(2,3-dioleyloxy-N-[2(Sperminecarboxamido)ethyl]-N,N-dimethyl-1-propanaminium trifluoroacetate) and the neutral lipid DOPE (dioleoyl phosphatidylethanolamine) supplied by GibcoBRL Life Technologies™) was diluted with 0.5 volumes of sterile double distilled water and added to the same volume of transfer vector / AcMNPV DNA mixture. The mixture was incubated at room temperature for 15 minutes. A 35 mm dish, seeded 24 h in advance with 1 x 10^6 cells, was washed twice with 1 ml of serum free TC100 medium, cells should look healthy and be about 50% confluent. 1 ml of serum free TC100 medium was added to the cells. The DNA / LipofectAMINE™ mixture was then pipetted into the dish, gently mixed and incubated at 28°C for 24 h. 1 ml of complete TC100 (10% foetal bovine serum) medium was added to the dish and incubated for a further 48 h at 28°C. The medium was harvested and stored at 4°C for further analysis by plaque assay.

To confirm the success of co-transfection 1 ml of complete TC100 containing 15 µl X-Gal (2% (w/v) X-Gal in dimethylformamide, stored at -20°C) was added to the cells. After 24 h the dish was examined for a blue coloration to confirm transfection (pBBH based constructs only).

2.28 Purification of Virus by Plaque Assay

Ref: The baculovirus expression system, King and Possee, (1992).

The co-transfection medium was diluted in complete TC100 medium using serial dilutions from undiluted to a 10^{-3} dilution. A negative control using complete TC100 medium was also included. Sf9 cells were grown to 50% confluence in 35 mm dishes by seeding 24 h before use with 1 x 10^6 cells. Culture medium was removed from the dishes and the cells inoculated with 100 µl of putative viral inoculum. The dishes were incubated for 1 h at room temperature. An overlay was prepared (TC100 medium with 5% (v/v) foetal bovine serum, 1% (v/v) penicillin / streptomycin solution, 1% (w/v) low melting point agarose) and incubated at 37°C. The inoculum was carefully removed and 2 ml of overlay were pipetted into each dish. When the overlay had solidified, 1 ml of complete TC100 medium was pipetted onto the overlay. The dishes were incubated at 28°C in a humidified plastic box for five days.

Plaque assays were analysed using X-Gal and neutral red staining, in order to visualise all viral plaques. Recombinant plaques formed from derivatives of the pBBH vector were blue and occlusion body negative. Recombinant plaques formed from derivatives of the pAC360 vector were colourless and occlusion body negative. Non-recombinant plaques were colourless and occlusion body positive.

To visualise recombinant plaques formed from pBBH vector derivatives the following protocol was used: Culture medium was removed from the overlay and replaced with 1 ml of complete TC100, containing 0.03% (w/v) X-Gal (15 µl / ml of 2% (w/v) X-Gal Lennox in dimethylformamide) and incubated at 28°C for 3 h. 1 ml of sterile PBS containing 0.025% (w/v) neutral red stain (50 µl / ml of 0.5% (w/v) neutral red stain solubilized in sterile double distilled water) was added and the incubation continued for a further 3 h. The stain was removed, the dishes inverted and the plaques allowed to develop in the dark for at least 2 h. Recombinant plaques were blue and occlusion body negative, while wild-type plaques were clear and occlusion body positive.

To visualise recombinant plaques formed from pAC360 vector derivatives the following protocol was used: Culture medium was removed from the overlay and replaced with 1 ml of sterile PBS containing 0.025% (w/v) neutral red stain was added and incubated for 4 h. The stain was removed, the dishes inverted and the plaques allowed to develop in the dark for at least 2 h, the plaques become clearer if left overnight. Recombinant plaques were clear and occlusion body negative, while wild-type plaques were clear and occlusion body positive.

Identified plaques were confirmed by microscopic analysis. Several well isolated putative recombinant plaques were selected for further analysis.

2.29 Plaque Purification

Ref: The baculovirus expression system, King and Possee, (1992).

Putative recombinant plaques were selected using a sterile glass Pasteur pipette. The plug of agarose containing viral particles was placed in a sterile bijou bottle containing 4 ml of TC100 medium and vortexed to disperse the virus particles in the

medium. Plaque picks were stored in the dark at 4°C (recombinant viral particles have been reported to be light sensitive (personal communication with Dr A. Wolstenholme)).

The plaque assay was repeated using serial dilutions from 0 to a 10^{-3} dilution. As a control, 2 dishes were inoculated with medium only. Cells were infected, incubated and stained according to protocol 2.28. Plaques were examined microscopically in order to identify contaminating wild-type virus. Pure plaques were picked and the plaque purification protocol was repeated until there were no wild-type plaques detected.

2.30 Titration of Viral Stocks by Plaque Assay

Ref: The baculovirus expression system, King and Possee, (1992).

The viral titre, measured in plaque forming units per ml (pfu / ml), was determined by modification of the plaque assay protocol. Serial dilutions of the viral stock, between 10^{-3} - 10^{-7} dilutions, were prepared in complete TC100 medium. 35 mm dishes of 50% confluent cells were inoculated with 100 µl of diluted virion. The inoculum was removed and the overlay applied, cells were incubated for 5 days and stained with X-Gal only (when determining the titre of pBBH derived vectors). Plaques were counted and the single dilution showing the maximum number of countable plaques was used to determine the titre.

2.31 Production of Small Virus Stocks

Ref: The baculovirus expression system, King and Possee, (1992).

25 cm^2 flasks were prepared 24 h in advance by seeding with 1.5×10^6 cells, resulting in 50% confluence. The medium was removed and the cells inoculated with 400 µl of plaque picked inoculum for 1 h at room temperature. The inoculum was discarded and replaced with 5 ml of complete TC100 medium and the flasks were incubated at 28°C for up to 7 days. Cells were microscopically observed during infection to ensure purity and viral infectivity. Culture medium containing viral particles was removed to sterile universal sample tubes and stored in the dark at 4°C. Recovered medium was used to infect cells for recombinant protein analysis.

2.32 Viral infection of Insect Cells for Recombinant Protein Analysis

Ref: The baculovirus expression system, King and Possee, (1992).

25 cm^2 flasks were prepared 24 h before use as described in protocol 2.31. The medium was discarded and the cells infected with 400 µl of viral inoculum. Cells were incubated with inoculum for 1 h, after which the inoculum was replaced with 5 ml of complete TC100 medium. Cells were incubated at 28°C for four days and the infection was monitored microscopically.

Cells were scraped from the flask surface, into the medium, using a cell scraper. The cells were pelleted in an Ole Diche bench top centrifuge at 20,000 g for 5 minutes. The cells were resuspended in 1.5 ml of TES buffer with protease inhibitors (10 mM Tris, 5 mM EDTA, 250 mM Sucrose, pH 7.2) and homogenised with 20 strokes from an electric teflon homogeniser. Membranes were centrifuged at 20,000 g and resuspended in 1 ml of TES buffer with protease inhibitors. Samples were assayed to determine protein concentration and were analysed by immunoblotting with a C-terminal polyclonal GLUT1 antibody. This determined whether putative recombinant viruses were producing the relevant protein.

2.33 Production of High Titre Viral Stocks

Ref: The baculovirus expression system, King and Possee, (1992).

Once a recombinant virus expressing the required protein had been identified a large viral stock was made for use in all further experiments.

A 250 ml spinner culture was prepared and grown until the cell density reached 5×10^5 cells / ml. Cells were infected with a low multiplicity of infection (MOI (0.1 - 0.2 pfu / cell)) as estimated by plaque assay. The required amount of inoculum was added to the spinner culture and the culture returned to stir at 28°C. Infected cultures were incubated for 7 days and the infection was monitored microscopically. Supernatants were separated from the cells by centrifugation at 6,000 g for 15 minutes at 4°C in a Sorvall high speed centrifuge. Supernatants containing the recombinant virions were stored in the dark at 4°C. Two aliquots of virus were subsequently removed and

cryogenically stored in liquid nitrogen. Samples were flash frozen on dry ice soaked in ethanol (-72°C), and then placed under liquid nitrogen (-196°C).

2.34 Production of Recombinant Protein for Further Experimentation

Ref: The baculovirus expression system, King and Possee, (1992).

Both Highfive cells and Sf9 cells were grown in spinner culture (5×10^5 cells / ml) or monolayer culture (grown to 50% confluence). Cells were infected with a low multiplicity of infection (0.1 pfu / cell (personal communication with Dr A. Wolstenholme suggested that protein expression was more effective with a low MOI, leading to two rounds of viral infection in culture)). Highfive cells and Sf9 cells were incubated at 28°C for 3 days or 4 days respectively. Cells were then recovered from culture, monolayer cells were freed from the surface by use of a cell scraper, all cells were pelleted by centrifugation at 6,000 g for 15 minutes at 4°C in a Sorvall high speed centrifuge.

Cells were resuspended in 5 mM sodium phosphate buffer (pH 7.4) with protease inhibitors and homogenised with 40 strokes from an electric teflon homogeniser. Membranes were centrifuged at 541,000 g (100,000 rpm in a Beckman Ultracentrifuge using a TLA-100.3 rotor) for 15 minutes at 4°C. Homogenisation and centrifugation was repeated twice more, in order to wash the membranes of soluble proteins. Membranes were resuspended in 5 mM sodium phosphate buffer with protease inhibitors and assayed to determine their protein concentrations.

2.35 Protein Analysis Methods

2.35 BCA Protein Assay

Protein concentrations were determined by the Pierce BCA (bicinchoninic acid) system for protein assay. The standard protein curve was made up using 0, 2, 4, 6, 8 and 10 µg of BSA stock (1 µg / µl), diluted with 5 mM sodium phosphate buffer or GLUT1 dialysis buffer, depending on sample. 10 ml of reagent A (1% bicinchoninic acid, 2% $NaCO_3 \cdot H_2O$, 0.16% sodium tartrate, 0.4% NaOH, 0.95% $NaHCO_3$) was mixed with

200 µl of reagent B (4% (w/v) $CuSO_4 \cdot H_2O$), 200 µl of the mixture was added to each sample. Samples were incubated at 37°C for 30 minutes and the plate was read on a dual wavelength Labsystems Multiskan plate reader at 450 nm and 540 nm.

2.36 SDS-Polyacrylamide Gel Electrophoresis (SDS-PAGE)

Electrophoresis was performed using a modification of the method of Hashimoto *et al.,* (1983), derived from the discontinuous buffer system of Laemmli, (1970). Samples were mixed with electrophoresis loading buffer (115 mM Tris, 10% (v/v) Glycerol, 2% (w/v) SDS, 5% (v/v) β-mercaptoethanol, 4 µg / ml (w/v) Bromophenol Blue, pH 6.8) and incubated at room temperature for 30 minutes before loading on the polyacrylamide gel. The polyacrylamide gel was run as either a 3 mm gel using the Protean II xi slab gel system (Bio-Rad) 16 x 20 cm plates or on the mini Atto gel system (6.5 x 9 cm gel size). Polyacrylamide gels were made, according to the manufacturer's instructions, with either 10 or 12% acrylamide (acrylamide / bisacrylamide stock was 30% T, 2.7% C (National Diagnostics, Flowgen, Lichfield, Staffordshire)). Resolving gel buffer (1.5 M Tris, 0.4% (w/v) SDS, pH 8.8), stacking gel buffer (0.5 M Tris, 0.4% (w/v) SDS, pH 6.8), 10% (w/v) ammonium persulfate (Bio-Rad) and N,N,N',N'-tetramethylethylenediamine (TEMED, Bio-Rad) were added to the acrylamide stock accordingly. Once assembled the upper and lower buffer chambers were filled with electrode buffer (0.025 M Tris, 0.1% (w/v) SDS, 0.192 M glycine, pH 8.3) and the 'wells' loaded with sample suspended in electrophoresis sample buffer. The Protean II xi slab gel system was electrophoresed for approximately 16 h (until the dye-front approached the bottom of the plates) using a constant current of 25 mA and internal cooling. The mini Atto gel system was run for 1½ h using a constant current of 70 mA. High molecular weight electrophoretic standards (myosin 205 kDa, β-galactosidase 116 kDa, phosphorylase B 97.4 kDa, bovine albumin 66 kDa, ovalbumin 45 kDa and carbonic anhydrase 29 kDa) were obtained from Sigma.

2.37 Visualisation of Protein on SDS-Polyacrylamide Gels

Following electrophoresis gels were stained in 0.2% (w/v) coomassie blue R-250 solubilized in fixative (30% (v/v) methanol, 10% (v/v) acetic acid) for 30 minutes at room temperature. Polyacrylamide gels were then destained in fixative, for 2 - 4 h.

2.38 Electrophoretic Transfer of SDS-PAGE Protein to Nitrocellulose

Samples were electrophoresed on the appropriate polyacrylamide gel, according to protocol 2.36. The polyacrylamide gel was taken, the stacking buffer removed and the gel soaked in transfer buffer (48 mM Tris, 0.0375% (w/v) SDS, 39 mM Glycine, pH 8.8) for 5 minutes. The electrophoretic cell consisted of 9 sheets of electrode paper (Pharmacia Biotech, St. Albans, Hertfordshire) soaked in transfer buffer, 1 piece of BioTrace® nitrocellulose blotting membrane (Gelman Sciences Ltd., Northampton) soaked in transfer buffer, a SDS-polyacrylamide gel and a further 9 sheets of electrode paper soaked in transfer buffer. The electrophoretic cell was placed between the plates of a Multiphor II NovaBlot electrophoretic transfer unit (Pharmacia Biotech). A current of 0.8 mA / cm^2 was applied for 110 minutes, after which the nitrocellulose was rinsed in double distilled water before staining with 0.1% (w/v) Ponceau S in 3% (w/v) trichloroacetic acid. The position of the molecular weight markers were recorded.

2.39 Immunoblotting for GLUT1

Immunoblotting was carried out at room temperature on a shaking table.

The dried nitrocellulose was rehydrated in TBS - Tween (10 mM Tris, 0.9% (w/v) NaCl, 0.1% (v/v) Tween 20, pH 7.4) before blocking with 5% (w/v) Marvel dried skimmed milk (Premier Beverages, Stafford) in TBS-Tween for 30 minutes. The milk was then discarded and the nitrocellulose washed in TBS-Tween. The nitrocellulose was incubated with the primary antibody at a dilution of 1:4000 in TBS-Tween, 1% (w/v) bovine serum albumin (BSA) for 90 minutes (the primary antibody was later re-used, being preserved by the addition of 0.03% (w/v) sodium azide and kept at 4°C). The primary antibody was removed and the nitrocellulose washed 6 times by 3 minute

washes with TBS-Tween. The nitrocellulose was then incubated with the secondary antibody at a dilution of 1:4000 anti-rabbit IgG conjugated to horseradish peroxidase in TBS-Tween with 1% (w/v) BSA, for 30 minutes. Following six 3 minute washes with TBS-Tween, the nitrocellulose was either incubated for 1 minute with Amersham's ECL detection reagent, or for 1 minute with Pierce's chemiluminescent detection reagent (detection reagents were used according to the manufacturer's instructions). The detection reagent was discarded and the nitrocellulose was placed between two transparent acetate sheets, before exposure to autoradiography film (Fuji medical X-ray film (13 x 18 cm) Fuji Photo Film Co. Ltd., Tokyo, Japan). The exposure time was adjusted until an image was visible on developed film.

2.40 Photolabelling of Membranes Expressing GLUT1

Homogenised insect cell membranes were (insect cell membranes or erythrocyte ghosts) resuspended in sodium phosphate buffer of Kreb-Ringer Hepes with protease inhibitors at 4°C and adjusted to a 1 ml volume. Membranes were incubated for 10 minutes with or without zinc sulphate, on a rotating wheel, before the addition of photolabel. Membranes were labelled with either 250 µCi of ATB-[2-^{3}H]BMPA (5 µCi / µl) or 2 µCi of ^{3}H-cytochalasin B (0.5 µCi / µl), which was added to each sample and the samples mixed on a rotating wheel. Samples were incubated for 5 minutes with photolabel before irradiation for 3½ minutes in a Rayonett RPR-100 photochemical reactor containing RPR-3000 lamps. Following irradiation the membranes were centrifuged at 13,400 g in a microcentrifuge, the supernatant discarded and the membranes resuspended in 1 ml of ice cold 5 mM sodium phosphate buffer containing protease inhibitors. The membranes were then washed a further two times, in order to remove free radioactivity. The membranes were solubilized in 1 ml of 2% (w/v) Thesit in 5 mM sodium phosphate buffer with protease inhibitors and incubated on ice for 20 minutes, before centrifugation at 13,400 g to remove the insoluble matter. The supernatant was subjected to GLUT1 immunoprecipitation (50 µl anti-serum conjugated to 5 mg protein A Sepharose beads) for two h at 4°C on a rotating wheel. The immunoprecipitate was washed 6 times with 1 ml of 1% (w/v) Thesit in PBS with protease inhibitors. Bound proteins were removed from the beads by the addition of

160 µl of electrophoresis sample buffer, 4% (w/v) SDS, for 30 minutes at room temperature. Samples were then analysed by SDS-PAGE, or by using the tricine gel system as described in protocol 2.42.

2.41 Photolabelling Gel Analysis

Photolabelled gels were stained with 0.2% coomassie blue, dissolved in fixative, (30% (v/v) methanol, 10% (v/v) acetic acid) for 1½ h to visualise and fix proteins. Photolabelled gel lanes were either cut to 6.5 mm slices or 3 mm slices, depending on the size of the gel, which were placed into scintillation counter vials and dried in an oven at 80°C for 2 - 3 h. Dried gel slices were solubilized in 30% (v/v) hydrogen peroxide with 2% (v/v) ammonium hydroxide in sealed vials for 2 h at 80°C. Samples were allowed to cool and 8 ml of scintillation fluid added (Optiphase Safe™). Samples were counted in a Packard 1500 TRI-CARB liquid scintillation counter using the tritium channel (0 - 12 KeV).

2.42 Tricine Gel Analysis

Tricine gels were electrophoresed on the mini Atto gel system (Atto corporation) and were used to resolve small photolabelled proteins. The gel was made up according to the method of Schägger, H. and Von Jagow, G., (1987). Mini Atto gel plates were assembled according to the manufacturer's instructions. The separating gel was made to 16% (w/v) acrylamide and 10% (v/v) glycerol in gel buffer (1M Tris-HCl, 0.1% (w/v) SDS, pH 8.45). The gel was polymerised by the addition of 0.033% (w/v) APS and 0.04% (v/v) TEMED, the spacer gel was poured onto the separating gel before polymerisation occurred. The spacer gel was 10% (w/v) acrylamide, in gel buffer (1M Tris-HCl, 0.1% (w/v) SDS, pH 8.45) and was polymerised by the addition of 0.024% (w/v) APS, 0.04% (v/v) TEMED. The stacking gel was poured after spacer gel polymerisation and was composed of 3.8% (w/v) acrylamide in gel buffer (0.744 M Tris-HCl, 0.074 (w/v) SDS, pH 8.45), polymerisation was initiated by the addition of 0.08% (w/v) APS, 0.08% (v/v) TEMED. The appropriate buffer chambers were filled with cathode buffer (0.1 M Tris, 0.1 M tricine, 0.1% (w/v) SDS, pH 8.25) and anode

buffer (0.2 M Tris-HCl, pH 8.9). Samples were loaded in standard electrophoresis sample buffer and the gel run at a constant current of 50 mA, until the dye-front approached the bottom of the plates. Following electrophoresis the gel was analysed by the same method as other photolabelling gels in protocol 2.41.

2.43 Purification of GLUT1 from Human Erythrocytes

GLUT1 was purified from human erythrocytes as described by Baldwin and Leinhard, (1989). 450 ml of blood was taken and diluted with wash buffer (5 mM sodium phosphate, 150 mM NaCl, pH 8.0). Erythrocytes were pelleted at 3,300 g in a Sorvall centrifuge for 10 minutes. The supernatant and white cells were removed and the wash repeated a further two times. The cells were then lysed by the addition of lysis buffer (5 mM sodium phosphate, pH 8.0) and the membranes pelleted by centrifugation at 21,500 g for 25 minutes. Lysis was repeated a further 5 times and erythrocyte ghosts were stored at -80°C.

Membrane ghosts were protein depleted by the addition of a base solution (15 mM NaOH, 2 mM EDTA, 0.2 M dithiothreitol). The base mixture was added to 40 ml of membranes to a final volume of 250 ml. The membranes were then centrifuged at 43,500 g for 15 minutes. The supernatant was discarded, the membranes washed once in 50 mM Tris, pH 7.4 at 2°C, and resuspended in the same buffer by homogenising with an electric teflon homogeniser. Protein depleted membranes were then stored at -80°C.

Protein depleted membranes were solubilized in 50 mM Tris-HCl, 2 mM dithiothreitol, 685 mM (1.45% (w/v)) octyl glucoside, pH 7.4, for 20 minutes and then centrifuged at 180,000 g for 1 h.

The solubilized fraction was applied to a DEAE cellulose column, pre-equilibrated in 50 mM Tris-HCl, 25 mM NaCl, 2 mM dithiothreitol, 34 mM octyl glucoside, pH 7.4. The sample was eluted using the same buffer and the eluate dialysed extensively against 50 mM sodium phosphate, 100 mM NaCl, 1 mM EDTA over 48 h. Finally, samples were analysed for purity by SDS-PAGE, protein assayed and used as an experimental control or protein standard.

2.44 Cytochalasin B Assays

Cytochalasin B assays were performed on either 250 µg of erythrocyte ghosts, 120 µg of erythrocyte protein depleted membranes, 36 µg of purified erythrocyte membranes or 1 mg of insect cells expressing the appropriate recombinant protein. Tritiated cytochalasin B (18.1 Ci / mmol) was used from a 50 µCi / 100 µl stock in ethanol and diluted to 0.02 µCi / 5 µl with PBS. Unlabelled cytochalasin B was diluted from a 1 mM stock, solubilized in ethanol, to 2 µM with PBS and was used at a range of concentrations from 0.096 µM to 0.48 µM. Unlabelled cytochalasin B was substituted with 0.5 M D-glucose to test glucose inhibition. Cytochalasin E was used at a concentration of 32 µM, in order to block non-specific cytochalasin B binding sites. Erythrocyte assays were performed in a total volume of 310 µl. Insect cell assays were performed in a total volume of 1 ml.

Assay components were combined and incubated at room temperature for 15 minutes. Membranes were pelleted at 13,400 g for 5 minutes and two 100 µl or 200 µl aliquots of supernatant were counted, depending on assay volume. The radioactivity detected in the supernatant represents unbound 'free' cytochalasin B. This was used to determine the amount of 'bound' and 'free' cytochalasin B. Results were plotted as a 'bound' / 'free' versus 'bound' Scatchard plot, from which the Bmax and Kd was determined.

2.45 Confocal Microscopy

Confocal scanning light microscopy was performed using a BioRad confocal imaging system (MRC500) with a Nikon 60 times (NA 1.40) magnification lens. The fluorescein isothiocyanate (FITC) antibody was stimulated by blue light emission at 488 nm (10mW) from an argon ion laser. The fluoresced image was analysed using the MRC500 confocal microscope operating software CoMOS Version 7.0a (BioRad Microscience Ltd., 1991-1994).

Spodoptera frugiperda cells were infected with virus 24 h and 36 h before use. Cells were combined and pelleted at 300 g in a bench top centrifuge. The supernatant was discarded and the cells were fixed in 7 ml 4% (w/v) paraformaldehyde in PBS for

20 minutes at room temperature on a shaking table. Cells were washed 3 times in 7 ml of PBS and permeabilised in 7 ml of 0.1% (w/v) saponin in PBS for 45 minutes. Permeabilised cells were centrifuged at 300 g for 45 seconds and the supernatant removed. The cell pellet was transferred to a microcentrifuge tube.

Affinity purified anti-rabbit polyclonal GLUT1 antibody was diluted 1:100 in PBS containing 0.1% (w/v) saponin, 1% (w/v) BSA and 3% (v/v) goat serum. Cells were resuspended in 125 µl of diluted GLUT1 antibody (1.57 mg / ml) and incubated at room temperature for 90 minutes on a shaking table. Cells were then washed 3 times with 500 µl of 0.1% (w/v) saponin in PBS. Cells were diluted in a 1:100 dilution of FITC-labelled goat anti-rabbit IgG antibody (1.57 mg / ml fluorescein conjugated affinipure goat anti-rabbit IgG with minimal cross reaction to human, mouse and rat serum proteins (code: 111-095-144, Jackson Immuno Research Laboratories Inc. USA)) in PBS containing 0.1% (w/v) saponin, 1% (w/v) BSA and 3% goat serum to give a final volume of 125 µl. The cells were then incubated for 1 h, in the dark, on a shaking table. Following incubation, cells were washed 3 times in 500 µl of PBS containing 0.1% (w/v) saponin and mounted onto a glass slide in 25 µl vector shield (Vector labs).

2.46 Purification of Egg Yolk Lipids

Ref: Personal communication with G. Schmitt, University of Bath.

Egg yolks were taken from six Chicken eggs and mixed with 3 volumes of a 2 : 1 chloroform : methanol mixture. The egg yolk / chloroform mixture was left for 5 minutes at room temperature in order to solubilize the lipid fraction and the precipitated proteins were filtered out using a 0.45 µm filter. The solubilized lipids were then reduced in volume by rotary evaporation and loaded onto a silica column. The column was eluted using three column volumes of chloroform, followed by three column volumes of 1 : 1 chloroform : methanol and finally by three column volumes of 1 : 9 chloroform : methanol. The solvent system resulted firstly in the elution of neutral lipids followed by the elution of increasingly polar lipids, for example phospholipids. Lipid fractions were analysed by thin layer chromatographic (TLC) analysis using the following solvent system: 65 parts chloroform, 35 parts methanol, 8 parts acetic acid, 4 parts water. The TLC plate was visualised using a molybdenate stain

(1.3 % molybdenum oxide in 4.2 M sulphuric acid) developed in an 80°C oven for 20 minutes.

2.47 Solubilization and Purification of Histidine Tagged Proteins

Homogenised membranes (2 mg / ml) were solubilized in buffer (solubilization buffer: 10 mM Hepes, 250 mM NaCl, 20% (v/v) Glycerol, 1.5 mg / ml Lipids, 1.5% (w/v) Octyl glucoside, 20 mM Imidazole, protease inhibitors, pH 7.9 (lipids were type II-S lipids from Soybean, Sigma catalogue code P5638)), and homogenised with 20 strokes from an electric teflon homogeniser and incubated on ice for 30 minutes. Following incubation, insoluble cell debris was removed by centrifugation at 20,000 g in a Beckman ultracentrifuge (TA100 rotor).

A 1 ml Pharmacia Biotech HiTrap Sepharose column was chelated with 10 ml of 0.1 M nickel sulphate using a Pharmacia Biotech FPLC unit (Gradient Programmer GP-250). The column was washed with 4 ml of distilled water and pre-equilibrated with 3 ml of wash buffer (10 mM Hepes, 250 mM NaCl, 20% (v/v) glycerol, 1.5 mg / ml lipids, 1% (w/v) octyl glucoside, 20 mM imidazole, protease inhibitors, pH 7.9), at a rate of 1 ml / min. Solubilized samples were loaded onto the column and 1.9 ml fractions collected. The column was washed with 10 ml of wash buffer and eluted with 5 ml of elution buffer (10 mM Hepes, 250 mM NaCl, 20% (v/v) glycerol, 1.5 mg / ml lipids, 1% (w/v) octyl glucoside, 300 mM imidazole, protease inhibitors, pH 7.9). Samples were dialysed against three 4 litre batches of GLUT1 dialysis buffer (50 mM Tris, 100 mM NaCl, 1 mM EDTA, pH 7.4) for a period of 48 h. Once dialysed, purified GLUT1 was stored at -80°C.

Protocol modifications

Preliminary experiments involved the use of a 5 ml Pharmacia Biotech HiTrap column eluted on a Pharmacia Biotech FPLC unit. The FPLC unit was programmed to generate a 25 ml wash followed by a 25 ml elution gradient from 0 to 200 mM imidazole. Columns run on the FPLC unit used the IMAC buffer system. The column was pre-equilibrated in IMAC 0 buffer and the sample loaded in the same buffer (10

Results

3.0 GLUT1 Point Mutations

Section 3.1 Introduction

Chinese hamster ovary (CHO) cells were transfected with one wild-type and 3 mutated glucose transporter constructs. The transfected cells were supplied to the laboratory by Muraoka (Kobe University, Japan). The CHO cell clones expressed the following point mutations: glycine 466 mutated to glutamic acid (G466E), phenylalanine 467 mutated to leucine (F467L) and arginine 468 mutated to leucine (R468L). Muraoka *et al.*, (1995) tested the CHO cells for glucose transporter expression using immunoblot analysis. Immunoblotting demonstrated the mutants to have similar expression levels (table 3.1).

		Western Blotting (%)
WT		100
G466E		106.6 ± 3.9 (n = 3)
F467L		107.3 ± 21.1 (n = 3)
R468L		126.0 ± 17.8 (n = 3)
Non-Transfected		11.3 ± 1.4 (n = 3)

Table 3.1, CHO cell glucose transporter expression levels. The levels of mutated GLUT1 were assessed by comparison with expression of the wild-type GLUT1 protein in CHO-K1 cells. Immunoblot analysis demonstrated that similar expression levels were attained by each mutant (Reproduced from Muraoka *et al.*, (1995)). The number of repeat experiments = 3 (n=3).

The location of the mutated amino acids can be seen in the 2-D representation of the GLUT1 glucose transporter on the following page, figure 3.1. For clarity only the C-terminal portion has been displayed. The mutated amino acids are located in the C-terminal hydrophilic tail of the glucose transporter.

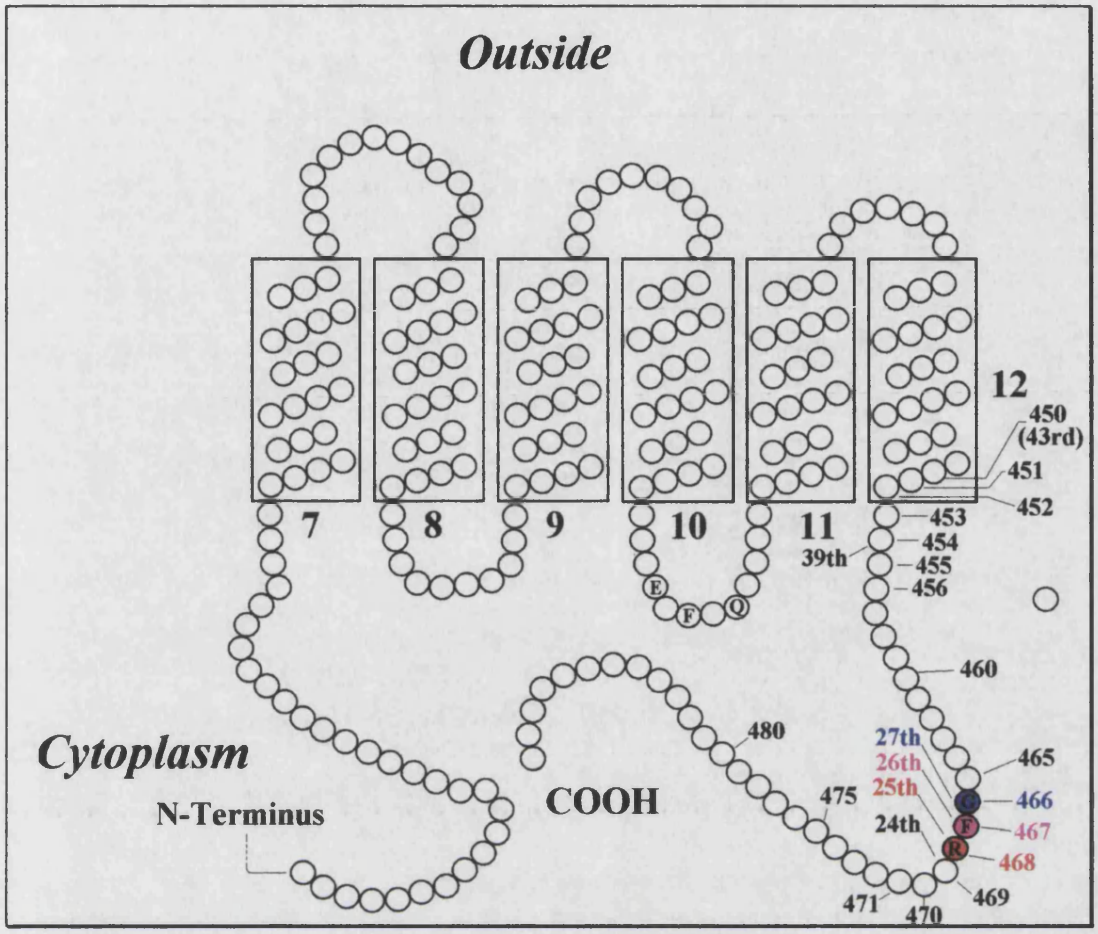

Figure 3.1, C-terminal portion of GLUT1. The diagram displays a modified version of the 2-dimensional representation of the 12 α-helix transporter model, according to Mueckler *et al.,* (1985). The 24th and 27th amino acids from the C-terminus are marked, as are the 466th, 467th, 468th and 469th amino acids from the N-terminus. The mutations G466E (Blue) F467L (Magenta) and R468L (Red) are denoted by the figures 466, 467 and 468, respectively.

Katagiri *et al.,* (1992), have determined the C-terminal region to be important for glucose transporter function. Katagiri *et al.,* (1992) substituted the final 39 amino acids of GLUT1 with the corresponding amino acids of GLUT2. Analysis of the resulting chimera showed that the observed kinetics of GLUT2 had been conferred to the GLUT1 / GLUT2 chimera. The Km of GLUT1 for 2-Deoxyglucose was 1.5 mM. However, the Km of the chimeric protein for 2-Deoxyglucose was 10 mM, a 6.6 fold increase (Km of GLUT2 for 2-Deoxyglucose is 10 mM). Figure 3.2 on the following page displays the C-terminal region between amino acids F450 and G471.

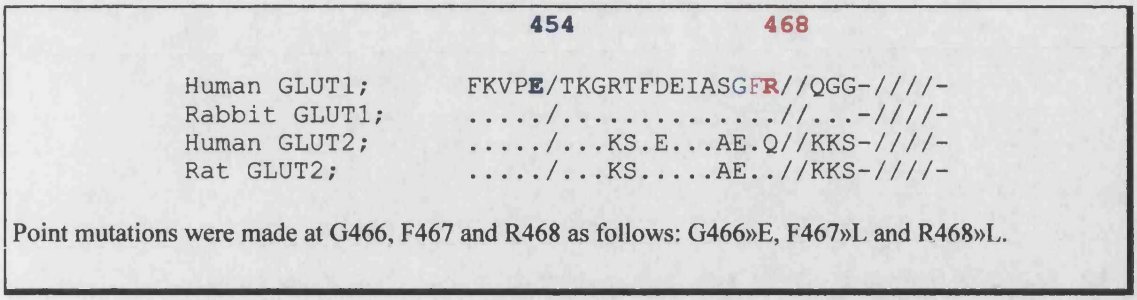

Figure 3.2, The 'critical' regions at the C-terminus of several glucose transporters. Taken from Muraoka *et al.,* (1995). The figure displays the sequence alignments of C-terminal amino acids in the 'critical' region of the C-terminus. The 'critical' region describes the area where C-terminal deletions result in a progressive, significant loss of activity.

Muraoka *et al.,* (1995) have produced several C-terminal deletion constructs. Study of the constructs showed that glucose transport was decrease by the removal of 24 or 25 C-terminal amino acids. The 24th C-terminal amino acid corresponds to amino acid Q469.

The three point mutations studied in this thesis were at amino acids R468, F467 and G466, which correspond to the 25th, 26th and 27th amino acids from the C-terminus, respectively. From figure 3.2, it can be seen that all of the amino acids in this region are conserved between human GLUT1 and rabbit GLUT1, indicating the region to be important for the function of the glucose transporter. The point mutation G466E exchanges the GLUT1 amino acid for the GLUT2 amino acid. Mutations F467L and R468L are situated at the region determined by C-terminal deletion to perturb transporter function.

Section 3.2

CHO Cell Transport Assays

CHO cells were assayed for uptake of 2-Deoxy-D-glucose and the results plotted in figure 3.3, the Km and Vmax values are displayed in table 3.2. Mori *et al.*, (1994) have previously shown that non-transfected CHO-K1 cells transport 2-Deoxy-D-glucose with the following kinetics: Km 2.6 mM (n=3) and Vmax 7.1 nmol/min/mg of protein (n=3).

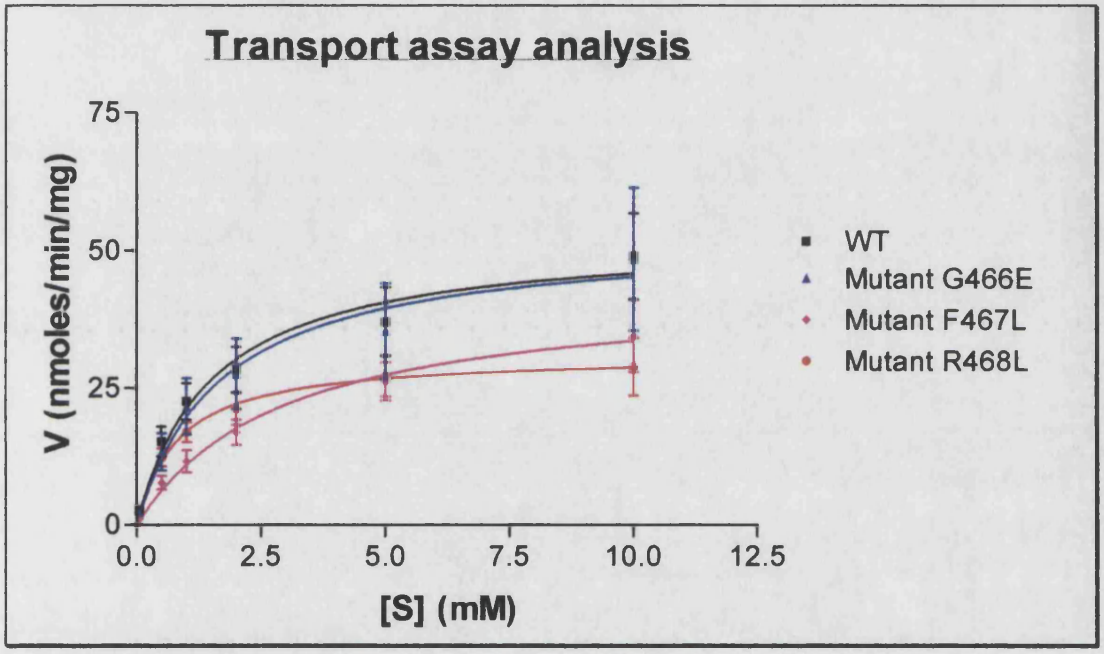

Figure 3.3, Uptake studies in CHO cell mutants. The figure displays the combined GLUT1 transporter assay results, (the number of repeat experiments is = 4 (n=4) except for the wild-type were the number of repeat experiments is = 5 (n=5)). Error bars indicate the standard error of the mean. The data obtained was fitted to the equation Y = Vmax x X / (Km + X).

	Km (mM) ± SEM	Vmax (nmoles/min/mg) ± SEM
WT	1.49 ± 0.17 (n = 5)	52.84 ± 9.19 (n = 5)
G466E	1.62 ± 0.16 (n = 4)	53.15 ± 14.48 (n = 4)
F467L	3.31 ± 0.77 (n = 4)	45.62 ± 8.71 (n = 4)
R468L	0.91 ± 0.11 (n = 4)	32.67 ± 4.72 (n = 4)

Table 3.2, Km and Vmax values for mutated glucose transporters. The table displays the calculated Km and Vmax values for the mutated glucose transporters.

Because the region of the C-terminus, R468 - G466, had previously been shown to be important by C-terminal deletion analysis it was thought that the introduction of point mutations would greatly affect the function of the glucose transporter. However, it was observed from the data, that there have been no substantial alterations in GLUT1 kinetics. For example, the kinetics of GLUT2 have certainly not been conferred upon the GLUT1 protein. Nevertheless, slight variations in transporter Km were observed in some mutants and have been demonstrated to be statistically significant, these results can be seen more clearly when plotted as follows in figure 3.4.

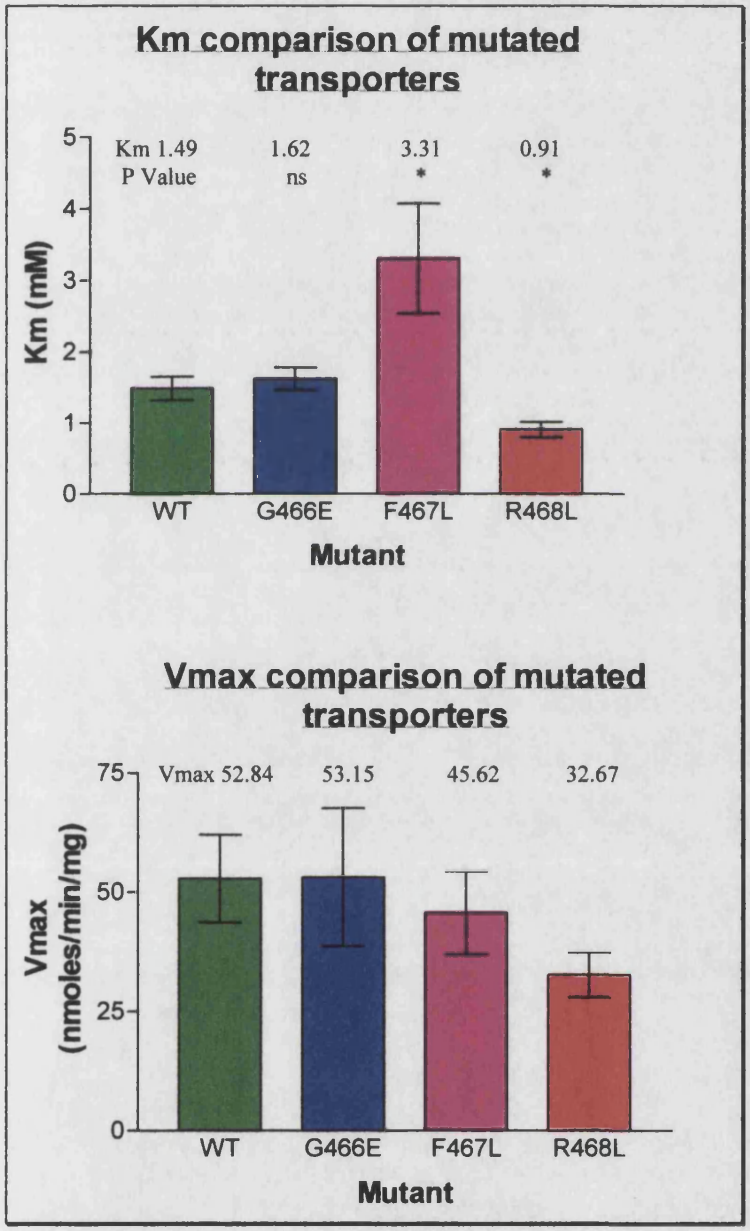

Figure 3.4, Km and Vmax comparison between mutants. The Km comparison with WT transporter shows a significant variation in the measured Km of mutant F467L and R468L. The P value is significant if P = <0.05; ns = none significant; * = significant. Mutant G466E P = 0.5822; mutant F468L P = 0.0360; R468L P = 0.0285. P values were derived from two tailed, unpaired t-test analysis, each mutant was compared with the wild-type GLUT1 data.

Mutant G466E does not have a significantly different Km value from the wild-type protein. However, t-tests have shown that there was a significant difference between the Km of mutant R468L and the wild-type protein and the Km of F467L and

the wild-type protein. None of the Vmax values were found to be significantly different. This result further demonstrates the importance of the C-terminal region of the glucose transporter in kinetic control.

Section 3.3
Discussion

The experiments carried out by Muraoka *et al.*, (1995) and Katagiri *et al.*, (1992) indicated that the C-terminal region is important for glucose transporter function, as the following two points show:

1) A 25 amino acid C-terminal GLUT1 deletion resulted in a Km of 0.92 ±0.14 mM and a Vmax of 20.2 ±1.15 nmoles/min/mg for 2-deoxy-D-glucose, similar to the R468L mutant (Muraoka *et al.*, (1995).
2) A chimeric protein composed of GLUT1 with the GLUT2 C-terminus produces a transporter with GLUT2 kinetics (Katagiri *et al.*, (1992).

The mutation of arginine 468 to leucine resulted in a significant reduction in the measured Km. Both arginine and leucine are large amino acids, having similar van der Waals volumes, being 148 and 124 $Å^3$, respectively. However, leucine is a non-polar, hydrophobic amino acid, whereas arginine is a hydrophilic amino acid carrying a positive charge at physiological pH. It is likely that this non-conservative substitution has altered the protein conformation in some way.

Phenylalanine 467 was exchanged for leucine. The phenylalanine 467 to leucine mutation did have the effect of lowering the glucose transporters affinity towards the substrate. Mutating glycine 466 to glutamic acid made no significant difference to transport activity.

In summary, the three point mutations studied did not substantially affect the function of GLUT1. It appears that glucose transporter function is controlled by a large region of protein (possibly the whole of the C-terminus) and that individual amino acids are less important. The overall structure would then influence the function of the transporter. C-terminal deletions and chimeric protein studies support this theory.

4.0 Construction of Recombinant Baculovirus Transfer Vectors

Section 4.1 Introduction

The insect cell system was chosen to express the modified glucose transporter constructs because:

a) A relatively large amount of protein can be readily produced
b) The system has been previously characterised, producing functional GLUT1 protein.

Insect cells are capable of targeting the full length glucose transporter to its correct location in the plasma membrane. Kuroda *et al.,* (1990) have shown that limited glycosylation occurs in insect cells.

Foreign proteins are expressed in the insect cell system by a baculoviral transfer vector, which must be modified to contain the cDNA of interest. The baculovirus transfer vector is a plasmid containing an *E. coli* origin of replication, a multiple cloning site downstream of a viral promoter site and baculovirus specific recombination sequences. The cDNA of interest is inserted into the multiple cloning site, followed by the amplification of the resulting plasmid in *E. coli.* The transfer vector can then be recombined with wild-type baculovirus DNA within insect cells and viable virus will then replicate. Because the foreign cDNA will replace the gene for the polyhedrin coat protein, recombinant viral particles are unable to produce the polyhedrin coat protein. The polyhedrin coat protein is clearly visible under the light microscope making it possible to select for the recombinant virus from the non-recombinant wild-type virus.

Two of the transfer vectors used in this thesis are fusion vectors. The pBBH transfer vector fuses a polyhistidine tag onto the N-terminal end of the expressed protein, allowing for purification upon a chelating nickel Sepharose column. The pAC360 transfer vector fuses a short sequence of the polyhedrin gene onto the start of the protein. This transfer vector was used in an attempt to increase the level of expression of the foreign protein. In both constructs the GLUT1 123 base pair non-coding region was eliminated.

Rabbit cDNA encoding the glucose transporter, isoform 1 (GLUT1), was supplied to the laboratory by Asano, in the plasmid pUC19 (Asano *et al.*, (1988)). The cDNA was inserted in the *Eco*RI restriction site as displayed in figure 4.1:

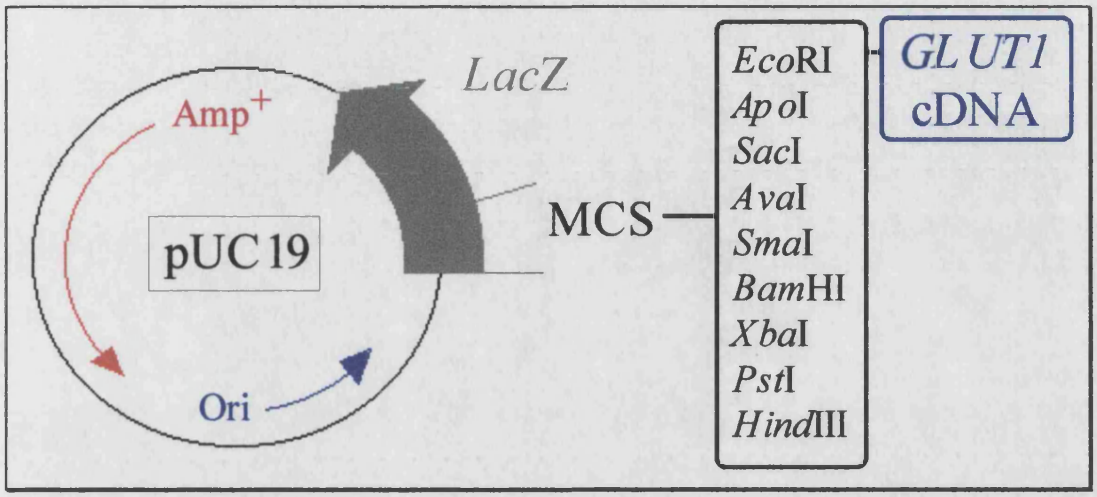

Figure 4.1, *GLUT1* cDNA contained in the vector pUC19.

pUC19:*GLUT1* served as the source DNA for all of the glucose transporter constructs. Table 4.1 defines the origin of these plasmids / viruses, the expressed protein sequence can be found in appendix 14.2.

Plasmid and Virus Generated by:	Plasmid construct
Present thesis	pLE12
Present thesis	pBBH:*GLUT1* (pLE14)
Plasmid constructed by Cope 1994 Virus produced in present thesis	pBBH:C-Term
Produced by Cope *et al.* (1994)	pVL1392: *GLUT1* (Baculovirus E4.2)
Produced by Cope *et al.* (1994)	pVL941:*GT52* (Baculovirus R12)

Table 4.1, History of vectors used within the present thesis. The production of pLE12 and pLE14 are described in this thesis. The plasmid pBBH:C-Term was produced by Cope (1994), but the virus was produced as described in this thesis. pVL:*GLUT1* (Baculovirus E4.2) and pVL:*GT52* (Baculovirus R12) were produced by Cope (1994).

The baculovirus transfer vector pLE12 codes for a GLUT1 fusion protein, expressing 15 amino acids from the polyhedrin coat protein. A 6 membered histidine sequence has been engineered into the first extracellular loop of GLUT1.

The baculovirus transfer vector pLE14 codes for a fusion protein containing a leader sequence encoding a 6 membered histidine sequence, an enterokinase site and then the full length GLUT1 protein.

The baculovirus transfer vector pBBH:C-Term was generated by Cope (1994). The C-terminal portion of the glucose transporter was subcloned from the plasmid pVL941:GT52, into the plasmid pBBH. The baculovirus transfer vector, pBBH:C-Term, expresses a leader sequence encoding 6 histidine residues, an enterokinase site and then the C-terminal portion of the GLUT1 protein. Baculovirus E4.2 expresses the full-length GLUT1 protein. Baculovirus R12 expresses the C-terminal portion of the GLUT1 protein.

Section 4.2

Construction of Plasmid pLE12

pUC19:*GLUT1*

pUC19:*GLUT1*, the starting material for all constructs developed can be clearly visualised in figure 4.2:

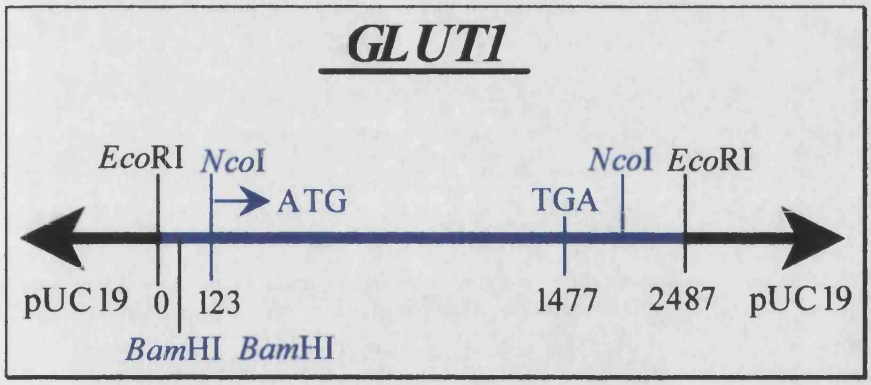

Figure 4.2, pUC19:*GLUT1* DNA containing the *GLUT1* cDNA. pUC19:*GLUT1* contains the *GLUT1* cDNA within two *Eco*RI sites. Base pairs 0-123 represent the 5' non-coding region and base pairs 1477-2487 represent the 3' non-coding region.

Epicurian Coli® SURE® competent cells (Supplied by Stratagene) were transformed with pUC19:*GLUT1* DNA and a large scale plasmid preparation was made using a Qiagen® maxi kit DNA binding column. As a diagnostic check, plasmid DNA was cut using *Nco*I and run on an agarose gel, with uncut DNA as a comparison. This confirmed the presence of two correctly sized bands, 3.653 kbp and 1.520 kbp. It was

concluded that the pUC19:*GLUT1* DNA was correct and of high quality and purity. A picture of the gel is displayed in figure 4.3.

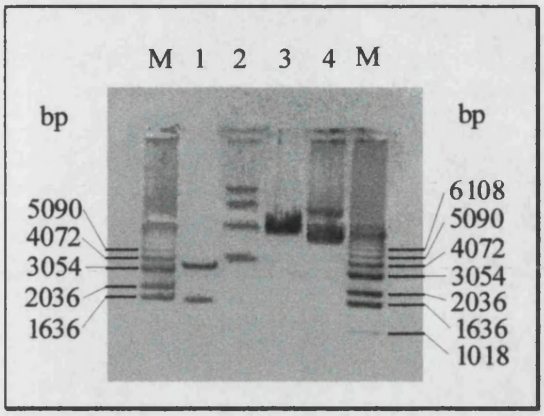

Figure 4.3, Digestion of pUC19:*GLUT1* with *Nco*I to check for the presence of *GLUT1* insert. A 0.8% agarose gel was loaded as follows: Lane M: 1 kbp marker (supplied by GibcoBRL); lane 1: 3 µl pUC19:*GLUT1* cut with *Nco*I; lane 2: 1 µl pUC19:*GLUT1*; lane 3: 3 µl pLE10 cut with *Nco*I; lane 4: 1 µl pLE10.

Section 4.3

Construction of pLE10 from pAC360

The plasmid pAC360 (supplied by Invitrogen) was the starting point for producing pLE10. pAC360 is a fusion vector and codes for a small portion of the baculovirus polyhedrin coat protein, expressed at the N-terminal end of the cloned protein. The cloning site of pAC360 has only one restriction site, *Bam*HI, displayed in figure 4.4. To take advantage of the two *Nco*I sites in the *GLUT1* cDNA (one of which cuts across the initiating ATG codon), the BamHI site of pAC360 was converted to an *Nco*I site by inserting a small linker oligonucleotide. The linker was designed to allow the *GLUT1* cDNA to be expressed in frame. The linker encoded *Bam*HI 'sticky' ends. On insertion the original *Bam*HI site was destroyed, leaving the *Nco*I site as the only constituent of the cloning site. The plasmid produced was then termed pLE10.

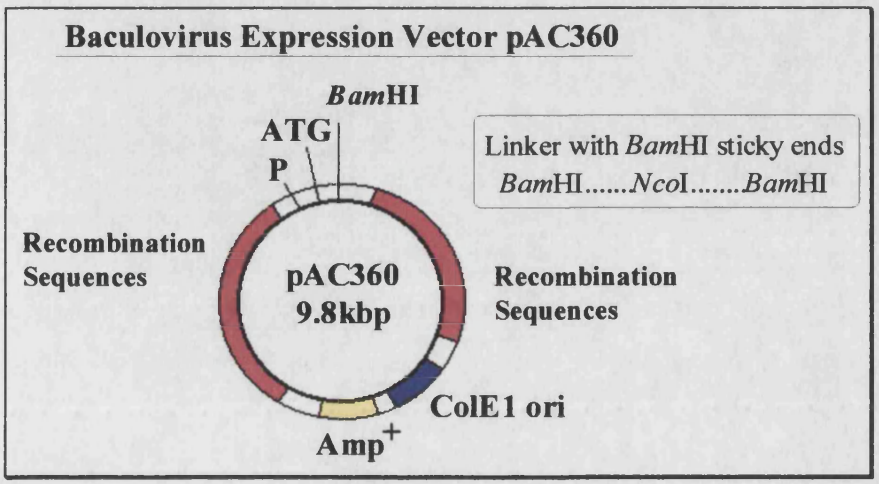

Figure 4.4, The baculovirus expression vector, pAC360. pAC360, a baculovirus transfer vector with a single *Bam*HI site in its cloning site.

The oligonucleotides (supplied by Seven Biotech) used to modify pAC360 were as follows:

Destroys BamHI site on insertion

BamHI sticky end ↓ NcoI Site ↓ BamHI sticky end

```
GAT CAT GCC ATG GA
    TA CGG TAC CT CTAG
```

The oligonucleotides were unphosphorylated to limit the formation of concatamers. *Bam*HI linearised pAC360 and linker were ligated at room temperature for 2 h. The ligated product was used to transform calcium chloride competent Top10 *Escherichia coli* (*E. coli*) cells. Following transformation 12 colonies were selected, amplified and the plasmid DNA extracted. DNA samples were cut separately with *Bam*HI / *Nco*I and compared. Plasmids cut by *Nco*I were found to contain the mutagenic linker. Plasmids cut by *Bam*HI do not contain the mutagenic linker. Only one out of 12 colonies, clone 3, appeared not to have taken up the linker, figure 4.5.

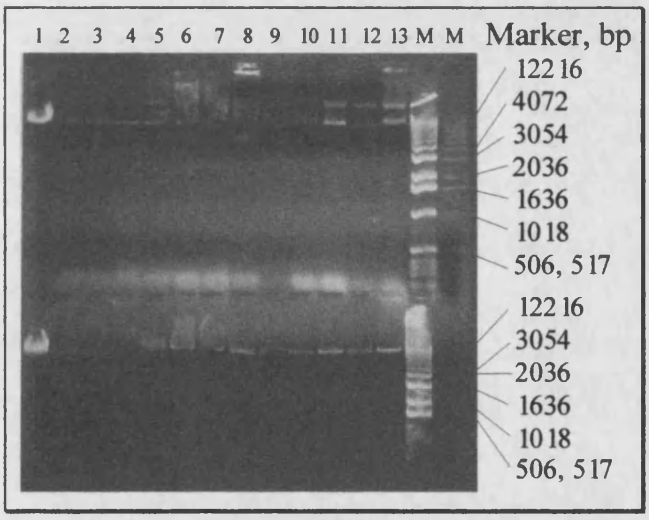

Figure 4.5, Construction of pLE10 from pAC360, demonstrating the absence of the *Bam*HI restriction site. A 0.8% agarose gel was loaded as follows: Lane 1: pAC360; lane 2: clone 1; lane 3: clone 2; lane 4: clone 3; lane5: clone 4; lane 6: clone 5; lane 7: clone 6; lane 8: clone 7; lane 9: clone8; lane 10: clone 9; lane 11: clone 10; lane 12: clone 11; lane 13: clone 12; M: 1 kbp marker.

Because it was possible for the oligonucleotide to insert bi-directionally (ie. in reverse), 3 plasmids containing the linker, clone 10, clone 11 and clone 12, were sequenced. DNA sequencing confirmed that clone 12 contained the correct linker sequence.

DNA sequencing also demonstrated the presence of aberrant linkers. The integrity of the oligonucleotide linkers was checked by end-labelling as described in the materials and methods section. End-labelling demonstrated the presence of more than one product (three major, and at least two minor products) indicating that the oligonucleotides were a mixture of products.

Section 4.4

Construction of pLE11 from pLE10

pLE11 is pLE10 containing the *GLUT1* cDNA, this is displayed in figure 4.6.

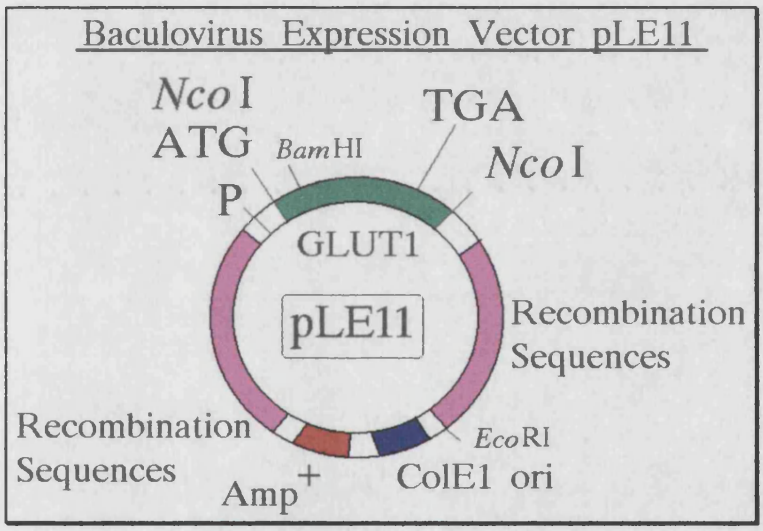

Figure 4.6, Plasmid map of pLE11. This vector contains the *GLUT1* cDNA in frame, in the correct orientation. The *Nco*I sites are found at either end of the *GLUT1* cDNA, and a unique *Bam*HI site exists in the first quarter of the cDNA.

*Nco*I cut pUC19:*GLUT1* was extracted from a low melting point agarose gel. *Nco*I cut pLE10 DNA was treated with calf intestinal alkaline phosphatase (CIP), to dephosphorylate the vector and prevent re-circularisation without insert.

pLE10 was ligated with *GLUT1* insert, at room temperature for 4 h. Following ligation, the resulting DNA mixture was transformed into Stratagene Epicurian Coli® SURE® competent cells. This resulted in several hundred colonies from which 12 colonies were selected, amplified and the plasmid extracted. The correctly inserted oligonucleotide was screened for by double digestion of the plasmid DNA with *Bam*HI and *Eco*RI. Following the identification of the correctly inserted cDNA, DNA sequencing was performed to confirm the integrity of the insert, the sequence is displayed in figure 4.7. The *GLUT1* cDNA was found to be inserted correctly.

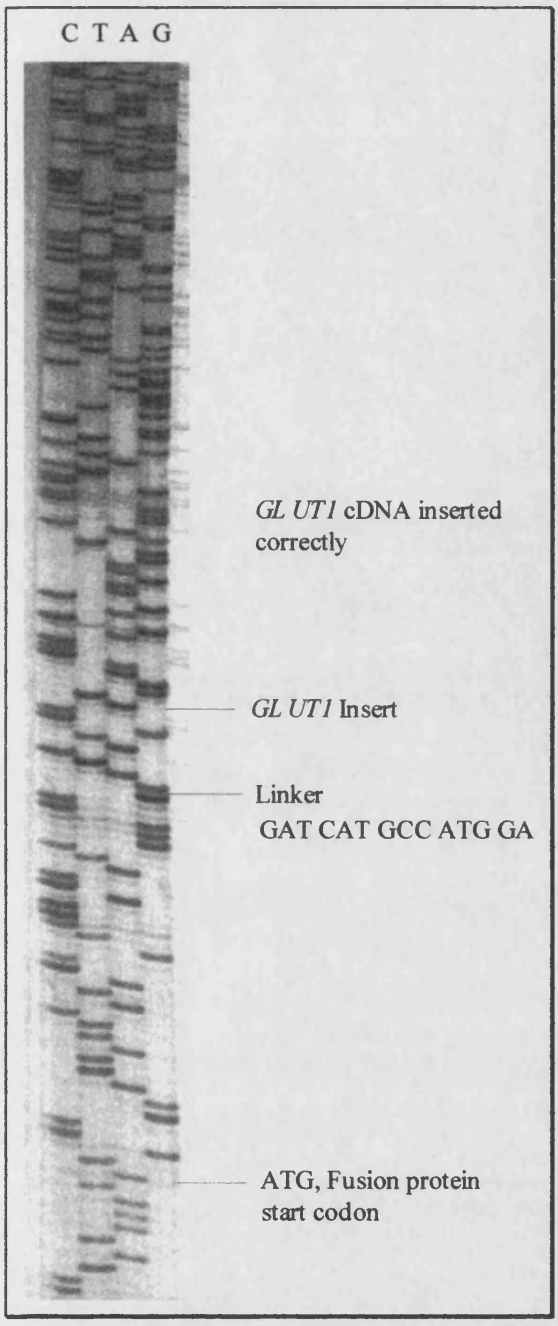

Figure 4.7, Sequencing of pLE11, clone 10. Sequencing reactions were performed according to section 2.26 in Materials and Methods. Bacterial clone 10 was shown by sequencing to contain the correctly inserted *GLUT1* cDNA. The full sequence is read as follows:
CCTATAAAT (start of fusion protein) ATG CCG GAT TAT TCA TAC CGT CCC ACC ATC GGG CCG (linker) GAT CAT GCC *(GLUT1)* ATG GAA CCC AGC AGC AAG AAG GTG ACG GGC CGC CTC ATG CTG GCC GTG GGA GGA GCA G...

Clone 10 is seen to contain the *GLUT1* cDNA in the correct orientation. The *GLUT1* sequence matches the published sequence exactly. Clone 10 was termed pLE11 and used in the next step, to produce the final vector pLE12.

Section 4.5

Construction of pLE12 from pLE11

This was the final stage in the construction of this baculovirus transfer vector and entailed the insertion of six codons, coding for histidine, into the unique *Bam*HI site present in the *GLUT1* cDNA (c.f. fig. 4.6). This was achieved by cutting the vector pLE11 with *Bam*HI and inserting a small linker encoding the six histidine residues. The linker had *Bam*HI sticky ends, destroying the *Bam*HI site on insertion and was composed of the following oligonucleotides (Supplied by VHBio):

```
G ATC ACG CAC CAT CAC CAT CAC CAT CA
      TGC GTG GTA GTG GTA GTG GTA GTC TAG
```

The histidine codons alternated between the two possibilities in the linker. It was hoped that this would result in improved expression by not requiring the repetitive use of any one type of tRNA molecule.

*Bam*HI cut pLE11 was ligated with the annealed oligonucleotides and transformed into Stratagene SURE® competent cells. This resulted in several hundred colonies, of which only 24 were picked for screening. Mini preparations were digested with *Bam*HI. Only 2 out of the 24 clones were linearised during this screening step, indicating that 22 of the clones had taken up the linker, therefore destroying the *Bam*HI site. The first five clones were manually sequenced confirming that three contained the linker inserted correctly, in frame. One contained the linker in reverse and one was a mis-sense construct. The sequence of the correct clone is displayed as text below:

GLUT1 » TTT GGC TAC AAC ACT GGA GTC ATC AAC GCC CCC CAG AAG GTG ATC GAG GAG TTC TAC AAC CAG ACG TG Linker » G ATC ACG CAT CAC CAT CAC CAT CAC CA « Linker *GLUT1* » G ATC CAC CGC TAT GGG GAG CGC ATC TTG CCC ACC A...

The linker can be seen to have inserted in the correct orientation and is intact. The *GLUT1* bases sequenced either side of the linker match the published sequence exactly, indicating the cDNA to be intact. The bacterial colony producing this construct

was amplified and the plasmid purified using a Qiagen® maxi kit DNA binding column. This clone was termed pLE12 and was used in subsequent experiments.

Section 4.6

Construction of pBBH:*GLUT1*, pLE14

The plasmid pBBH is a baculovirus transfer vector (supplied by Invitrogen). The cloned DNA is expressed as a fusion protein product with a polyhistidine sequence at the N-terminal end. This allows for the purification of the recombinant protein on a chelating nickel Sepharose column. A schematic diagram of pBBH is displayed in figure 4.8.

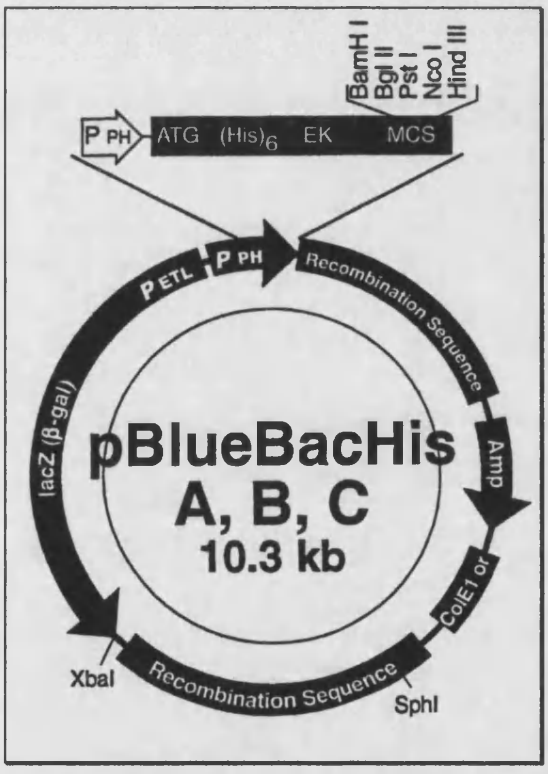

Figure 4.8, The baculovirus transfer vector p Bac Blue His. The transfer vector pBBH comes in three forms, allowing for protein expression in three different reading frames. *GLUT1* derived from pUC19:*GLUT1* was inserted into the *Nco*I site of pBBH B to allow the expression of the *GLUT1* cDNA in frame. The fusion protein added on the N-terminal end of the protein is displayed at the top of the vector. Following the initiating ATG start codon 6 histidine residues are expressed, with a short run of amino acids, before a recognition site for the enzyme enterokinase (Recognition sequence: Asp, Asp, Asp, Asp, Lys//). The multiple cloning site falls shortly after the enterokinase site. The diagram was taken from Invitrogen's technical advice.

*Nco*I digested pUC19:*GLUT1* was excised from a low melting point agarose gel. *Nco*I digested pBBH B DNA was treated with calf intestinal alkaline phosphatase (CIP) to dephosphorylate the vector and prevent re-cirularisation without insert. The *GLUT1* cDNA insert was ligated into the pBBH B transfer vector, at room temperature for 4 h.

Following ligation, the resulting DNA mixture was transformed into Stratagene Epicurian Coli® SURE® competent cells. This resulted in several hundred colonies from which 12 colonies were selected, amplified and the plasmid extracted. The insert was detected by digestion with the restriction enzyme *Nco*I. DNA containing the *GLUT1* insert was seen to be cut twice with *Nco*I.

Clones 13, 14, 15, 18, 20, 23 and 24 were all shown to contain the *GLUT1* cDNA. The orientation of the *GLUT1* insert was determined by digesting the clones with *Bam*HI. All clones which had been shown to contain an insert by digestion with *Nco*I, but which did not show an insert with *Bam*HI (insert is actually too small to be seen on these gels) contain the *GLUT1* cDNA in the correct orientation. Clones 15, 23 and 24 were all shown to contain correctly inserted *GLUT1* cDNA and clone 15 plasmid DNA was taken and the sequence confirmed using manual DNA sequencing, figure 4.9.

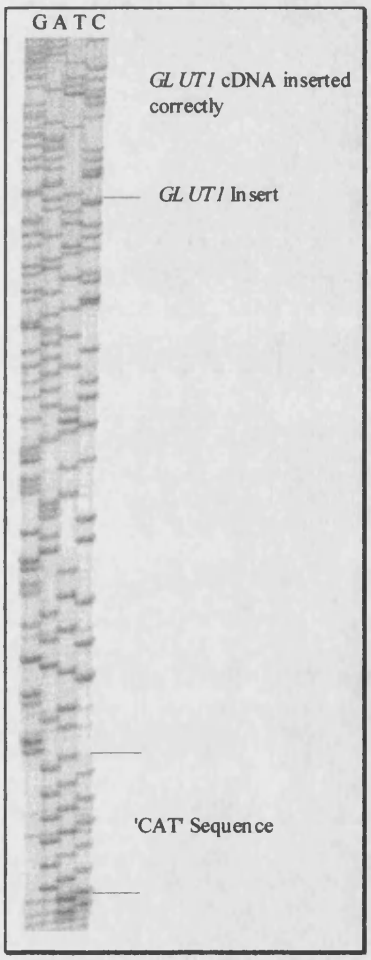

Figure 4.9, Sequencing of putative pLE14, clone 15. Sequencing reactions were performed according to section 2.26 in Materials and Methods. Sequencing demonstrated clone 15 to be correct. The GLUT1 cDNA has been inserted in the correct frame and orientation. The sequence read is an exact match to the published sequence. The full sequence read is as follows:

```
Fusion protein with polyhistidine tag » T TCT CAT CAT CAT CAT CAT CAT
  GGT ATG GCT AGC ATG ACT GGT GGA CAG CAA ATG GGT CGG GAT CTG TAC GAC
  GAT GAC GAT AAG GAT CCG AGC TCG AGA TCT GCA GCT GGT ACC GLUT1 » ATG
  GAA CCC AGC AGC AAG AAG GTG ACG GGC CGC CTC ATG C
```

Clone 15 has been confirmed to contain the correct insert, in the correct orientation and reading frame. Clone 15 was termed pLE14.

Section 4.7

Discussion

In summary, both constructs generated were sequenced and were determined to contain inserts in the correct frame and orientation. Furthermore, the inserts were determined to be faithful to the published sequence. These constructs were used in subsequent work. As additional information, extracts of published DNA sequences are contained in the appendix of this thesis.

5.0 Expression of Proteins Encoded by Recombinant Baculovirus Transfer Vectors

Section 5.1 Introduction

The p Bac Blue His (pBBH) range of baculovirus transfer vectors allowed for the co-expression of the β-galactosidase gene with the cloned gene of interest (as separate gene products). The enzyme β-galactosidase acts on the colourless artificial substrate X-gal (5-bromo-4-chloro-3-indoyl-β-D-galactoside) to produce an insoluble blue precipitate. This made it possible to select for recombinant viral particles by incubation with the chromogenic substrate X-gal. Recombinant viral plaques, expressing β-galactosidase, produce a blue coloration surrounding the viral plaque. Whereas wild-type virus, which has not recombined with the transfer vector, does not contain the β-galactosidase gene and is therefore unable to convert X-gal into the coloured product. Furthermore, infection with wild-type virus produces polyhedra which can be clearly seen under the microscope within the infected cell. Both the absence of polyhedra and the presence of a blue coloration leads to the rapid identification of putative recombinant viral plaques.

However, baculovirus transfer vectors based on the plasmids pVL1392, pVL941 and pAC360 express only the proteins engineered into the cloning site. Putative recombinant viral plaques must be screened by microscopic observation in order to determine that plaques are polyhedrin negative.

Section 5.2

Co-Transfection and Protein Expression of Recombinant Baculovirus Transfer Vectors pLE14 (HIS-GLUT1) and pBBH:*GT52* (HIS-C-TERM) with AcMNPV in Sf9 Cells

The baculovirus transfer vectors pLE14 and pBBH:*GT52* coded for the HIS-GLUT1 and HIS-C-TERM proteins, respectively. Both vectors were taken separately and mixed with linear AcMNPV DNA (wild-type baculovirus expressing the polyhedrin protein). Vector and AcMNPV DNA were co-transfected as described in the materials

and methods section 2.27. Recombinant plaques were observed to be polyhedrin negative and to turn blue on the addition of the chromogenic substrate X-gal. Recombinant plaques were screened for expression of HIS-GLUT1 and HIS-C-TERM by immunoblotting (figure 5.1).

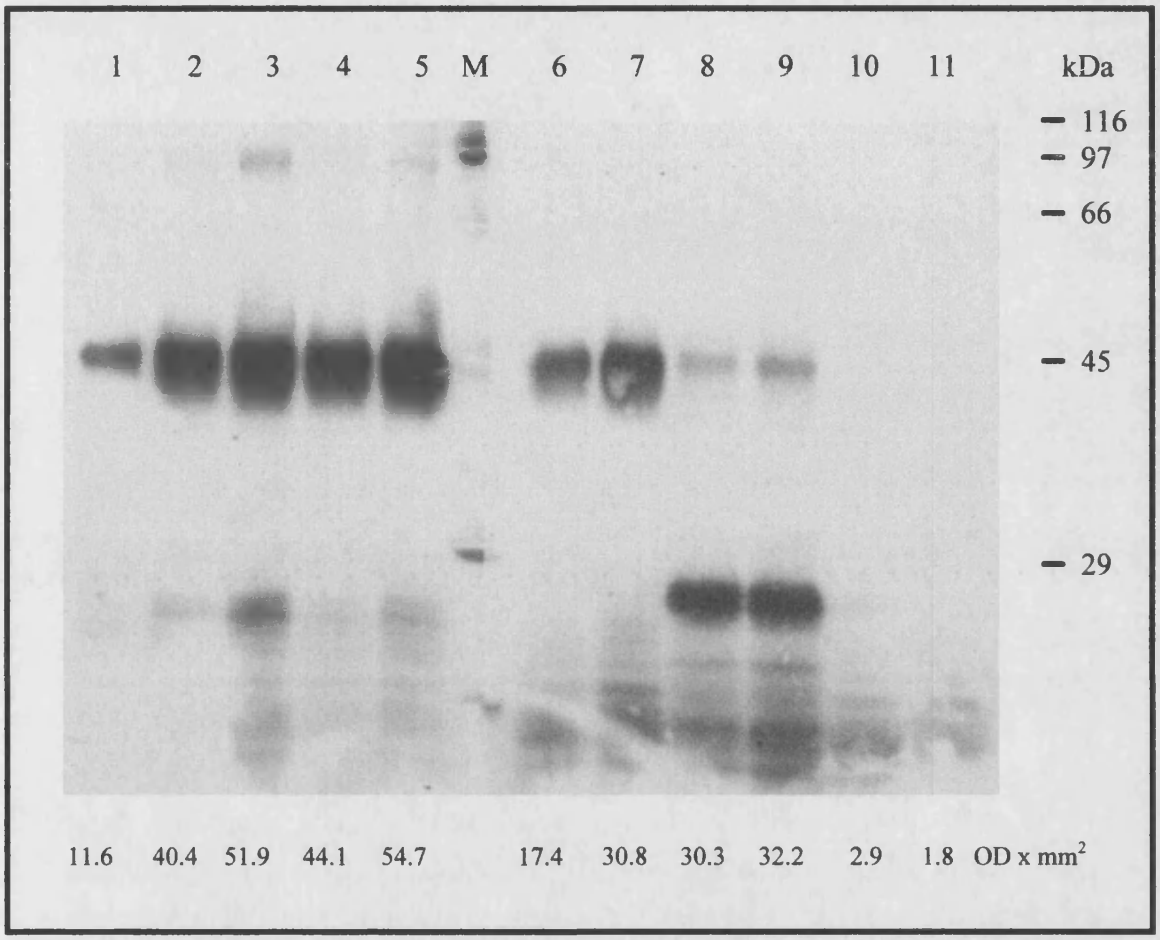

Figure 5.1, Recombinant protein expression assessed by immunoblot assay. A 10% polyacrylamide gel was loaded as follows: Lane 1: 30 μg of Sf9 cells expressing HIS-GLUT1 (clone A); lane 2: 30 μg of Sf9 cells expressing HIS-GLUT1 (clone B); lane 3: 40 μg of Sf9 cells expressing HIS-GLUT1 (clone B); lane 4: 30 μg of Sf9 cells expressing HIS-GLUT1 (clone C); lane 5: 40 μg of Sf9 cells expressing HIS-GLUT1 (clone C); lane M: High molecular weight marker; lane 6: 30 μg of Sf9 cells expressing HIS-GLUT1 (clone D); lane 7: 60 μg of Sf9 cells expressing HIS-GLUT1 (clone D); lane 8: 30 μg of Sf9 cells expressing HIS-C-TERM (clone E); lane 9: 40 μg of Sf9 cells expressing HIS-C-TERM (clone E); lane 10: 30 μg of Sf9 cells expressing HIS-C-TERM (clone F); lane 11: 30 μg of Sf9 cells expressing HIS-C-TERM (clone F); lane M: High molecular weight marker.

Optical densitometry analysis demonstrated that clones C and E, expressing the HIS-GLUT1 and HIS-C-TERM proteins respectively, expressed the most recombinant protein. Viral inoculum from clones C and E were taken for further plaque purification

and experimental analysis. Viral stocks were made by spinner culture. Typical viral titres obtained are displayed in table 5.1, section 5.5.

Section 5.3

Recombinant Protein Expression in Sf9 Cells

Recombinant viruses E4.2 and R12 were described by Cope *et al.,* (1994) and express the GLUT1 and C-TERM protein products, respectively. Large viral stocks were made from the smaller stocks provided. Viral titres were calculated by plaque assay.

Plaque purified recombinant virus was used to infect Sf9 cells. The cells were then analysed by immunoblot assay, figures 5.2 and 5.3.

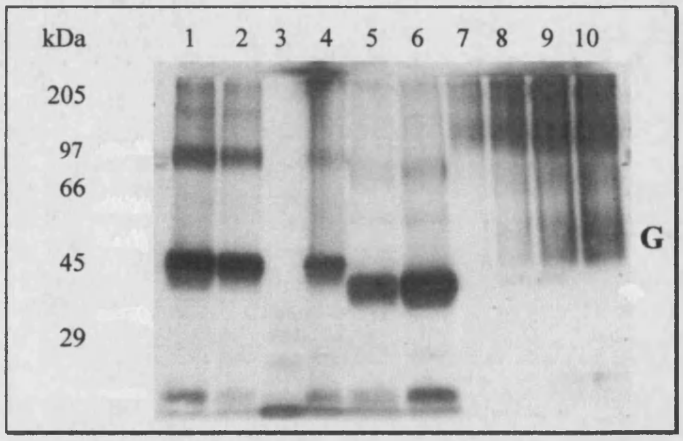

Figure 5.2, Expression of recombinant proteins GLUT1 and HIS-GLUT1. A 10% polyacrylamide gel was loaded as follows: Lane 1: 40 µg of Sf9 cells expressing HIS-GLUT1 (clone 8); lane 2: 30 µg of Sf9 cells expressing HIS-GLUT1 (clone 8); lane 3: 30 µg of Sf9 cells expressing GLUT1 (clone 31); lane 4: 30 µg of Sf9 cells expressing HIS-GLUT1 (clone 32); lane 5: 30 µg of Sf9 cells expressing GLUT1 (clone 34); lane 6: 30 µg of Sf9 cells expressing GLUT1 (clone 35); lane 7: 100 ng human GLUT1; lane 8: 200 ng human GLUT1; lane 9: 400 ng human GLUT1; lane 10: 500 ng human GLUT1. Human GLUT1 standard is marked with the letter G.

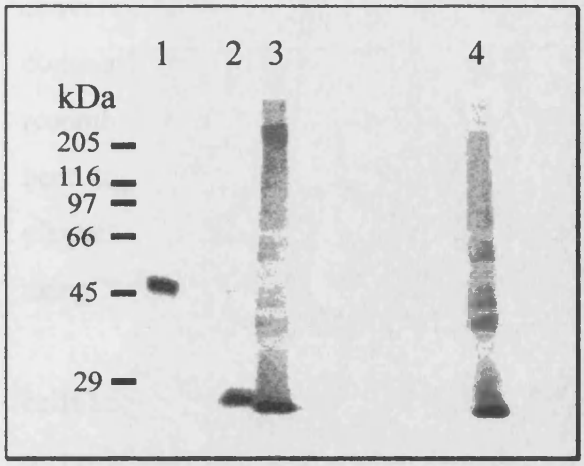

Figure 5.3, Expression of recombinant proteins C-TERM and HIS-C-TERM. A 10% polyacrylamide gel was loaded as follows: Lane 1: 30 µg of Sf9 cells expressing HIS-GLUT1; lane 2: 30 µg of Sf9 cells expressing HIS-C-TERM; lane 3: 30 µg of Sf9 cells expressing C-TERM; lane 4: 15 µg of Sf9 cells expressing C-TERM. NB. Image has been background corrected to allow visualisation of all bands.

Figures 5.2 and 5.3 demonstrated that all of the plaque purified recombinant proteins are expressed in Sf9 cells. The difference in apparent molecular weight between the histidine tagged and non-histidine tagged proteins (the histidine tagged proteins run more slowly through the gel) is thought to be attributable to the presence of the polyhistidine tag, the enterokinase recognition sequence and the linker amino acids in the modified protein.

Section 5.4

Co-Transfection of Transfer Vector pLE12 (G-HIS-LUT1) with AcMNPV and Bac-N-Blue DNA in Sf9 Cells

Co-transfection of pLE12 into Sf9 cells was attempted using linearised AcMNPV DNA. As a control, co-transfection was performed using the already successful transfer vector pLE14. Sf9 cells were co-transfected according to the materials and methods, section 2.27. Plaque assays performed on the putative viral inoculum did not reveal the presence of any recombinant viral plaques. However, since there were very few polyhedrin positive plaques present, it was conceivable that there was a problem with either the linear AcMNPV DNA or the Lipofectamine, or both. For this reason co-transfection was attempted using fresh triple cut Bac-N-Blue™ viral DNA (supplied by Invitrogen) which also had the advantage of reducing the number of non-recombinant viral plaques produced (non-recombinant viral plaques were reported by Invitrogen to be less than 10%). A 72 h incubation period exposure of the control

cells, co-transfected with pLE14, to the chromogenic substrate X-gal resulted in the conversion of X-gal from a colourless solution into a blue solution. This result was consistent with the recombination of the control vector with viral DNA, producing a recombinant virus expressing β-galactosidase. This indicated that co-transfection had been successful in the control. However, when pLE12 polyhedrin negative recombinant plaques were screened for none could be identified (pLE12 could not be screened for using X-gal as the vector does not co-express β-galactosidase).

It is possible that the protein encoded by the vector pLE12 is toxic to the insect cells and caused cell death before protein expression. Alternatively there may have been a problem with either the conditions of co-transfection, or the vector being co-transfected.

Section 5.5

Viral Titres

Viral stock titres are displayed below in table 5.1. Stock viruses were used to infect cells at a low multiplicity of infection (moi), approximately 0.1 plaque forming units per cell (Chen *et al.*, (1997)). Protein expression levels are discussed in chapters 6 and 7.

Recombinant virus	Expression vector	Recombinant protein	Titre (pfu/ml) (Passage Number, S: suspension culture derived)
LE12	pLE12	G-HIS-LUT1	-
LE14	pLE14	HIS-GLUT1	$1.2x10^6$ (P6, S)
BBH:*GT52*	pBBH:*GT52*	HIS-C-TERM	$1.1x10^6$ (P6, S)
E4.2	pVL1392:*GLUT1*	GLUT1	$1.7x10^6$ (P5, S)
R12	pVL941:*GT52*	C-TERM	$1.36x10^6$ (P5, S)

Table 5.1, Displaying viral origin and titre. pLE12 could not be co-transfected and so does not have a titre. Baculovirus vectors pLE14 and pBBH:*GT52* were co-transfected as described (section 5.2) and their titres are displayed. Viruses E4.2 and R12 were produced from small lab stocks.

Section 5.6

Time Course of Expression - Immunoblot Analysis

In order to determine the optimal time period for expression of recombinant protein, a time course of expression was carried out. Samples were taken from a spinner culture at 0, 24, 48, 72, 96 and 168 h for analysis by immunoblot assay. Time courses were run using both Sf9 cells and Highfive cells. The resulting immunoblots are displayed in figures 5.4 and 5.5.

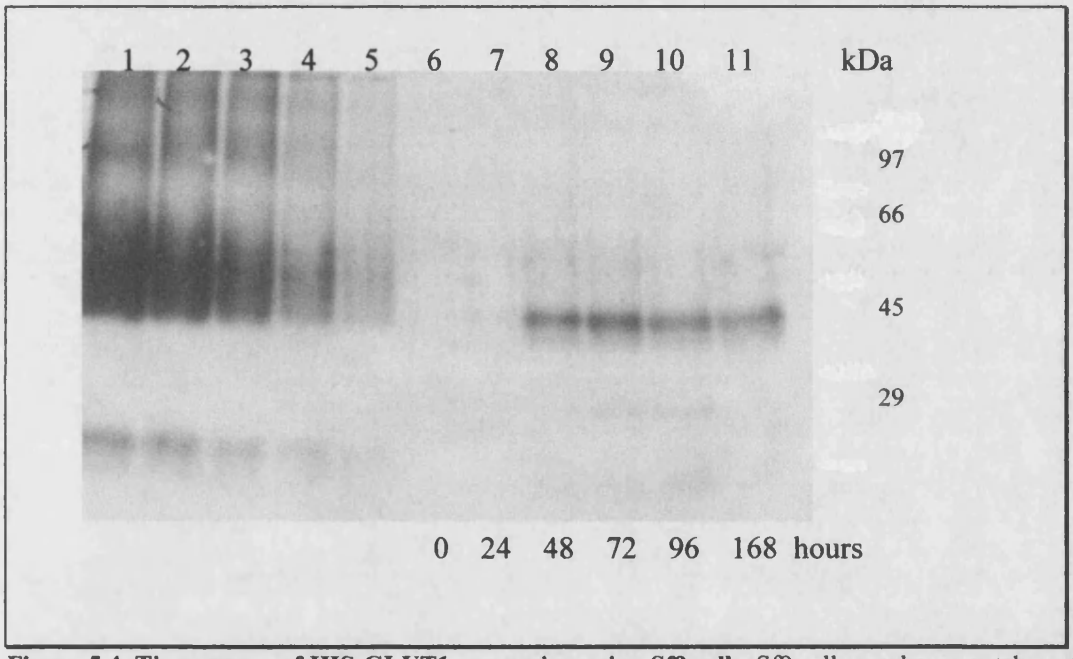

Figure 5.4, Time course of HIS-GLUT1 expression using Sf9 cells. Sf9 cell samples were taken at the appropriate time points (ie. 0, 24, 48, 72, 96 and 168 h) and run on a 10% polyacrylamide gel as follows: Lane 1: 100 ng human GLUT1 standard; lane 2: 75 ng human GLUT1 standard; lane 3: 50 ng human GLUT1 standard; lane 4: 25 ng human GLUT1 standard; lane 5: 10 ng human GLUT1 standard; lane 6: 0 h post infection, HIS-GLUT1; lane 7: 24 h post infection, HIS-GLUT1; lane 8: 48 h post infection, HIS-GLUT1; lane 9: 72 h post infection, HIS-GLUT1; lane 10: 96 h post infection, HIS-GLUT1; lane 11: 168 h post infection, HIS-GLUT1.

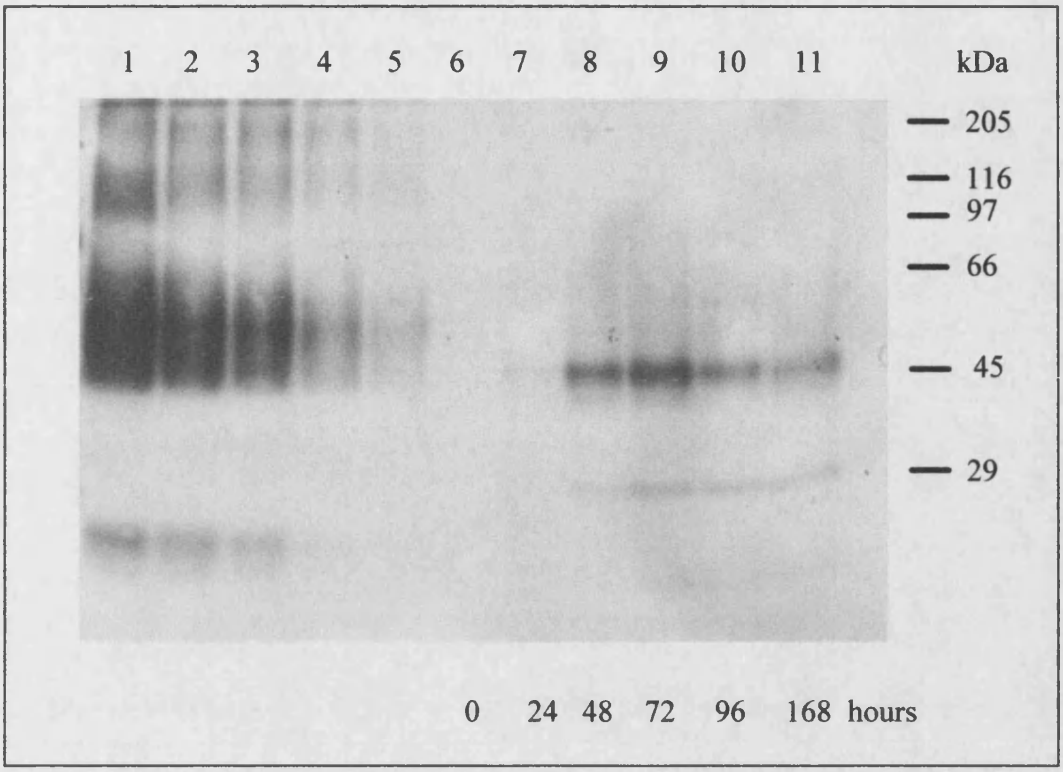

Figure 5.5, Time course of HIS-GLUT1 expression using Highfive cells. Highfive cell samples were taken at the appropriate time points (ie. 0, 24, 48, 72, 96 and 168 h) and run on a 10% polyacrylamide gel as follows: Lane 1: 100 ng human GLUT1 standard; lane 2: 75 ng human GLUT1 standard; lane 3: 50 ng human GLUT1 standard; lane 4: 25 ng human GLUT1 standard; lane 5: 10 ng human GLUT1 standard; lane 6: 0 h post infection, HIS-GLUT1; lane 7: 24 h post infection, HIS-GLUT1; lane 8: 48 h post infection, HIS-GLUT1; lane 9: 72 h post infection, HIS-GLUT1; lane 10: 96 h post infection, HIS-GLUT1; lane 11: 168 h post infection, HIS-GLUT1.

The immunoblots have been analysed by densitometric analysis using a BioRad scanner with molecular analyst software. These results can be plotted graphically and are displayed in figure 5.6

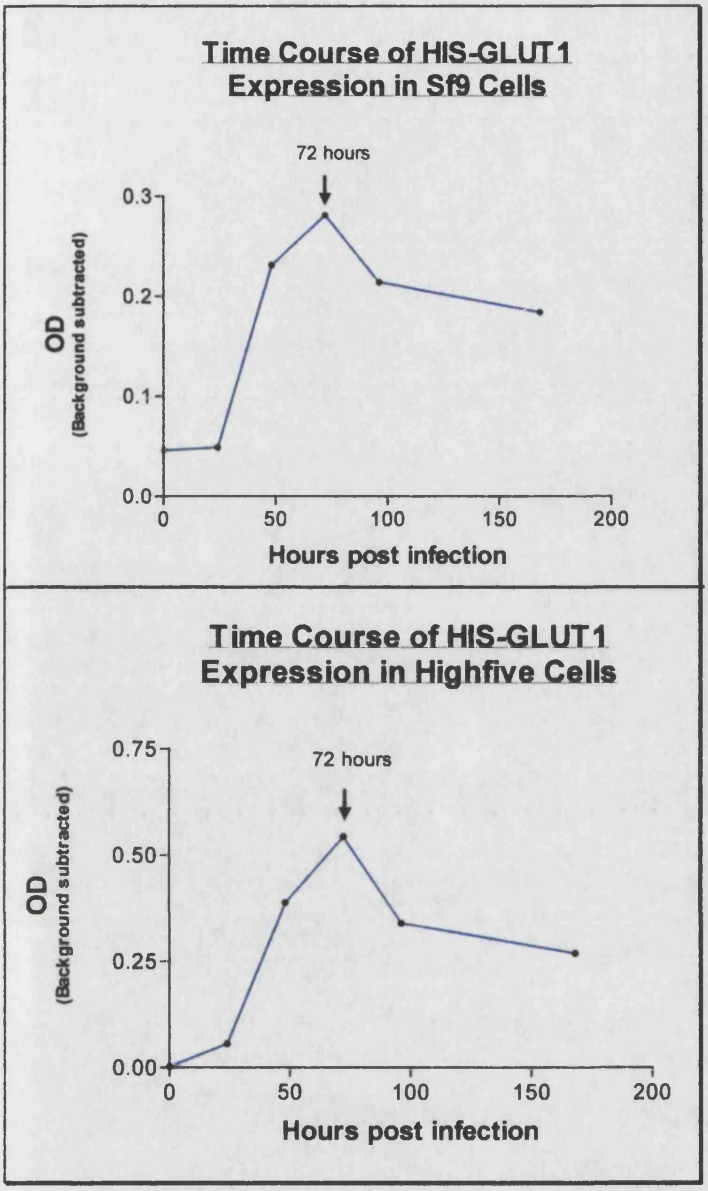

Figure 5.6, Graphical interpretation of HIS-GLUT1 time course in both Sf9 and Highfive cells. The optical density data were taken and plotted against hours post infection. The graphs clearly show maximum expression to be at 72 h post infection.

Immunoblot analysis demonstrated that maximum protein expression occurred at 72 h (3 days) post infection. Cells expressing recombinant protein were therefore always harvested at 72 h post infection. Following 72 h post infection the levels of recombinant proteins went into a decline phase. This may be due to cell lysis followed by the subsequent release of proteases into the growth medium.

Section 5.7

Time Course of Expression - Microscopic Analysis

The progress of cell infection was also monitored microscopically. This gave an indication of the progression of viral infection and allowed for the observation of any wild-type baculovirus contamination. As a comparison a photograph of Sf9 cells, infected with wild-type baculovirus is displayed below, figure 5.7.

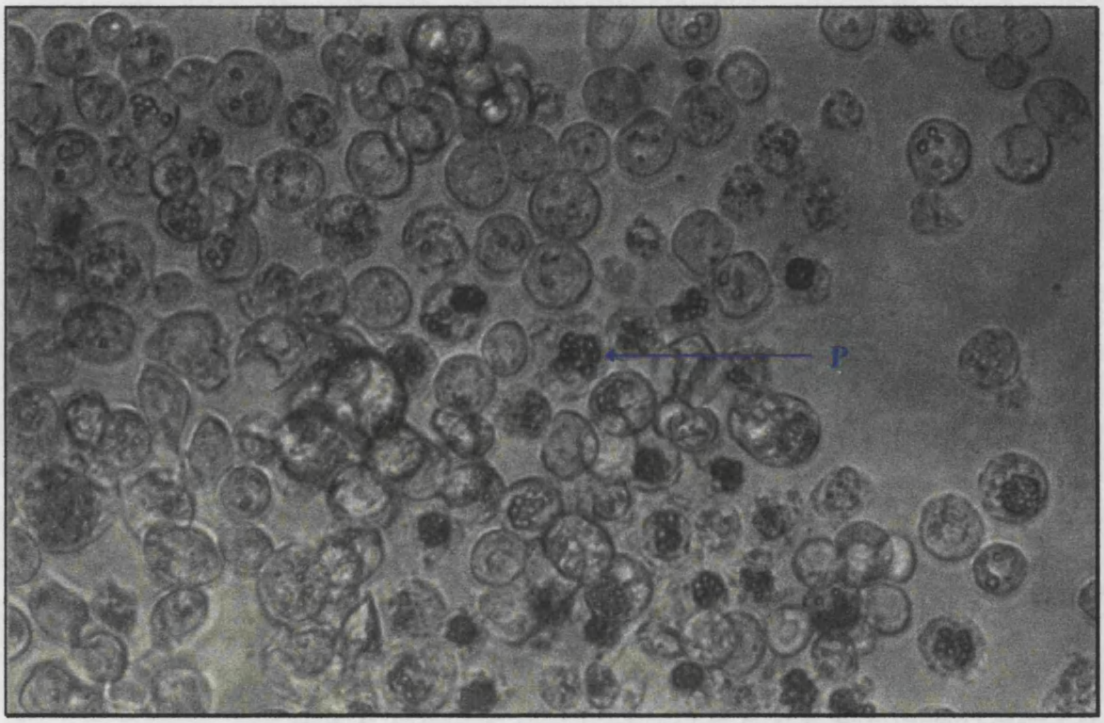

Figure 5.7, Sf9 cells infected with wild-type baculovirus. Cells were infected with wild-type baculovirus for 96 h and then observed under a light microscope. Occlusion bodies (polyhedrin) are clearly visible as small spherical objects seen within the cells, denoted by the letter P.

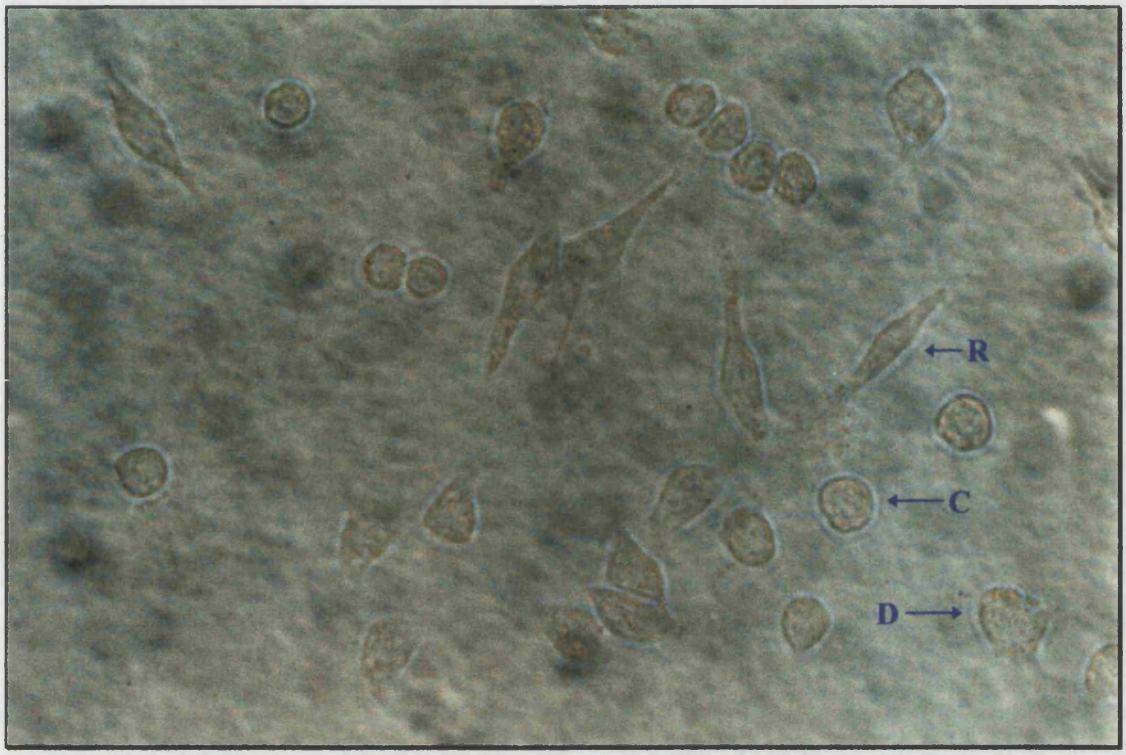

Figure 5.8, Uninfected control cells. Uninfected Sf9 cells have a smooth surface and form spherical shapes during cell growth, cell C is an example of this. During cell division they become elongated and rod shaped, illustrated by cell R. The lower right hand corner of the picture shows a dead cell, cell D. Dead cells have an uneven, crenellated surface due to the breakdown of the plasma membrane.

Uninfected cells have the above healthy appearance, demonstrated by the cells marked C and R. Before infection with recombinant virus and during passaging, cells were checked to ensure they were viable and uninfected with recombinant or wild-type virus. The following figures 5.9a-d and 5.10a-d display a time course of infection in Sf9 cells using two recombinant viruses, expressing HIS-GLUT1 and HIS-C-TERM respectively. Examples of infected cells are denoted by the letter I and healthy cells by the letter C. All of the cells infected with recombinant virus are observed to be uninfected with wild-type virus.

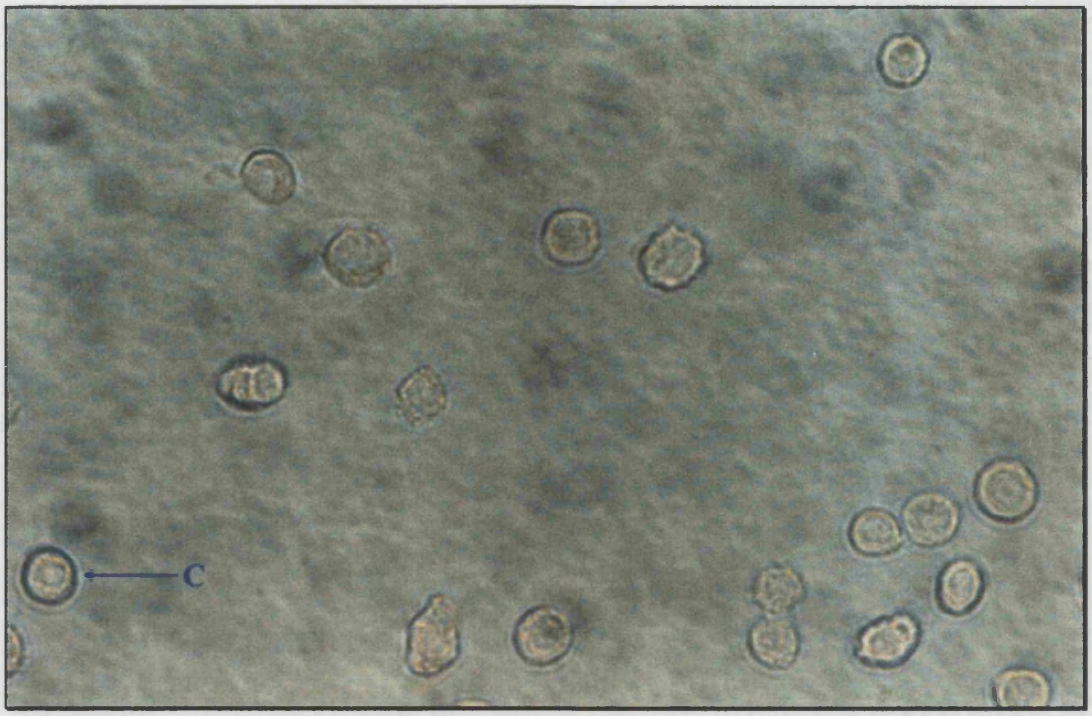

Figure 5.9a, Sf9 cells expressing HIS-GLUT1 24 hours post infection. The letter C illustrates a healthy cell.

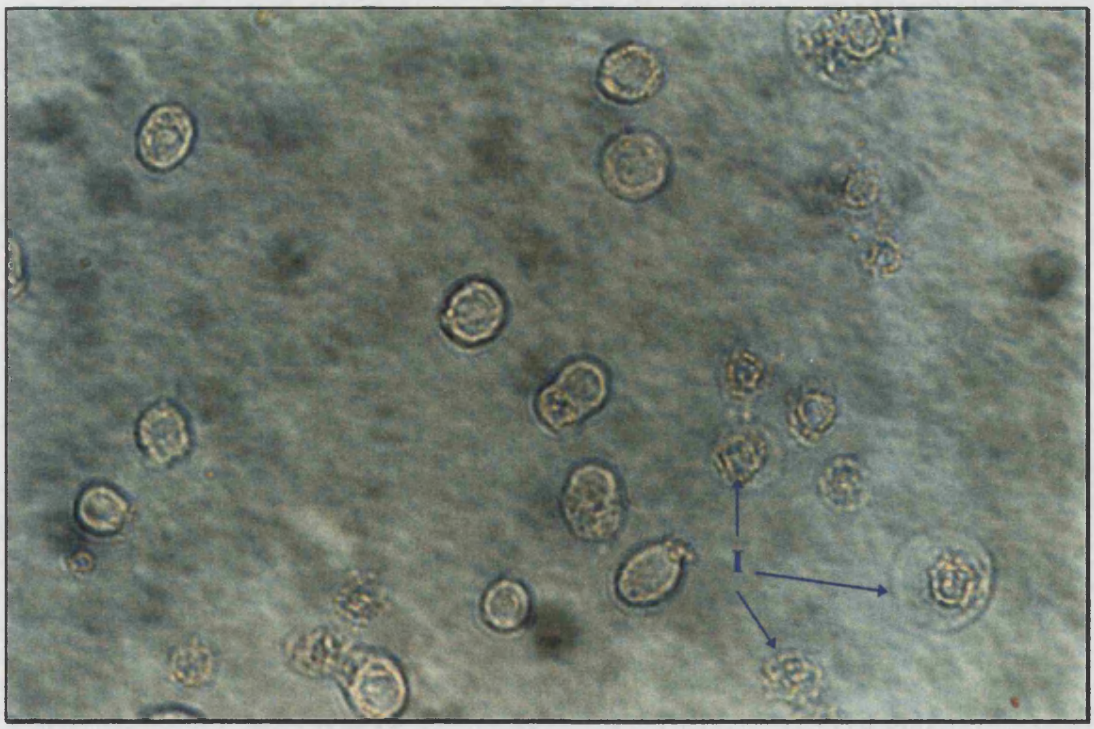

Figure 5.9b, Sf9 cells expressing HIS-GLUT1 48 hours post infection. The letter I illustrates an infected cell.

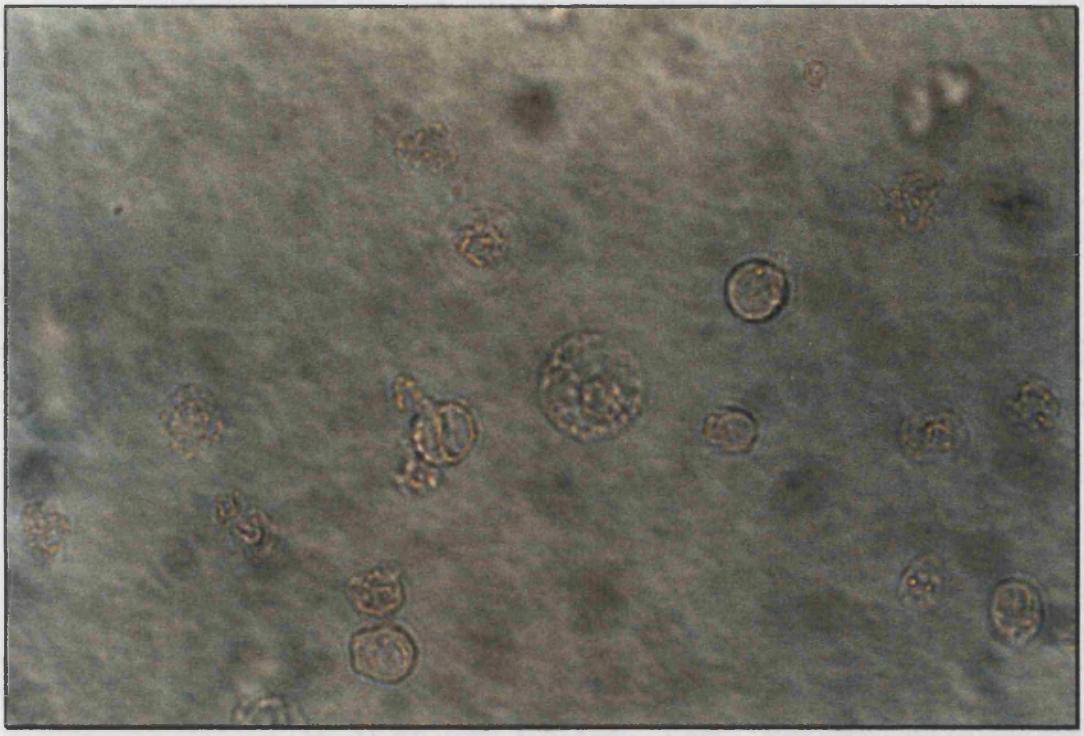

Figure 5.9c, Sf9 cells expressing HIS-GLUT1 72 hours post infection.

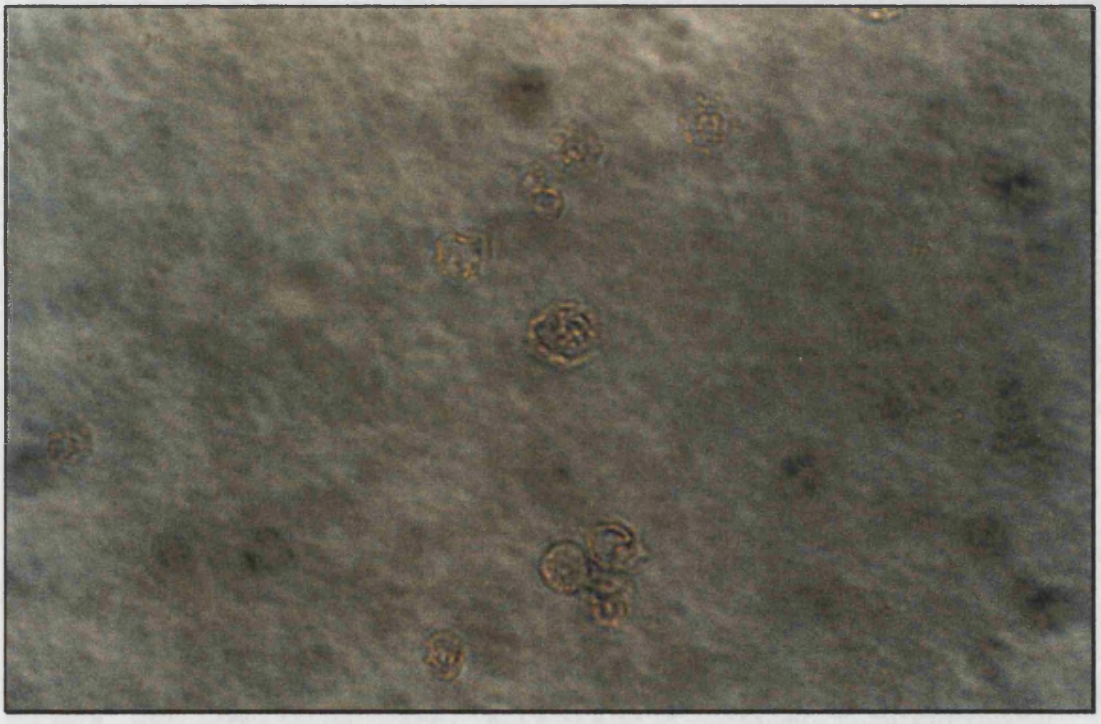

Figure 5.10d, Sf9 cells expressing HIS-GLUT1 96 hours post infection

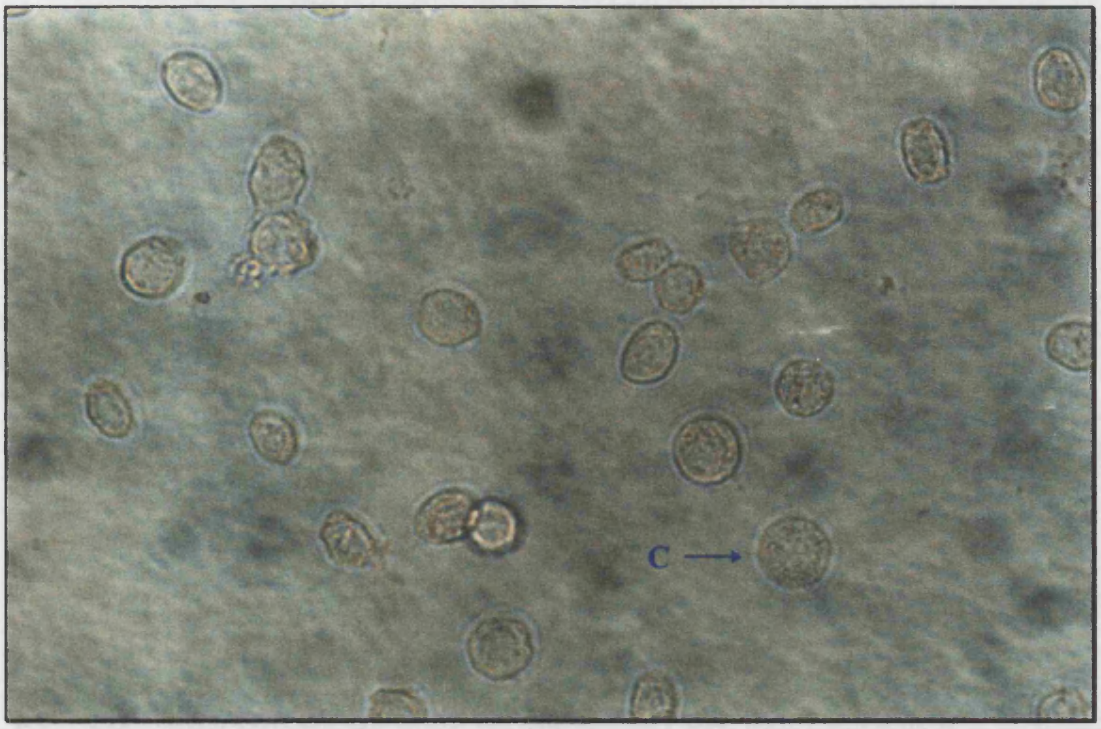

Figure 5.11a, Sf9 cells expressing HIS-C-TERM 24 hours post infection. The letter C illustrates a healthy cell.

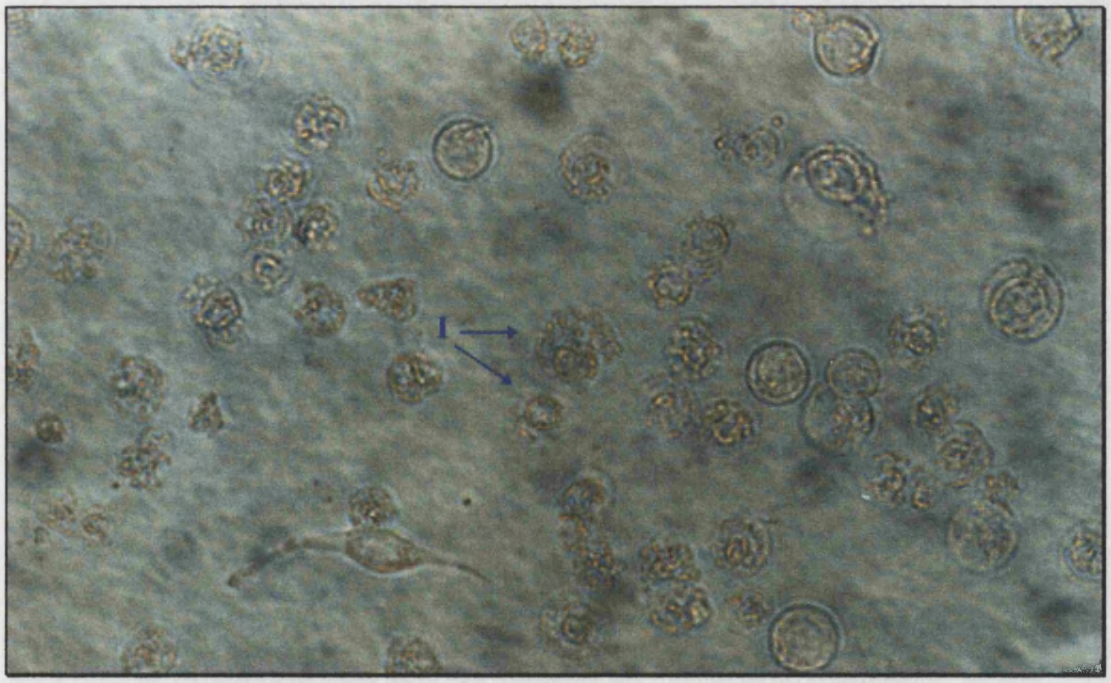

Figure 5.11b, Sf9 cells expressing HIS-C-TERM 48 hours post infection. The letter I illustrates an infected cell.

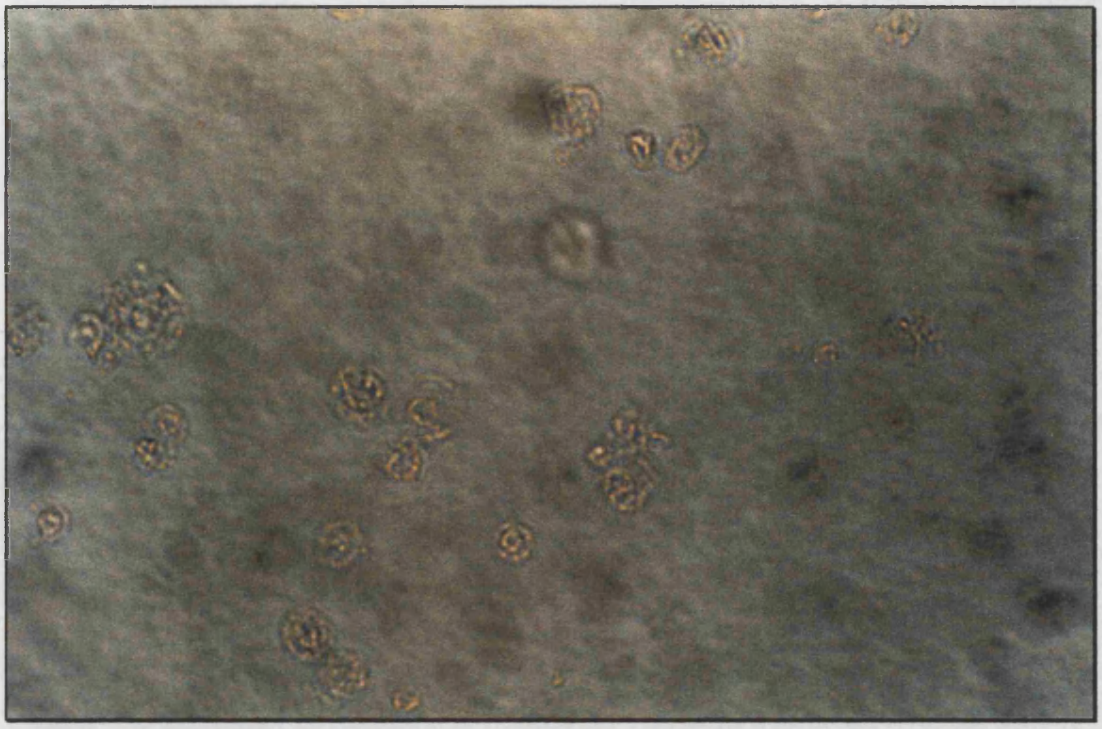

Figure 5.11c, Sf9 cells expressing HIS-C-TERM 72 hours post infection.

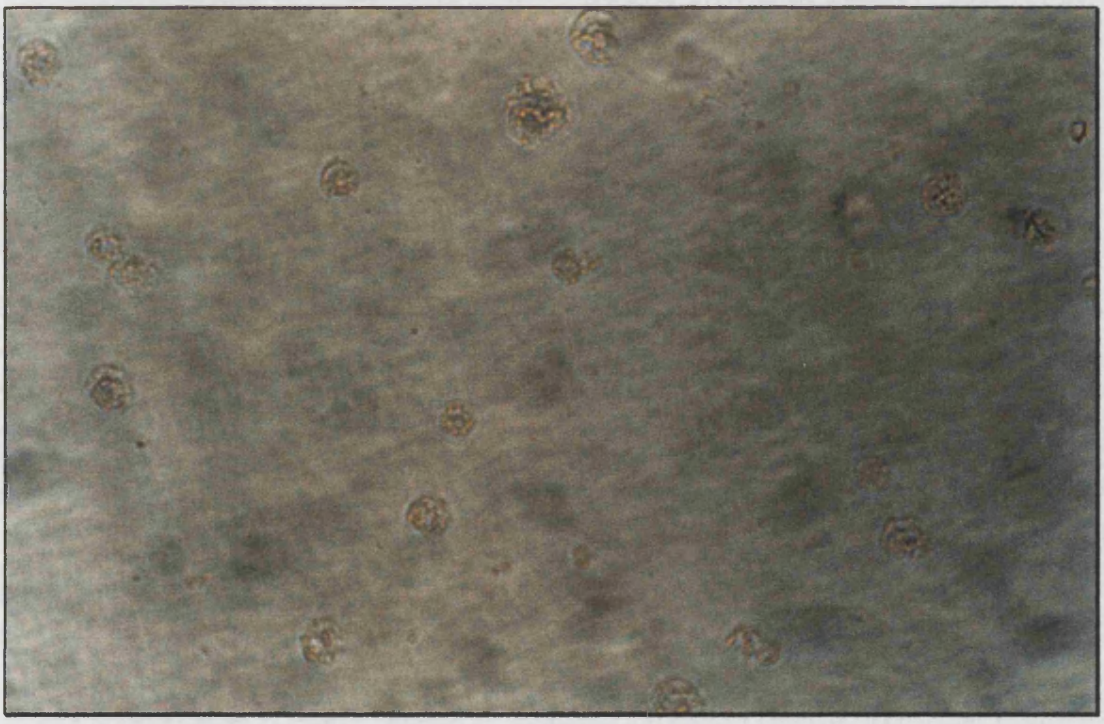

Figure 5.11d, Sf9 cells expressing HIS-C-TERM 96 hours post infection

The above time course shows that the cells began to look infected at 48 h post infection and are completely lysed at 72 h post infection. Infected cells have an uneven surface and become crenellated. Infected cells finally undergo cell lysis, this results in the breaking of the plasma membrane. The cell contents empty into the medium and cell proteases are released along with other biomolecules. The time course demonstrated the recombinant virus to be pure, having no wild-type baculovirus contamination.

Section 5.8
Discussion

Immunoblotting was consistent with the recombinant viruses producing the required recombinant protein. Immunoblot time course analysis revealed that maximum recombinant protein expression was at 72 h post infection, following which there was a decline in the levels of recombinant protein. Microscopic analysis of infection revealed that the cells began to look infected by 48 h post infection and are almost all dead by 72 h post infection. Microscopic analysis also revealed that the recombinant virus is pure and free of any wild-type baculovirus contamination. Time course analysis has determined the optimum time for recombinant protein recovery to be 72 h (3 days) post infection.

6.0 Confocal Microscopy

Section 6.1 Introduction

Confocal scanning light microscopy was used to analyse the expression of the four recombinant proteins: GLUT1, HIS-GLUT1, HIS-C-TERM and C-TERM, using a BioRad confocal imaging system (MRC500). Constructs were detected with affinity purified GLUT1 antibody which was in turn detected using a fluorescein isothiocyanate (FITC) conjugated antibody. Phase-contrast and immunofluorescent images were analysed in order to determine where the expressed proteins were targeted.

Section 6.2 GLUT1

Sf9 cells were infected for 24 and 36 h, following infection the cells were combined. Using the confocal microscope cells were selected for study at a point before cell lysis had occurred. Confocal microscopy images of GLUT1 are displayed in figure 6.2. Uninfected control cells are displayed below (figure 6.1). The control does not show any cross reaction between the GLUT1 / immunofluorescent antibody complexes and native Sf9 cell proteins.

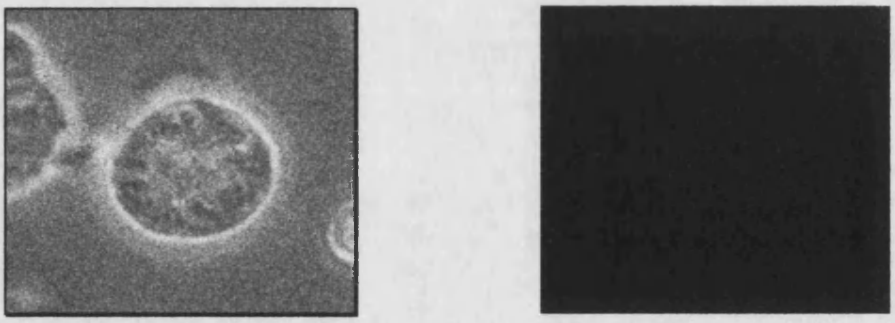

A B

Figure 6.1, Uninfected Sf9 cell control. Panel A displays the phase-contrast image, showing an uninfected cell and panel B displays the corresponding immunofluorescent image.

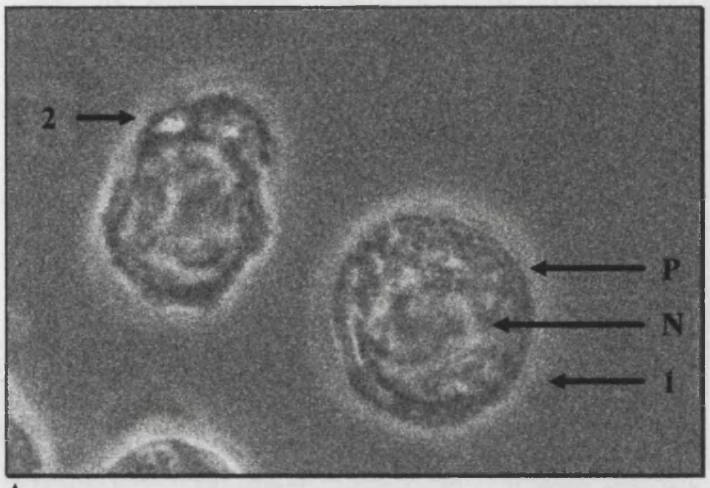

A

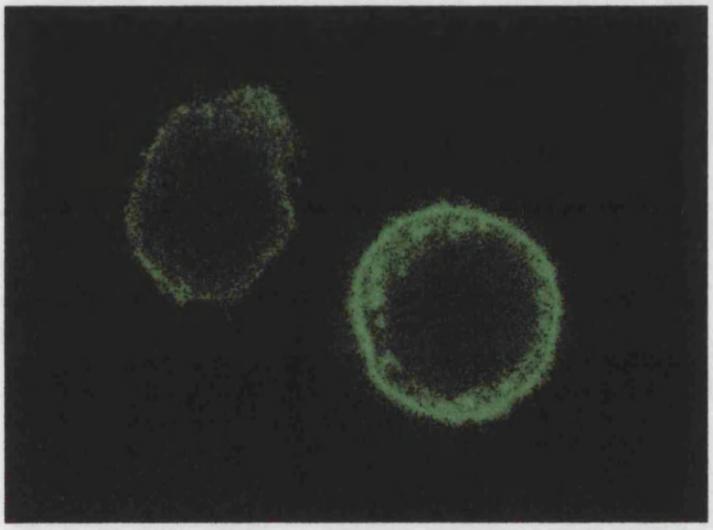

B

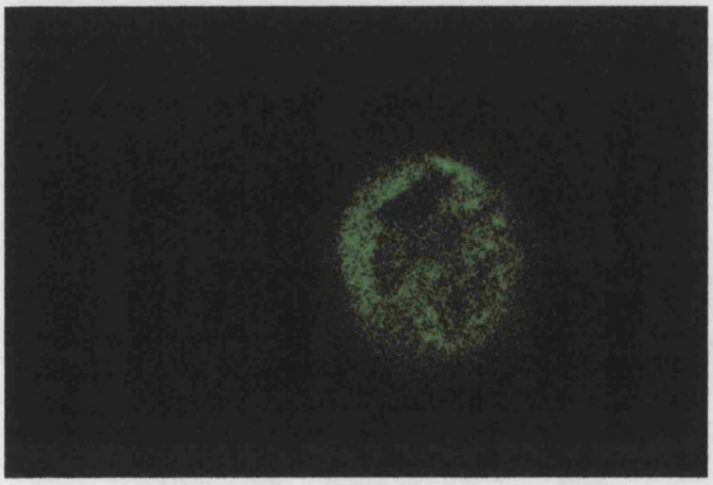

C

15 μm

Figure 6.2, Phase-contrast and immunofluorescent images of Sf9 cells expressing GLUT1.. Panel A: phase-contrast image (the plasma membrane is indicated by the letter P and the nuclear membrane by the letter N); panel B: cell cross section immunofluorescent image (cell 1 appears to be intact and expresses GLUT1 in the plasma membrane); Panel C: cell surface immunofluorescent image.

The confocal scanning light microscope images displayed a clear ring of fluorescence around the cell with a punctate surface distribution. This indicated that the GLUT1 protein was targeted to and inserted in the plasma membrane of the cell.

Confocal microscopy of the full length GLUT1 construct has demonstrated that there was good expression and correct targeting of the protein to the plasma membrane of the cell. This also inferred that Sf9 cells allowed for the correct folding of the glucose transporter.

Section 6.3 HIS-GLUT1

Sf9 cells were infected with the recombinant virus encoding the protein HIS-GLUT1 and the results of confocal scanning microscopy are shown in figures 6.3.

Confocal scanning light microscopy revealed a ring of fluorescence around the cell, thus demonstrating that the HIS-GLUT1 construct was also targeted to the plasma membrane. Distribution at the cell surface and internal structures was identical to that of the GLUT1 protein, cell surface distribution was punctate. This suggested that the HIS-GLUT1 protein was transported and targeted in an identical fashion to the GLUT1 protein. This indicated that the addition of a polyhistidine tag (histidine residues, enterokinase site and 'spacer' amino acids) does not affected the folding, targeting and insertion characteristics of the glucose transporter protein.

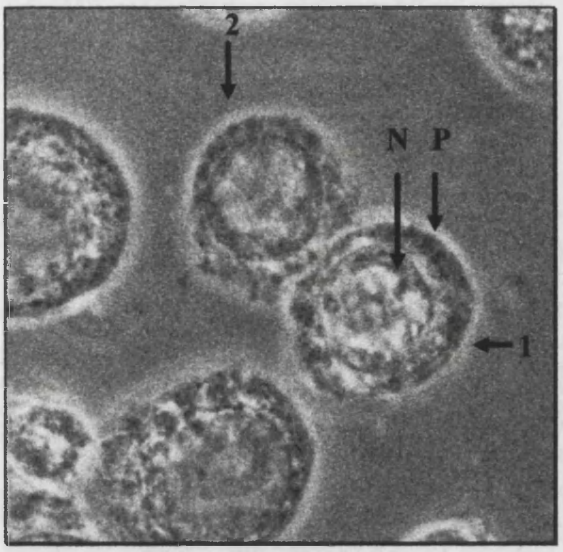

A

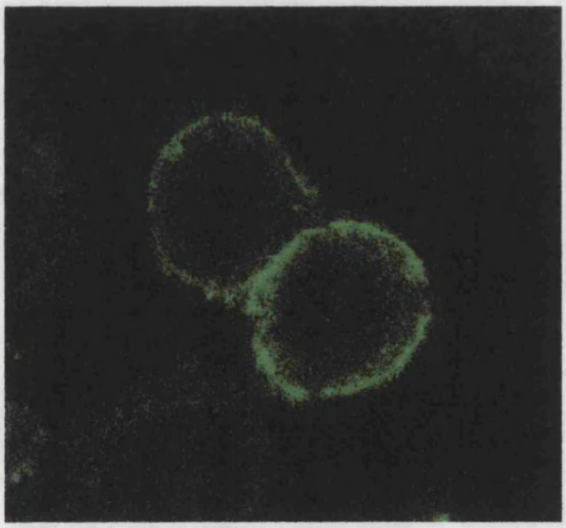

B

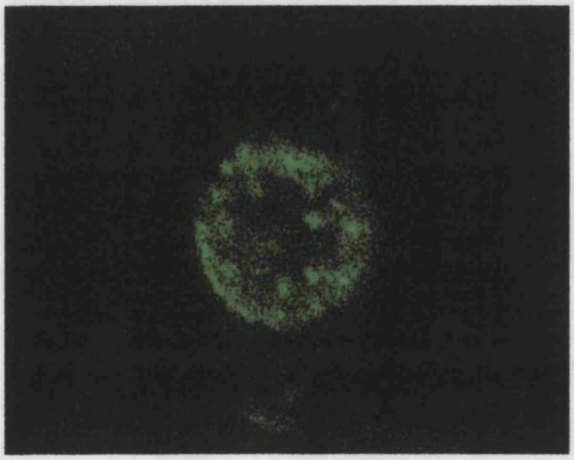

C

15 μm

Figure 6.3, Phase-contrast and immunofluorescent images of Sf9 cells expressing HIS-GLUT1. Panel A: phase-contrast image (the nucleus is indicated in cell 1 by the letter N, the letter P denotes the plasma membrane); Panel B: cell cross section immunofluorescent image (cell 1 appears intact and expresses HIS-GLUT1 in the plasma membrane); panel C: cell surface immunofluorescent image.

Section 6.4 C-TERM

Sf9 cells were infected with the recombinant virus encoding the C-TERM protein. The cells were examined using immunofluorescent confocal microscopy. The phase-contrast and immunofluorescent images are displayed in figures 6.4.

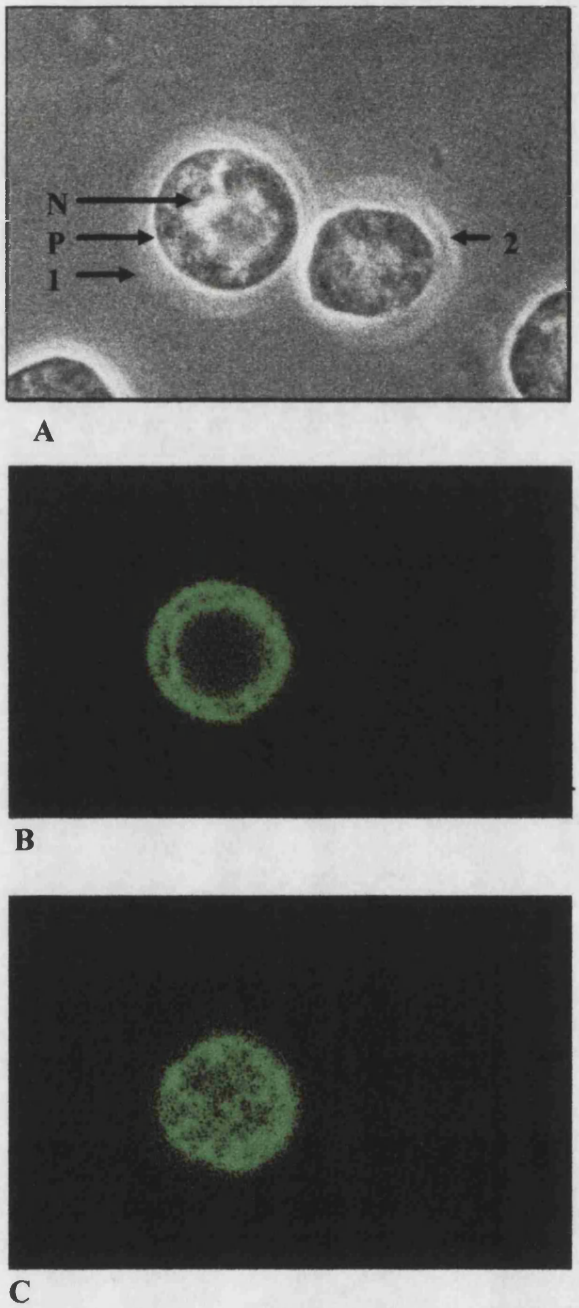

Figure 6.4, Phase-contrast and immunofluorescent images of Sf9 cells expressing C-TERM. Panel A: phase contrast image (the letter N denotes the nuclear membrane and the letter P the plasma membrane); Panel B: cell cross section immunofluorescent image (only cell 1 is expressing C-TERM protein); Panel C: cell surface immunofluorescent image.

Targeting of the C-TERM protein was markedly altered in comparison to targeting of the full length glucose transporter; C-TERM protein appeared to be aberrantly targeted within the Sf9 cell. However, a significant proportion of the C-TERM protein was correctly targeted to the plasma membrane. The C-TERM protein had a punctate surface distribution.

Section 6.5 HIS-C-TERM

Sf9 cells were infected with virus coding for the HIS-C-TERM protein. The cells were examined using immunofluorescent confocal microscopy. Phase-contrast and immunofluorescent images of cells expressing the HIS-C-TERM protein are displayed in figures 6.5

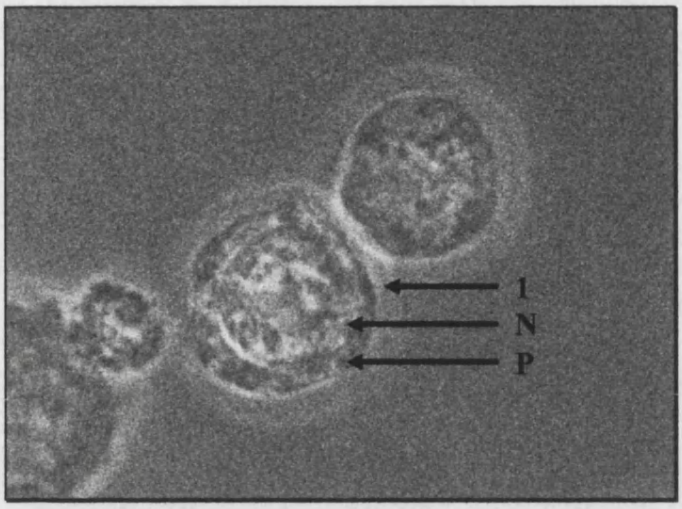

A

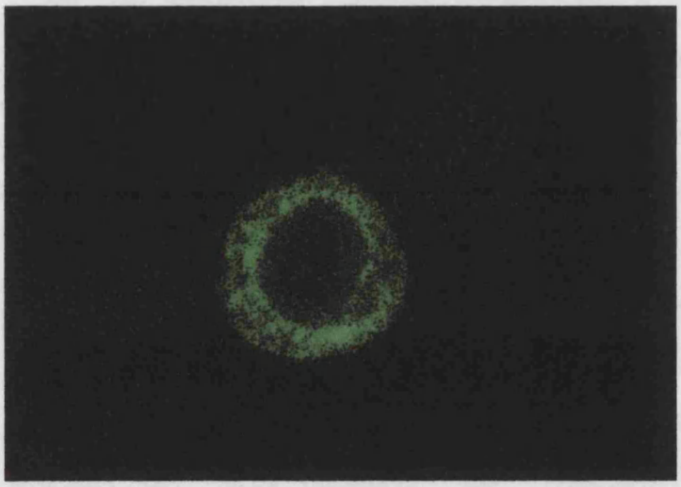

B

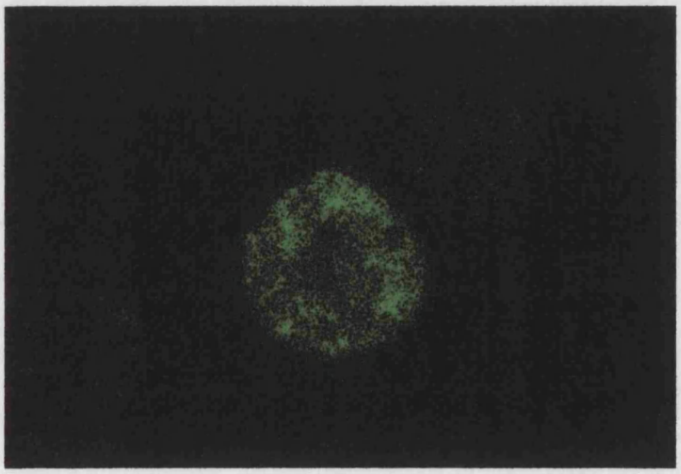

C

15 μm

Figure 6.5, Phase-contrast and immunofluorescent images of Sf9 cells expressing HIS-C-TERM. Panel A: phase contrast image (the letter N denotes the nuclear membrane and the letter P denotes the plasma membrane); Panel B: cell cross section immunofluorescent image; Panel C: cell surface immunofluorescent image.

Despite the addition of a polyhistidine tag and spacer sequence (containing an enterokinase site and several amino acids from the baculovirus polyhedrin protein), the HIS-C-TERM protein appears to have been targeted in a similar fashion to the C-TERM protein, having a punctate surface distribution. A significant amount of C-terminal construct was expressed in the plasma membrane and was therefore correctly targeted to this location. A proportion of the protein was observed to be localised around the nucleus. It was proposed that this represented protein which had not been exported from the endoplasmic reticulum, a structure which is continuous with the nuclear membrane. The rest of the protein appeared to be contained within cytoplasmic membranes and was distributed throughout the cytoplasm.

Section 6.6 Discussion

Confocal scanning light microscopy demonstrated that all of the recombinant protein constructs were expressed in the Sf9 cell system. However, not all of the constructs were targeted in the same manner. All constructs demonstrated a similar plasma membrane surface distribution, described as punctate. In all constructs the modification of the N-terminal sequence, by the addition of the polyhistidine tag, had very little effect on the targeting of the recombinant protein.

GLUT1 sequestered in internal structures may be a result of overexpression of the recombinant protein. Overexpression may result in the transport machinery becoming saturated and incapable of handling the protein correctly. This may result in the sequestering of the protein in internal, membranous structures, near to the cell surface.

C-TERM protein was observed to be localised within cytoplasmic membranes and a band of strong fluorescence also surrounds the nucleus. The strong band of fluorescence surrounding the nucleus may represent protein that has not been transported out of the endoplasmic reticulm. This may be due to incorrect folding of the protein. It is possible that while correctly folded protein is translocated to the cell surface, C-TERM protein which folds more slowly may be retained within the internal structures of the cell.

7.0 Expression Systems and the Quantitation of Expressed Recombinant Protein

Section 7.1 Introduction

Recombinant protein expression was assessed by two techniques, immunoblotting and a cytochalasin B binding assay. Immunoblotting indicates the quantity of expressed protein present, whereas, the cytochalasin B assay assesses how much of this protein is functional. This chapter looks at expression based on immunoblot analysis. Furthermore, two different types of insect cells were compared for use in recombinant protein expression.

Section 7.2
Expression of HIS-GLUT1 and GLUT1 in Sf9 Cells

Recombinant protein expression was assessed by quantitative immunoblot analysis. Expressed proteins were compared with human GLUT1 standards of known protein concentration. Purified human GLUT1 standard was obtained from human erythrocytes, using the method described by Baldwin and Leinhard, (1989). This method is known to give pure GLUT1 protein (as assessed by PAGE followed by silver staining) and measurement of the protein content by protein assay reports the concentration of reconstituted human GLUT1. Figure 7.1 compares the HIS-GLUT1 and GLUT1 protein constructs with the purified human GLUT1 standard.

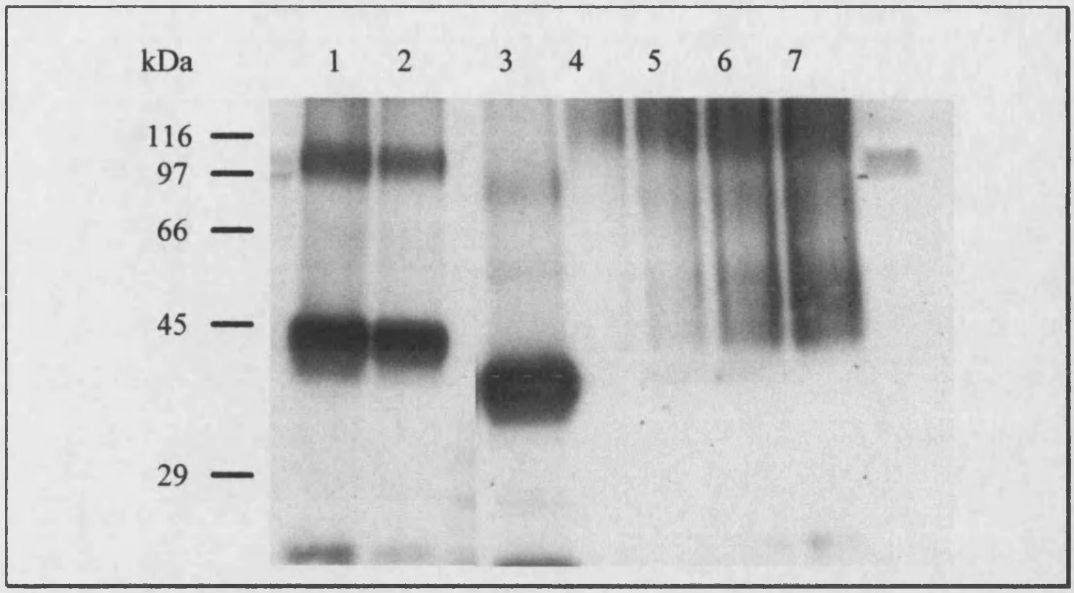

Figure 7.1, Expression of recombinant virus expressing E4.2 and HIS-GLUT1. A 10% polyacrylamide gel was loaded as follows: Lane 1: 40 µg clone 8, HIS-GLUT1; lane 2: 30 µg clone 8, HIS-GLUT1; lane 3: 30 µg clone 35, GLUT1; lane 4: 100 ng human GLUT1; lane 5: 200 ng human GLUT1; lane 6: 400 ng human GLUT1; lane 7: 500 ng human GLUT1.

The immunoblot was densitometrically analysed and the HIS-GLUT1 and GLUT1 proteins were compared to the human GLUT1 standard. The amount of recombinant protein present could then be calculated, the results of this calculation are displayed in table 7.1. The same procedure was followed for the HIS-C-TERM and C-TERM proteins, the immunoblots are displayed in figures 7.2 and 7.3.

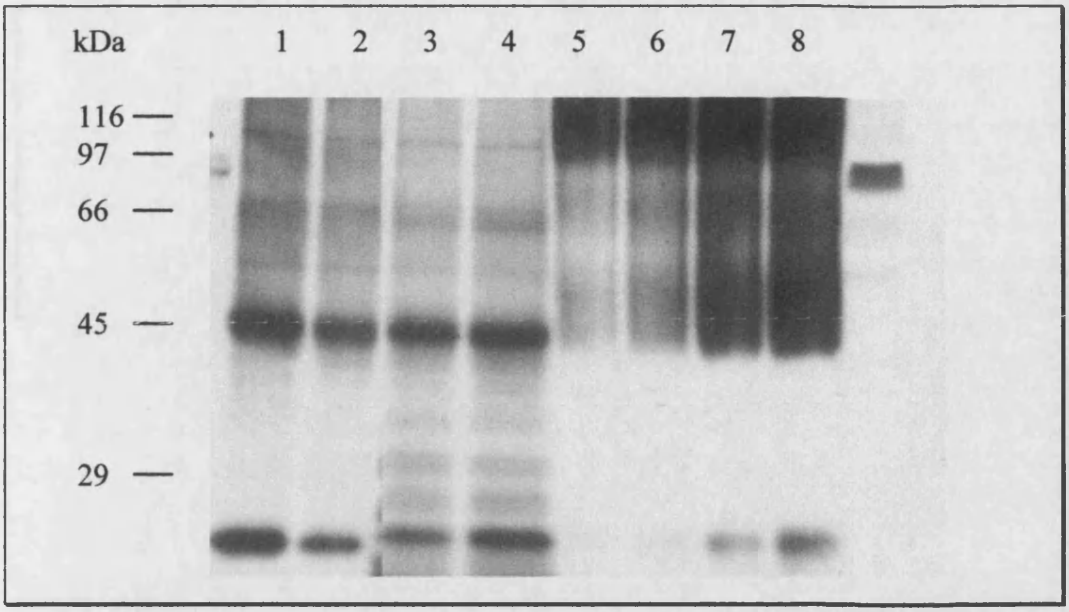

Figure 7.2, Expression of recombinant virus expressing HIS-C-TERM. A 12% polyacrylamide gel was loaded as follows: Lane 1: 40 µg, HIS-C-TERM; lane 2: 30 µg, HIS-C-TERM; lane 3: 10 µg, HIS-C-TERM; lane 4: 20 µg, HIS-C-TERM; lane 5: 100 ng human GLUT1; lane 6: 200 ng human GLUT1; lane 7: 400 ng human GLUT1; lane 8: 500 ng human GLUT1.

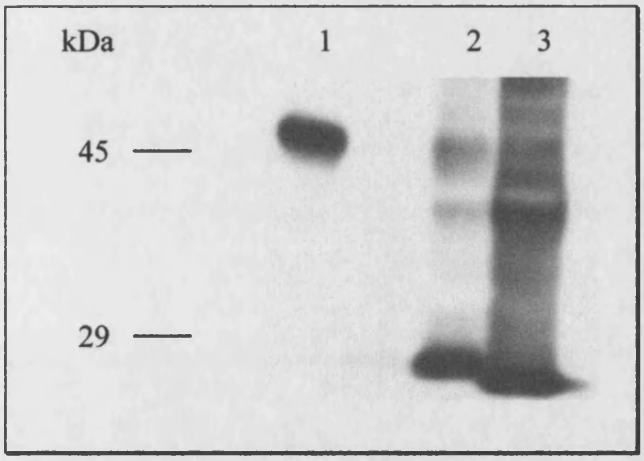

Figure 7.3, Expression of recombinant virus expressing, HIS-GLUT1, HIS-C-TERM and C-TERM. A 12% polyacrylamide gel was loaded as follows: Lane 1: 30 µg, HIS-GLUT1; lane 2: 30 µg, HIS-C-TERM; lane 3: 30 µg, C-TERM.

The C-TERM protein, displayed in figure 7.3, was compared with the already characterised HIS-GLUT1 and HIS-C-TERM proteins. Table 7.1 summarises the mean expression level of expressed recombinant proteins.

Recombinant protein	µg of recombinant protein / mg of Sf9 cell protein	pmoles of recombinant protein / mg of Sf9 cell protein
HIS-GLUT1	24 µg / mg	527 pmoles / mg (n=2)
GLUT1	32 µg / mg	700 pmoles / mg (n=1)
HIS-C-TERM	12 µg / mg	272 pmoles / mg (n=4)
C-TERM	13 µg / mg	296 pmoles / mg (n=1)

Table 7.1, Average recombinant protein expression. Summary of average expression figures for recombinant proteins.

The GLUT1 construct was observed to have the highest level of expression at 700 pmoles of GLUT1 / mg of Sf9 cell protein. In comparison the HIS-GLUT1 construct expressed lower levels of protein at 527 pmoles of HIS-GLUT1 / mg of Sf9 cell protein. C-terminal expression was approximately half that of HIS-GLUT1 expression, at 272 pmoles of HIS-C-TERM / mg of Sf9 cell protein and 296 pmoles of C-TERM / mg of Sf9 cell protein. However, as the quantity of oligomers was not taken into account during scanning, the apparently lower level of C-terminal construct expression was probably due to the formation of oligomers. This would result in the distribution of the protein to more than one region of the polyacrylamide gel.

A small variation in the level of protein expression was observed between the HIS-GLUT1 and GLUT1 proteins. However, because the number of repeat experiments were small it was not possible to determine if there were any significant difference in the level of expression. There was very little difference observed between the level of protein expression for both the HIS-C-TERM and the C-TERM proteins.

Section 7.3

Comparison of Expression Between Highfive and Sf9 Cells

Two different types of insect cells were tested for the expression of recombinant protein, *Spodoptera frugiperda* ovarian cells (Sf9 cells) and *Trichoplusia ni* cells (Highfive cells). The following immunoblot (figure 7.4) demonstrates the increase in expression attained when using Highfive cells instead of Sf9 cells.

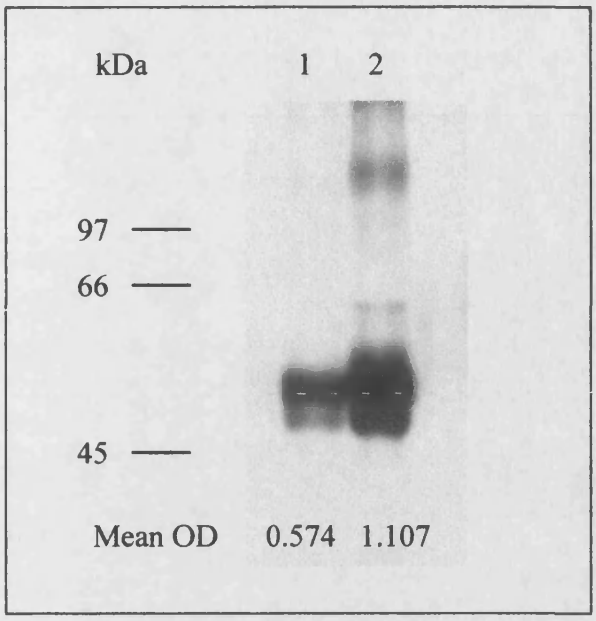

Figure 7.4, Sf9 and Highfive cells expressing the protein HIS-GLUT1. A 10% polyacrylamide gel was loaded as follows: Lane 1: 15 μg of Sf9 cells expressing HIS-GLUT1; lane 2: 15 μg of Highfive cells expressing HIS-GLUT1.

Analysis of the immunoblot demonstrated a 1.9 fold increase in expression in Highfive cells when compared with Sf9 cells.

Section 7.4

Discussion

The amount of protein expressed in insect cells has been determined by immunoblot analysis. However, there are several problems in using this method of protein determination. For example, comparing a heavily glycosylated protein with a moderately glycosylated protein; measuring accurately the optical densities on a film; controlling the amount of protein in varying forms of aggregation; determining the purity and protein concentration of the standard. Even with these difficulties this method has resulted in protein determinations which are comparable with literature values (Yi *et al.*, (1992) and Cope *et al.*, (1994)).

The use of Highfive cells demonstrated a significant increase in the level of recombinant protein expressed. However, Highfive cells grow at a much slower rate than Sf9 cells, therefore increasing the time required to culture the cells before viral infection.

8.0 Cytochalasin B Studies on Expressed Recombinant Protein

Section 8.1 Introduction

Cytochalasin B is a fungal toxin with a high affinity to the internal binding site of the GLUT1 protein. Cytochalasin B assays were carried out to determine the quantity of functional recombinant glucose transporter expressed in Sf9 cells. The cytochalasin B assay was originally developed by Lin *et al.*, (1974). However, Baldwin *et al.*, (1982) and Yi *et al.*, (1992) have since used the method of cytochalasin B equilibrium dialysis to successfully determine the glucose transporter content of human erythrocytes and insect cells, respectively. The method used in this thesis was modified from that of Jung and Rampal, (1977). Separation of the bound cytochalasin B and the free cytochalasin B was achieved by centrifugation.

Yi *et al.*, (1992) have determined that cytochalasin B has no affinity towards the native insect cell glucose transporter. However, cytochalasin B is lipophilic in nature and therefore has an affinity towards the cell membrane lipid. Non-specific binding towards the cell membrane generated a background which could be corrected for by assaying uninfected Sf9 cells. Cytochalasin E was used to block any non-specific binding sites present. Binding is assumed to be stochiometric, ie. one cytochalasin B molecule binds to one glucose transporter molecule.

The cytochalasin B assay was tested by assaying purified human erythrocyte GLUT1. Once the literature values had been obtained for human GLUT1, the assay was used to determine the amount of recombinant glucose transporter expressed in insect cells. Assaying human GLUT1 also served to confirm the integrity of the purified human GLUT1 protein. The human GLUT1 protein was then used as a control against unknown GLUT1 concentrations during quantitative immunoblot analysis.

Cytochalasin B assays have been used throughout this thesis to determine the amount of functional GLUT1 and HIS-GLUT1 protein present. Cytochalasin B assays were also used during the purification of the HIS-GLUT1 protein, in an attempt to determine protein stability and the increase in protein activity on purification.

Section 8.2

Cytochalasin B Assays - Erythrocytes

Cytochalasin B assays were carried out according to the method described in the Materials and Methods section (2.44). Purified human GLUT1 was assayed to determine the integrity of the protein and to confirm that the assay was functioning correctly. The results are displayed in figures 8.2 and 8.3.

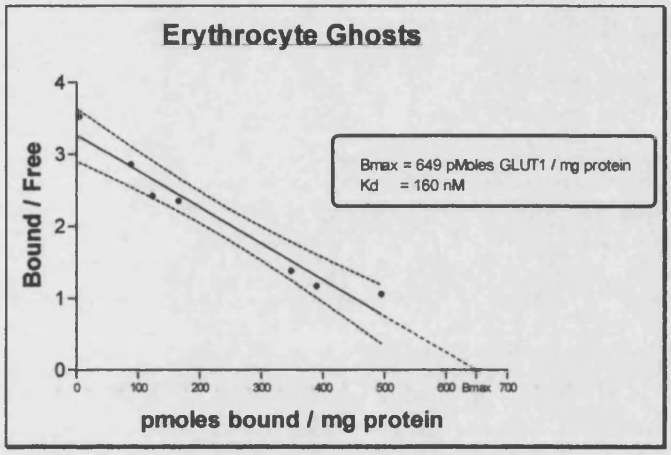

Figure 8.2, Cytochalasin B assay of erythrocyte ghosts. Cytochalasin B binding was analysed by Scatchard plot, 95% confidence intervals have been displayed as an indication of error.

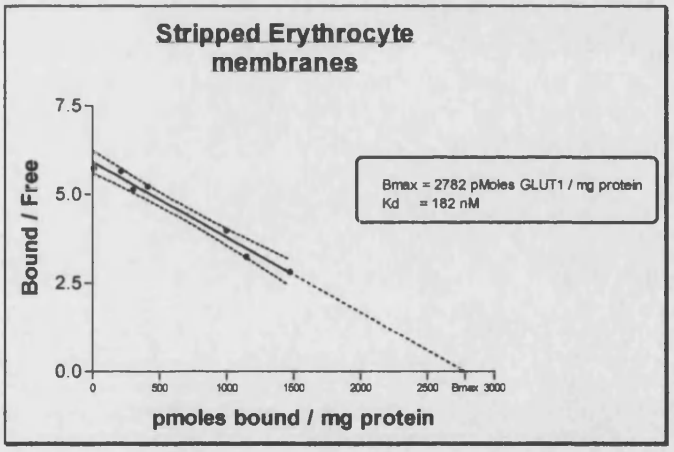

Figure 8.3, Cytochalasin B assay of stripped erythrocyte membranes. Cytochalasin B binding was analysed by Scatchard plot, 95% confidence intervals have been displayed as an indication of error.

Cytochalasin B assays have determined that a suspension of erythrocyte ghosts (prepared according to Baldwin and Lienhard, (1989)) contained 649 pmoles of active GLUT1 / mg of protein. Alkali stripped erythrocyte membranes were found to contain 2782 pmoles of active GLUT1 / mg of protein. The Kd of cytochalasin B binding to erythrocyte ghosts and stripped erythrocyte membranes were calculated to be 160 nM and 182 nM, respectively. The average molecular weight of human erythrocyte GLUT1 has been calculated to be 55 kDa. From the average molecular weight it was calculated

that the amount of GLUT1 in erythrocyte ghosts and stripped membranes was 36 µg of GLUT1 / mg protein and 153 µg of GLUT1 / mg protein, respectively. Glucose inhibition for erythrocyte ghosts and stripped membranes was 76% and 75%, respectively. Glucose inhibition figures demonstrated that the GLUT1 binding site recognises the natural ligand with a high affinity.

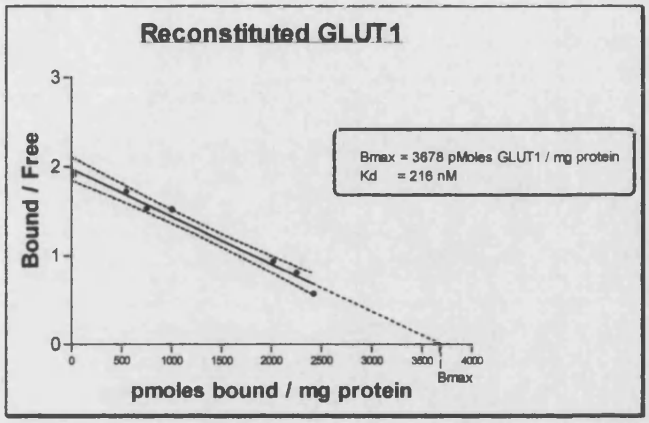

Figure 8.4, Cytochalasin B assay of reconstituted, purified, human GLUT1. Cytochalasin B binding was analysed by Scatchard plot, 95% confidence intervals have been displayed as an indication of error.

Following the reconstitution of DEAE cellulose purified human GLUT1, cytochalasin B analysis reported that there were 3678 pmoles of active GLUT1 / mg of protein present, with a calculated Kd of 216 nM. This equated to 202 µg of active GLUT1 / mg of protein. Glucose inhibition was determined to be 91.5%. PAGE indicated that the reconstituted GLUT1 was more than 95% pure. Purified human GLUT1 was used as a standard during quantitative immunoblotting of insect cells. Baldwin *et al.*, (1979) have reported Bmax and Kd values as follows: erythrocyte ghosts, Bmax 620 pmoles / mg and Kd 100 nM; stripped erythrocyte membranes, Bmax 2200 pmoles / mg and Kd 140 nM; reconstituted GLUT1, Bmax 6700 pmoles / mg and Kd 130 nM. In the presence of 200 mM D-glucose, glucose inhibition was 80%. These values were similar to those obtained in this study, therefore it was concluded that the erythrocyte GLUT1 was fully functional.

Section 8.3

Cytochalasin B Assays - Sf9 Expressed Protein

Sf9 cells expressing the HIS-GLUT1 and GLUT1 proteins were assayed for cytochalasin B binding. Background cytochalasin B binding was calculated by assaying

uninfected Sf9 cells. The results of cytochalasin B binding to Sf9 cell membranes expressing the HIS-GLUT1 protein, with and without background subtraction, are displayed in figure 8.5.

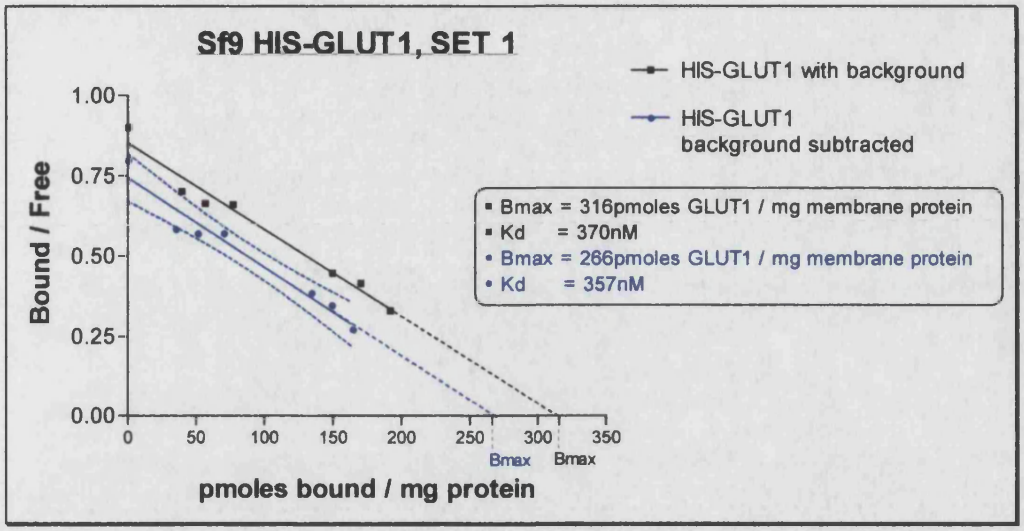

Figure 8.5, Sf9 HIS-GLUT1 Set 1 cytochalasin B binding assay, with and without background correction. Cytochalasin B binding was analysed by Scatchard plot, 95% confidence intervals have been displayed as an indication of error.

Without background correction, 1 mg of Sf9 cells expressing HIS-GLUT1 bound 316 pmoles of cytochalasin B with a Kd of 370 nM. Following background correction, 1 mg of Sf9 cells expressing HIS-GLUT1 bound 266 pmoles of cytochalasin B with a Kd of 357 nM. Glucose inhibition was determined to be 82%. The data showed that 1 mg of uninfected Sf9 cell membranes bound 49 pmoles cytochalasin B / mg of membrane protein. The following cytochalasin B assays have been corrected for this background.

Results showed that following background correction, Sf9 cells expressing HIS-GLUT1 bound 266 pmoles of cytochalasin B / mg of membrane protein. The average molecular weight of recombinant GLUT1 in the Sf9 cell was calculated to be 46 kDa. It was estimated that 12 µg of HIS-GLUT1 were expressed / mg of membrane protein. Cytochalasin B binding was repeated using a second batch of cells and termed HIS-GLUT1 set 2, figure 8.6.

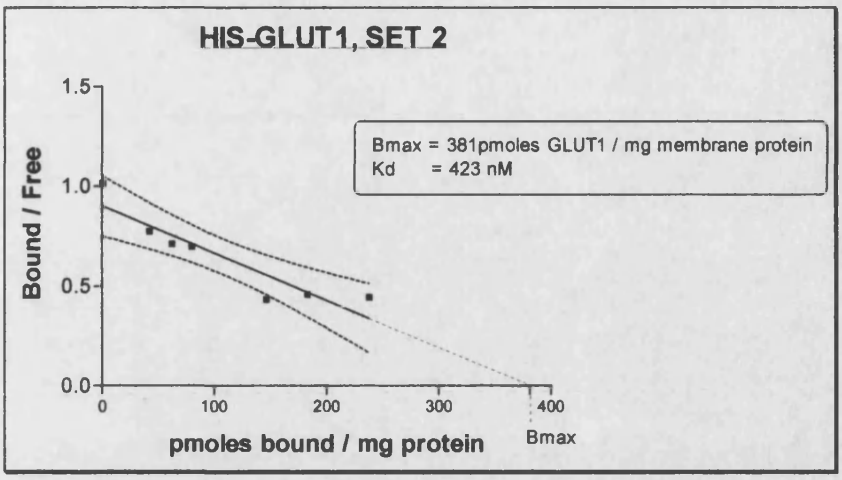

Figure 8.6, Sf9 HIS-GLUT1 Set 2 cytochalasin B assay, with background correction. Cytochalasin B binding was analysed by Scatchard plot, 95% confidence intervals have been displayed as an indication of error.

1 mg of set 2 Sf9 cells expressing HIS-GLUT1 bound 381 pmoles of cytochalasin B with a Kd of 423 nM. It was estimated that 18 μg of functional HIS-GLUT1 were expressed / mg of membrane protein. Glucose inhibition was calculated to be 73%. The HIS-GLUT1 set 2 recombinant protein resulted in higher Bmax and Kd values in comparison to HIS-GLUT1 set 1. The differences seen in these data is due to cell variability. For this reason large batches of cells were prepared, analysed and used in several experiments. This allowed for comparison between experiments.

Wild-type GLUT1 protein was expressed in Sf9 cells as a control. The amount of cytochalasin B binding sites were assayed in the following experiment, figure 8.7.

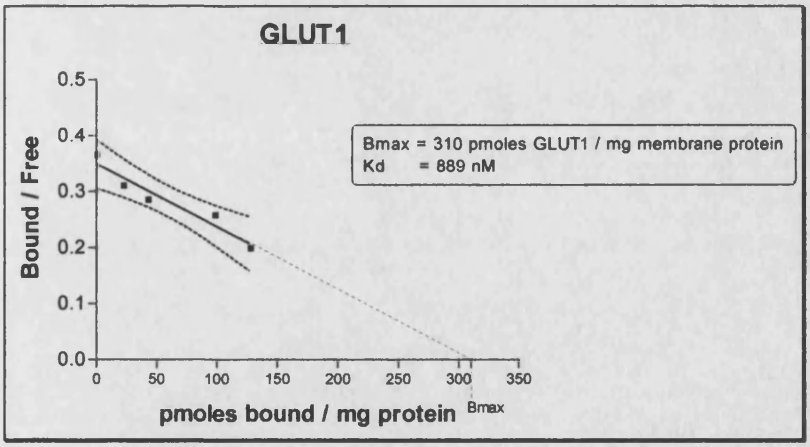

Figure 8.7, Sf9 GLUT1 Cytochalasin B assay, with background correction. Cytochalasin B binding was analysed by Scatchard plot, 95% confidence intervals have been displayed as an indication of error.

Following background correction 1 mg of Sf9 cells expressing GLUT1 bound 310 pmoles of cytochalasin B with a Kd of 889 nM. It was estimated that 14 μg of functional GLUT1 were expressed / mg of membrane protein. The glucose inhibition was determined to be 81%.

Section 8.4

Discussion

Table 8.1 summarises the results of the cytochalasin B assays. The expression levels achieved in Sf9 cells were similar to those achieved by Yi *et al.*, (1992) when expressing GLUT1 (0.23 and 0.29 nmoles / mg) and Weinglass and Baldwin, (1996) when expressing C-terminally histidine tagged GLUT1 (0.33 nmoles / mg).

Protein	Bmax (pmoles / mg)	Kd (nM)	Glucose inhibition (%)
Human erythrocyte ghosts	649 pmoles / mg	160 nM	76%
Stripped erythrocyte membranes	2782 pmoles / mg	182 nM	75%
Reconstituted GLUT1	3678 pmoles / mg	216 nM	91.5%
HIS-GLUT1 Set 1	266 pmoles / mg	357 nM	82%
HIS-GLUT1 Set 2	381 pmoles / mg	423 nM	73%
GLUT 1	310 pmoles / mg	889 nM	81%

Figure 8.9, Summary of cytochalasin B assay results.

Glucose inhibition in all forms of the glucose transporter were of similar levels. This demonstrated that all forms of the transporter responded in an identical way towards the natural substrate, recognising glucose with a high enough affinity to displace cytochalasin B. This showed that the specificity of Sf9 GLUT1 and HIS-GLUT1 for the natural substrate has not been dramatically altered.

Yi *et al.*, (1992) have reported a high level of inactive protein (80%) when GLUT1 was expressed in Sf9 cells. In the present study the levels of inactive Sf9 expressed GLUT1 and HIS-GLUT1 protein were 55% and 39%, respectively (the total amount of GLUT1 construct having been determined by quantitative immunoblotting). The lower amount of inactive HIS-GLUT1 protein observed may be an effect of expressing a polyhistidine tag on the start of the protein, since no other changes to the protein structure have been made. The addition of the tag may enable the HIS-GLUT1 protein to form a more stable structure. Carlsson *et al.*, (1996) have reported a decrease in protein expression when using long polyhistidine tags. A decreased level of expression may allow for correct protein folding to occur, without saturation of the

protein folding machinery. Alternatively, Yi *et al.,* (1992) may have over estimated the total amount of GLUT1 protein present by immunoblot analysis. This would then give the impression that there was a high level of inactive protein.

Because cytochalasin B has a greatly reduced affinity towards the C-terminal constructs it was not possible to obtain accurate cytochalasin B binding data in this study. The amount of C-terminal recombinant protein could therefore only be judged by quantitative immunoblot assay.

9.0 Time, Temperature and Metal-ion Dependent Aggregation

Section 9.1 Introduction

During photolabelling studies it was observed that the GLUT1 protein constructs were sensitive to aggregation. Experiments were carried out in order to determine the cause of the aggregation. Although aggregates seemed to be very difficult to completely eliminate from experiments, several rules appeared to govern the level of aggregation which occurred. The factors hypothesised to affect aggregation are as follows:

1) The protein concentration of the sample
2) The temperature of the sample
3) The metal ion (zinc ion) concentration (polyhistidine tagged proteins)
4) The length of time that the protein is held in non-native conditions

Section 9.2

Protein Concentration and Temperature Dependency of Aggregation

It was observed that during photolabelling studies of erythrocyte GLUT1, high protein concentrations lead to an increase in the amount of aggregation observed. Photolabelling experiments using human erythrocyte membranes stored at a concentration of 440 µg / ml yielded a large tetrameric aggregation peak at 205 kDa, figure 9.1. The tetrameric peak was hypothesised to consist of four GLUT1 molecules. A reduction in the storage concentration of human erythrocyte membranes to 50 µg / ml resulted in the reduction of the aggregation peak, figure 9.2. Aggregation was thought to increase in more concentrated samples due to the closer proximity of protein molecules.

Neither of the HIS-C-TERM or the HIS-GLUT1 protein samples were as concentrated as the human erythrocyte GLUT1 protein. This would prevent much of the aggregation generated by this mechanism.

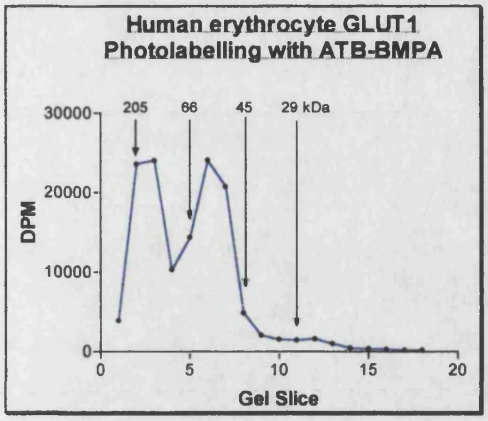

Figure 9.1, Photolabelling high concentrations of erythrocyte GLUT1. 440 µg / ml of human erythrocyte membranes were labelled. An intensely labelled tetrameric peak appears at approximately 205 kDa. This was attributed to the high protein concentration of the sample.

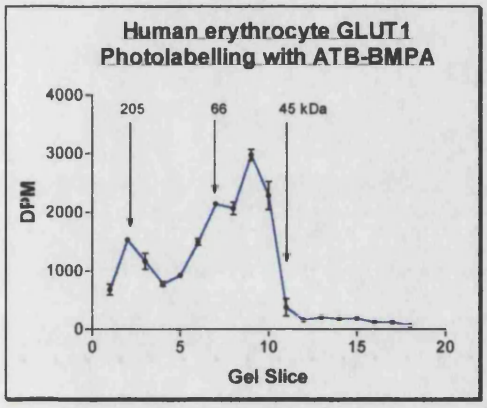

Figure 9.2, Photolabelling low concentrations of erythrocyte GLUT1. 50 µg / ml of human erythrocyte membranes were labelled. The error bars display the standard error of the mean (SEM). The amount of labelled tetramer is greatly reduced in this experiment. This was due to the lower storage concentration of the human erythrocyte GLUT1.

Furthermore, samples were never boiled in sample buffer before loading onto polyacrylamide gels because of reported increases in aggregation (personal communication with Dr A Clark and Dr J Yang). During photolabelling experiments samples were incubated on ice or at 4°C whenever possible to limit aggregation.

Section 9.3

HIS-C-TERM Zinc Dependent Aggregation

It was hypothesised that zinc ions had the effect of increasing the aggregation levels of the HIS-C-TERM protein, the aggregation being moderated by the presence of the polyhistidine tag. The theory was tested by exposing the HIS-C-TERM protein to varying concentrations of zinc. The resulting protein mixture was analysed by immunoblotting, figure 9.3.

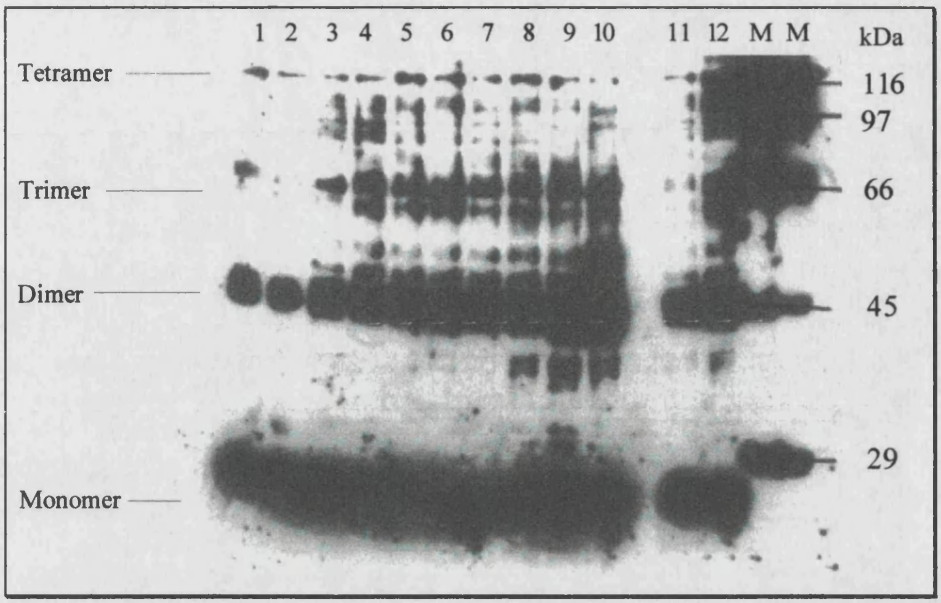

Figure 9.3, Immunoblot analysis of zinc induced aggregation in the HIS-C-TERM protein. 30 µg (13 pmoles) aliquots of homogenised Highfive cell membranes expressing HIS-C-TERM were incubated with varying concentrations of zinc for 15 minutes. A 12% polyacrylamide gel was loaded with the protein samples as follows: Lane 1: 41 nM zinc; lane 2: 82 nM zinc; lane 3: 123 nM zinc; lane 4: 164 nM zinc; lane 5: 205 nM zinc; lane 6: 410 nM zinc; lane 7: 1.25 µM zinc; lane 8: 2.5 µM zinc; lane 9: 50 µM zinc; lane 10: 75 µM zinc; lane 11: HIS-C-TERM in 5 mM Phosphate buffer; lane 12: HIS-C-TERM in KRH buffer; lane M: High molecular weight marker.

Figure 9.3 was analysed densitometrically and the results displayed in figure 9.4.

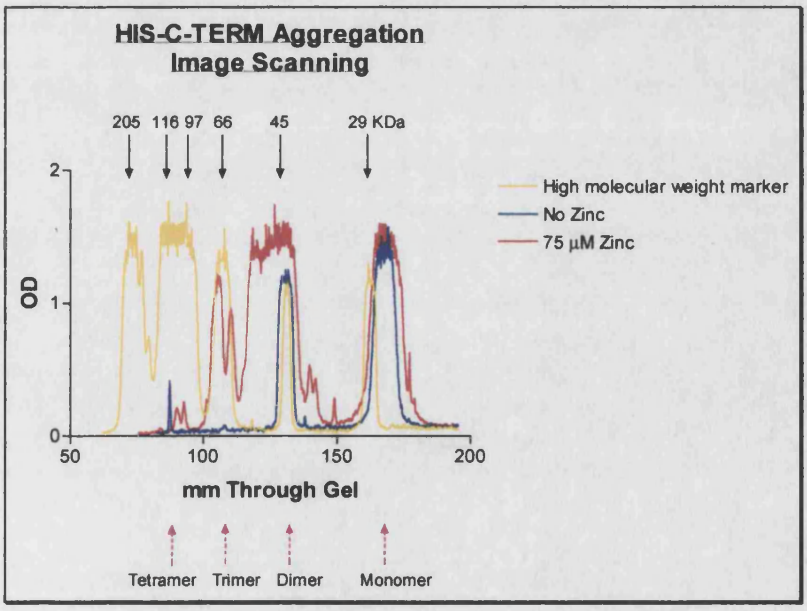

Figure 9.4, Densitometric analysis of zinc induced aggregation in the HIS-C-TERM protein. The high molecular weight marker can be seen to be present in similar amounts throughout the molecular weight range. The addition of 75 µM zinc resulted in increased formation of aggregates, specifically dimer and trimer.

Immunoblotting demonstrated that the level of HIS-C-TERM aggregation increased with increasing zinc concentration. Imaging of the proposed octameric form of HIS-C-TERM was difficult. This was thought to be because it was present only in small amounts. However, photolabelling experiments demonstrated that the octamer and trimer bind the most radiolabel. This suggested that the HIS-C-TERM aggregates either have a higher affinity towards the radioligand than that displayed by the monomeric form of the protein or the protein binding the photolabel at 205 kDa was not the HIS-C-TERM protein. Densitometric analysis showed an even transfer of the molecular weight marker throughout the blot, indicating that the high molecular weight proteins were transferred as efficiently as the low molecular weight proteins.

It was observed that the addition of varying concentrations of zinc had very little effect on the peak height of monomeric HIS-C-TERM protein. However, two other regions of interest exist, the dimer (40 - 60 kDa) and timer / tetramer (60 - 116 kDa) regions. Aggregation in these regions showed a marked increase on the addition of zinc. The amount of aggregation was quantified by determining the 'area beneath the curve' (measured in arbitrary units) from the densitometric analysis. The 'area beneath the curve' between 40 - 116 kDa was calculated and plotted against the concentration of zinc. The relationship was found to fit a hyperbolic curve, figure 9.5.

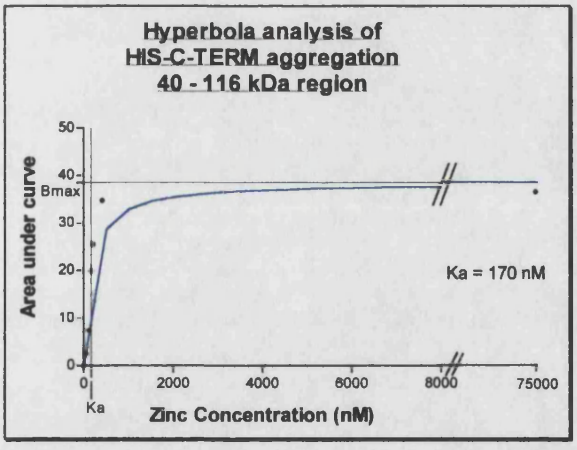

Figure 9.5, Densitometric analysis of the 40 - 116 kDa region. The area under the curve (arbitrary units) was background subtracted and plotted against zinc concentration.

Aggregation appears to be governed by a hyperbolic relationship, Ka 170 nM. At the Ka 1 zinc ion is bound to 2 HIS-C-TERM molecules which approximates to the point of maximum radio ligand binding as determined by photolabelling (photolabelling determined that there were 2.5 HIS-C-TERM molecules : 1 zinc ion at maximum ligand binding). It is thought that during photolabelling maximum radioligand binding was

achieved below the level of maximum aggregation. Maximum aggregation of the HIS-C-TERM protein may involve several ions of zinc per HIS-C-TERM molecule.

Section 9.4

HIS-GLUT1 Zinc Dependent Aggregation

The HIS-GLUT1 protein was tested for increased levels of aggregation on the addition of zinc. The immunoblot is displayed in figure 9.6. It was observed that zinc increased the level of aggregation of the HIS-GLUT1 protein. No aggregation can be observed on this blot above 116 kDa due to the low quantities of protein present. The marker was demonstrated, by densitometric analysis (figure 9.7) to be present in equal amounts across the full molecular weight range of the blot. This indicated that protein transfer had been efficient throughout the molecular weight range.

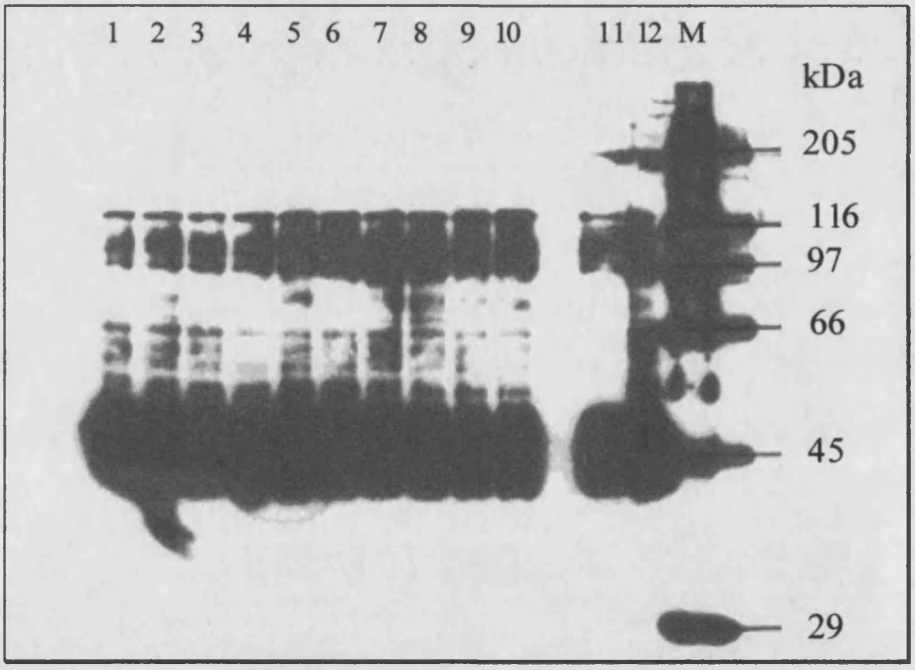

Figure 9.6, Immunoblot analysis of zinc induced aggregation in the HIS-GLUT1 protein. 30 μg (13 pmoles) aliquots of Highfive cell membranes expressing HIS-GLUT1 were incubated with varying concentrations of zinc for 15 minutes. A 10% polyacrylamide gel was loaded as follows: Lane 1: 41 nM zinc; lane 2: 82 nM zinc; lane 3: 123 nM zinc; lane 4: 164 nM zinc; lane 5: 205 nM zinc; lane 6: 410 nM zinc; lane 7: 1.25 μM zinc; lane 8: 2.5 μM zinc; lane 9: 50 μM zinc; lane 10: 75 μM zinc; lane 11: HIS-GLUT1 in 5 mM Phosphate buffer; lane 12: HIS-GLUT1 in KRH buffer; lane M: High molecular weight marker.

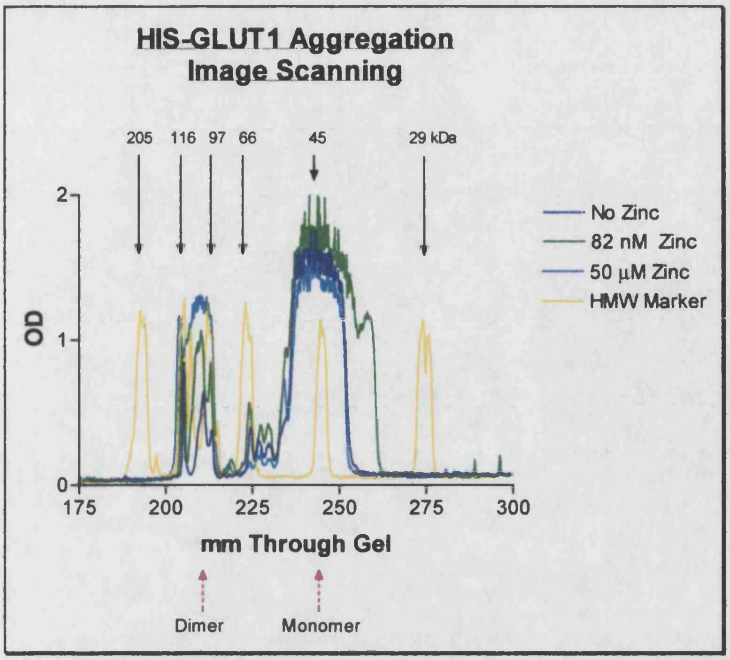

Figure 9.7, Densitometric analysis of zinc induced aggregation in the HIS-GLUT1 protein. The high molecular weight marker can be seen to be present at similar levels throughout the molecular weight range of the gel. The addition of zinc results in the increased level of aggregation in comparison with the 'no zinc' control.

The immunoblot and densitometric scan clearly show an increase in the amount of proposed dimer at 97 kDa on the addition of zinc to the sample. In order to determine a relationship between the concentration of zinc and the level of aggregation, the 'area beneath the curves' in the region 60 - 116 kDa were analysed and plotted against the zinc concentration. These data are displayed in figure 9.8.

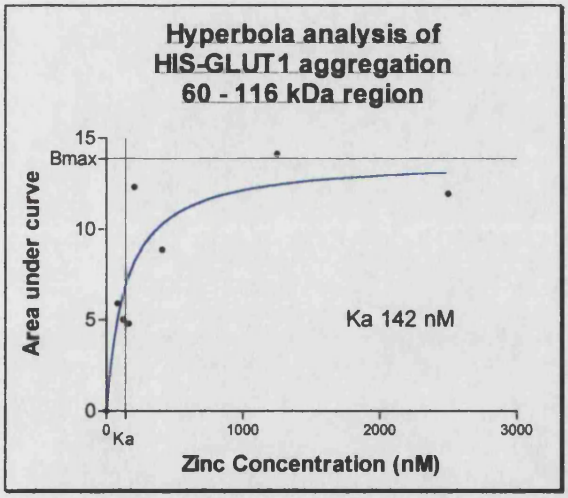

Figure 9.8, Densitometric analysis of the 60 - 116 kDa region. The area under the curve (arbitrary units) was background subtracted and plotted against zinc concentration. The amount of HIS-GLUT1 protein used was 13 pmoles. The relationship is best described as hyperbolic. The Ka equates to the addition of 5.7 pmoles of zinc.

HIS-GLUT1 zinc dependent aggregation appeared to be governed by a hyperbolic relationship. The Ka of aggregation was determined to be 142 nM, which is equivalent to the binding of 1 zinc ion : 2 HIS-GLUT1 molecules. Maximum radioligand binding, as determined by photolabelling, was 1 zinc ion : 1.64 HIS-GLUT1

molecules. In conclusion, maximum photolabelling occurred well below the maximum level of aggregation.

Section 9.5

HIS-GLUT1 Time dependent aggregation

Time dependent aggregation was tested for using the HIS-GLUT1 protein. Time courses were run using HIS-GLUT1 incubated with stochiometric amounts of zinc to promote aggregation throughout the time course. This experiment was again designed to mimic the incubation of protein with zinc during photolabelling.

The only visible form of aggregation was a band running above 205 kDa. This band became apparent after 10 minutes of incubation with stochiometric quantities of zinc. The densitometric analysis of the immunoblot is displayed in figure 9.9.

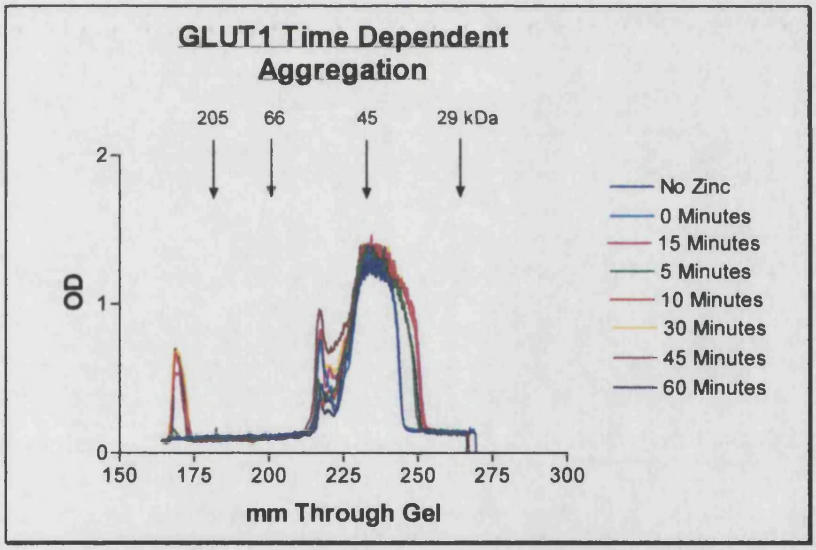

Figure 9.9, Densitometric analysis of HIS-GLUT1 time dependent aggregation. The plot demonstrated how the whole molecular weight range was affected over 60 minutes of the time course. The aggregate running above 205 kDa showed the most time dependent variation.

Aggregation was observed to increase in a time dependent manner, but would be much slower in the absence of zinc. The incubatory periods during photolabelling were reduced accordingly in an attempt to reduce the levels of aggregation.

Section 9.6

Discussion

In conclusion, it appears that aggregation is indeed governed by the proposed factors listed in the introduction. The largest increases in aggregation were observed by varying the concentrations of zinc in both the HIS-GLUT1 and HIS-C-TERM proteins.

Increases in aggregation on a time dependent basis correlate with the observed levels of aggregation seen in photolabelling. Photolabelling experiments performed during a shorter time frame resulted in less aggregation.

Aggregation during photolabelling was never completely eliminated because it was not possible to control all of the conditions, indeed several experiments actively encouraged aggregation. Furthermore, the polyhistidine tag itself appeared to encourage aggregation in the presence of metal ions.

10.0 Photolabelling

Section 10.1 Introduction

Photolabelling experiments were undertaken to investigate the activity of expressed recombinant glucose transporters. It was hypothesised that the C-terminal glucose transporter constructs would lack any radioligand binding activity, as determined by Cope *et al.*, (1994). Experiments were designed using anti C-terminal antibodies and zinc. This was done in an attempt to produce functional HIS-C-TERM protein capable of radioligand binding. It was theorised that the anti C-terminal antibodies may form a surface for the HIS-C-TERM protein to pack against, similar to that achieved by Iwata *et al.*, (1995) when crystallising cytochrome C oxidase. Zinc ions were introduced in the hope that the polyhistidine tags would bind to the zinc, forming a stable, active complex. However, experiments indicated that the HIS-C-TERM protein was capable of ligand binding in the absence of other factors. Anti C-terminal antibodies had little effect, though the addition of zinc ions to the protein had a remarkable effect.

Photolabelling studies were performed according to the method described in the Materials and Methods section. Variables have been described for each individual experiment. The following photolabels were used: 2-*N*-4-(1-azi-2,2,2-trifluoroethyl)-benzoyl-1,3-[^{3}H]-bis-(D-mannos-4-yloxy)-2-propylamine (ATB-[2-^{3}H]BMPA) (synthesised by Prof. G. D. Holman) and cytochalasin B. These chemicals bind to the exofacial and endofacial binding site of the glucose transporter respectively (figure 10.1).

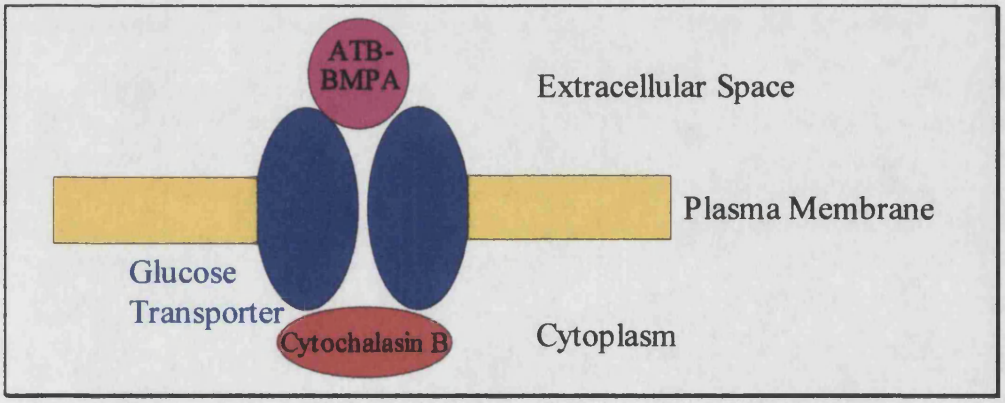

Figure 10.1, Binding locations of ATB-BMPA and cytochalasin B. The photolabels ATB-BMPA and cytochalasin B bind to external and internal binding sites respectively (but not at the same time).

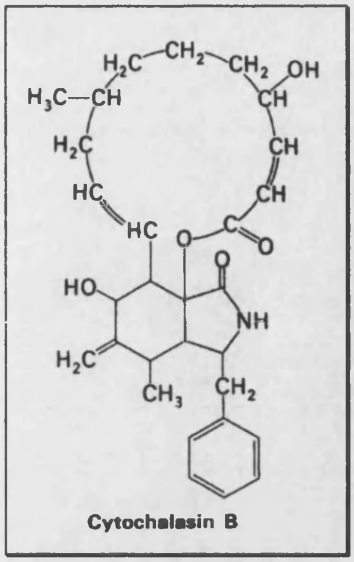

Figure 10.2, Cytochalasin B. A fungal toxin which has a high affinity to the internal binding site of the glucose transporter.

The structure of cytochalasin B is displayed in figure 10.2. Cytochalasin B has a high affinity towards the internal binding site of the glucose transporter. By irradiating the glucose transporter-cytochalasin B complex with high energy ultra violet radiation it is possible for cytochalasin B to become covalently bound to the glucose transporter protein. UV irradiation is thought to photo-activate tryptophan residues on the glucose transporter, possibly tryptophan 388 and tryptophan 412. These tryptophan residues are thought to be closely associated with the internal binding site of the glucose transporter (Inukai *et al.,* 1994). Once activated the tryptophan residues form a stable covalent bond with the cytochalasin B molecule. The cytochalasin B molecule carries a tritium label making detection of the complex possible using standard radiolabel detection techniques.

The ATB-BMPA (figure 10.3) used was first characterised by Clark and Holman, (1990). ATB-BMPA has a high affinity towards the external binding site of the glucose transporter. UV irradiation of the ATB-BMPA and glucose transporter complex results in the photo-activation of the azi group on ATB-BMPA. The azi group then reacts with the glucose transporter to form a covalently bound complex. The ATB-BMPA molecule carries a tritium label which can be detected by standard radiolabel detection techniques.

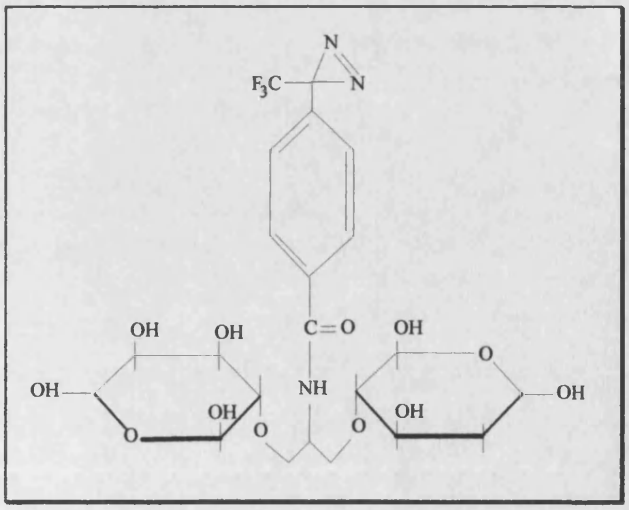

Figure 10.3, The photolabel ATB-BMPA. The photolabel ATB-BMPA is displayed with the azi (N=N) group at the top. ATB-BMPA was kindly synthesised by Professor G.D. Holman, University of Bath.

Section 10.2

C-Terminal Photolabelling

Photolabelling was performed as described in the Materials and Methods section. The glucose transporter constructs were radiolabelled with the appropriate affinity label and UV irradiated to covalently bond the label to the protein. The labelled protein was then separated on a polyacrylamide gel. Following electrophoresis the gel was cut into sections and the radioactivity in each section counted. A control experiment was performed using 2 mg of uninfected Sf9 cells, 2 mg of Sf9 cells expressing HIS-GLUT1 and 2 mg of Sf9 cells expressing GLUT1. The Sf9 cells were homogenised, protein assayed and photolabelled in 5 mM phosphate buffer using ATB-BMPA, figure 10.4.

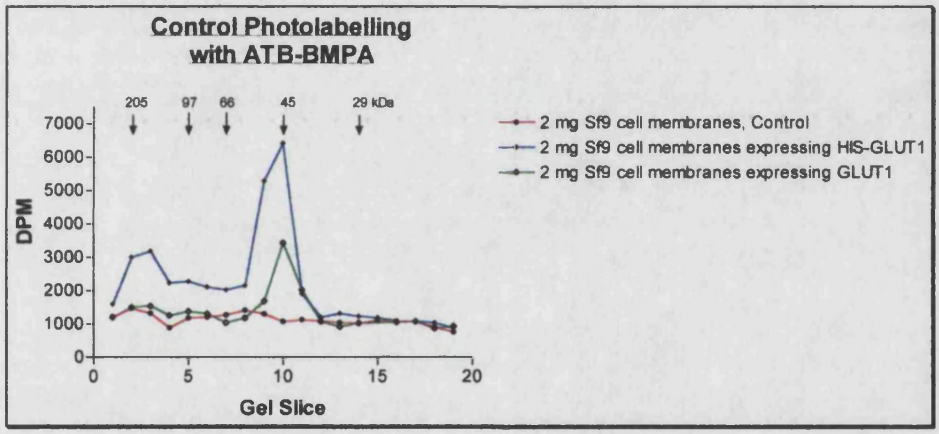

Figure 10.4, Photolabelling control with ATB-[2-^{3}H]BMPA. Sf9 cells were solubilized in 1 ml of 5 mM phosphate buffer containing 2% Thesit and protease inhibitors.

ATB-[2-^{3}H]BMPA binding to uninfected Sf9 cells was observed to be non-specific resulting in a background of about 1000 DPM / gel slice. It was noted that the background does not act to cause any specific peak height amplifications.

When analysing these data there appeared to be a discrepancy in peak height between the photolabelling of the HIS-GLUT1 and GLUT1 recombinant proteins. 2 mg of Sf9 membranes expressing the HIS-GLUT1 protein appear to have produced a much higher photolabelling peak than the 2 mg of Sf9 membranes expressing the GLUT1 protein. However, immunoblot analysis has demonstrated there to be slightly more GLUT1 than HIS-GLUT1 present / mg of protein in these batches of cells (table 7.1).

Cytochalasin B assays performed in chapter 8 also indicated that the HIS-GLUT1 protein has a higher activity when compared with the GLUT1 protein. It is hypothesised that the polyhistidine tag, on the HIS-GLUT1 protein, causes the recombinant protein to be expressed more slowly during viral infection. Slower expression could allow for the correct folding and insertion of the HIS-GLUT1 protein into the membrane. This may be achieved by preventing the saturation of protein processing machinery with non-native protein. One reason for the decrease in expression rate of HIS-GLUT1 may be the high requirement for histidine in the expression of this protein, a phenomenon also observed by Carlsson *et al.,* (1996) when expressing polyhistidine tagged proteins. In addition, the extra protein sequence present at the start of the HIS-GLUT1 protein may act to increase the stability of the protein product. Thus, further decreasing the levels of non-functional HIS-GLUT1 present.

Experiments performed by Cope *et al.*, (1994) using insect cells demonstrated the C-terminal portion of the glucose transporter to be responsible for binding ligand. However, photolabelling was never achieved in the absence of the N-terminal portion. The following work was carried out to further the study by Cope *et al.,* (1994).

The following experiment, figure 10.5, showed the result of photolabelling the C-terminal portion of the glucose transporter with ATB-BMPA.

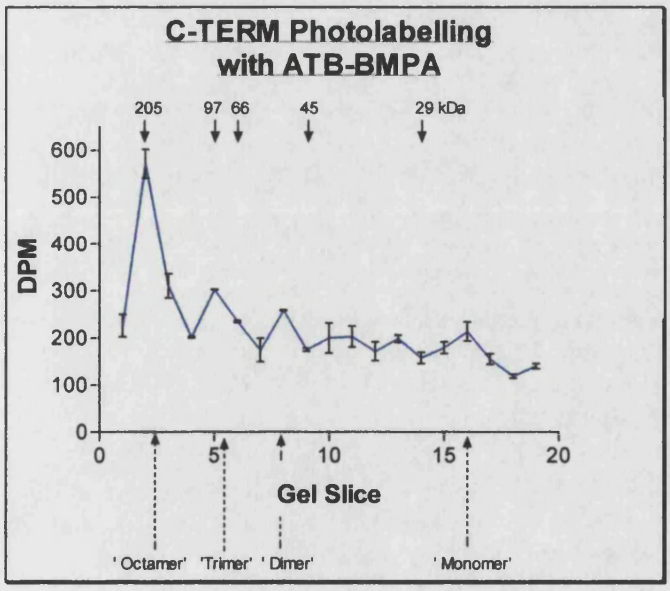

Figure 10.5, Photolabelling C-TERM with ATB-[2-^{3}H]BMPA. 3 mg of homogenised Highfive cell membranes expressing C-TERM were labelled and solubilized in 1 ml of 5 mM phosphate buffer containing 2% Thesit and protease inhibitors. Samples were electrophoresed on a 12% polyacrylamide photolabelling gel.

It was difficult to detect any photolabel that had bound to the C-terminal monomer due to the poor signal to noise ratio. It was concluded that the C-terminal portion bound little, if any photolabel. On many of the C-terminal photolabelling gels a

large peak was observed at a molecular weight of 205 kDa. The association of eight C-terminal 26 kDa monomeric units would correspond to a peak at 205 kDa. It is suggested that the association of eight monomeric units could form an octamer, two monomeric units may form a dimer and three monomeric units may form a trimer.

The ability of the HIS-C-TERM protein to bind radioligand was tested. Sf9 cell membranes expressing the HIS-C-TERM protein were photolabelled with the photolabel ATB-[2-^{3}H]BMPA, figure 10.6.

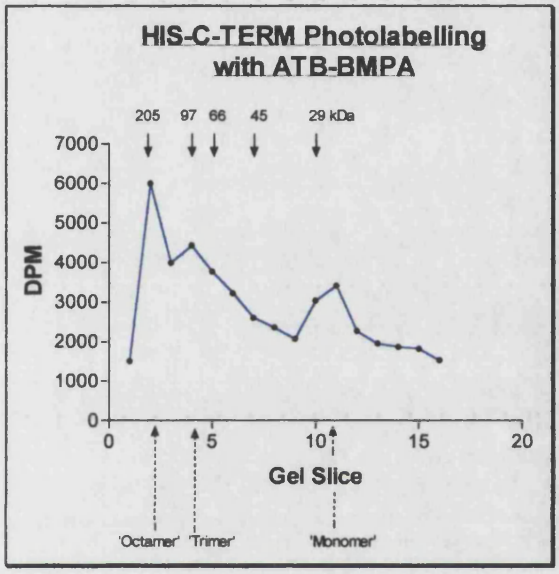

Figure 10.6, Photolabelling HIS-C-TERM with ATB-[2-^{3}H]BMPA. 3 mg of Highfive cell membranes expressing HIS-C-TERM were labelled and solubilized in 1 ml of 5 mM phosphate buffer containing 2% Thesit and protease inhibitors. Samples were electrophoresed on a 12% polyacrylamide photolabelling gel.

Photolabelling of the HIS-C-TERM protein resulted in a radiolabelled protein running near the 29 kDa marker. This molecular weight corresponds to the monomeric form of the glucose transporter. However, glucose displacement studies of HIS-C-TERM ATB-BMPA binding were inconclusive, figure 10.7.

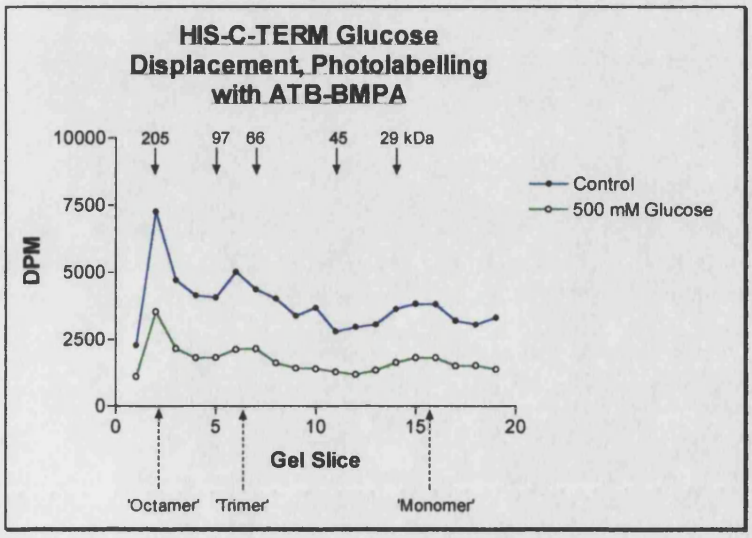

Figure 10.7, Glucose displacement studies, using the recombinant protein HIS-C-TERM. 3 mg of Highfive cell membranes expressing HIS-C-TERM were labelled and solubilized in 1 ml of 5 mM phosphate buffer containing 2% Thesit and protease inhibitors, with or without 0.5 M D-glucose. Samples were electrophoresed on a 12% polyacrylamide gel.

Glucose displacement photolabelling demonstrated a decrease in total photolabelling, however, labelling of individual peaks was not significantly reduced. The background labelling may have been reduced due to the glucose molecule displacing photolabel which was non-specifically bound to the cell membrane and HIS-C-TERM protein. In this experiment there did not appear to be any specific labelling of the HIS-C-TERM protein. This may have been due to a loss of activity during the experiment as the monomer has not bound as much label as in previous experiments.

Electrophoresis was performed using a tricine gel system (as described in the Materials and Methods section) to ensure that the labelling observed in figure 10.6 was not due to a small, undefined protein running at the end of the gel. Tricine gel analysis allowed for a more precise determination of the size of the photolabelled protein, figure 10.8.

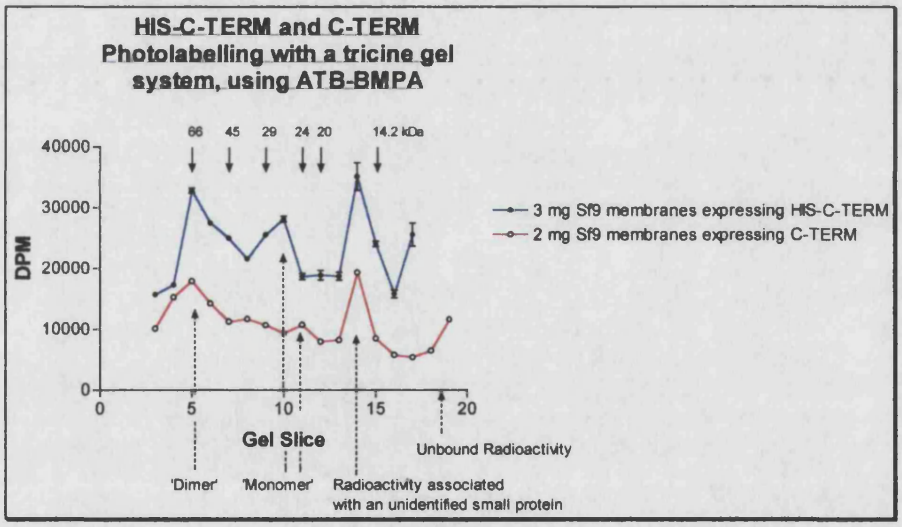

Figure 10.8, Tricine gel photolabel, of HIS-C-TERM and C-TERM expressed in Sf9 cell membranes. 3 mg and 2 mg of Sf9 cell membranes expressing HIS-C-TERM and C-TERM, respectively, were labelled and electrophoresed on a 16% tricene photolabelling gel.

Figure 10.8 suggests that there is a specific protein being labelled at approximately 26 kDa in Sf9 cell membranes expressing HIS-C-TERM protein. Sf9 cell membranes expressing C-TERM protein were observed not to bind any photolabel. The immunoprecipitation step has been omitted in an attempt to visualise all of the photolabelled proteins. This allowed for the detection of the free radioactivity in the photolabelled sample. A smaller protein of approximately 16 kDa was observed which

produced a large photolabelled peak. This peak was not normally observed when immunoprecipitation was included in the protocol.

Photolabelling with the glucose analogue ATB-[2-^{3}H]BMPA was used to demonstrate binding to the exofacial binding site of the HIS-C-TERM protein. By using this label alone it cannot be determined whether the protein has a functional internal site. For example, it may be that the protein is locked into one conformation, capable only of binding ligand at its exofacial site. To determine if the HIS-C-TERM construct had a functional internal site cytochalasin B photolabelling was performed, figure 10.9.

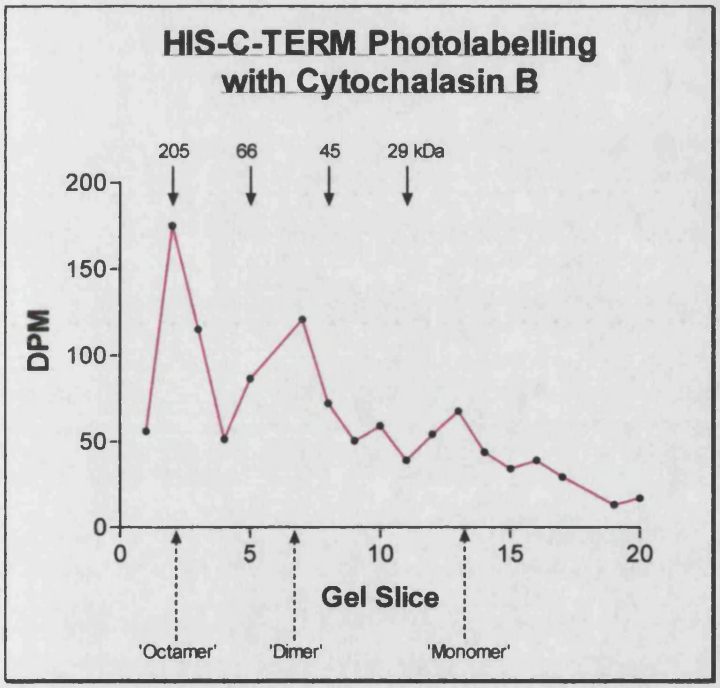

Figure 10.9, Photolabelling HIS-C-TERM with H^3-Cytochalasin B. 600 µg of Sf9 cell membranes expressing HIS-C-TERM were labelled and electrophoresed on a 12% polyacrylamide photolabelling gel. Gel slice 6 did not solubilize and has therefore been omitted from the results.

Cytochalasin B photolabelling resulted in a labelled peak at approximately 26 kDa, this would correspond to the expected size of the HIS-C-TERM protein.. The low levels of radioactivity in this experiment were due to the smaller amounts of radioactive label used.

Photolabelling experiments suggested that both internal and external binding sites are intact and capable of binding ligand. However, it was not possible to demonstrate glucose displacement of the HIS-C-TERM construct. More work would be required to determine if the HIS-C-TERM protein is capable of functioning as a monomeric unit.

Section 10.3

The Effect of Zinc on Human Erythrocyte GLUT1

The HIS-C-TERM protein was engineered with a polyhistidine tag on the N-terminal end. This provided the recombinant protein with a metal binding site. Because the HIS-C-TERM protein was capable of binding to metal ions, the question was posed, 'Is the activity of HIS-C-TERM affected by metal ion concentration?' To answer this question it was first determined whether there were any effects of zinc ions on the wild-type form of the protein. For this purpose, human erythrocyte GLUT1 was photolabelled with varying concentrations of zinc ions, (zinc ions were derived from the compound zinc sulphate in aqueous solution), figures 10.10.

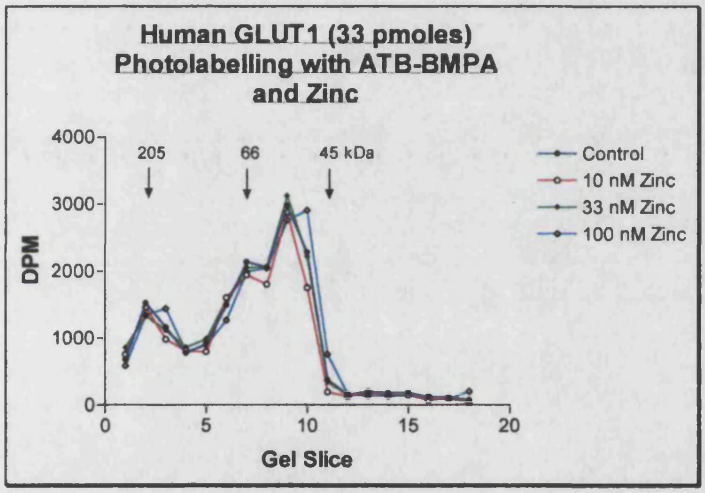

Figure 10.10, Photolabelling human GLUT1 with varying concentrations of zinc. 50 µg (33 pmoles) of human erythrocyte GLUT1 were incubated with varying concentrations of zinc, labelled and electrophoresed on a 10% polyacrylamide photolabelling gel.

The experiment (figure 10.10) demonstrated that there was very little deviation in radioligand binding activity between the presence and the absence of low concentrations of zinc ions in solution. In both cases, the addition of zinc does not significantly increase or decrease photolabel binding. It was therefore concluded that low zinc concentrations had no effect on the activity of the human GLUT1 protein.

The following experiment (figure 10.11) demonstrated that high concentrations of zinc inhibit ligand binding, possibly by interfering with the electrostatic forces within the protein. Disruption of electrostatic forces may result in the alteration of the protein's conformation.

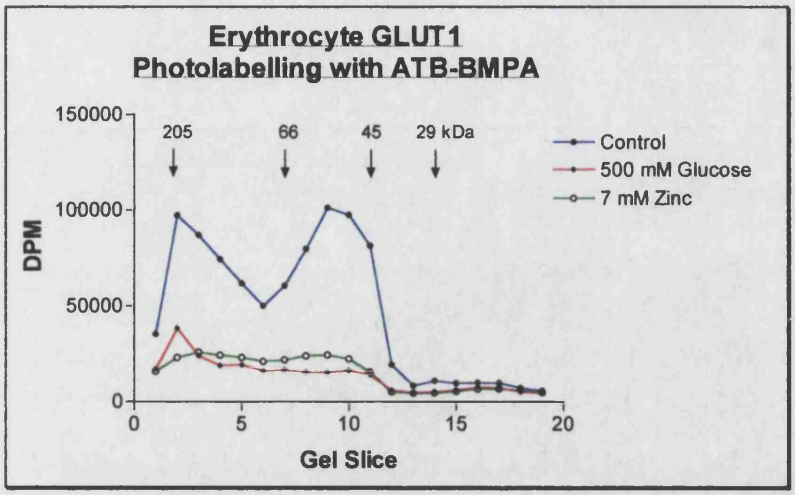

Figure 10.11, High levels of zinc inhibit ligand binding. 500 µg (325 pmoles of human erythrocyte GLUT1, were incubated with zinc or D-glucose for 10 minutes. Erythrocyte membranes were labelled and electrophoresed on a 10% polyacrylamide gel.

It was hypothesised that low concentrations of zinc do not have a significant effect on the activity of wild-type human GLUT1 protein, whereas high concentrations of zinc do have detrimental effects on the activity of human GLUT1 protein.

Section 10.4

The Effect of Zinc on HIS-C-TERM Photolabelling with ATB-[2-^{3}H]BMPA

Figure 10.12 demonstrates the effect of high levels of zinc upon the HIS-C-TERM protein. High levels of zinc can be seen to have an inhibitory effect on ligand binding.

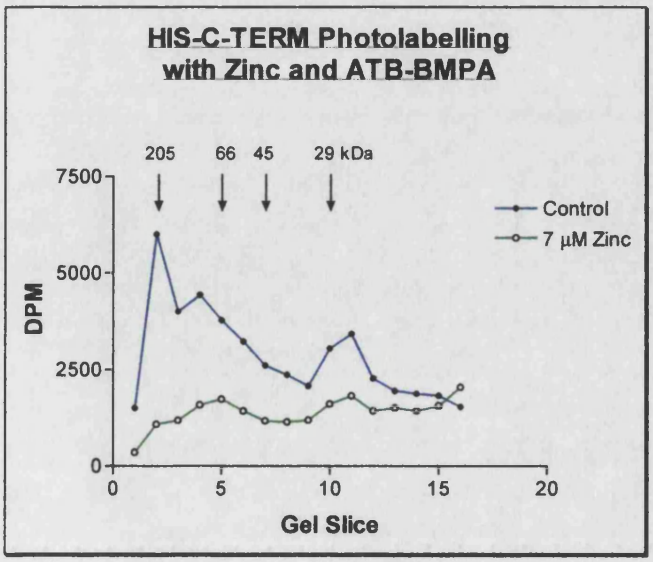

Figure 10.12, Zinc can have a negative effect on ligand binding. 3 mg of homogenised Highfive cell membranes expressing HIS-C-TERM (1305 pmoles) were incubated with or without zinc for 10 minutes. Samples were electrophoresed on a 12% polyacrylamide photolabelling gel.

It seems likely that in the presence of large quantities of zinc the tertiary structure of the protein is disrupted. This may be due to the disruption of electrostatic bonds within the protein. In the case of the polyhistidine tagged proteins, excessive amounts of metal ions may result in the polyhistidine tag becoming saturated with metal ions, causing steric hindrance to the ligand binding regions of the protein. It was hypothesised that in the presence of high concentrations of metal ions both mechanisms would occur. Further experiments have indicated that stochiometric concentrations of zinc act to enhance the ligand binding activity of the HIS-C-TERM protein, probably through metal ion interactions with the polyhistidine tag, figures 10.13 - 10.14.

Quantitative immunoblot assays were used to measure the amount of recombinant protein used in each experiment. Both the amount of recombinant protein present and the amount of zinc ions present were calculated. From these calculations the ratio of components at maximum ligand binding (as determined by photolabelling) was determined.

The amount of Highfive expressed HIS-C-TERM protein was determined by immunoblot assay to be 435 pmoles / mg (1305 pmoles / 3 mg) of membrane protein. This is equivalent to 435 pmoles of metal binding sites which should, theoretically, be capable of metal ion binding.

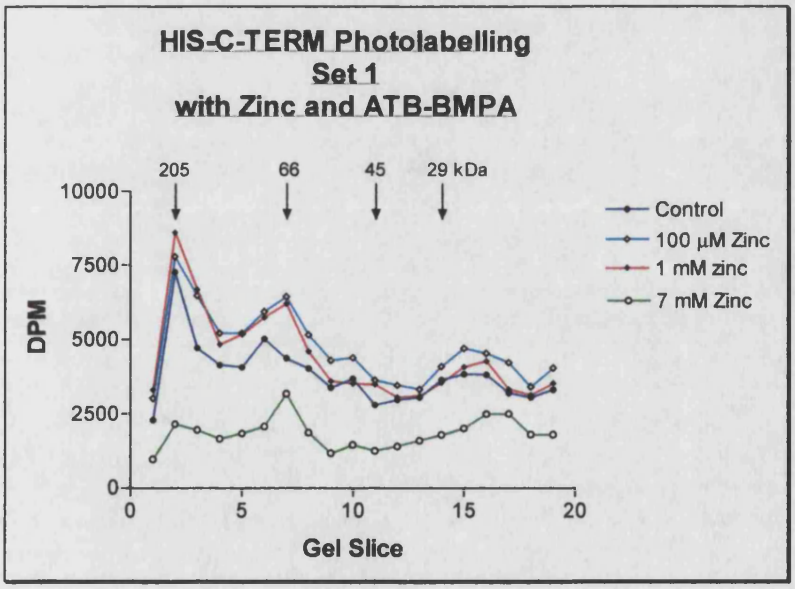

Figure 10.13, Zinc can have a beneficial effect on ligand binding. 3 mg of homogenised Highfive cell membranes expressing HIS-C-TERM (1305 pmoles) were incubated with varying amounts of zinc for 15 minutes and labelled. Samples were electrophoresed on a 12% polyacrylamide gel.

The above experiment (figure 10.13) indicated that the addition of small amounts of zinc had a beneficial effect on radio-ligand binding. It was observed that the addition of 100 µM of zinc had the most effect on photolabelling. Higher zinc concentrations

acted to decrease the level of photolabelling. The trend indicated that there was an optimum amount of zinc required for maximum ligand binding.

Because the osmolarity of 5 mM phosphate buffer was very low it was hypothesised that the HIS-C-TERM protein was losing activity and that the use of a physiological buffer would be more appropriate. The following experiment was performed in Kreb-Ringer hepes buffer, in order to test this hypothesis, figure 10.14.

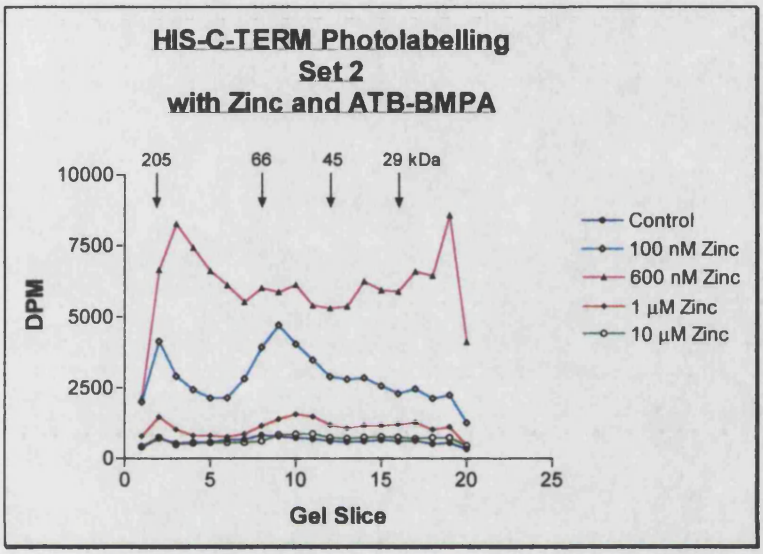

Figure 10.14, Zinc can have a beneficial effect on ligand binding. 3 mg of homogenised Highfive cell membranes, in KRH buffer with protease inhibitors, expressing HIS-C-TERM (1305 pmoles) were incubated with varying amounts of zinc for 35 minutes. Samples were labelled and electrophoresed on a 12% polyacrylamide gel.

Incubation in Kreb-Ringer hepes (KRH) buffer appeared to reduce the binding capacity of the HIS-C-TERM protein, in the absence of zinc, to negligible amounts. This may be due to high levels of metal ions contained within the KRH buffer (1.25 mM magnesium, 4.7 mM potassium, 1.25 mM calcium ions) having the same effect as the addition of excessive amounts of zinc ions. The addition of small amounts of zinc ions to this sample had a beneficial effect, similar to that seen in the previous experiment, figure 10.13. It is possible that the zinc ions compete for binding sites with other metal ions present. Zinc ions have a greater affinity towards the polyhistidine tag than magnesium, calcium or potassium ions. On the addition of 600 nM zinc a large increase in labelled monomeric units occurred. By plotting the total area beneath the curve (figure 10.15) against the amount of zinc, a second order polynomial plot can be fitted to the points. A theoretical maximal effect would be achieved by the addition of 515 pmoles of zinc, this would be equal to 2.5 HIS-C-TERM molecules being associated with 1 zinc ion.

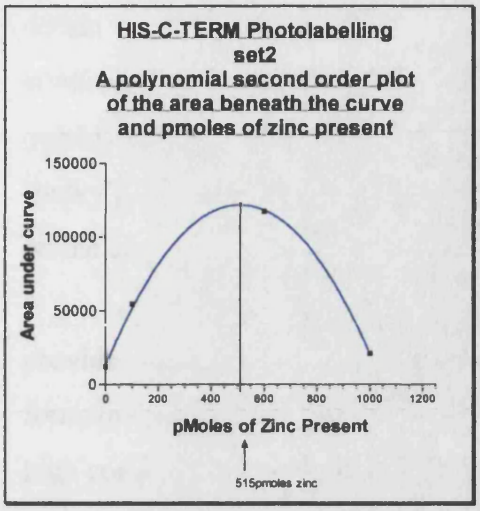

Figure 10.15, A polynomial plot between the integral area beneath the curve and pmoles of zinc present. The areas beneath the curve (arbitrary units) were taken from figure 10.14. For each individual zinc concentration the area below the entire curve was calculated and plotted against the zinc concentration for that curve. Zinc has its theoretical maximal beneficial effect at 515 pmoles/3mg protein.

Section 10.5

Summary of HIS-C-TERM Photolabelling

Results presented here suggested that the protein, HIS-C-TERM can be photolabelled using the radioactive ligands cytochalasin B and ATB-BMPA. However, glucose displacement analysis was inconclusive, so it was not possible to state if the binding was specific towards the C-terminal half of the glucose transporter. However, if the binding activity exhibited by the HIS-C-TERM construct was found to be specific it may provide further evidence for the function of the N-terminal region of the wild-type glucose transporter. The addition of the polyhistidine tag at the start of the HIS-C-TERM protein may have allowed this construct to take on a stable structure.

Examination of several photolabelling experiments indicated that the C-terminal portion was capable of binding more radio-ligand when in the proposed dimeric or octameric form. It was suggested that by forming a dimeric unit the HIS-C-TERM protein mimicked the wild-type form of the protein, where both C-terminal sub-units are capable of ligand binding. It has been shown that the wild-type glucose transporter is capable of associating (Hebert and Carruthers, (1992)) and may function as an complex. It is possible that the C-terminal portion of the protein is forming a similar structure from dimeric units.

It was demonstrated that zinc had both a positive and negative effect upon the HIS-C-TERM protein. At high zinc concentrations, the metal ions have an inhibitory effect on radio-ligand binding. This may be due to the disruption of electrostatic bonds

within the protein, this was also observed during photolabelling of the human erythrocyte GLUT1 protein. Further to this, the metal ions may well act to saturate the polyhistidine tag. Saturation of the polyhistidine tag could make the N-terminus too 'bulky', causing steric hindrance. This may disrupt the protein, preventing it from taking on the correct conformation for ligand binding.

At low concentrations, free metal ions scavenged by the polyhistidine group may provide sites for other HIS-C-TERM units to bind to. This would allow for the formation of the proposed dimers, trimers and octamers. However, in the presence of high concentrations of zinc, figure 10.12, a depletion of octameric and dimeric units was observed. A consequence of saturating the polyhistidine tag appears to be the prevention of protein interactions via metal ion binding sites.

Section 10.6

HIS-GLUT1 Photolabelling

ATB-BMPA photolabelling, of the protein HIS-GLUT1, has already been demonstrated in figure 10.4. The experiment, displayed in figure 10.4, showed that the HIS-GLUT1 protein was capable of binding radioligand at the external binding site. Cytochalasin B binding to the HIS-GLUT1 protein is demonstrated in the following experiment, figure 10.16.

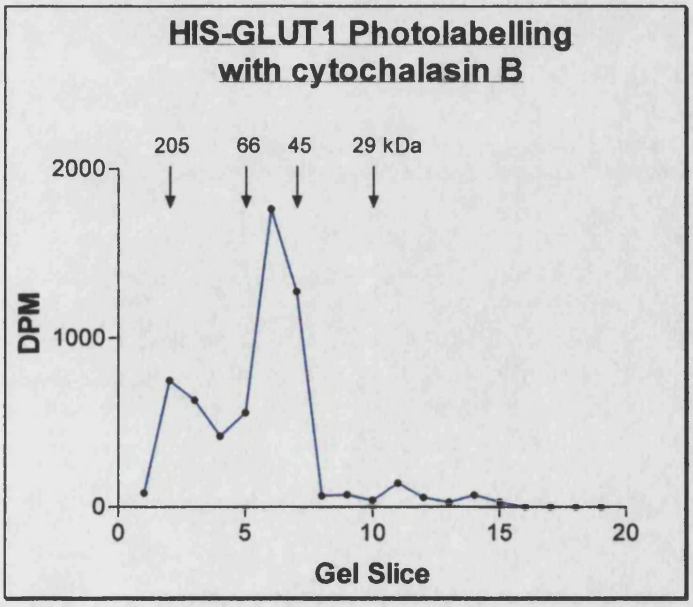

Figure 10.16, HIS-GLUT1 Photolabelling with cytochalasin B. 1.6 mg of homogenised Highfive cell membranes, in 5 mM phosphate buffer with protease inhibitors, expressing HIS-GLUT1. Samples were labelled and electrophoresed on a 12% polyacrylamide photolabelling gel.

The 50 kDa peak, figure 10.16, represents the proposed monomeric form of the HIS-GLUT1 protein. The peak at 205 kDa represents the proposed tetrameric form of the protein. The HIS-GLUT1 protein appears to be capable of binding radioligand at its internal binding site. This indicated that the internal binding site was intact and that the protein was likely to have a wild-type conformation Glucose displacement of the ATB-BMPA labelling was demonstrated in figure 10.17.

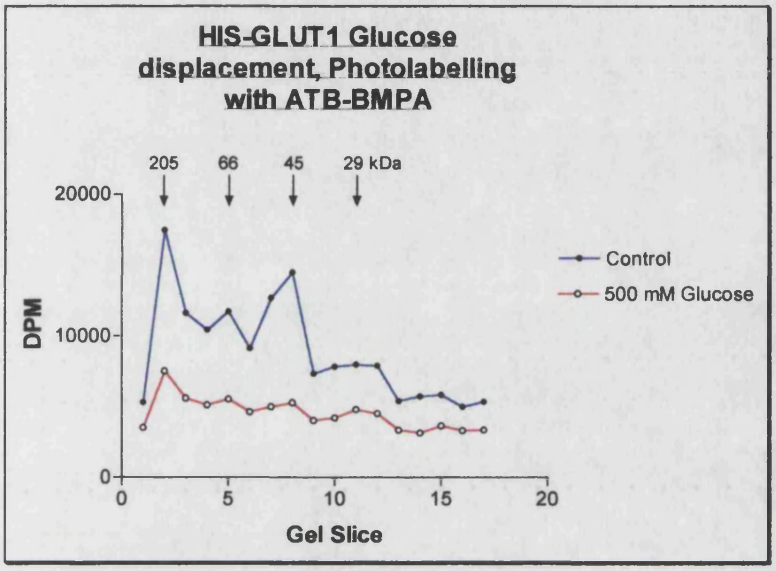

Figure 10.17, HIS-GLUT1 Photolabelling, displaying D-glucose displacement. 1.6 mg of Highfive cell membranes expressing HIS-GLUT1 were homogenised in 5 mM phosphate buffer with protease inhibitors,. Samples were labelled and electrophoresed on a 10% polyacrylamide gel.

Glucose displacement studies demonstrated that the HIS-GLUT1 protein was capable of recognising its natural substrate, D-glucose and is likely to be in a wild type conformation. High levels of labelling were observed in the proposed tetrameric peak region (205 kDa). This may be a result of longer incubation times with the radioligand at room temperature. The photolabelling experiment displayed in figure 10.4 was performed on ice and the protein was incubated with ATB-BMPA for less than 4 minutes.

Section 10.7

The Effect of Zinc on HIS-GLUT Photolabelling with ATB-[2-^{3}H]BMPA

Zinc has been observed to have both a positive and negative effect on the HIS-C-TERM protein. Figure 10.18 displays the effect of incubating 696 pmoles of HIS-GLUT1 with 7 µmoles of zinc. The 45 kDa peak is greatly reduced which is

thought to be due to the disruption of electrostatic bonds within the protein, this in turn may disrupt protein conformation. The proposed tetramer, at 205 kDa, was completely eliminated.

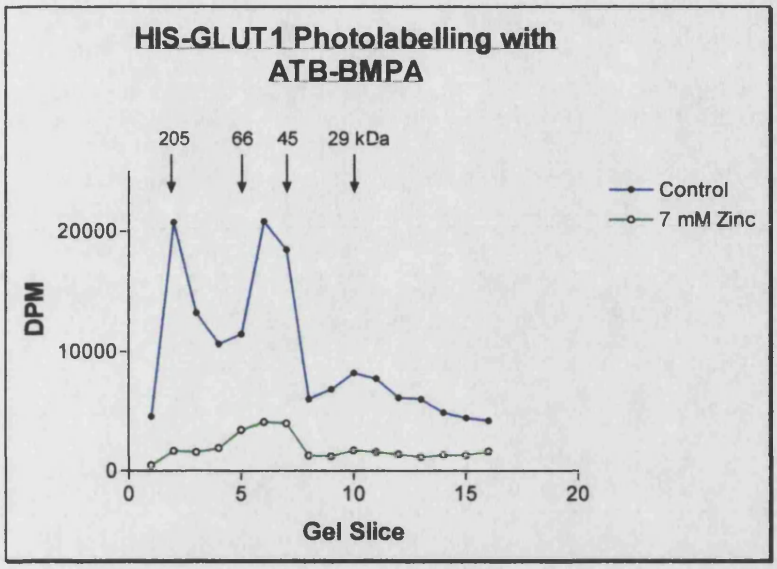

Figure 10.18, HIS-GLUT1 photolabelling, exhibiting the negative effect of zinc on ligand binding. 1.6 mg of homogenised Highfive cell membranes expressing HIS-GLUT1 (696 pmoles HIS-GLUT1) were incubated with or without zinc for 10 minutes. Samples were labelled and electrophoresed on a 12% polyacrylamide gel.

Radioligand binding appeared to be greatly reduced by the addition of large amounts of zinc. The following 3 experiments display the effects of small amounts of zinc upon the HIS-GLUT1 protein, figures 10.19 - 10.22.

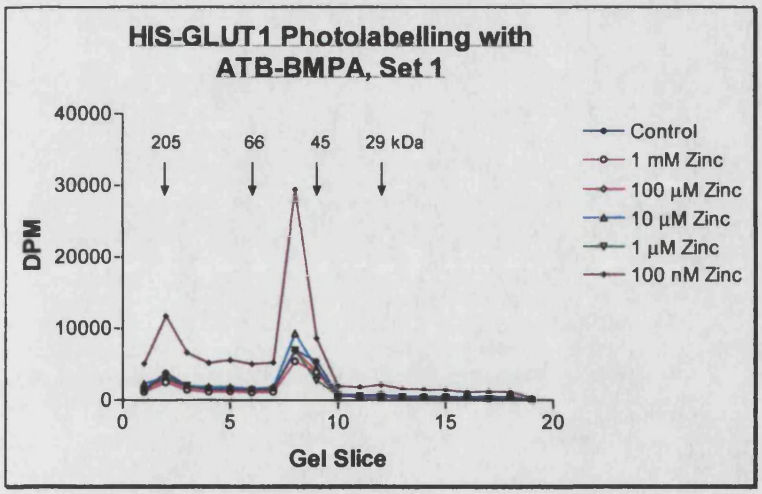

Figure 10.19, HIS-GLUT1 Photolabelling, exhibiting the effect of zinc on ligand binding. 2 mg of homogenised Highfive cell membranes expressing HIS-GLUT1 were incubated with or without zinc in 5 mM phosphate buffer for 5 minutes. Samples were labelled and electrophoresed on a 10% polyacrylamide photolabelling gel.

The experiment displayed in figure 10.19, showed a significant increase in photolabel binding in the presence of small amounts of zinc. The levels of aggregation were also reduced in this experiment, which was attributed to the short incubation times (10 minutes) with zinc and ATB-BMPA. It was though that the longer incubation times

were responsible for increasing the level of aggregation observed. The experiment was repeated with a longer incubation time, the results are displayed in figure 10.20.

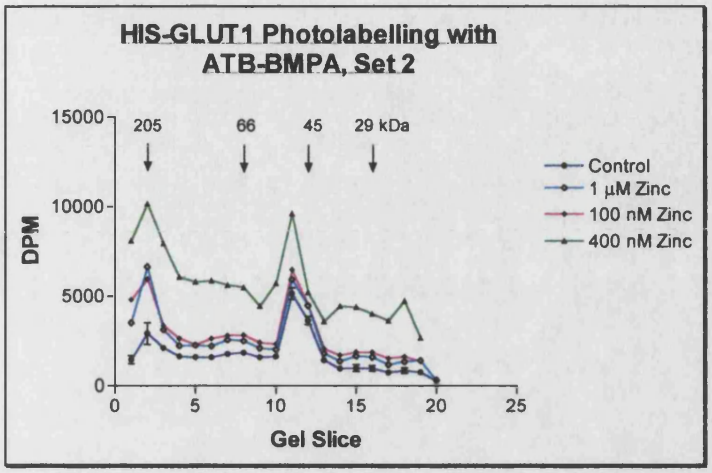

Figure 10.20, HIS-GLUT1 Photolabelling, exhibiting the effect of zinc on ligand binding. 2 mg of homogenised Highfive cell membranes expressing HIS-GLUT1 were incubated with or without zinc for 35 minutes. Samples were labelled and electrophoresed on a 10% polyacrylamide photolabelling gel.

The above experiment, figure 10.20, again demonstrated an increase in bound photolabel on the addition of small amounts of zinc. Data from this experiment was used to plot the area beneath the curve against the amount of zinc added, figure 10.21, and was found to fit a polynomial relationship. A maximum theoretical response was predicted at 530 pmoles zinc. The areas calculated include the aggregation peaks. At maximum radioligand binding a ratio of protein : metal ions of 1.64 HIS-GLUT1 : 1 zinc ion was observed.

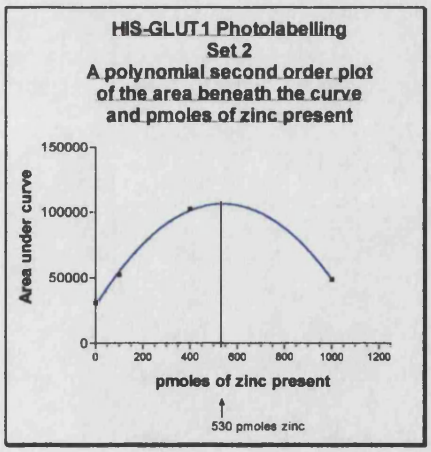

Figure 10.21, A polynomial plot between the integral area beneath the curve and pmoles of zinc present. The areas beneath the curve (arbitrary units) were taken from figure 10.20. For each individual zinc concentration the area below the entire curve was calculated and plotted against the zinc concentration for that curve. Zinc has its theoretical maximal beneficial effect at 530 pmoles/2mg protein.

Because of the low osmolarity of 5 mM phosphate buffer a physiological buffer was tested to ensure that the HIS-GLUT1 protein was not taking on a novel

conformation in the low osmolar buffer. KRH buffer was used as the physiological buffer. The results of this experiment are displayed below in figure 10.22.

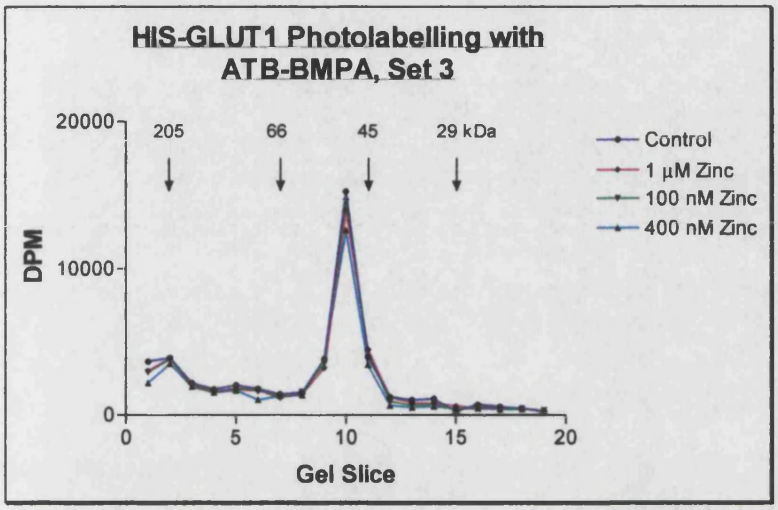

Figure 10.22, HIS-GLUT1 photolabelling, exhibiting the effect of zinc on ligand binding. 3 mg of homogenised Highfive cell membranes expressing HIS-GLUT1 (1305 pmoles HIS-GLUT1) were incubated with or without zinc for 5 minutes in KRH buffer with protease inhibitors. Samples were labelled and electrophoresed on a 10% polyacrylamide gel.

In the above experiment, figure 10.22, Highfive cells expressing the HIS-GLUT1 protein construct were homogenised in KRH buffer. Very few aggregates were observed, probably due to the short incubation times and high concentrations of metal ions present in the KRH buffer. Incubation with KRH buffer also appeared to eliminate any response from the addition of small amounts of zinc. This may have been because the HIS-GLUT1 protein had already been stimulated to bind the maximum amount of radioligand by the metal ions present in the KRH buffer, saturating the polyhistidine tags with metal ions.

When resuspended in KRH buffer, the result of adding zinc to the HIS-GLUT1 protein was different to the result obtained from adding zinc to the HIS-C-TERM protein. The HIS-GLUT1 protein, unlike the HIS-C-TERM protein, appeared to be fully functional as a metal ion saturated monomer. This may be because the N-terminal portion of the protein acts to 'shield' the binding site from any effect that the metal ion saturated polyhistidine site may have on the protein structure.

Section 10.8

Summary of HIS-GLUT1 Photolabelling

It has been demonstrated that the HIS-GLUT1 protein has affinity for the radioligands cytochalasin B and ATB-BMPA. This demonstrated that both the internal and external binding sites of the HIS-GLUT1 protein have a conformation similar to that of the wild-type protein. Furthermore, it was shown that binding of the ligand ATB-[2-^{3}H]BMPA was D-glucose displaceable, indicating that the external binding site has retained its affinity for its natural substrate, glucose. These data, together with cytochalasin B assay results, indicate that the recombinant protein HIS-GLUT1 still recognises its natural substrate at both the external and internal sites. Unfortunately, it was not possible to measure D-glucose transport across the membrane of infected insect cells due to the cell membranes becoming 'leaky' following viral infection. However, experiments carried out by Dr Annette Schürmann (Institute for Pharmacology and Toxicology, Aachen, Germany) on reconstituted HIS-GLUT1 from Sf9 cells (University of Bath) demonstrated that an increased level of D-glucose transport was obtained from HIS-GLUT1 transfected Sf9 cells (unpublished data) in comparison with uninfected Sf9 cells.

Under certain reaction conditions the addition of zinc had a beneficial effect on the binding of radioligand. It was possible that the zinc ions caused an association of glucose transporters that was beneficial to ligand binding. Alternatively, the bound zinc ions may have conferred a slightly different protein structure which allowed more photolabel to bind.

10.9 Discussion

Experiments suggested that the HIS-C-TERM protein was capable of binding glucose analogues. Unfortunately, in the absence of glucose displacement data this cannot be confirmed. However, if the HIS-C-TERM construct is capable of functioning as a single unit, then this rules out the possibility of the N-terminal portion being involved in the external glucose binding site. It is therefore more likely that the glutamine 161 mutation, generated by Mueckler *et al.,* (1994) causes a massive

structural change transmitted through the protein structure, rather than being involved directly in the binding site itself. Both the HIS-C-TERM and C-TERM proteins were shown to be expressed at similar levels in the Sf9 cell (by immunoblotting), demonstrating that any differences observed were not simply due to different levels of expression.

It was hypothesised that the C-TERM protein may represent the original ancestral protein, which existed before the proposed gene duplication event (Szkutnicka *et al.,* (1989). The ancestral protein may have had a very low capacity for transporting glucose. Glucose transport across the membrane would therefore have been very slow. Evolutionary pressures may have then acted to select a mutated form of the glucose transporter. A form which was generated from a gene duplication event. The gene duplication event may have produced a glucose transporter which had a higher capacity for transporting glucose.

11.0 Purification of Polyhistidine Tagged GLUT1

Section 11.1 Introduction

The recombinant proteins HIS-GLUT1 and HIS-C-TERM were N-terminally polyhistidine tagged to aid purification while using a chelating nickel Sepharose column. This technique can result in a pure protein. If large quantities of purified HIS-GLUT1 and HIS-C-TERM protein were obtained it would be possible to start crystallisation trials on the proteins. This could result in 3-dimensional X-ray crystallographic analysis or 2-dimensional electron diffraction analysis being performed. This structural information would confirm or disprove the proposed 3-dimensional theoretical structures for the glucose transporter protein.

It was hypothesised that the HIS-C-TERM construct would have a higher affinity towards the matrix and would prove simpler to purify. It was further hypothesised that its compact, simpler structure would prove easier to crystallise and analyse by X-ray crystallographic analysis.

Section 11.2 Cell Fractionation

Sf9 cells expressing the HIS-GLUT1 protein were homogenised and fractionated at an appropriate speed for 15 minutes using a Beckman ultracentrifuge, table 11.1. The HIS-GLUT1 protein was found to be present in three of the four fractions by immunoblot analysis. The HIS-GLUT1 protein was not fully recovered by centrifugation for 15 minutes at 22,000 g. This suggested that the HIS-GLUT1 protein was associated with internal membranes and structures, other than the plasma membrane. This data was consistent with confocal microscopy studies that suggested some of the HIS-GLUT1 protein was mis-targeted to internal cellular structures. The presence of HIS-GLUT1 in the 22,000 - 541,000 g fraction is shown on the immunoblot, figure 11.1. The immunoblot was densitometrically analysed and the results are displayed in figure 11.2 and table 11.2.

Fraction	Fraction contents
0 - 350 g	Whole cells, large membrane fragments
350 - 22,000 g	Membrane fragments
22,000 - 541,000 g	Microsomal fraction, very small membrane fragments
Supernatant	Soluble cytoplasmic proteins

Table 11.1, Fractionation of Sf9 cells expressing HIS-GLUT1.. HIS-GLUT1 was found to be present in the first 3 fractions but not in the 541,000 g supernatant.

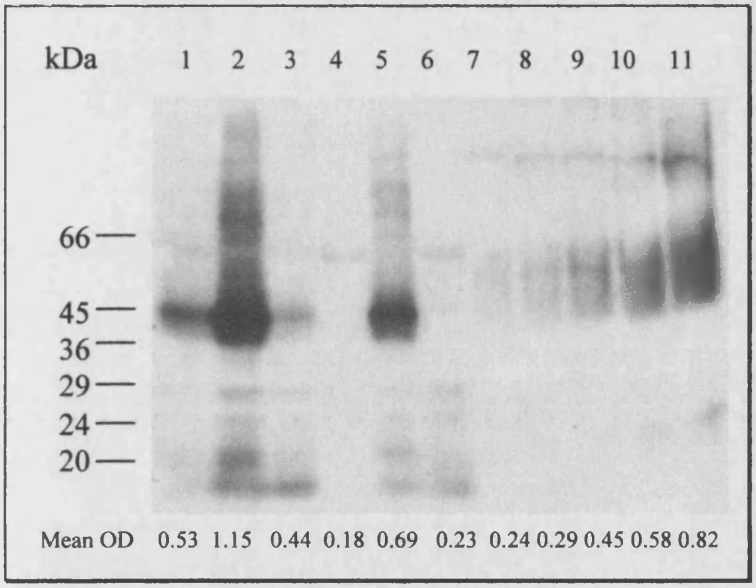

Figure 11.1, Immunoblot assay to determine the composition of membrane fractions. Sf9 cells were homogenised and the membranes pelleted in a Beckman ultracentrifuge. 20 µg of protein was loaded on a 10% polyacrylamide gel as follows: Lane 1: 20 µg of fraction A supernatant (supernatant from an 15 minute centrifugation of homogenised Sf9 cells at 22,000 g); lane 2: 20 µg of fraction A pellet (Sample A, 0 - 22,000 g for 15 minutes); lane 3: 20 µg of fraction B pellet (fraction B: Fraction A, pelleted at 541,000 g for 15 minutes); lane 4: 20 µg of fraction C, from fraction B supernatant (fraction C: Fraction B, 541,000 g supernatant); lane 5: 20 µg of Sf9 cells expressing HIS-GLUT1; lane 6: 20 µg non-transfected Sf9 cells; lane 7: human GLUT1 standard, 10 ng; lane 8: human GLUT1 standard, 25 ng; lane 9: human GLUT1 standard, 50 ng; lane 10: human GLUT1 standard, 75 ng; lane 11: human GLUT1 standard, 100 ng.

Centrifugation for 15 minutes at 541,000 g was observed to pellet all of the membranes with associated HIS-GLUT1 protein. The immunoblot was analysed using a BioRad scanner with molecular analyst software for the PC. A standard curve was generated from the human GLUT1 standard and is displayed below in figure 11.2. The amount of recombinant protein in each sample was determined and is displayed in table 11.2.

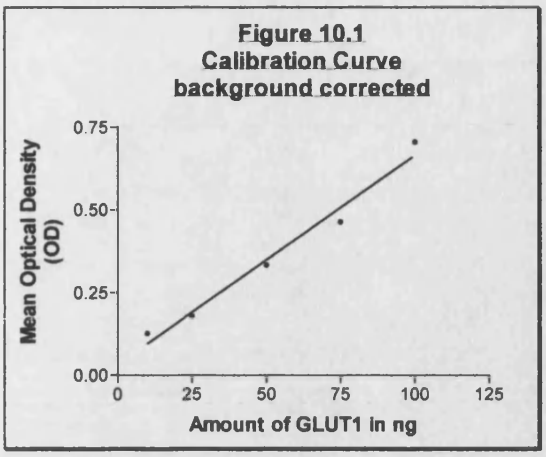

Figure 11.2, Immunoblotting calibration curve to determine the composition of membrane fractions (cf. figure 11.1). Figure 11.1 was densitometrically analysed and the data generated from the standards plotted. From this standard curve the amount of unknown HIS-GLUT1 was calculated, table 11.2.

Lane	Total Amount of HIS-GLUT1 in µg / 150 ml culture
Lane 5: Starting material	252 µg
Lane 2: 22,000 g pellet	96 µg
Lane 1: 22,000 g supernatant	146 µg
Lane 3: 541,000 g pellet	122 µg
Lane 4: 541,000 g supernatant	4 µg

Table 11.2, The table displays the calculated distribution of fractionated HIS-GLUT1 protein.

The immunoblot displayed in figure 11.1 demonstrated that the HIS-GLUT1 protein was associated with the three fractions between 0 - 541,000 g. The HIS-GLUT1 protein was not found in the 541,000 g supernatant, demonstrating it to be insoluble and entirely associated with cellular membranes. It was observed from the densitometry data (table 11.2) that 58% of the protein was lost by centrifugation at 22,000 g for 15 minutes (146 µg were lost and only 96 µg were recovered). Centrifugation of the 22,000 g supernatant at 541,000 g for 15 minutes resulted in the recovery of 122 µg of recombinant protein, which constituted most of the lost protein. To ensure total recovery of the HIS-GLUT1 protein, cell homogenates were routinely centrifuged at 541,000 g for 15 minutes.

Further analysis of the cell wash supernatant demonstrated a significant amount of soluble protein with an apparent molecular weight of 66 kDa, figure 11.3.

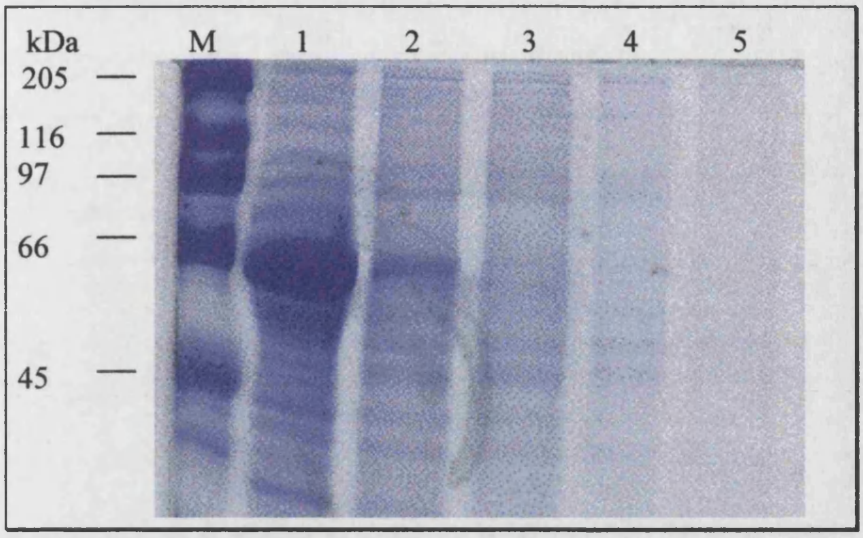

Figure 11.3, Coomassie stained gel demonstrating the presence of a soluble protein at 66 kDa. Sf9 cells expressing HIS-GLUT1 were washed in a 1 ml volume of 5 mM phosphate buffer and 40 µl aliquots were taken and loaded on a 10% polyacrylamide gel as follows: Lane 1: 40 µl of 1st supernatant; lane 2: 40 µl of 2nd supernatant; lane 3: 40 µl of 3rd supernatant; lane 4: 40 µl of 4th supernatant; lane 5: 40 µl of 5th supernatant.

The large protein band running at 66 kDa was thought to be bovine serum albumin (BSA), derived from the foetal calf serum that the cells were incubated in during growth. The BSA may either be adhering to the cell membranes or it may be taken up and retained within the cell. The above experiment indicated that most of the BSA was removed after about three washes with buffer. However, it would be possible to completely eliminate BSA from the system by adapting the insect cells to grow in a serum free medium. In order to routinely remove the BSA, cells were homogenised and washed 3 times using 5 mM phosphate buffer containing protease inhibitors.

Section 11.3

Detergent Analysis

Four detergents were selected for screening (based on economy, availability and physical properties) these were: Thesit, SB12 (Zwittergent® 3-12), Octyl glucoside and Triton X-100. Detergents were tested for their ability to solubilize homogenised insect cells. Following solubilization samples were centrifuged to remove unsolubilized material. Equal amounts of protein were taken from the solubilized supernatant and unsolubilized pellet for analysis by immunoblot assay. All four detergents appeared to solubilize HIS-GLUT1 and HIS-C-TERM at room temperature, but at 4°C triton X-100

did not solubilize either protein construct efficiently. For this reason triton X-100 was not selected for further testing. None of the detergents used were capable of completely solubilizing the HIS-GLUT1 or the HIS-C-TERM proteins. Thesit, SB12 (Zwittergent® 3-12) and Octyl glucoside were tested for use on a Pharmacia Biotech HiTrap™ affinity column.

Section 11.4 FPLC Analysis

Detergent - Thesit

Cells were prepared and solubilized in 5 mM phosphate buffer containing 1% Thesit with protease inhibitors. Protein was solubilized at a ratio of 2 mg of protein to 1 ml of detergent. The insoluble material was pelleted at 164,000 g in a Beckman ultracentrifuge for 15 minutes and was loaded onto a 5 ml (bed volume) Pharmacia Biotech metal chelating column, previously charged with 15 ml of 0.1 M nickel sulphate. The column was washed using 25 ml of IMAC buffer containing 1% Thesit, protease inhibitors and no imidazole. Elution was over a 25 ml gradient ending in IMAC 200 buffer containing 1% Thesit, protease inhibitors and 200 mM imidazole (ie., forming a gradient between 0 and 200 mM imidazole) on a Pharmacia FPLC unit. The column was run three times, once with no protein as a control, once with HIS-GLUT1 and once with HIS-C-TERM, figures 11.4 - 11.6.

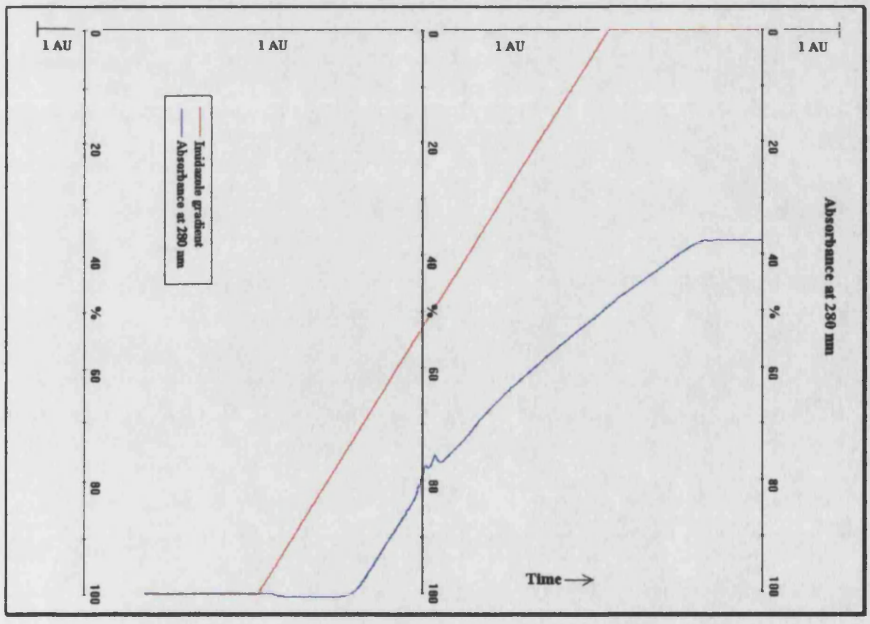

Figure 11.4, FPLC control using a nickel column. A Pharmacia Biotech HiTrap column (charged with nickel) was run with no protein using 5 mM phosphate buffer containing 1% Thesit. The red line represents the imidazole gradient and the blue line the increase in absorption at 280 nm. The column had been previously used for histidine tagged protein purification which explains the minor peak in the elution line.

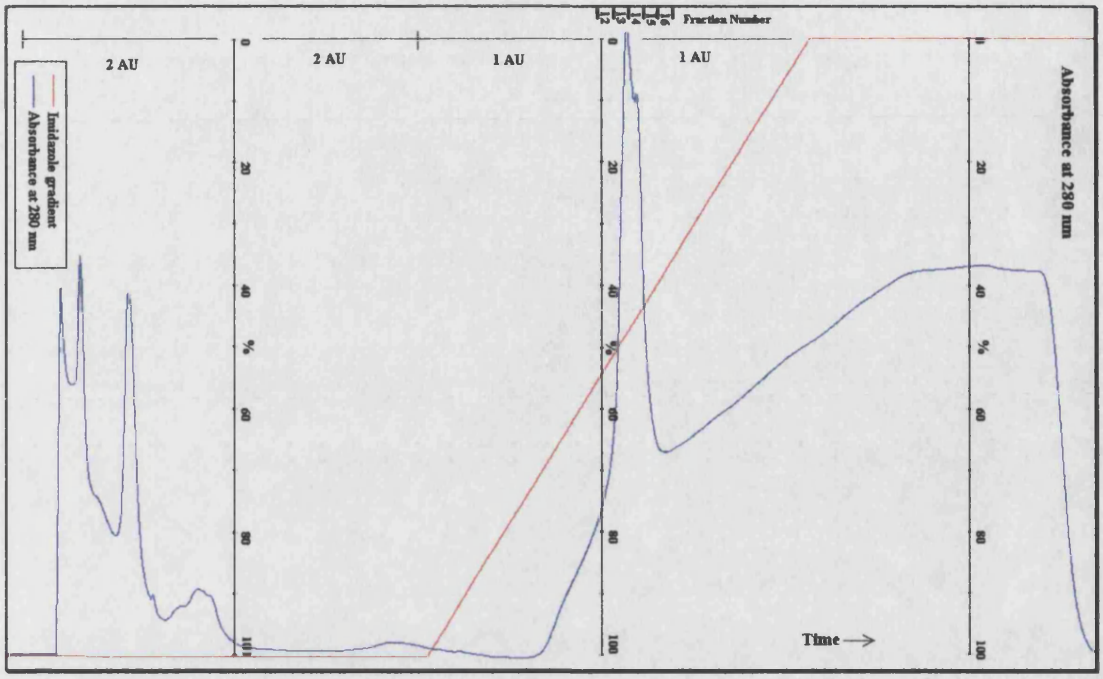

Figure 11.5, FPLC elution of HIS-GLUT1 using a nickel column. A Pharmacia Biotech HiTrap column (charged with nickel) was loaded with HIS-GLUT1 protein. The red line represents the imidazole gradient and the blue line the increase in absorption at 280 nm. The wash was monitored at a sensitivity of 2 AU and the elution at a sensitivity of 1 AU.

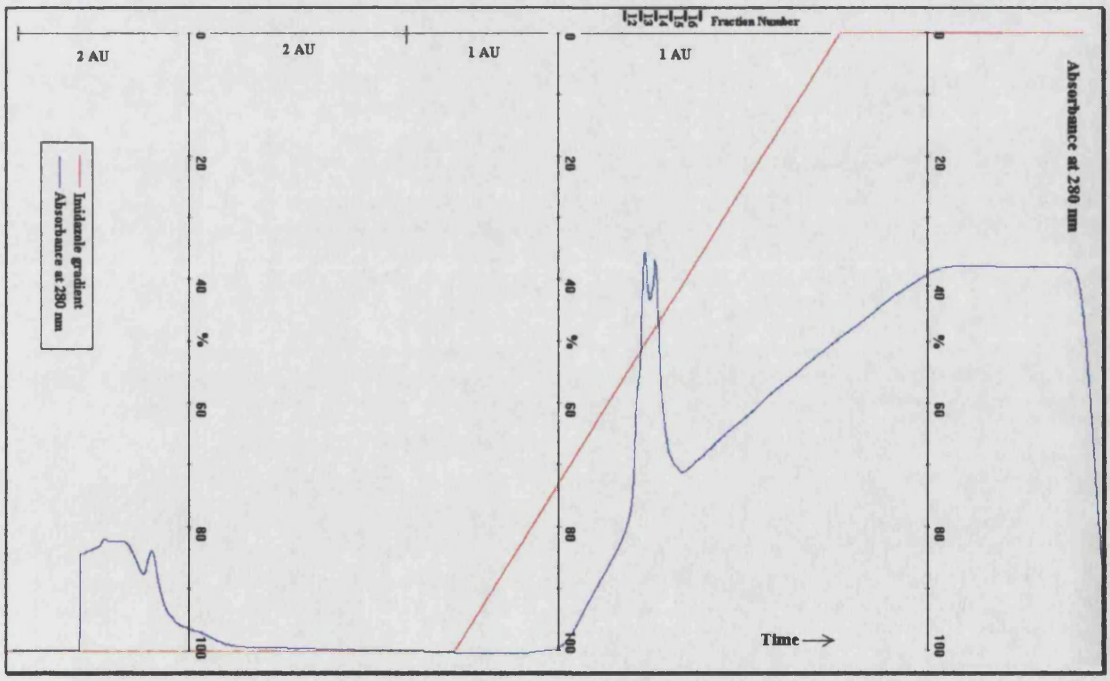

Figure 11.6, FPLC elution of HIS-C-TERM using a nickel column. A Pharmacia Biotech HiTrap column (charged with nickel) was loaded with HIS-C-TERM protein. The red line represents the imidazole gradient and the blue line the increase in absorption at 280 nm. The wash was monitored at a sensitivity of 2 AU and the elution at a sensitivity of 1 AU.

Protein elution was observed to occur at 35% of the total imidazole gradient, (70 mM imidazole). In both FPLC plots, figures 11.5 and 11.6, the elution peak forms a twin peak, the first indication that the HIS-GLUT1 and HIS-C-TERM proteins have not been eluted as pure proteins. Column fractions were analysed by SDS-PAGE followed by Coomassie Blue staining and by immunoblot analysis. Immunoblotting revealed that the HIS-GLUT1 protein had been specifically eluted in the peak fractions 13, 14 and 15. However, Coomassie staining revealed that there were many impurities present in the peak fractions. It was observed that the imidazole content of the fractions interfered with the protein assay system used, therefore constant volumes were loaded on the gel to visualise eluted proteins.

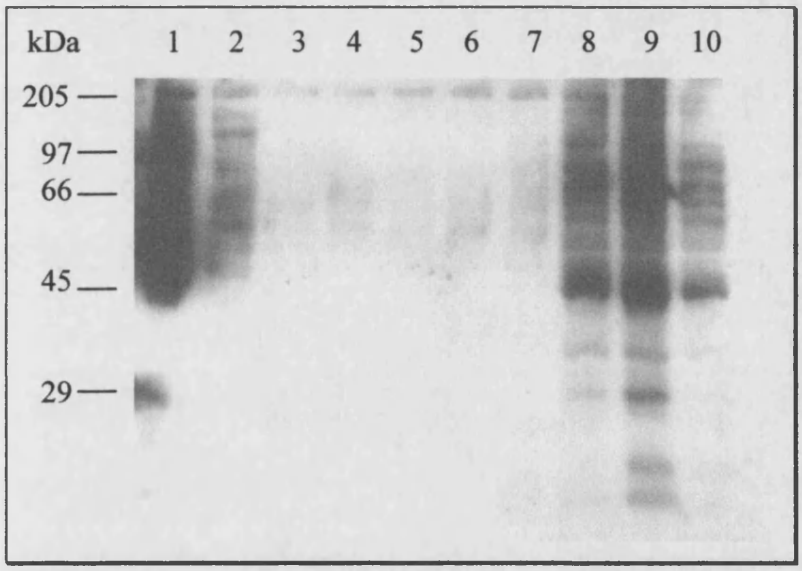

Figure 11.7, Immunoblot analysis of Thesit solubilized HIS-GLUT1 eluted from a HiTrap nickel column. Solubilized Sf9 cells were eluted from a Pharmacia Biotech HiTrap nickel column and electrophoresed on a 12% polyacrylamide gel as follows: Lane 1: 40 µl of sample loaded on column; lane 2: 40 µl of column wash; lane 3: 40 µl of fraction 8; lane 4: 40 µl of fraction 9; lane 5: 40 µl of fraction 10; lane 6: 40 µl of fraction 11; lane 7: 40 µl of fraction 12; lane 8: 40 µl of fraction 13; lane 9: 40 µl of fraction 14; lane 10: 40 µl of fraction 15; lane 11: 40 µl of fraction 16; lane 12: 40 µl of fraction 17.

SDS-PAGE analysis was repeated for the HIS-C-TERM protein. Coomassie staining revealed many impurities in the peak fractions. However, immunoblot analysis demonstrated that very little HIS-C-TERM protein was detectable in the peak fractions, figure 11.8.

Modifications were made to the purification protocol using the Thesit detergent system, but had no effect on the results. Modifications included increasing the detergent concentration to 2% Thesit in order to achieve better solubilization and the inclusion of 20 mM imidazole in the wash buffer to reduce non-specific binding to the column.

The use of Thesit was discontinued following the attempted purification of recombinant protein. There were also further concerns that the peroxide and aldehyde impurities of Thesit may well be damaging the recombinant protein.

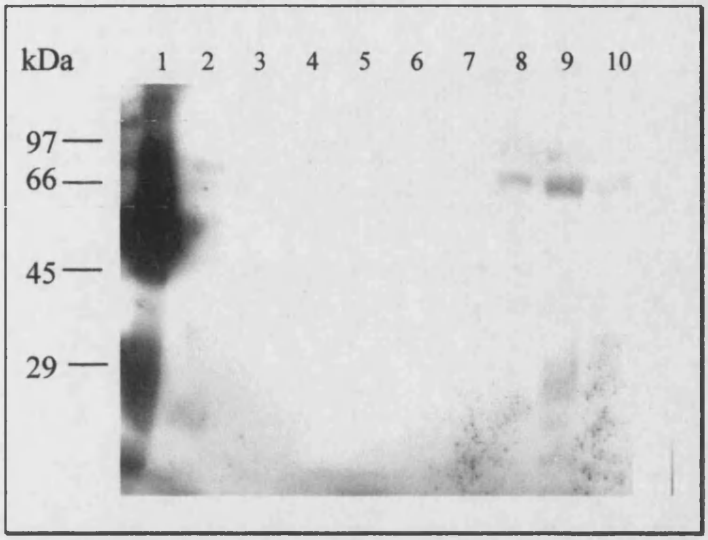

Figure 11.8, Immunoblot analysis of Thesit solubilized HIS-C-TERM eluted from a HiTrap nickel column. Solubilized Sf9 cells were collected from a Pharmacia Biotech HiTrap nickel column using a Pharmacia Biotech FPLC unit and electrophoresed on a 12% polyacrylamide gel as follows: Lane 1: 40 µl of sample loaded on column; lane 2: 40 µl of column wash; lane 3: 40 µl of fraction 7; lane 4: 40 µl of fraction 8; lane 5: 40 µl of fraction 9; lane 6: 40 µl of fraction 10; lane 7: 40 µl of fraction 11; lane 8: 40 µl of fraction 12; lane 9: 40 µl of fraction 13; lane 10: 40 µl of fraction 14.

Detergent - SB12

SB12 derivatives were reported by Pourcher *et al.*, (1995) to be suitable detergents for solubilizing the polyhistidine tagged melibiose permease. SB12 was tested as a possible detergent system for solubilizing the HIS-GLUT1 protein. The HIS-GLUT1 protein was solubilized in 5 mM phosphate buffer containing 2% SB12 with protease inhibitors (2 mg protein : 1 ml detergent). The column was washed with 25 ml of IMAC 20 buffer and then eluted over a 25 ml gradient up to a final concentration of 200 mM imidazole, using IMAC 200 buffer. The FPLC plot is displayed in figure 11.9.

There were no specific elution peaks visible throughout the graduated increase in imidazole concentration. Furthermore, it was apparent that the detergent SB12 altered the oxidation state of the immobilised metal ions. The application of SB12 (with or without solubilized protein) to either a nickel column or copper column turned the column a brown colour or yellow colour, respectively. The coloration could only be removed by washing the column using 7 M hydrochloric acid.

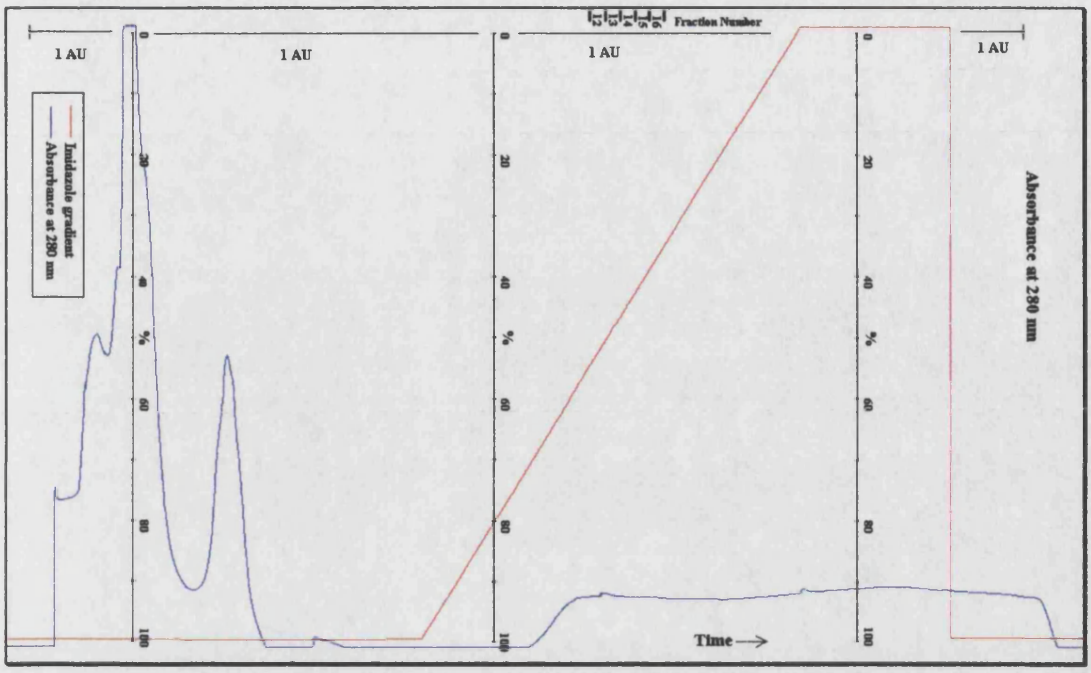

Figure 11.9, FPLC elution of HIS-GLUT1 using a nickel column. A Pharmacia Biotech HiTrap column (charged with nickel) was loaded with HIS-GLUT1 protein solubilized in 5 mM phosphate buffer containing 2% SB12 with protease inhibitors. The red line represents the imidazole gradient and the blue line the increase in absorption at 280 nm. The FPLC was monitored at a sensitivity of 1 AU.

The chemical alteration of the column, by the detergent SB12, clearly destroyed any affinity towards the histidine tagged protein. Thus the detergent was eliminated from further screening.

Detergent - Octyl Glucoside

The detergent Octyl Glucoside is less economical, but has been the detergent of choice for solubilizing erythrocyte GLUT1 for many years. Test columns were run using octyl glucoside.

A Pharmacia Biotech HiTrap column was charged with 0.1 M nickel sulphate and loaded with 10 mg of protein solubilized in 5 ml of 5 mM phosphate buffer containing 1.35% octyl glucoside with protease inhibitors. The protein was loaded on to the column and eluted using a Pharmacia FPLC unit. The column was washed with 25 ml of IMAC 20 buffer containing 100 mM sodium chloride, 20 mM imidazole and 0.75% octyl glucoside. The column was eluted over a 25 ml gradient. The 100% final

elution buffer was composed of IMAC 200 buffer containing 100 mM sodium chloride, 200 mM imidazole and 0.75% octyl glucoside.

The column run was repeated with the same buffers, using a 20 ml wash and a 7 ml elution gradient. For comparison, the column was run using copper as the immobilised metal ion. The same buffer conditions were used on the copper column as described above. A 20 ml wash and a 15 ml elution gradient were used during the run.

The FPLC plots of the HIS-GLUT1 protein on both nickel and copper columns are displayed on the following pages, figures 11.10, 11.11 and 11.12. All column runs resulted in sharp elution peaks. Fractions were analysed on polyacrylamide gels using Coomassie staining and immunoblot analysis.

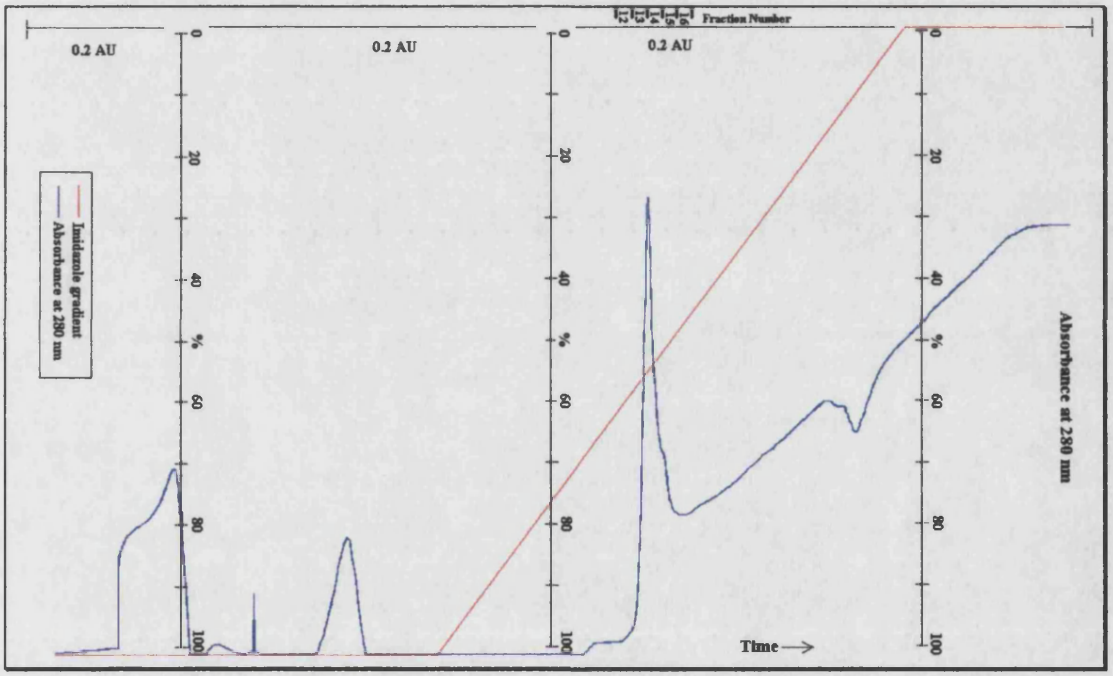

Figure 11.10, FPLC elution of HIS-GLUT1 using a nickel column. A Pharmacia Biotech HiTrap column (charged with nickel) was loaded with HIS-GLUT1 protein. The red line represents the imidazole gradient and the blue line the increase in absorption at 280 nm. The FPLC was monitored at a sensitivity of 0.2 AU.

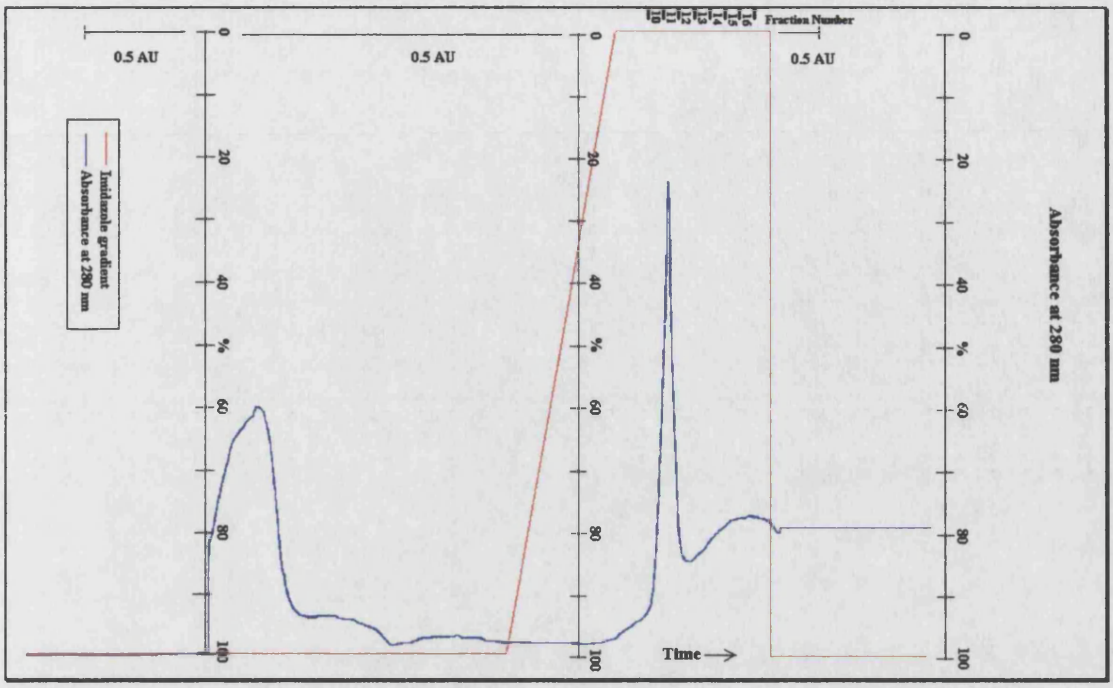

Figure 11.11, FPLC elution of HIS-GLUT1 using a nickel column. A Pharmacia Biotech HiTrap column (charged with nickel) was loaded with HIS-GLUT1 protein. The column was washed with 20 ml of wash buffer and eluted over a 7 ml gradient. The red line represents the imidazole gradient and the blue line the increase in absorption at 280 nm. The FPLC was monitored at a sensitivity of 0.5 AU.

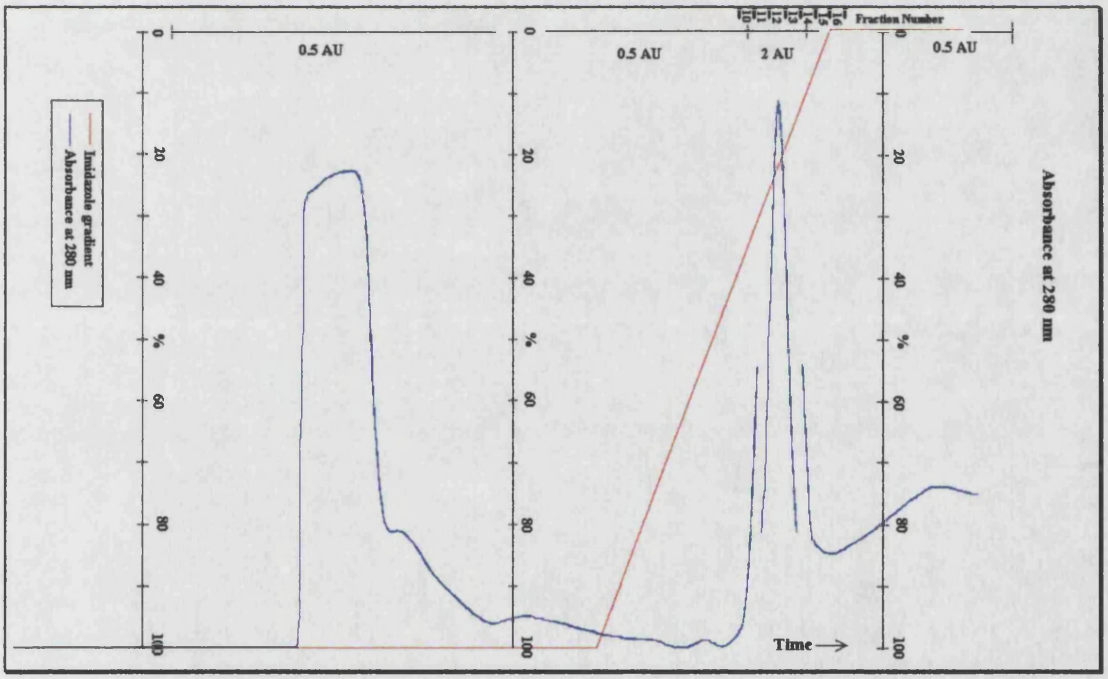

Figure 11.12, FPLC elution of HIS-GLUT1 using a copper column. A Pharmacia Biotech HiTrap column (charged with copper) was loaded with HIS-GLUT1 protein. The red line represents the imidazole gradient and the blue line the increase in absorption at 280 nm.

FPLC samples from the nickel Sepharose column (figure 11.10) were analysed by immunoblot assay and by Coomassie staining, figure 11.13 and figure 11.14, respectively. The FPLC plot displayed in figure 11.10 indicated that the major protein band was eluted at about 30% of 200 mM imidazole (60 mM imidazole), and was contained within fraction 14 (peak fraction). The FPLC plot displayed in figure 11.11 demonstrated that the wash and the elution of the HIS-GLUT1 protein can be performed using much smaller volumes of buffer. Thus making the process more economical.

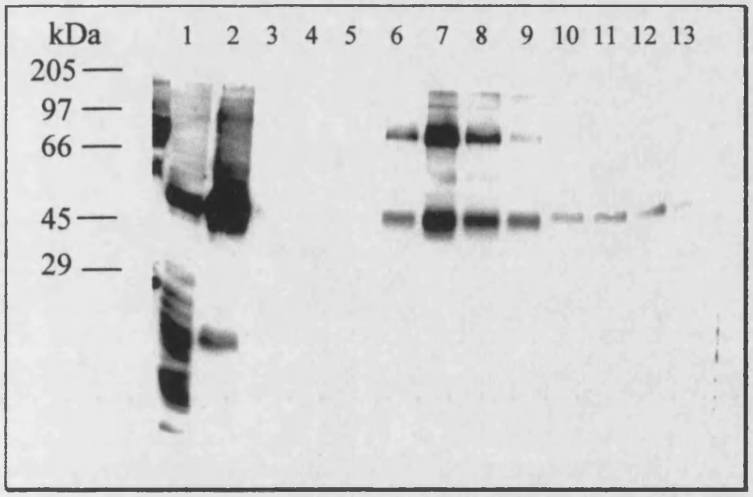

Figure 11.13, Immunoblot analysis of octyl glucoside solubilized HIS-GLUT1 eluted from a nickel column (cf. figure 11.10). Solubilized Sf9 cells were loaded on to a Pharmacia Biotech HiTrap column charged with nickel ions and electrophoresed on a 12% polyacrylamide gel as follows: Lane 1: 40 µl taken from insoluble cell debris following octyl glucoside solubilization; lane 2: 40 µl taken from 5 ml of solubilized Sf9 cells expressing HIS-GLUT1; lane 3: 40 µl of column wash; lane 4: 40 µl of fraction 11; lane 5: 40 µl of fraction 12; lane 6: 40 µl of fraction 13; lane 7: 40 µl of fraction 14; lane 8: 40 µl of fraction 15; lane 9: 40 µl of fraction 16; lane 10: 40 µl of fraction 24; lane 11: 40 µl of fraction 25; lane 12: 40 µl of fraction 26; lane 13: 40 µl of fraction 27.

Immunoblot analysis has demonstrated that fraction 14 was the peak fraction. This corresponded to the peak fraction observed by FPLC absorption analysis. Smaller amounts of HIS-GLUT1 were eluted in the fractions following fraction 14. After solubilization an insoluble pellet of cell debris remained. This was resuspended in 1 ml of buffer, of which 40 µl was loaded in lane 1. This allowed for comparison with the 40 µl sample of solubilized HIS-GLUT1 contained in 5 ml of buffer, lane 2 (figure 11.13 and 11.14). It was observed that the majority (about 90%) of the HIS-GLUT1 protein had been solubilized by octyl glucoside.

Comparison of the immunoblot (figure 11.13) with a Coomassie stained polyacrylamide gel (figure 11.14) loaded with the same fractions revealed that fraction 14 was not a pure fraction.

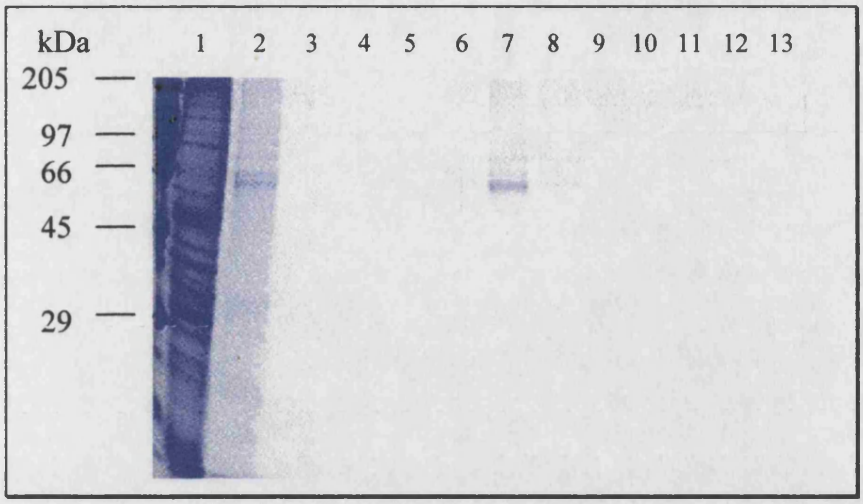

Figure 11.14, Coomassie stained polyacrylamide gel of purified HIS-GLUT1 eluted from a nickel column (cf. figure 11.10). Solubilized Sf9 cells were loaded on to a Pharmacia Biotech HiTrap column charged with nickel ions and electrophoresed on a 12% polyacrylamide gel as follows: Lane 1: 40 µl taken from insoluble cell debris following octyl glucoside solubilization; lane 2: 40 µl taken from 5 ml of solubilized Sf9 cells expressing HIS-GLUT1; lane 3: 40 µl of column wash; lane 4: 40 µl of fraction 11; lane 5: 40 µl of fraction 12; lane 6: 40 µl of fraction 13; lane 7: 40 µl of fraction 14; lane 8: 40 µl of fraction 15; lane 9: 40 µl of fraction 16; lane 10: 40 µl of fraction 24; lane 11: 40 µl of fraction 25; lane 12: 40 µl of fraction 26; lane 13: 40 µl of fraction 27.

Coomassie staining indicated that fraction 14 contained an impurity which had an apparent molecular weight of 66 kDa. In an attempt to alter the binding characteristics of the column, the column was run using copper as the metal ion. It was hypothesised that copper ions may change the binding affinity of either HIS-GLUT1, or the contaminants, or both.

Sf9 cells expressing HIS-GLUT1 were solubilized and loaded on a column charged with 0.1 M copper sulphate. Figure 11.12 displays the FPLC elution profile of HIS-GLUT1 protein using an immobilised copper column. A protein fraction containing HIS-GLUT1 was eluted at approximately 50% of 200 mM imidazole (100 mM imidazole) demonstrating that the retained proteins had a higher affinity towards the copper ions. Unfortunately the affinity of the column towards contaminating proteins was also increased.

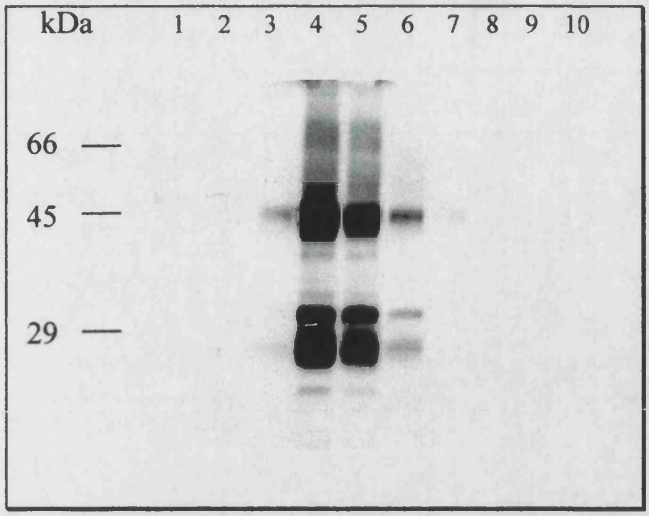

Figure 11.15, Immunoblot analysis of HIS-GLUT1 eluted from a copper column. Solubilized Sf9 cells were loaded on to a Pharmacia Biotech HiTrap column charged with copper ions and electrophoresed on a 12% polyacrylamide gel as follows: Lane 1: 40 µl of fraction 9; lane 2: 40 µl of fraction 10; lane 3: 40 µl of fraction 11; lane 4: 40 µl of fraction 12; lane 5: 40 µl of fraction 13; lane 6: 40 µl of fraction 14; lane 7: 40 µl of fraction 15; lane 8: 40 µl of fraction 16; lane 9: 40 µl of fraction 17; lane 10: 40 µl of fraction 18. Fractions 12 and 13 were observed to contain the peak fractions of HIS-GLUT1 and corresponded to the observed peak on the FPLC plot.

The bands appearing at 29 kDa on the immunoblot may be due to degradation of the HIS-GLUT1 protein. The above immunoblot was compared with the corresponding Coomassie stained polyacrylamide gel, figure 11.16.

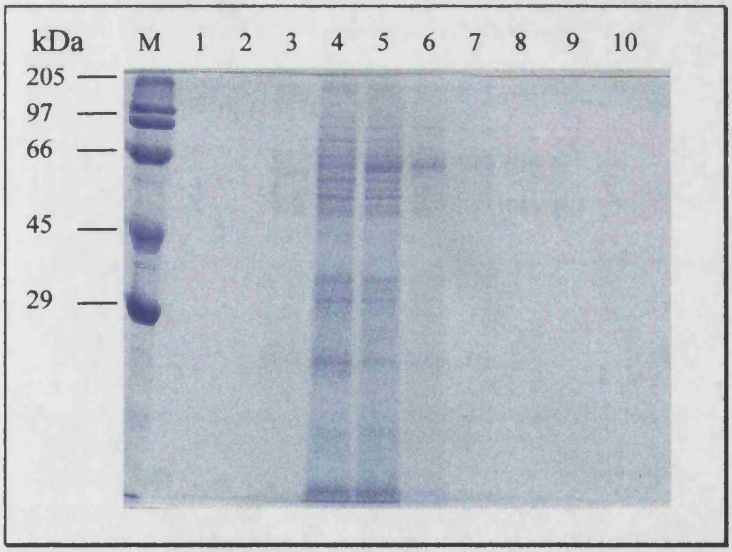

Figure 11.16, Coomassie stained polyacrylamide gel analysis of HIS-GLUT1 eluted from a copper column. Solubilized Sf9 cells were loaded on to a Pharmacia Biotech HiTrap column charged with copper ions and electrophoresed on a 12% polyacrylamide gel as follows: Lane 1: 40 µl of fraction 9; lane 2: 40 µl of fraction 10; lane 3: 40 µl of fraction 11; lane 4: 40 µl of fraction 12; lane 5: 40 µl of fraction 13; lane 6: 40 µl of fraction 14; lane 7: 40 µl of fraction 15; lane 8: 40 µl of fraction 16; lane 9: 40 µl of fraction 17; lane 10: 40 µl of fraction 18.

Coomassie staining revealed that many contaminating proteins were co-eluted with the HIS-GLUT1 protein. Major contaminating bands appeared at 25 and 66 kDa. Because the affinity of the contaminating proteins also appeared to have been increased,

studies using copper ions were discontinued and experiments continued using nickel ions.

These initial experiments have demonstrated that the recombinant protein, HIS-GLUT1, has an appreciable affinity towards immobilised metal ions on a Sepharose column. This suggests that:

a) The histidine tag is being expressed and is present on the protein
b) The histidine tag protrudes far enough out of the protein structure to allow for specific binding of immobilised metal ions to occur.

Because the HIS-GLUT1 protein was eluted in one main elution peak, as observed by FPLC analysis, it was possible to elute the HIS-GLUT1 protein using a step gradient. Following the application of the IMAC 20 (20 mM imidazole buffer) wash buffer, IMAC 200 (200 mM imidazole buffer) elution buffer was applied. Further analysis was performed using octyl glucoside on a nickel column.

Section 11.5

Ion Exchange Column - Anion Exchange using DEAE Cellulose

In order to eliminate contaminating proteins, the possibility of including a second column was investigated. A DEAE (diethyl amino ethyl) cellulose column was selected for testing. This column was chosen because it had been previously successful in the purification of human GLUT1 from erythrocytes (Baldwin and Lienhard, (1989)).

As a control erythrocyte GLUT1 was purified using a DEAE cellulose column. Erythrocyte ghosts were solubilized in 5 mM phosphate buffer containing 1.35% octyl glucoside with protease inhibitors at pH 7.4. The column was eluted using a step gradient containing increasing concentrations of sodium chloride (50 - 500 mM). The fractions were analysed by immunoblot analysis and the results displayed in figure 11.17 below.

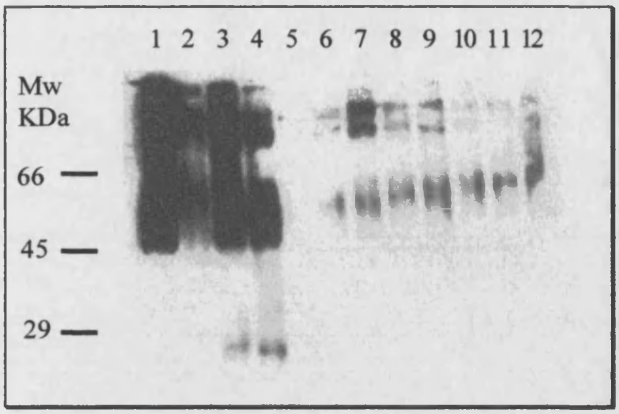

Figure 11.17, Immunoblot analysis of erythrocyte GLUT1 eluted from a DEAE cellulose column. Human erythrocyte ghosts were solubilized run on a DEAE cellulose column. 4 ml fractions were collected and 20 µl aliquots were taken and electrophoresed on a 10% polyacrylamide gel as follows: Lane 1: 20 µl of solubilized membranes; lane 2: 20 µl of 3 ml column load; lane 3: 20 µl of 50 mM NaCl; lane 4: 20 µl of 50 mM NaCl; lane 5: 20 µl of 100 mM NaCl; lane 6: 20 µl of 100 mM NaCl; lane 7: 20 µl of 200 mM NaCl; lane 8: 20 µl of 200 mM NaCl; lane 9: 20 µl of 300 mM NaCl; lane 10: 20 µl of 400 mM NaCl; lane 11: 20 µl of 500 mM NaCl; lane 12: 20 µl of 1 M NaCl.

Erythrocyte GLUT1 was observed to be eluted at a concentration of only 50 mM NaCl, indicating that erythrocyte GLUT1 had little or no affinity towards the DEAE cellulose column. A small amount of erythrocyte GLUT1 appeared to be retained on the column. This retention was probably due to protein being caught in the matrix of the column and would be completely removed by the 50 mM sodium chloride wash if continued.

Sf9 Expressed HIS-GLUT1

Sf9 cell membranes expressing HIS-GLUT1 were homogenised and solubilized in 5 mM phosphate buffer containing 1.35% octyl glucoside. A DEAE cellulose column was prepared (bed volume, 8 ml) and the solubilized cell protein loaded on to the column. The column was eluted using a step gradient. The step gradient consisted of 4 ml volumes of elution buffer containing 5 mM phosphate buffer with protease inhibitors, 0.75% octyl glucoside and increasing concentrations of sodium chloride (50 - 500 mM). 4 ml fractions were collected from the column and 40 µl aliquots were taken from each fraction and analysed by immunoblotting and polyacrylamide gel analysis.

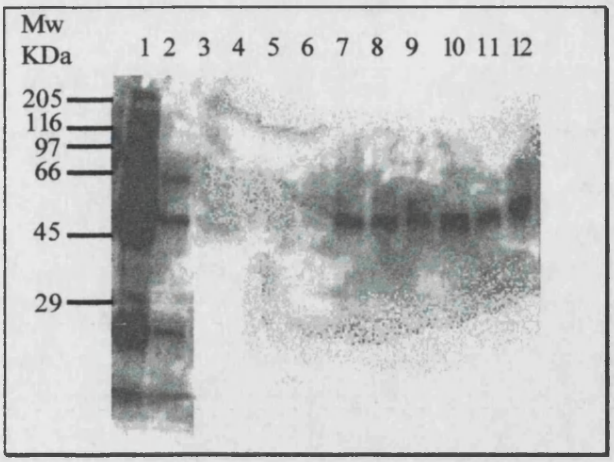

Figure 11.18, Immunoblot analysis of HIS-GLUT1 protein eluted from a DEAE cellulose column. Sf9 cells were solubilized loaded on to a DEAE cellulose column. 4 ml fractions were collected and 40 µl aliquots were taken and electrophoresed on a 12% polyacrylamide gel as follows: Lane 1: 40 µl of solubilized membrane; lane 2: 40 µl of 50 mM NaCl; lane 3: 40 µl of 50 mM NaCl; lane 4: 40 µl of 50 mM NaCl; lane 5: 40 µl of 100 mM NaCl; lane 6: 40 µl of 100 mM NaCl; lane 7: 40 µl of 200 mM NaCl; lane 8: 40 µl of 200 mM NaCl; lane 9: 40 µl of 300 mM NaCl; lane 10: 40 µl of 400 mM NaCl; lane 11: 40 µl of 500 mM NaCl; lane 12: 40 µl of 500 mM NaCl.

Comparison of the immunoblot with the Coomassie stained polyacrylamide gel, figure 11.19, indicated that the majority of contaminants were not retained on the column at 50 mM sodium chloride.

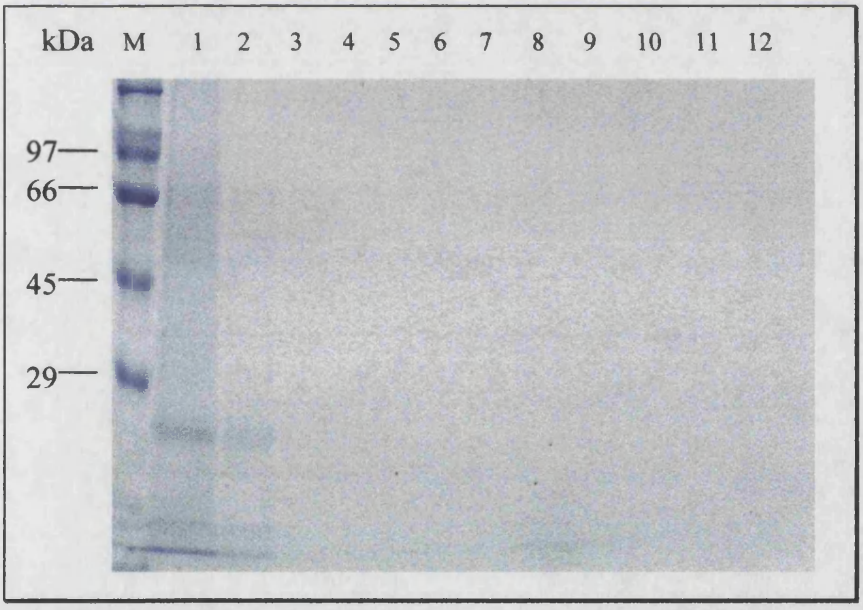

Figure 11.19, Coomassie stained polyacrylamide gel analysis of HIS-GLUT1 eluted from a DEAE cellulose column. Sf9 cells were solubilized and loaded on to a DEAE cellulose column. 4 ml fractions were collected and 40 µl aliquots were taken and electrophoresed on a 12% polyacrylamide gel as follows: Lane 1: 40 µl of solubilized membrane; lane 2: 40 µl of 50 mM NaCl; lane 3: 40 µl of 50 mM NaCl; lane 4: 40 µl of 50 mM NaCl; lane 5: 40 µl of 100 mM NaCl; lane 6: 40 µl of 100 mM NaCl; lane 7: 40 µl of 200 mM NaCl; lane 8: 40 µl of 200 mM NaCl; lane 9: 40 µl of 300 mM NaCl; lane 10: 40 µl of 400 mM NaCl; lane 11: 40 µl of 500 mM NaCl; lane 12: 40 µl of 500 mM NaCl.

Several contaminating proteins were observed to be eluted from the DEAE cellulose column on the application of 50 mM sodium chloride elution buffer. However, the HIS-GLUT1 protein was retained and only eluted on the application of 200 mM sodium chloride. The affinity displayed by the HIS-GLUT1 protein towards the DEAE cellulose column was not as predicted. It was proposed that the increase in HIS-GLUT1 affinity was as a direct result of the addition of the enterokinase site before the N-terminal polyhistidine tag. The addition of several aspartic acid residues, which at pH 7.4 would be negatively charged, appeared to have resulted in an increased negative charge on the surface of the protein. This provided further evidence to suggest that the polyhistidine tag and preceding amino acids were protruding from the surface of the protein and were accessible to metal ions.

The use of the DEAE cellulose column, in combination with the nickel column, carries disadvantages as well as advantages. The inclusion of this column in the protocol serves to increase the amount of time that the HIS-GLUT1 protein is incubated with the detergent octyl glucoside. This is important as erythrocyte GLUT1 has been reported, by Baldwin and Lienhard, (1989), to undergo degradation and loss of activity with long periods of incubation in the detergent octyl glucoside. Inclusion of the DEAE cellulose column also leads to a greater loss of HIS-GLUT1 protein throughout the purification protocol. For these reasons the DEAE cellulose column was not included as part of the purification strategy.

Section 11.6

Isolation of Egg Yolk Lipids for Reconstitution of the Glucose Transporter

Following column chromatography it was necessary to reconstitute the HIS-GLUT1 protein into lipid vesicles. Two types of phospholipid were used: type II-S soybean phospholipids (Sigma) and egg yolk phospholipids. Egg yolk phospholipids were isolated from egg yolks and purified according to the protocol described in the Materials and Methods section. Lipid fractions were collected and analysed by thin layer chromatography (TLC), figure 11.20.

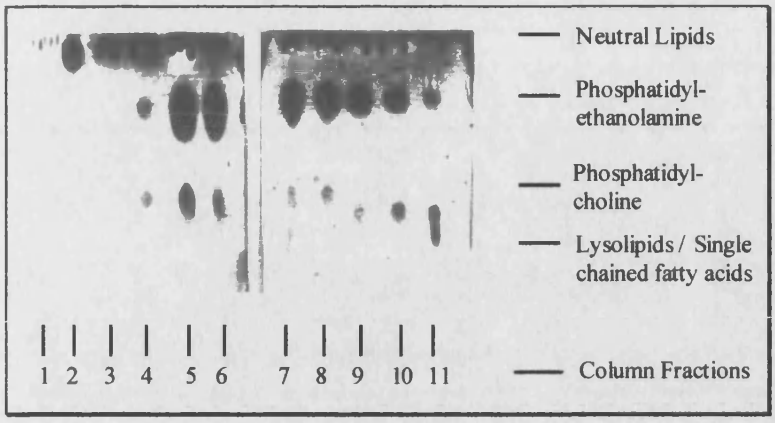

Figure 11.20, TLC analysis of egg yolk lipids separated on a silica column. Fractions 4, 5 and 10 were combined to give approximately equal amounts of phosphatidylcholine and phosphatidylethanolamine in the final mixture.

TLC analysis demonstrated the egg yolk lipids to be rich in phosphatidylethanolamine. In order to obtain a lipid mixture with equal amounts of phosphatidylethanolamine and phosphatidylcholine fractions 4, 5 and 10 were taken, combined and termed as fraction B. Fractions were combined because too much phosphatidylethanolamine could lead to the disruption of membrane vesicles. Fractions 1 and 2 contained only neutral lipids and were discarded. The remaining fractions were combined and termed as fraction A. The samples generated were then re-tested by TLC analysis, displayed in figure 20.21.

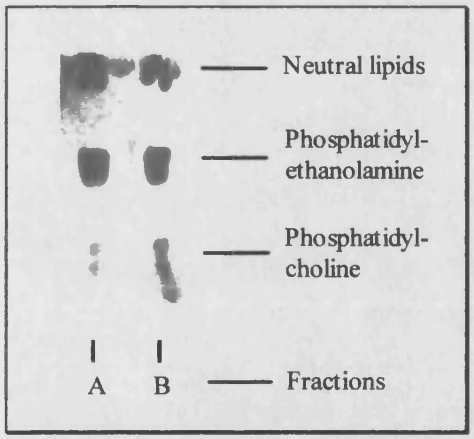

Figure 11.21, TLC analysis of combined egg yolk lipids (cf. figure 11.20). Fraction B was considered to contain approximately equal amounts of phosphatidylcholine and phosphatidylethanolamine.

Fraction B contained 610 mg of lipid with a density of 0.828 g / cm^3 and was used for the reconstitution of the glucose transporter.

Both egg yolk lipids and soybean lipids produced good results on reconstitution of the HIS-GLUT1 and HIS-C-TERM proteins. However most of the experiments performed in this thesis used soybean lipids. This was because the soybean lipids proved to be more soluble in the detergent octyl glucoside than the egg yolk lipids.

Section 11.7 Protein Stability in Octyl Glucoside

Baldwin and Leinhard, (1989) have reported that human erythrocyte GLUT1 is unstable in the detergent octyl glucoside. Incubation in octyl glucoside was reported to result in the loss of glucose binding activity on a time dependent basis. The stability of the recombinant constructs GLUT1, HIS-GLUT1 and HIS-C-TERM were also questioned and tested by incubating the proteins with octyl glucoside for varying amounts of time. The amount and activity of the recombinant protein following incubation was detected by immunoblot and cytochalasin B assay.

Immunoblot Analysis

Samples of homogenised Sf9 cell membranes expressing HIS-GLUT1, HIS-C-TERM and GLUT1 were incubated in 5 mM phosphate buffer containing 1.5% octyl glucoside with protease inhibitors. Aliquots were taken over a time course of 6½ h and analysed by immunoblotting, the results are displayed in figures 11.22 - 11.24.

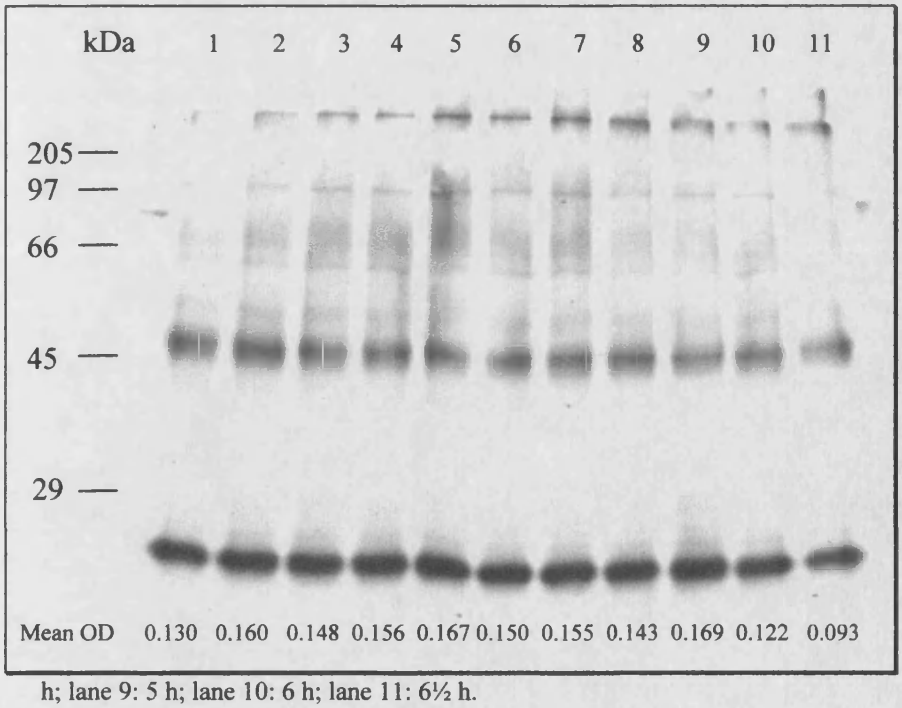

Figure 11.22, HIS-C-TERM incubated with octyl glucoside. Sf9 cells expressing HIS-C-TERM were incubated with 1.5% octyl glucoside and loaded onto a 12% polyacrylamide gel as follows: Lane 1: 0 minutes; lane 2: 30 minutes; lane 3: 1 h; lane 4: 1½ h; lane 5: 2 h; lane 6: 2½ h; lane 7: 3 h; lane 8: 4 h; lane 9: 5 h; lane 10: 6 h; lane 11: 6½ h.

The HIS-C-TERM immuno reactive protein band does not show a significant decrease in intensity throughout the time course, as determined from optical density measurements. These results were mirrored by the HIS-GLUT1 and GLUT1 proteins displayed in figures 11.23 and 11.24. The mean optical density data is displayed on the immunoblots.

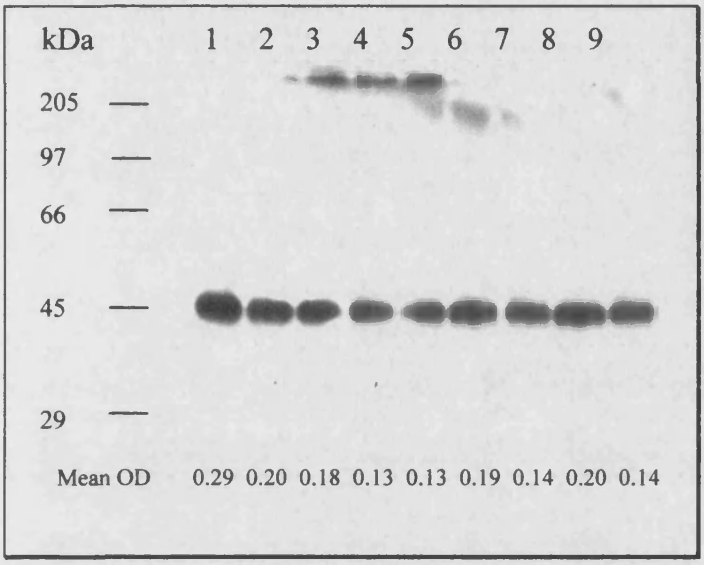

Figure 11.23, HIS-GLUT1 incubated with octyl glucoside. Sf9 cells expressing HIS-GLUT1 were incubated with 1.5% octyl glucoside and loaded onto a 10% polyacrylamide gel as follows: Lane 1: 0 minutes; lane 2: 30 minutes; lane 3: 1 h; lane 4: 1½ h; lane 5: 2 h; lane 6: 2½ h; lane 7: 3 h; lane 8: 4 h; lane 9: 5 h.

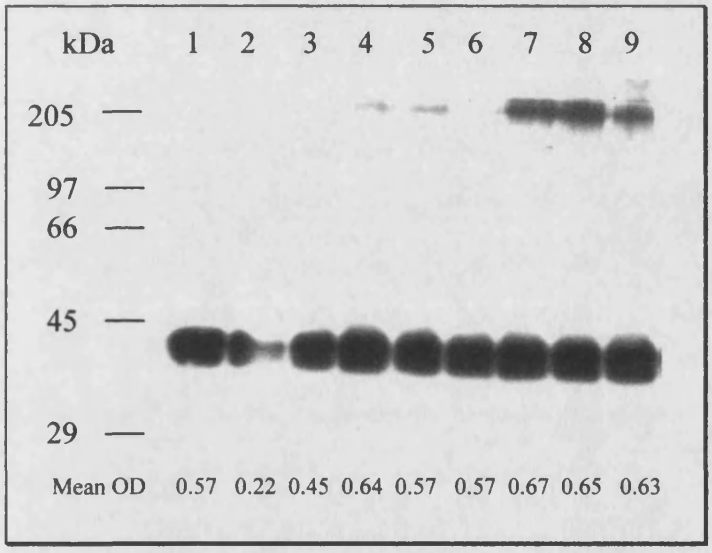

Figure 11.24, GLUT1 incubated with octyl glucoside. Sf9 cells expressing GLUT1 were incubated with 1.5% octyl glucoside and loaded onto a 10% polyacrylamide gel as follows: Lane 1: 0 minutes; lane 2: 30 minutes; lane 3: 1 h; lane 4: 1½ h; lane 5: 2 h; lane 6: 2½ h; lane 7: 3 h; lane 8: 4 h; lane 9: 5 h.

Immunoblot analysis has demonstrated that there was no significant degradation of Sf9 expressed HIS-C-TERM, HIS-GLUT1 or GLUT1 during incubation with octyl glucoside. Variation is thought to be due to transfer inefficiency. The HIS-GLUT1 protein was taken for further analysis by cytochalasin B assay.

Cytochalasin B Assay - HIS-GLUT1 Activity in Octyl Glucoside

Homogenised Sf9 cell membranes, expressing HIS-GLUT1, were incubated for up to 7 h in 5 mM phosphate buffer containing 1.5% octyl glucoside with protease inhibitors. 1 mg samples were taken throughout the time course and dialysed; reconstitution was in soybean type II-S lipids. Samples were assayed using a standard cytochalasin B assay as described in the Materials and Methods section. The total amount of free and bound ligand at each time point was calculated and the Bmax plotted, figure 11.25

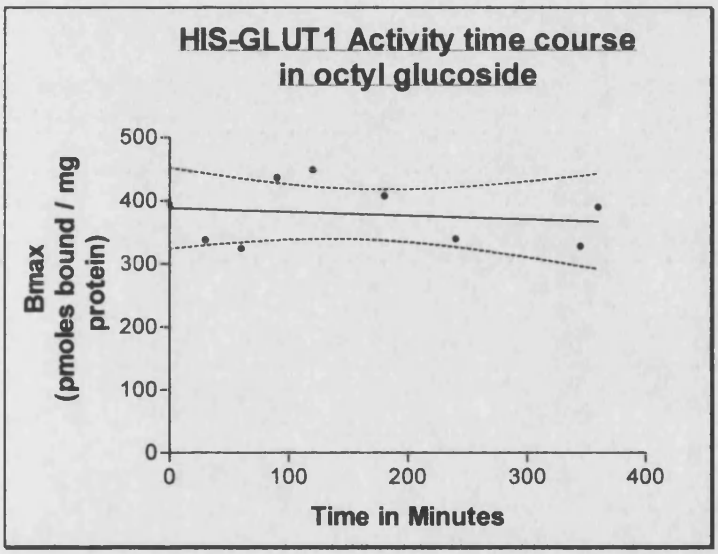

Figure 11.25, Time course of activity of HIS-GLUT1 in the presence of octyl glucoside. HIS-GLUT1 was exposed to octyl glucoside over a period of 7 h. The Bmax values from cytochalasin B assays were calculated and plotted. The line was found not to deviate significantly from the horizontal (P=0.67).

Throughout the time course there was very little decrease in HIS-GLUT1 affinity towards the radioligand, cytochalasin B. The line of best fit was not found to deviate significantly from the horizontal (P=0.67). It was concluded that over the time period tested there was very little deterioration of HIS-GLUT1 activity.

HIS-GLUT1 Activity in Octyl Glucoside with Substrate Protection

It was theorised that octyl glucoside could be recognised by the GLUT1 protein as a substrate mimic. Octyl glucoside could bind to the GLUT1 substrate binding site and reduce the activity of the transporter, by either blocking the site, or by denaturing the protein. The detergent octyl glucoside appeared to have had very little effect on the

activity of the HIS-GLUT1 protein in the absence of glucose. Nevertheless, the time course was also performed in the presence of 0.5 M D-glucose, in an attempt to protect the binding site from octyl glucoside. The results of this are displayed in figure 11.26.

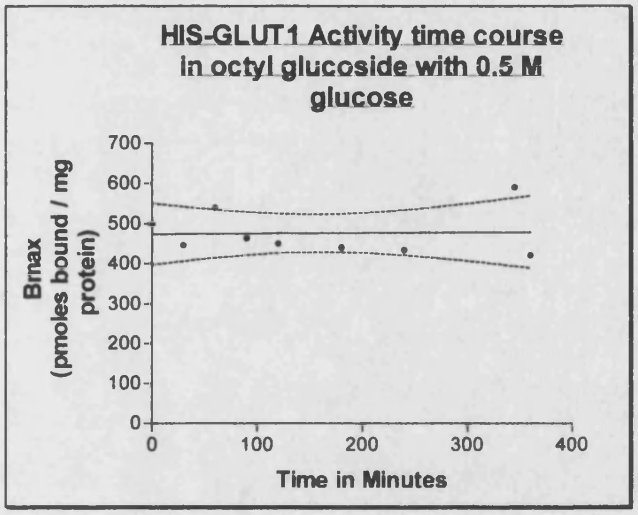

Figure 11.26, Time course of activity of HIS-GLUT1 in the presence of octyl glucoside and 0.5 M D-glucose. HIS-GLUT1 was exposed to octyl glucoside and 0.5 M D-glucose over a period of 7 h. The Bmax values from cytochalasin B assays were calculated and plotted. The line was found not to deviate significantly from the horizontal (P=0.92).

The addition of 0.5 M D-glucose appeared to have very little effect on the HIS-GLUT1 protein activity. In both time courses there were no significant losses of activity over the 7 h time period. Immunoblotting also demonstrated very little observable deterioration in the HIS-GLUT1 protein and it was concluded that octyl glucoside had little effect on the Sf9 expressed proteins over the 7 h time period observed. It is possible that the HIS-GLUT1 protein would be affected by incubation with octyl glucoside over longer time periods, but since the solubilization and chromatographic stages of purification were accomplished within 3 h, this was not tested.

Section 11.8
GLUT1 Control Column

To determine that the GLUT1 protein does not have an intrinsic affinity towards the nickel column the following experiment was performed. A 1 ml Sepharose chelating column was charged with 0.1 M nickel sulphate and pre-equilibrated with the wash buffer. 4 mg of homogenised Sf9 cells expressing GLUT1 were solubilized and loaded on the column. The column was washed with 10 ml of wash buffer and eluted with 5 ml

of elution buffer, 2 ml fractions were collected and analysed by immunoblot assay, displayed in figure 11.27.

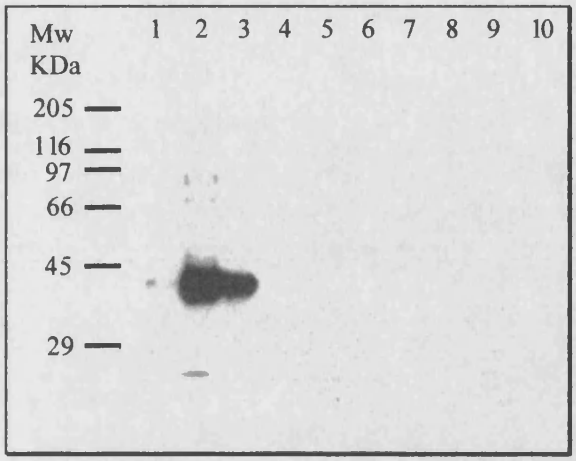

Figure 11.27, Immunoblot of Sf9 expressed GLUT1 protein eluted from a nickel column. 4 mg of Sf9 cells expressing GLUT1 were solubilized and loaded onto a 1 ml nickel chelating Sepharose column charged with 0.1 M nickel sulphate. 40 µl aliquots from each fraction were loaded on a 10% polyacrylamide gel as follows: lane 1: fraction 1; lane 2: fraction 2; lane 3: fraction 3; lane 4: fraction 4; lane 5: fraction 5; lane 6: fraction 6; lane 7: fraction 7; lane 8: fraction 8; lane 9: fraction 9; lane 10: fraction 10. Fractions 1 represents the load, fractions 2 - 6 represent the wash and fractions 7 - 10 represent the elution.

GLUT1 was seen to elute from the column in the wash buffer. None of the GLUT1 protein was retained upon the column following the wash, this suggested that the addition of the polyhistidine tag confers nickel ion affinity up on the GLUT1 protein.

Sf9 Control Column

An Sf9 control column was run to determine whether any Sf9 proteins have an affinity towards the nickel column. A 1 ml nickel chelating Sepharose column was charged with 0.1 M nickel sulphate and pre-equilibrated with wash buffer. 4 mg of uninfected Sf9 cells were homogenised, solubilized and loaded on to the column. The column was washed using 10 ml of wash buffer and eluted using 5 ml of elution buffer. 1.9 ml fractions were collected from the column. 40 µl samples were taken from the collected fractions and analysed by immunoblotting, no immunospecific bands were revealed by immunoblot analysis. In order to clearly visualise the contaminating Sf9 cell proteins with an affinity towards the nickel column larger amounts of dialysed protein were loaded onto a polyacrylamide gel for analysis. Dialysed protein samples were concentrated by chloroform / methanol precipitation and visualised by silver staining.

The gel compares the protein content of the wash, fraction 1, with the elution, fraction 9. The results are displayed in figure 11.28.

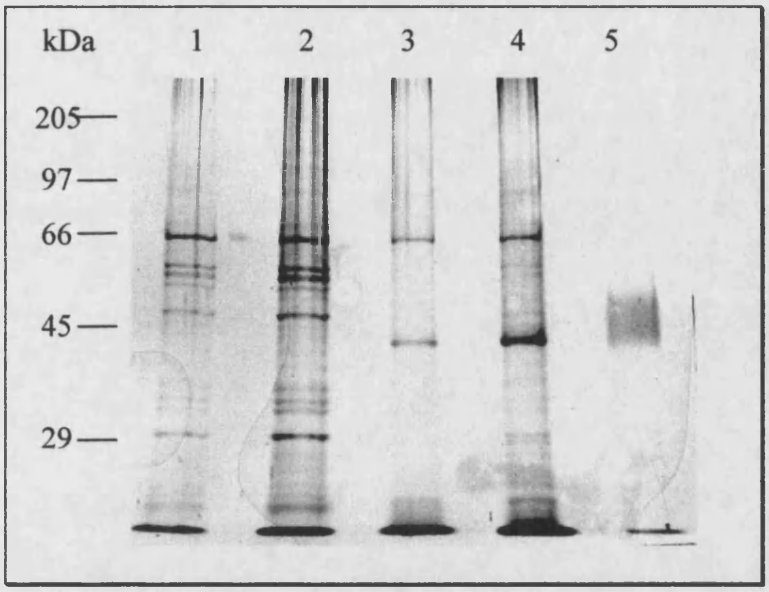

Figure 11.28, Silver stained polyacrylamide gel of Sf9 cell proteins eluted from a nickel column. Samples from dialysed fractions were loaded in two different amounts on a 10% polyacrylamide gel as follows: Lane 1: 35 µl of fraction 1; lane 2: 71 µl of fraction 1; lane 3: 612 µl of fraction 9; lane 4: 1020 µl of fraction 9; lane 5: 2 µg human GLUT1 standard.

Several protein bands were observed in the column wash, fraction 1, which have no affinity towards the column. However, in fraction 9 there appeared to be at least two contaminating Sf9 proteins with a high affinity towards the column. These proteins are present at 66 and 45 kDa and are only eluted with high concentrations of imidazole. The protein at 66 kDa is thought to be BSA, used during Sf9 cell incubation. This could be eliminated by adapting the cells to grow in serum free medium. The origin on the 45 kDa band is unknown, but previous results suggest that it could be removed by the use of a DEAE cellulose column.

Section 11.9

Purification of HIS-GLUT1 Expressed in Sf9 Cells

A 1 ml HiTrap™ column was charged with 0.1 M nickel sulphate and pre-equilibrated with 3 ml of wash buffer. 4 mg of Sf9 cells expressing HIS-GLUT1 were homogenised, solubilized and loaded on to the column. 1.9 ml fractions were collected and 40 µl aliquots were taken from each fraction. The aliquots were analysed

by immunoblot assay, figure 11.30, and by PAGE followed by Coomassie blue staining. Fractions were then dialysed against GLUT1 dialysis buffer for further analysis.

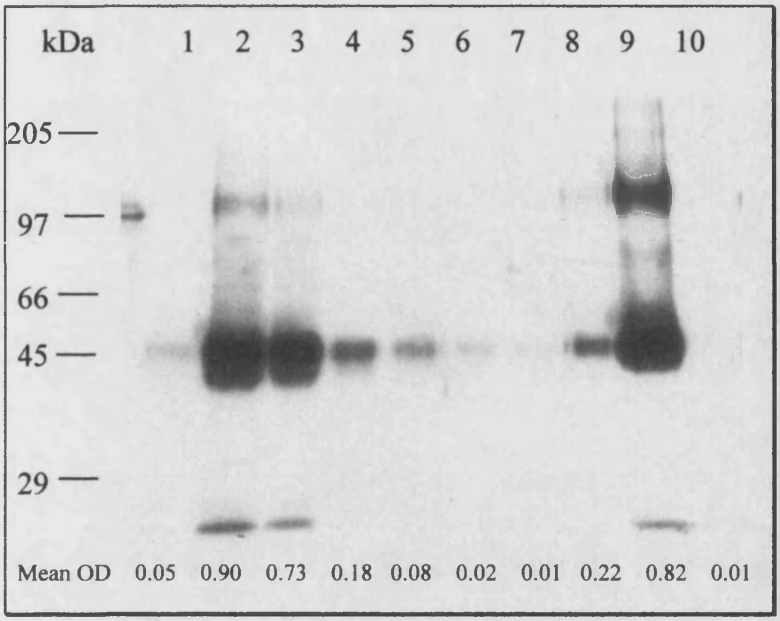

Figure 11.30, Immunoblot of Sf9 expressed HIS-GLUT1 protein eluted from a nickel column. 40 µl from each column fraction were loaded on to a 10% polyacrylamide gel as follows: lane 1: fraction 1; lane 2: fraction 2; lane 3: fraction 3; lane 4: fraction 4; lane 5: fraction 5; lane 6: fraction 6; lane 7: fraction 7; lane 8: fraction 8; lane 9: fraction 9; lane 10: fraction 10. Fraction 1 represents the load, fractions 2 - 6 represent the wash and fractions 7 - 10 represent the elution.

PAGE followed by Coomassie staining revealed that there was very little protein present in any of the fractions, other than fractions 2 and 3. However, immunoblotting demonstrated that HIS-GLUT1 protein was retained and specifically eluted in fractions 8 and 9. A high level of HIS-GLUT1 flow through was observed in fractions 2 and 3 (more than 50%) and will be discussed later (figures 11.32 and 11.33).

In order to determine how many contaminating proteins were present, dialysed fractions 2 and 9 were taken and concentrated by chloroform / methanol precipitation. Samples were loaded onto a 10% polyacrylamide gel and visualised using the BioRad silver stain plus system, figure 11.31.

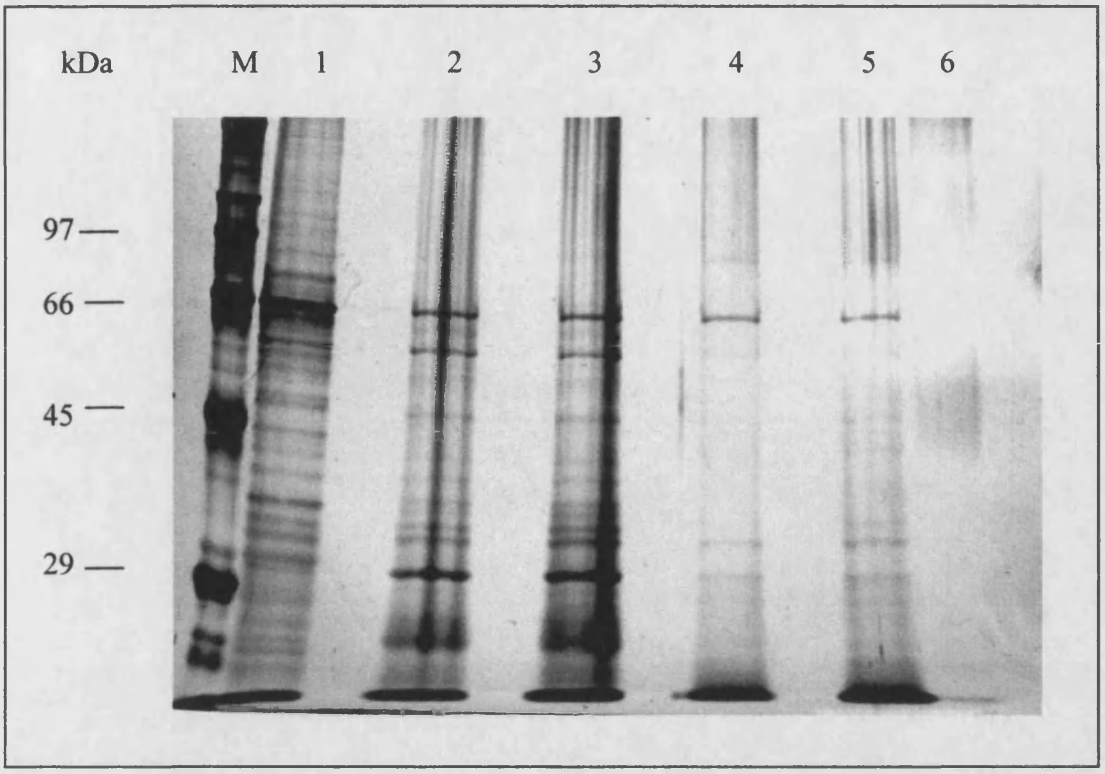

Figure 11.31, Silver stained polyacrylamide gel of Sf9 expressed HIS-GLUT1 protein eluted from a nickel column. Samples from dialysed fractions 2 and 9 were taken and loaded in two different amounts on a 10% polyacrylamide gel as follows: Lane M: high molecular weight marker; lane 1: 2 μg of Sf9 membranes expressing HIS-GLUT1; lane 2: 10 μg (40 μl) of fraction 2; lane 3: 20 μg (79 μl) of fraction 2; lane 4: 150 μg (557 μl) of fraction 9; lane 5: 250 μg (929 μl) of fraction 9; lane 6: 2 μg of human GLUT1 standard.

Following dialysis residual amounts of imidazole appeared to have remained in the sample and have made the protein assay results unreliable. From comparison with the Sf9 standard it was estimated that there were between 2 - 3 μg of protein in lane 5.

The 66 kDa band, assumed to be BSA, was observed in both fractions 2 and 9, its presence was also observed in uninfected Sf9 cells. The 66 kDa protein (BSA) is clearly the major contaminating protein co-eluting with the HIS-GLUT1 protein. Other visible contaminating proteins were present at approximately 30 and 90 kDa. Although it was difficult to determine the origin of these proteins, wild-type viral coat protein (polyhedrin) and degraded HIS-GLUT1 protein are both possibilities that have been eliminated. Polyhedrin protein was discounted because it has a slightly different apparent molecular weight. Degraded HIS-GLUT1 protein was discounted because the band had no immunoreactivity, protease inhibitors were present and low temperatures

(< 4°C) were maintained throughout the experiment. Samples were analysed by quantitative immunoblotting to determine the amount of HIS-GLUT1 protein contained within each fraction, figure 11.32 and 11.33.

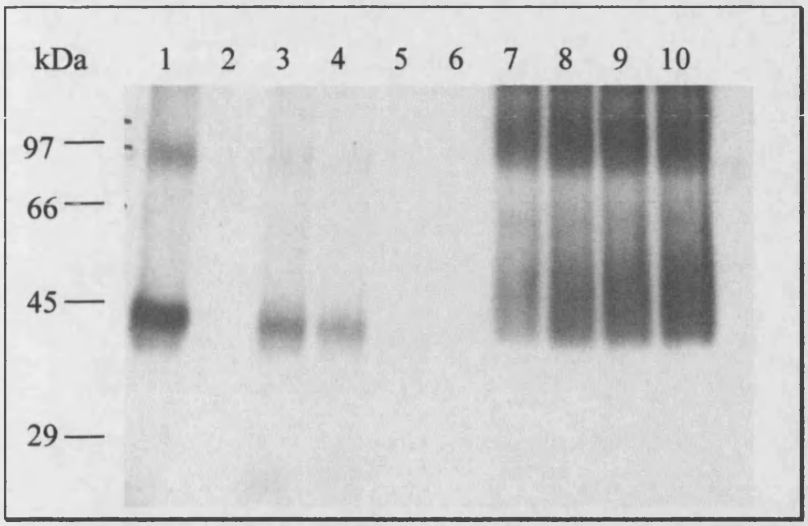

Figure 11.32, Immunoblot of Sf9 expressed HIS-GLUT1 protein eluted from a nickel column. Concentrated samples were loaded on to a 10% polyacrylamide gel as follows: lane 1: 20 µg Sf9 cells expressing HIS-GLUT1; lane 2: 65 µl of fraction 1; lane 3: 75 µl fraction 2; lane 4: 97 µl of fraction 3; lane 5: 129 µl of fraction 4; lane 6: 121 µl of fraction 5; lane 7: 200 ng human GLUT1 standard; lane 8: 400 ng human GLUT1 standard; lane 9: 500 ng human GLUT1 standard; lane 10: 600 ng human GLUT1 standard.

Fraction	Mean OD	amount in ng	pmoles / mg
			µg / ml
Sf9 cell control	0.397	428 ng / 20 µg	465 pmoles / mg
1	0.050	0 ng / 65 µl	0 µg / ml
2	0.178	155 ng / 75 µl	2.1 µg / ml
3	0.119	82 ng / 97 µl	0.9 µg / ml
4	0.041	0 ng / 129 µl	0 µg / ml
5	0.031	0 ng / 121 µl	0 µg / ml

Table 11.3, Densitometric analysis of figure 11.32. The above table demonstrates the amount of HIS-GLUT1 found in fractions 1 - 5 in µg / ml.

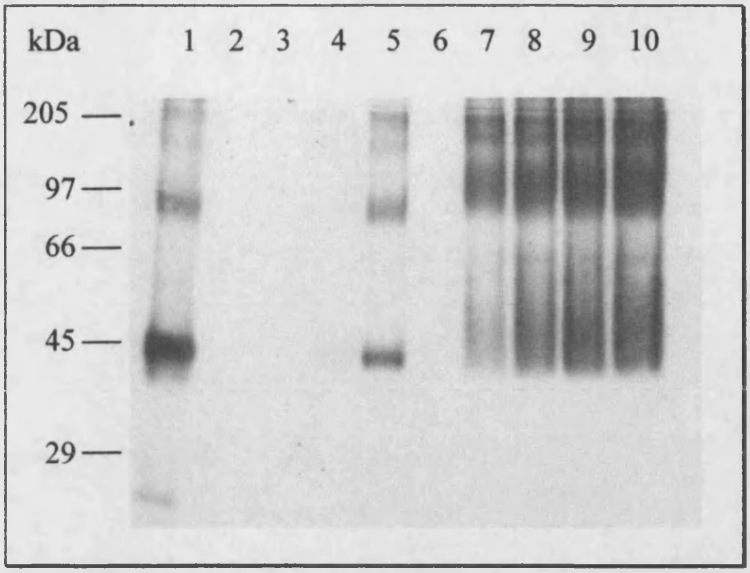

Figure 11.33, Immunoblot of Sf9 expressed HIS-GLUT1 protein eluted from a nickel column. Concentrated samples were loaded on to a 10% polyacrylamide gel as follows: lane 1: 20 µg Sf9 cells expressing HIS-GLUT1; lane 2: 119 µl of fraction 6; lane 3: 123 µl fraction 7; lane 4: 160 µl of fraction 8; lane 5: 75 µl of fraction 9; lane 6: 127 µl of fraction 10; lane 7: 200 ng human GLUT1 standard; lane 8: 400 ng human GLUT1 standard; lane 9: 500 ng human GLUT1 standard; lane 10: 600 ng human GLUT1 standard.

Fraction	Mean OD	amount in ng	pmoles / mg
			µg / ml
Sf9 cell control	0.286	507 ng / 20 µg	551 pmoles / mg
6		0 ng / 119 µl	0 µg / ml
7		0 ng / 123 µl	0 µg / ml
8		0 ng / 160 µl	0 µg / ml
9	0.071	170 ng / 75 µl	2.3 µg / ml
10		0 ng / 127 µl	0 µg / ml

Table 11.4, Densitometric analysis of figure 11.32. The above table demonstrates the amount of HIS-GLUT1 found in fractions 6 - 10, in µg / ml.

HIS-GLUT1 Yield

The column yield for HIS-GLUT1 protein has been calculated for a 500 ml culture of Sf9 cells. The calculations are as follows: 33 mg of washed membranes were obtained from a 500 ml Sf9 cell culture. The Sf9 cells in this experiment expressed HIS-GLUT1 at 507 pmoles / mg of membrane protein (mean of densitometric data, tables 11.3 and 11.4). Therefore, 507 pmoles x 33 mg = 16.7 nmoles of HIS-GLUT1 were expressed / 500 ml culture, which is equal to 770 µg of HIS-GLUT1 expressed / 500 ml culture.

4 mg of Sf9 cell membranes expressing HIS-GLUT1 were purified on an immobilised nickel column. The 4 mg of membranes contained 93.3 μg of HIS-GLUT1. Following purification, the retained HIS-GLUT1 protein was completely eluted in fraction 9 and was calculated by immunoblot analysis to contain 2.3 μg / ml of HIS-GLUT1. The fraction size was 1.9 ml and therefore the fraction contained 4.3 μg of purified HIS-GLUT1.

Therefore, the total yield from a 500 ml Sf9 cell culture expressing HIS-GLUT1 was 36 μg of purified HIS-GLUT1. From the original culture only 5% of the HIS-GLUT1 was recovered.

The amount of HIS-GLUT1 protein lost in the wash fractions is shown as follows: Fractions 2 and 3 contain 2.1 and 0.9 μg / ml of HIS-GLUT1, respectively. This represents a total of 5.6 μg of HIS-GLUT1. The HIS-GLUT1 protein lost in the wash step for a 500 ml culture was therefore 45.8 μg of HIS-GLUT1, this represents 6% of the HIS-GLUT1 from the original culture. This suggests that 89% of the HIS-GLUT1 protein has been lost from the 500 ml culture. This protein may have been lost during solubilization of the membranes, running the column and by experimental error. It was previously observed that not all of the HIS-GLUT1 protein was solubilized by detergent, some of the HIS-GLUT1 protein remained in the unsolubilized cell pellet.

From the yield calculations it can be seen that 46% of the HIS-GLUT1 protein was retained on the column and that 54% is eluted off in the wash buffer. This ratio of approximately 1 : 1 was maintained throughout all of the purification experiments. This was probably a result of the HIS-GLUT1 protein having a low affinity towards the nickel column, possibly due to the polyhistidine tag being masked by amino acid tertiary structure or by being partially buried in the detergent micelle / lipid bilayer. It was thought that the yield could be improved by increasing the affinity of the polyhistidine tag towards the nickel column, this could be achieved by placing the tag on the hydrophilic C-terminal end of the protein. A substantial amount of protein has been lost during the solubilization step, this could be improved by selecting a more efficient detergent system.

The HIS-GLUT1 protein was not clearly visible with silver stain analysis (figure 11.31). It is known that certain types of protein are detected by the silver stain system with a lower sensitivity. These proteins include glycosylated proteins such as the

GLUT1 and HIS-GLUT1 proteins. A low sensitivity of detection was supported by the human GLUT1 2 µg standard, which was barely visible and was known to be pure, having no other contaminating proteins to mask its presence.

In conclusion, the total yield from a 500 ml Sf9 cell culture expressing HIS-GLUT1 was 36 µg of purified HIS-GLUT1, the original culture having contained 770 µg HIS-GLUT1. However, it was clear that the final product was not completely pure and there are still contaminating bands within it.

Section 11.10

Purification of HIS-GLUT1 Expressed in Highfive Cells

4 mg of Highfive cells expressing HIS-GLUT1 were purified on a 1 ml nickel chelating Sepharose column. The column was run as in section 11.8, except that it was washed using only 8 ml of wash buffer. 40 µl samples were taken from each fraction and analysed by immunoblot assay and by PAGE with Coomassie protein staining. Fractions 2 and 3 were the only fractions which contained enough protein to allow for visualisation using Coomassie staining. Immunoblotting indicated which fractions contained HIS-GLUT1 protein, the blot is displayed in figure 11.34.

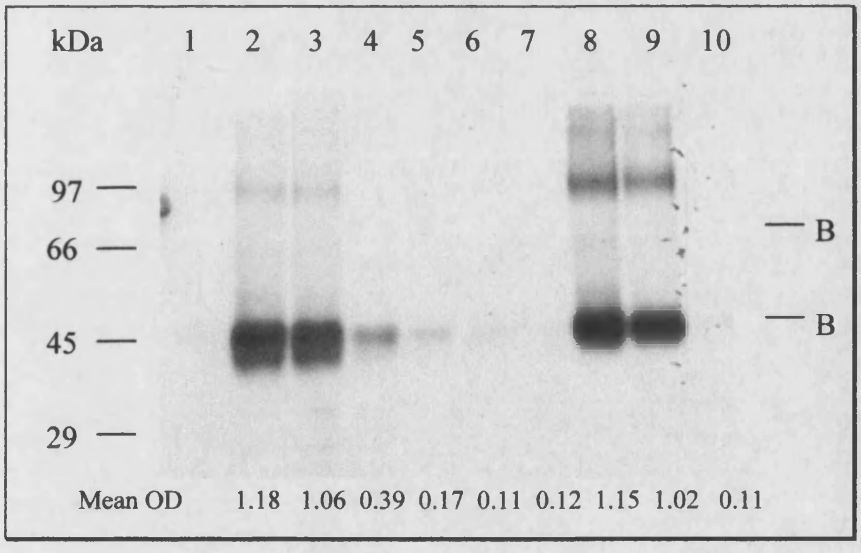

Figure 11.34, Immunoblot of Highfive expressed HIS-GLUT1 protein eluted from a nickel column. 40 µl from each fraction were loaded on a 10% polyacrylamide gel as follows: lane 1: fraction 1; lane 2: fraction 2; lane 3: fraction 3; lane 4: fraction 4; lane 5: fraction 5; lane 6: fraction 6; lane 7: fraction 7; lane 8: fraction 8; lane 9: fraction 9; lane 10: fraction 10. Fraction 1 represents the load, fractions 2 - 6 represent the wash and fractions 7 - 10 represent the elution. The letter B marks the position of visible banding observed on the nitrocellulose, following Ponceau S staining.

Densitometric analysis showed that approximately 50% of the HIS-GLUT1 protein was eluted from the column during the column wash. The same pattern was maintained even when only half the amount of protein was loaded on the column, it is therefore unlikely to be a result of column saturation as the ratio of retained protein would fluctuate. In order to determine the amount of HIS-GLUT1 protein present in fractions 3 and 9, figure 11.34, the fractions were assessed by quantitative immunoblotting, figure 11.35.

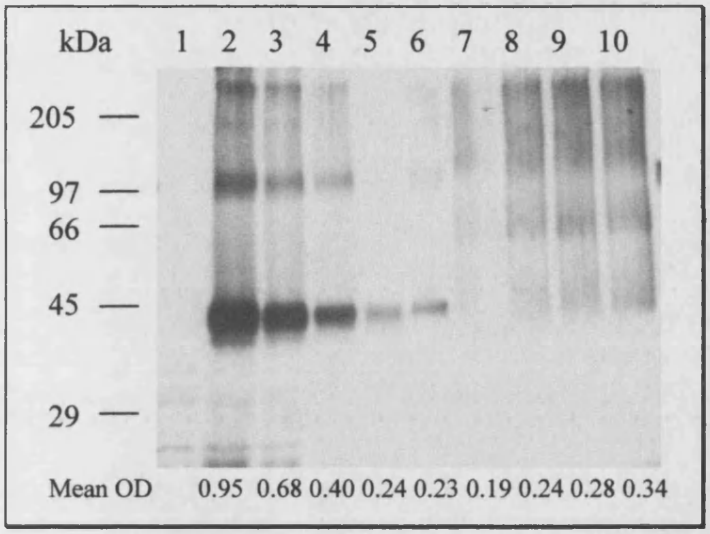

Figure 11.35, Quantitative immunoblot of Highfive expressed HIS-GLUT1. Concentrated samples were taken from fractions 3 and 9 and loaded onto a 10% polyacrylamide gel as follows: Lane 1: 30 µg uninfected Sf9 cell membranes; Lane 2: 30 µg of Highfive cell membranes expressing HIS-GLUT1; Lane 3: 20 µg of Highfive cell membranes expressing HIS-GLUT1; Lane 4: 10 µg of Highfive cell membranes expressing HIS-GLUT1; Lane 5: 25 µl of fraction 3; lane 6: 25 µl of fraction 9; lane 7: 200 ng of human GLUT1 standard; lane 8: 400 ng of human GLUT1 standard; lane 9: 500 ng of human GLUT1 standard; lane 10: 600 ng of human GLUT1 standard.

Fraction	Mean OD	amount in ng / µl	µg / ml
2		338 ng / 20 µl	16.9 µg / ml
3	0.239	359 ng / 25 µl	14.3 µg / ml
8		398 ng / 25 µl	19.9 µg / ml
9	0.230	333 ng / 25 µl	13.3 µg / ml
Mean Highfive expression values		80 µg / mg	1.7 nmoles / mg

Table 11.5, Densitometric analysis of figure 11.36. The above table demonstrates the amount of HIS-GLUT1 found in fractions 2, 3, 8 and 9, in µg / ml. Fractions 2 and 8 were analysed from a separate blot, which is not shown.

Both the wash fractions and the elution fractions were observed to contain similar amounts of HIS-GLUT1. It was calculated from immunoblot analysis that fractions 2 and 3 and fractions 8 and 9, contained 31 and 33 µg / ml, respectively. Experimental

evidence again demonstrated a 1 : 1 ratio between the HIS-GLUT1 eluted in the wash fraction and the HIS-GLUT1 eluted in the elution fraction. This suggested the presence of two distinct sub groups of HIS-GLUT1 protein. One subgroup has a high affinity towards the column and the other has a low affinity towards the column. Dialysed fractions were concentrated in a Beckman ultracentrifuge at 541,000 g for 30 minutes. Samples were analysed on a 10% polyacrylamide gel and the proteins visualised using the BioRad silver stain plus system, figure 11.36.

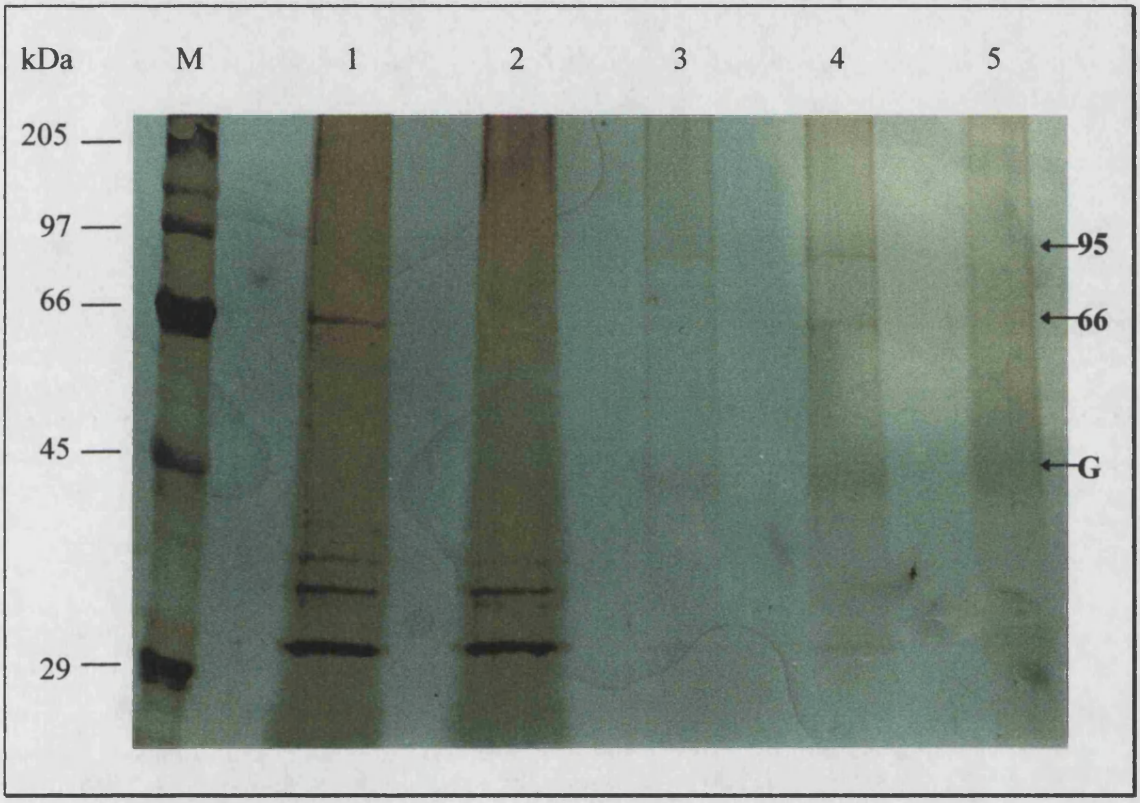

Figure 11.36, Silver stained analysis of column purified HIS-GLUT1. Fractions 3 and 9 were concentrated and loaded onto a 10% polyacrylamide gel as follows: Lane M: high molecular weight marker; lane 1: 500 µl of fraction 3; lane 2: 750 µl of fraction 3; lane 3: 500 µl of fraction 9; lane 4: 750 µl of fraction 9; lane 5: 2 µg of human GLUT1 standard. The GLUT1 and HIS-GLUT1 bands are indicated with a G and the 66 and 95 kDa contaminating bands are indicated with the figures 66 and 95.

Fraction 3 (the wash fraction) was observed to contain many bands and the HIS-GLUT1 protein can not be seen at all. However, in fraction 9 (the elution fraction) the HIS-GLUT1 protein is clearly visible as a diffuse band running at 45 kDa. The HIS-GLUT1 protein band is less diffuse than the human GLUT1 standard because of the reduced level of glycosylation in insect cells. Immunoblot analysis suggested that there

should be 10 μg of HIS-GLUT1 present in 750 μl of fraction 9, these data suggested that silver staining has a decreased sensitivity with respect to the HIS-GLUT1 protein. Two contaminating bands were observed, as characterised previously, 66 kDa BSA band and the 95 kDa band. Analysis of fractions 2 and 8 from the same column run gave similar results.

In an attempt to obtain pure HIS-GLUT1 protein, a column was taken and over-loaded with HIS-GLUT1. It was hypothesised that an excess of HIS-GLUT1 protein may compete off the contaminating proteins. A 1 ml chelating Sepharose column, charged with nickel, was over loaded with 40 mg of octyl glucoside solubilized Sf9 cell membranes expressing HIS-GLUT1. Following analysis on a 10% polyacrylamide gel stained with Coomassie blue, the 95 kDa band and other fainter contaminating bands were still evident. It was concluded that the excessive over loading of HIS-GLUT1 protein on the nickel column had no beneficial effect upon HIS-GLUT1 protein purification.

HIS-GLUT1 Yield

The column yield of HIS-GLUT1 protein has been calculated for a 500 ml culture of Highfive cells. The calculations are as follows: 24 mg of washed membranes were obtained from 500 ml of Highfive cell culture. The Highfive cells in this experiment expressed HIS-GLUT1 protein at 1.7 nmoles HIS-GLUT1 / mg of membrane protein (mean of densitometric data, table 11.5). Therefore, 1.7 nmoles x 24 mg = 41.8 nmoles of HIS-GLUT1 were expressed / 500 ml culture, which was equal to 1.9 mg of HIS-GLUT1 expressed / 500 ml culture.

4 mg of Highfive cell membranes expressing HIS-GLUT1 were purified on an immobilised nickel column. The 4 mg of membranes contained 321 μg of HIS-GLUT1 protein. Following purification, the retained HIS-GLUT1 protein was eluted in fractions 8 and 9 and was calculated by immunoblot assay to contain 19.9 and 13.3 μg / ml of HIS-GLUT1, respectively. The fraction size was 1.9 ml and therefore fractions 8 and 9 contained 63.1 μg / 3.8 ml of purified HIS-GLUT1 protein. The total yield from a 500 ml Highfive cell culture expressing HIS-GLUT1 was 378.5 μg of purified HIS-GLUT1. From the original culture 20% of the HIS-GLUT1 protein was recovered.

The HIS-GLUT1 protein lost in the wash fractions is shown as follows: Fractions 2 and 3 contain 16.9 and 14.3 μg / ml of HIS-GLUT1, respectively. This represents a total of 59.4 μg of HIS-GLUT1. The HIS-GLUT1 protein lost in the wash step for a 500 ml culture was therefore 356.3 μg of HIS-GLUT1 protein, this represents 19% of the HIS-GLUT1 from the original culture.

From the yield calculations it can be seen that 51% of the HIS-GLUT1 protein was retained on the column and that 49% was eluted in the wash buffer. This is probably a result of the HIS-GLUT1 protein having a low affinity towards the nickel column, by the polyhistidine tag being masked by amino acid tertiary structure or by being partially buried in the detergent micelle / lipid bilayer. 61% of the HIS-GLUT1 from the 500 ml culture was lost during solubilization (some HIS-GLUT protein remained in the unsolubilized cell pellet), running the column and as experimental error. This was considerably less than that lost during HIS-GLUT1 protein purification from Sf9 cells. This may have been partly due to the Highfive cell membrane being more effectively solubilized by the detergent system used. The yield could be improved by increasing the affinity of the polyhistidine tagged protein towards the nickel column. This could be accomplished by placing the tag on the hydrophilic C-terminal end of the glucose transporter.

Section 11.11

Purification of the HIS-C-TERM Protein Expressed in Sf9 Cells

The HIS-C-TERM protein was expressed with an N-terminal polyhistidine tag to allow for purification of the protein by immobilised metal ion liquid chromatography. 2 mg of homogenised Sf9 cells expressing the HIS-C-TERM protein were solubilized and loaded on to a chelating Sepharose nickel column. The column was washed with 9 ml of wash buffer and eluted with 5 ml of elution buffer. 1.5 ml fractions were collected and 40 μl aliquots were taken from each fraction. The aliquots were analysed by immunoblot assay, figure 11.37 and on a 12% polyacrylamide gel followed by Coomassie blue staining, results not shown. The only detectable protein present, by Coomassie staining was in fraction 2. There were no other proteins detectable on the gel. The immunoblot assay is displayed in figure 11.37.

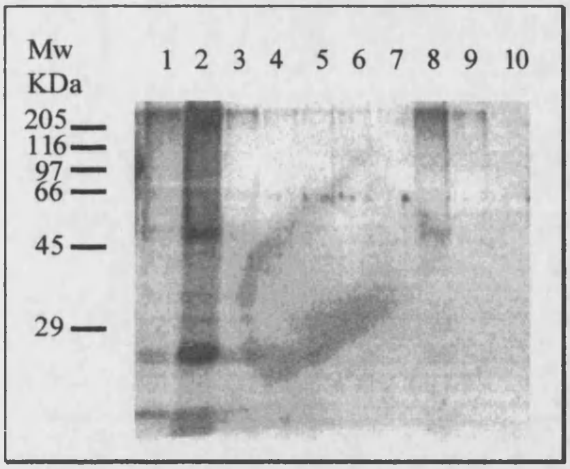

Figure 11.37, Immunoblot of Sf9 expressed HIS-C-TERM protein eluted from a nickel column. 40 µl aliquots were taken from each column fraction and loaded onto a 12% polyacrylamide gel as follows: lane 1: fraction 1; lane 2: fraction 2; lane 3: fraction 3; lane 4: fraction 4; lane 5: fraction 5; lane 6: fraction 6; lane 7: fraction 7; lane 8: fraction 8; lane 9: fraction 9; lane 10: fraction 10.

The HIS-C-TERM protein appeared to have little or no affinity towards the column. The majority of the HIS-C-TERM protein appeared to have been eluted off during the column wash. Only a very small fraction of the protein was observed to have been retained by the column. The retained protein was eluted from the column in fraction 8, resulting in a very faint monomer and dimer band at approximately 27 and 50 kDa, respectively.

Section 11.12 Protein Purification Discussion

Table 11.6 summarises the data obtained from purification trials carried out on the HIS-GLUT1 protein expressed in Sf9 and Highfive insect cells.

Sf9 Expressed HIS-GLUT1		
	Before Purification	After Purification
Yield	770 µg of HIS-GLUT1 / 500 ml of culture	36 µg of HIS-GLUT1 / 500 ml of culture (6% recovery)
Highfive Expressed HIS-GLUT1		
Yield	1.92 mg of HIS-GLUT1 / 500 ml of culture	379 µg of HIS-GLUT1 / 500 ml of culture (20% recovery)
Purity	8% Pure	Approximately 40 % Pure

Table 11.6, Summary of data. The above table summarises the data obtained from purification trials on HIS-GLUT1 protein expressed in Sf9 and Highfive cells.

During purification a 5 fold increase in purity was achieved. It was estimated that the resulting HIS-GLUT1 protein was 40 % pure. Further purification of the constructs proved difficult without fundamental modifications to the procedure. Modifications may include the elimination of the 66 kDa BSA band, by incubating and infecting the insect

cells in a serum free environment. It could take several weeks to adapt the cells to such a system but may well be worth the effort so as to eliminate the contaminating proteins. Throughout the procedure the 66 kDa band, thought to be BSA, proved to be a very persistent contaminant. The unidentified protein, running at 97 kDa, could be removed by including a DEAE cellulose column within the purification protocol. Initial studies suggested that a DEAE cellulose column would act as a useful primary column, providing an initial sample clean up. The sample could then be refined upon a nickel column. One disadvantage however would be the increased loss of HIS-GLUT1 protein due to an increased number of purification steps.

The HIS-GLUT1 protein appeared to have a low affinity towards the nickel column and the HIS-C-TERM protein appeared to have no affinity towards the nickel column. It was hypothesised that the affinity of the HIS-GLUT1 protein towards the nickel column may in some way be affected by the conformation of the protein. The polyhistidine tag may not be completely free of the protein structure. The polyhistidine tag may well be 'shielded' by other residues present in the N-terminal sequence or be buried in the detergent micelle / lipid bilayer. By random chance about 50% of the polyhistidine tags would be free of this structure and capable of binding immobilised nickel ions with a certain degree of affinity; the other polyhistidine tags would be buried within the protein structure. By separating the polyhistidine tag further from the protein, with a longer hydrophilic 'spacer', or by placing it at the end of the hydrophilic C-terminus, it may be possible to increase the affinity of the HIS-GLUT1 protein towards the nickel column. This may result in the HIS-GLUT1 protein competing off the contaminating Sf9 cell proteins, resulting in a purified polyhistidine tagged protein product. In the case of the HIS-C-TERM protein the polyhistidine tag may have been completely obscured by the detergent micelle.

Weinglass and Baldwin, (1996) have demonstrated a 90% level of purification of the glucose transporter protein, based on the use of a C-terminally placed polyhistidine tag. The final 39 amino acids of the GLUT1 protein are predicted to be free of the membrane and may even be involved in the kinetic control of the transporter. The C-terminal end of the GLUT1 protein is already known to be accessible to cytoplasmic proteins, and provides the necessary distance required between the GLUT1 protein and affinity matrix, making the polyhistidine tag accessible to the immobilised nickel ions.

Final Discussion

12.0 Final Discussion

Studies involving point mutation analysis of the human GLUT1 C-terminal tail in CHO cells revealed that although there was a significant perturbation of transporter activity by the R468L mutation the kinetics of the GLUT2 protein were not conferred upon the GLUT1 protein. It was concluded that the kinetic function of the glucose transporter was controlled by the overall conformation of a much larger region (possibly the whole of the cytoplasmic C-terminal tail) and that no one amino acid appeared to be critical for this function. This conclusion is consistent with results obtained from C-terminal deletion analysis and chimeric protein studies.

Confocal microscopy demonstrated that the full length glucose transporter constructs, with or without a polyhistidine tag, were targeted to the plasma membrane. However, plasma membrane targeting was perturbed in both C-terminal constructs. The C-terminal constructs were not exclusively targeted to the plasma membrane, instead only a small proportion of the protein ended up there. Protein mis-folding cannot explain the amount of recombinant protein targeted to cytoplasmic membranes other than the endoplasmic reticulum. Mis-folded protein should be exclusively retained in the endoplasmic reticulum and protein released into the Golgi apparatus should be targeted immediately to the plasma membrane. It is possible that there is a specific intracellular targeting motif contained within the C-terminal portion of the glucose transporter recognised by Sf9 cells. However, more research would be required to prove or disprove this theory. The polyhistidine tag and linking amino acids were observed to have no effect on the localisation of any of the constructs. This demonstrated that the polyhistidine tag does not disrupt or aid in the targeting of the protein.

Photolabelling of the C-terminal glucose transporter construct (C-TERM) did not result in any significant level of photolabelling. Photolabelling of the polyhistidine tagged C-terminal glucose transporter construct (HIS-C-TERM) was inconclusive due to poor glucose displacement data. It was not possible to prove that the polyhistidine tagged C-terminal half was capable of glucose transport due to the insect cells becoming permeable on viral infection.

If the polyhistidine tagged C-terminal construct was capable of transporting substrate across the membrane this would provide further evidence to support the glucose transporter theory of origin to have been by a gene duplication event (Szkutnicka *et al.*, (1989)). Indeed, the C-terminal construct may have been the original ancestral glucose transporter. Wu *et al.*, (1996) have found that the C-terminal portion of the lactose transporter was capable of lactose transport in the absence of the N-terminal half. However, the C-terminal portion was only

capable of this when modified by the addition of 5 amino acids on the N-terminal end of the C-terminal construct.

The present study has shown that a genetically modified form of the rabbit glucose transporter protein, expressing a polyhistidine tag on the N-terminal end, does not result in the purification of that protein to homogeneity upon a Pharmacia Biotech HiTrap™ nickel column. Neither is the column successful in the purification of a genetically truncated glucose transporter construct (HIS-C-TERM), with a polyhistidine tag attached to the N-terminal end. In both cases it is hypothesised that this is due to the polyhistidine tag either being 'shielded' by the protein structure or by being partially buried in the detergent micelle when in solution.

It is possible that the binding affinity of the polyhistidine tagged constructs could have been improved by either extending the amino acid spacer region (the region between the polyhistidine tag and the protein), increasing the number of histidine residues forming the tag or by placing the tag on the C-terminal end of the transporter. The C-terminal tail was predicted to be highly hydrophilic by hydropathy plot analysis (figure 1.1) and appears to be accessible to soluble components within the cytoplasm. A structure that is readily accessible to soluble cellular components should theoretically provide an ideal site for the positioning of a polyhistidine tag and allow for complete access to the tag by immobilised metal ions. Placing the polyhistidine tag at the end of the protein would also provide a secondary benefit, it would result in the complete elimination of partially expressed products from the final purified product (partially expressed products will not possess a polyhistidine tag and will therefore not be bound by the nickel column). The purification experiments performed in this study may indicate that the N-terminal end of the glucose transporter is closely associated with the lipid bilayer, and may be barely free of the membrane. Davies *et al.,* (1987a&b) have observed that anti N-terminal antibodies displayed little affinity towards the glucose transporter protein. This also indicated that in the native state the N-terminal tail may be partially buried within the membrane.

Weinglass and Baldwin, (1996) have reported on the expression of a C-terminal polyhistidine tagged glucose transporter construct in insect cells. Following solubilization in the detergent octyl glucoside they reported a 90% level of purification. Weinglass and Baldwin, (1996) did not report which proteins were causing contamination of their polyhistidine tagged protein. However, it seems likely that the contaminants could have been proteins such as BSA from the foetal calf serum. These contaminants could have been removed by the inclusion of a primary DEAE cellulose column in the purification protocol or by growing the cells in a serum free medium system.

13.0 Future Work

Observations made by confocal microscopy suggested that there may be targeting information contained within the glucose transporter recognised by the Sf9 cell. The insect cell system could be used to examine any targeting information that may be present. The construction of N-terminal deletion mutants followed by insect cell expression and analysis by confocal microscopy could help to determine the exact nature of any signal sequence present within the transporter.

At present, the baculovirus expression system offers the most rapid way forwards for GLUT1 protein purification. However, before the system can be used for the purification of the glucose transporter consideration will need to be given to re-designing the polyhistidine tagged construct. Purification to homogeneity could be achieved by engineering the polyhistidine tag onto the end of the C-terminal tail. It is thought that this would result in a protein with a higher affinity towards the immobilised nickel Sepharose column. Alternatively, it may be possible to increase the affinity of the N-terminally attached polyhistidine tag towards the immobilised metal ions by inserting a glycine linker between the polyhistidine tag and the glucose transporter. This would prevent the GLUT1 protein from interfering with column affinity. A further increase in affinity could be achieved by increasing the length of the polyhistidine tag from six histidine residues to either eight or ten residues. However, this may result in a decreased level of protein expression. The expression of a polyhistidine tagged glucose transporter with an increased affinity towards the column would allow for the use of more stringent washing protocol in order to remove contaminating proteins.

To ensure the removal of contaminating proteins (ie. BSA), insect cells should be adapted to and incubated in a serum free medium. Furthermore, a DEAE cellulose column should be included in the purification protocol as a primary column. If this was done in addition to redesigning the polyhistidine tag then pure glucose transporter protein may well be obtained from the baculovirus system.

Further thought may be needed with respect to the detergent system used. Mascher, (1989) and Haneskog *et al.*, (1996) have determined that human erythrocyte GLUT1, solubilized in the detergent octyl glucoside, resulted in GLUT1 protein in the dimeric and oligomeric form. Mascher *et al.*, (1989) and Haneskog *et al.*, (1996) have

further shown that GLUT1 solubilized in the detergents SDS and Thesit ($C_{12}E_8$) was in a largely monomeric form. This is perhaps not such an important consideration during the chromatographic step, but it may be a necessary consideration for the attempted crystallisation of the protein. Varying amounts of aggregates may make the protein difficult or impossible to crystallise. However, crystallisation of the monomeric form may prove easier. Boulter and Wang (1997) have had success solubilizing and purifying the human erythrocyte GLUT1 using a maltoside detergent. This detergent has been used in crystallising many other membrane proteins and may be useful in the crystallisation of the glucose transporter, hopefully restricting the formation of GLUT1 oligomers.

The baculovirus expression system does have disadvantages when expressing protein for use in protein crystallisation studies as a substantial amount of pure protein is required. The baculovirus expression system requires a lot of time and resources in order to produce large quantities of recombinant protein. Researchers are now investigating the possibility of expressing large amounts of functional protein in the yeast expression system. This offers the advantage of a continuous culture system and the economic production of vast quantities of protein in a relatively short period of time.

However, the baculovirus system does have certain advantages over the yeast expression system. Insect cells produce a glucose transporter that is glycosylated. This may prove to be essential for the correct function of the protein and may even be necessary to allow the protein to adopt its true wild-type conformation. Insect cells target the polyhistidine tagged protein to the plasma membrane and allow it to fold correctly, adopting an active conformation. Finally, glucose transporter expression in the insect cell system has been well characterised and functional glucose transporter protein is known to be expressed.

The baculovirus expression system has proved to be a useful system in which to express the glucose transporter. It has been demonstrated to yield fully functional polyhistidine tagged glucose transporter, which can be partially purified on an immobilised metal ion Sepharose column. Persistence with this system should result in the complete purification to homogeneity of recombinant glucose transporter expressed in insect cells. The pure protein can then be used to start crystallisation studies.

Appendix

14.0 Appendix

Recombinant Protein Sequences

Fusion vector pLE12

MPDYSYRPTI GPDHA ---- *GLUT1* ------

Fusion vector pLE14

Histidine tag ↓ ↓ Enterokinase site (Recognition sequence DDDDK//) ↓

MRGSHHHHHH GMASMTGGQQ MGRDLYDDDD KDPSSRSAAG A -*GLUT1*-

Non-fusion vector pVL:*GLUT1* (Full length glucose transporter)

```
1   MEPSSKKVTG  RLMLAVGGAV  LGSLQFGYNT  GVINAPQKVI  EEFYNQTWIH
51  RYGERILPTT  LTTLWSLSVA  IFSVGGMIGS  FSVGLFVNRF  GRRNSMLMMN
101 LLAFVSAVLM  GFSKLAKSFE  MLILGRFIIG  VYCGLTTGFV  PMYVGEVSPT
151 ALRGALGTLH  QLGIVVGILI  AQVFGLDSIM  GNEDLWPLLL  SVIFVPALLQ
201 CIVLPLCPES  PRFLLINRNE  ENRAKSVLKK  LRGNADVTRD  LQEMKEESRQ
251 MMREKKVTIL  ELFRSPAYRQ  PILSAVVLQL  SQQLSGINAV  FYYSTSIFEK
301 AGVQQPVYAT  IGSGIVNTAF  TVVSLFVVER  AGRRTLHLIG  LAGMAACAVL
351 MTIALALLEQ  LPWMSYLSIV  AIFGFVAFFE  VGPGPIPWFI  VAELFSQGPR
401 PAAVAVAGFS  NWTSNFIVGM  CFQYVEQLCG  PYVFIIFTVL  LVLFFIFTYF
451 KVPETKGRTF  DEIASGFRQG  GASQSDKTPE  ELFHPLGADS  QV*
```

pVL941:*GT52* (C-terminal portion of GLUT1)

```
254     EKKVTIL  ELFRSPAYRQ  PILSAVVLQL  SQQLSGINAV  FYYSTSIFEK
301 AGVQQPVYAT  IGSGIVNTAF  TVVSLFVVER  AGRRTLHLIG  LAGMAACAVL
351 MTIALALLEQ  LPWMSYLSIV  AIFGFVAFFE  VGPGPIPWFI  VAELFSQGPR
401 PAAVAVAGFS  NWTSNFIVGM  CFQYVEQLCG  PYVFIIFTVL  LVLFFIFTYF
451 KVPETKGRTF  DEIASGFRQG  GASQSDKTPE  ELFHPLGADS  QV*
```

Nucleotides at the start of the *GLUT1* cDNA (Taken from Asano *et al.* (1988)):

```
GCC ATG GAA CCC AGC AGC AAG AAG GTG ACG GGC CGC CTC ATG CTG GCC GTG
GGA GGA GCA GTG CTC GGC TCC CTG CAG TTT GGC TAC AAC ACT GGA GTC ATC
AAC GCC CCC CAG AAG GTG ATC GAG GAG TTC TAC AAC CAG ACG TGG ATC CAC
CGC TAT GGG GAG CGC ATC TTG CCC ACC ACG CTC ACC ACG CTG TGG TCC CTC
TCG GTG GCC ATC TTC TCC GTC GGG GGA ATG ATT GGC
```

The two restriction sites *Nco*I and *Bam*HI are marked respectively.

References

Baldwin, S. A. (1993).
Mammalian passive glucose transporters: members of an ubiquitous family of active and passive transport proteins.
Biochimica et Biophysica Acta, Vol. 1154, pp. 17 - 49.

Baldwin, S. A., Kan, O., Whetton, A. D., Martin, S., Fawcett, H. A. C., Flint, D. J. and Wilde, C. J. (1994).
Regulation of the glucose transporter GLUT1 in mammalian cells.
Biochemical Society Transactions, Vol. 22, pp. 814 - 817.

Barnett, J. E. G., Holman, G. D. and Munday, K. A. (1973a).
Structural Requirements for Binding to the Sugar-Transport System of the Human Erythrocyte.
Biochem. J., Vol. 131, pp. 211 - 221.

Barnett, J. E. G., Holman, G. D. and Munday, K. A. (1973b).
An Explanation of the Asymmetric Binding of Sugars to the Human Erythrocyte Sugar-Transport Systems.
Biochem. J., Vol. 135, pp. 539 - 541.

Barnett, J. E. G., Holman, G. D., Chalkley, R. A. and Munday, K. A. (1975).
Evidence for Two Asymmetric Conformational States in the Human Erythrocyte Sugar-Transport System.
Biochem. J., Vol. 145, pp. 417 - 429.

Bell, G. I., Burant, C. F., Takeda, J. and Gould, G. W. (1993).
Structure and Function of Mammalian Facilitative Sugar Transporters.
The Journal of Biological Chemistry, Vol. 268, No. 26, pp. 19161 - 19164.

Birnboim, H. C. and Doly, J. (1979).
A Rapid Alkaline Extraction Procedure for Screening Recombinant Plasmid DNA.
Nucleic Acids Research, Vol. 7, No. 6, pp. 1513 - 1523.

Blaurock, A. E. (1982).
Analysis of Bacteriorhodopsin Structure by X-Ray Diffraction.
Methods in Enzymology, Vol. 88, pp. 124 - 132.

Boulter, J. M. and Wang, D. N. (1997).
Purification and Characterization of GLUT-1 from Human Erythrocytes.
Glucose transporter meeting, Copper Mountain, Colorado, 1997.

Burant, C. F., Takeda, J., Brot-Laroche, E., Bell, G. I. and Davidson, N. O. (1992).
Fructose transporter in human spermatozoa and small intestine is GLUT5.
J. Biol. Chem., Vol. 267, pp. 14523 - 14526.

Carlsson, J., Mosbach, K. and Bülow, L. (1996).
Affinity Precipitation and Site-Specific Immobilization of Proteins Carrying Polyhistidine Tails.
Biotechnology and Bioengineering, Vol. 51, pp. 221 - 228.

Carruthers, A. and Helgerson, A. (1989).
The Human Erythrocyte Sugar Transporter Is Also a Nucleotide Binding Protein.
Biochemistry, Vol. 28, pp. 8337 - 8346.

Chen, L., Buters, J. T., Hardwick, J. P., Tamura, S., Penman, B. W., Gonzalez, F. J. and Crespi, C. L. (1997).
Coexpression of cytochrome P450 2A6 and human NADPH-P450 oxidoreductase in the baculovirus system.
Drug Metab. Dispos., Vol. 25, pp. 399 - 405.

Chin, J. J., Jung, E. K. Y., Chen, V. and Jung, C. Y. (1987).
Structural basis of human erythrocyte glucose transporter function in proteoliposome vesicles: Circular dichroism measurements.
Proc. Natl. Acad. Sci. USA, Vol. 84, pp. 4113 - 4116.

Clark, A. E. and Holman, G. D. (1990).
Exofacial photolabelling of the human erythrocyte glucose transporter with an azitrifluoroethylbenzoyl-substituted bismannose.
Biochem. J., Vol. 269, pp. 615 - 622.

Connolly, T. J., Carruthers, A. and Melchior, D. L. (1985a).
Effect of Bilayer Cholesterol Content on Reconstituted Human Erythrocyte Sugar Transporter Activity.
The Journal of Biological Chemistry, Vol. 260, No. 5, pp. 2617 - 2620.

Connolly, T. J., Carruthers, A. and Melchior, D. L. (1985b).
Effects of Bilayer Cholesterol on Human Erythrocyte Hexose Transport Protein Activity in Synthetic Lecithin Bilayers.
Biochemistry, Vol. 24, pp. 2865 - 2873.

Cope, D. L., Holman, G. D., Baldwin, S. A. and Wolstenholme, A. J. (1994).
Domain assembly of the GLUT1 glucose transporter.
Biochem. J., Vol. 300, pp. 291 - 294.

Dauterive, R., Laroux, S., Bunn, R. C., Chaisson, A., Sanson, T. and Reed, B. C. (1996).
C-terminal Mutations That Alter the Turnover Number for 3-O-Methylglucose Transport by GLUT1 and GLUT4.
The Journal of Biological Chemistry, Vol. 271, No. 19, pp. 11414 - 11421.

Davies, A., Meeran, K., Cairns, M. T. and Baldwin, S. A. (1987a).
Antibodies as probes of the human erythrocyte glucose transporter.
Biochemical Society Transactions, Vol. 15, pp. 436 - 437.

Davies, A., Meeran, K., Cairns, M. T. and Baldwin, S. A. (1987b).
Peptide-specific Antibodies as Probes of the Orientation of the Glucose Transporter in the Human Erythrocyte Membrane.
The Journal of Biological Chemistry, Vol. 262, No. 19. pp. 9347 - 9352.

Davies, A., Ciardelli, T. L., Lienhard, G. E., Boyle, J. M., Whetton, A. D. and Baldwin, S. A. (1990).
Site-specific antibodies as probes of the topology and function of the human erythrocyte glucose transporter.
Biochem. J., Vol. 266, pp. 799 - 808.

Deisenhofer, J., Epp, O., Miki, K., Huber, R. and Michel, H. (1984).
X-ray Structure Analysis of a Membrane Protein Complex
Electron Density Map at 3 Å Resolution and a Model of the Chromophores of the Photosynthetic Reaction Center from *Rhodopseudomonas viridis.*
J. Mol. Biol., Vol. 180, pp. 385 - 398.

Deisenhofer, J., Epp, O., Miki, K., Huber, R. and Michel, H. (1985).
Structure of the protein subunits in the photosynthetic reaction centre of *Rhodopseudomonas viridis* at 3 Å resolution.
Nature, Vol. 318, pp. 618 - 624.

Ducarme, P., Rahman, M., Lins, L. and Brasseur, R. (1996).
The erythrocyte / brain glucose transporter (GLUT1) may adopt a 2-channel transmembrane-alpha / beta structure.
Journal of Molecular Modeling, Vol. 2, No. 2, pp. 27 - 45.

Due, A. D., Zhi-chao, Q., Thomas, J. M., Buchs, A., Powers, A. C. and May, J. M. (1995).
Role of the C-Terminal Tail of the GLUT1 Glucose Transporter in Its Expression and Function in *Xenopus laevis* Oocytes.
Biochemistry, Vol. 34, pp. 5462 - 5471.

Eisenberg, D., Schwarz, E., Komaromy, M. and Wall, R. (1984).
Analysis of membrane and surface protein sequences with the hydrophobic moment plot.
J. Mol. Biol., Vol. 179, pp. 125 - 142.

Feugeas, J., Néel, D., Pavia, A. A., Laham, A., Goussault, Y. and Derappe, C. (1990).
Glycosylation of the human erythrocyte glucose transporter is essential for glucose transport activity.
Biochimica et Biophysical Acta, Vol. 1030, pp. 60 - 64.

Fischbarg, J., Cheung, M., Czegledy, F., Li, J., Iserovich, P., Kuang, K., Hubbard, J., Garner, M., Rosen, O. M., Golde, D. W. and Vera, J. C. (1993).
Evidence that facilitative glucose transporters may fold as β-barrels.
Proc. Natl. Acad. Sci. USA, Vol. 90, pp. 11658 - 11662.

Fuchs, R. and Blakesley, R. (1983).
Guide to the Use of Type II Restriction Endonucleases.
Methods in Enzymology, Vol. 100, pp. 3 - 38.

Gould, G. W., Thomas, H. M., Jess, T. J. and Bell, G. I. (1991).
Expression of human glucose transporters in Xenopus oocytes: Kinetic characterization and substrate specificities of the erythrocyte, liver, and brain isoforms.
Biochemistry, Vol. 30, pp. 5139 - 5145.

Haneskog, L., Andersson, L., Brekkan, E., Englund, A., Kameyama, K., Liljas, L., Greijer, E., Fischbarg, J. and Lundahl, P. (1996).
Monomeric human red cell glucose transporter (Glut1) in non-ionic detergent solution and a semi-elliptical torus model for detergent binding to membrane proteins.
Biochimica et Biophysica Acta, Vol. 1282, pp. 39 - 47.

Hashimoto, F., Horigome, T., Kanbayashi, M., Yoshida, K. and Sugano, H. (1983).
An Improved Method for Separation of Low-Molecular-Weight Polypeptides by Electrophoresis in Sodium Dodecyl Sulfate - Polyacrylamide Gel.
Analytical Biochemistry, Vol. 129, pp 192 - 199.

Hashiramoto, M., Kadowaki, T., Clark, A. E., Muraoka, A., Momomura, K., Sakura, H., Tobe, K., Akanuma, Y., Yazaki, Y., Holman, G. D. and Kasuga, M. (1992).
Site-directed Mutagenesis of GLUT1 in Helix 7 Residue 282 Results in Perturbation of Exofacial Ligand Binding.
The Journal of Biological Chemistry, Vol. 267, No. 25, pp. 17502 - 17507.

Haspel, H. C., Wilk, E. W., Birnbaum, M. J., Cushman, S. W. and Rosen, O. M. (1986).
Glucose deprivation and hexose transporter polypeptides of murine fibroblasts.
J. Biol. Chem., Vol. 261, pp. 6778 - 6789.

Hebert, D. N. and Carruthers, A. (1986).
Direct Evidence for ATP Modulation of Sugar Transport in Human Erythrocyte Ghosts.
The Journal of Biological Chemistry, Vol. 261, No. 22, pp. 10093 - 10099.

Hebert, D. N. and Carruthers, A. (1992).
Glucose Transporter Oligomeric Structure Determines Transporter Function.
The Journal of Biological Chemistry, Vol. 267, No. 33, pp. 23829 - 23838.

Helgerson, A. L. and Carruthers, A. (1989).
Analysis of Protein-Mediated 3-O-Methylglucose Transport in Rat Erythrocytes:
Rejection of the Alternating Conformation Carrier Model for Sugar Transport.
Biochemistry, Vol. 28, pp. 4580 - 4594.

Henderson, R. and Unwin, P. N. T. (1975).
Three-dimensional model of purple membrane obtained by electron microscopy.
Nature, Vol. 257, pp. 28 - 32.

Hiraki, Y., de Herreros, A. G. and Birnbaum, M. J. (1989).
Transformation stimulates glucose transporter gene expression in the absence of protein kinase C.
Proc. Natl. Acad. Sci. U.S.A., Vol. 86, pp. 8252 - 8256.

Hodgson, P. A., Osguthorpe, D. J. and Holman, G. D. (1992).
Molecular modeling of the human erythrocyte glucose transporter.
11th Annual Molecular Graphics Society Meeting.

Holman, G. D. and Rees, W. D. (1982).
Side-specific analogues for the rat adipocyte sugar transport system.
Biochimica et Biophysica Acta, Vol. 685, pp. 78 - 86.

Holman, G. D. and Rees, W. D. (1987).
Photolabelling of the hexose transporter at external and internal sites: fragmentation patterns and evidence for a conformational change.
Biochimica et Biophysica Acta, Vol. 897, pp. 395 - 405.

Hresko, R. C., Kruse, M., Strube, M. and Mueckler, M. (1994).
Topology of the GLUT1 Glucose Transporter Deduced from Glycosylation Scanning Mutagenesis.
The Journal of Biological Chemistry, Vol. 269, No. 32, pp. 20482 - 20488.

Inukai, K., Asano, T., Katagiri, H., Anai, M., Funaki, M., Ishihara, H., Tsukuda, K., Kikuchi, M., Yazaki, Y. and Oka, Y. (1994).
Replacement of both tryptophan residues at 388 and 412 completely abolished cytochalasin B photolabelling of the GLUT1 glucose transporter.
Biochem. J., Vol. 302, pp. 355 - 361.

Iwata, S., Ostermeier, C., Ludwig, B. and Michel, H. (1995).
Structure at 2.8 Å resolution of cytochrome c oxidase from *Paracoccus denitrificans*.
Nature, Vol. 376, pp. 660 - 669.

Jähnig, F. (1990).
Structure predictions of membrane proteins are not that bad.
TIBS, Vol. 15, pp. 93 - 95.

Jung, C. Y. and Rampal, A. L. (1977).
Cytochalasin B Binding Sites and Glucose Transport Carrier in Human Erythrocyte Ghosts.
The Journal of Biological Chemistry, Vol. 252, No. 15, pp. 5456 - 5463.

Jung, C. Y., Hsu, T. L., Hah, J. S., Cha, C. and Haas, M. N. (1980).
Glucose Transport Carrier of Human Erythrocytes.
The Journal of Biological Chemistry, Vol. 255, No. 2, pp. 361 - 364.

Kasahara, T. and Kasahara, M. (1996).
Expression of the rat GLUT1 glucose transporter in the yeast *Saccharomyces cerevisiae*.
Biochem. J., Vol. 315, pp. 177 - 182.

Katagiri, H., Asano, T., Ishihara, H., Tsukuda, K., Lin, J., Inukai, K., Kikuchi, M., Yazaki, Y. and Oka, Y. (1992).
Replacement of Intracellular C-terminal Domain of GLUT1 Glucose Transporter with That of GLUT2 Increases V_{max} and K_m of Transport Activity.
The Journal of Biological Chemistry, Vol. 267, No. 31, pp. 22550 - 22555.

Keller, K., Strube, M. and Mueckler, M. (1989).
Functional expression of the human HepG2 and rat adipocyte glucose transporters in Xenopus oocytes. Comparison of kinetic parameters.
J. Biol. Chem., Vol. 264, pp. 18884 - 18889.

King, L. A. and Possee, R. D. (1992).
The Baculovirus Expression System
A laboratory guide.
Chapman & Hall, ISBN 0 412 37150 2.

Kuroda, K., Hauser, C., Rott, R., Klenk, H. and Doerfler, W. (1986).
Expression of the influenza virus haemagglutinin in insect cells by a baculovirus vector.
The EMBO Journal, Vol. 5, No. 6, pp. 1359 - 1365.

Kuroda, K., Geyer, H., Geyer, R., Doerfler, W. and Klenk, H. D. (1990).
The oligosaccharides of influenza virus hemagglutinin expressed in insect cells by a baculovirus vector.
Virology, Vol. 174, pp. 418 - 429.

Laemmli, U. K. (1970).
Cleavage of Structural Proteins during the Assembly of the Head of Bacteriophage T4.
Nature, Vol. 227, pp. 680 - 685.

Li, J. and Tooth, P. (1987).
Size and shape of the *Escherichia coli* lactose permease measured in filamentous arrays.
Biochemistry, Vol. 26, pp. 4816 - 4823.

Lin, S., Santi, D. V. and Spudich, J. A. (1974).
Biochemical Studies on the Mode of Action of Cytochalasin B.
The Journal of Biological Chemistry, Vol. 249, No. 7, pp. 2268 - 2274.

Lin, J., Asano, T., Katagiri, H., Tsukuda, K., Ishihara, H., Inukai, K., Yazaki, Y. and Oka, Y. (1992).
Deletion of C-terminal 12 amino acids of GLUT1 protein does not abolish the transport activity.
Biochemical and Biophysical Research Communications, Vol. 184, No. 2, pp. 865 - 870.

Loddenkötter, B., Kammerer, B., Fischer, K. and Flügge, U. (1993).
Expression of the functional mature chloroplast triose phosphate translocator in yeast internal membranes and purification of the histidine-tagged protein by a single metal-affinity chromatography step.
Proc. Natl. Acad. Sci. USA, Vol. 90, pp. 2155 - 2159.

Maiden, M. C. J., Davis, E. O., Baldwin, S. A., Moore, D. C. M. and Henderson, P. J. F. (1987).
Mammalian and bacterial sugar transport proteins are homologous.
Nature, Vol. 325, pp. 641 - 643.

Mascher, E. (1989).
Chromatographic studies of the human red cell glucose transporter in sodium dodecyl sulfate and in octyl glucoside.
Acta Univ. Ups., Vol. 217, ISBN. 91-554-2435-X, p. 43.

Michel, H. (1982).
Three-dimensional Crystals of a Membrane Protein Complex
The Photosynthetic Reaction Centre from *Rhodopseudomonas viridis*.
J. Mol. Biol., Vol. 158, pp. 567 - 572.

Mori, H., Hashiramoto, M., Clark, A. E., Yang, J., Muraoka, A., Tamori, Y., Kasuga, M. and Holman, G. D. (1994).
Substitution of Tyrosine 293 of GLUT1 Locks the Transporter into an Outward Facing Conformation.
The Journal of Biological Chemistry, Vol. 269, No. 15, pp. 11578 - 11583.

Mueckler, M., Caruso, C., Baldwin, S. A., Panico, M., Blench, I., Morris, H. R., Allard, W. J., Lienhard, G. E. and Lodish, H. F. (1985).
Sequence and Structure of a Human Glucose Transporter.
Science, Vol. 229, pp. 941 - 945.

Mueckler, M., Weng, W. and Kruse, M. (1994).
Glutamine 161 of GLUT1 Glucose Transporter Is Critical for Transport Activity and Exofacial Ligand Binding.
The Journal of Biological Chemistry, Vol. 269, No. 32, pp. 20533 - 20538.

Muraoka, A., Hashiramoto, M., Clark, A. E., Edwards, L. C., Sakura, H., Kadowaki, T., Holman, G. D. and Kasuga, M. (1995).
Analysis of the structural features of the C-terminus of GLUT1 that are required for transport catalytic activity.
Biochem. J., Vol. 311, pp. 699 - 704.

Narayana, N., Cox, S., Shaltiel, S., Taylor, S. and Xuong, N. (1997).
Crystal Structure of a Polyhistidine - Tagged Recombinant Catalytic Subunit of cAMP-Dependent Protein Kinase Complexed with the Peptide Inhibitor PKI(5-24) and Adenosine.
Biochemistry, Vol. 36, pp. 4438 - 4448.

Oka, Y., Asano, T., Shibasaki, Y., Lin, J., Tsukuda, K., Katagiri, H., Akanuma, Y. and Takaku, F. (1990).
C-terminal truncated glucose transporter is locked into an inward-facing form without transport activity.
Nature, Vol. 345, pp. 550 - 553.

Ortells, M. O. and Lunt, G. G. (1996).
A mixed helix-beta-sheet model of the transmembrane region of the nicotinic acetylcholine receptor.
Protein Eng., Vol. 9, pp 51 - 59.

Ostermeier, C., Harrenga, A., Ermler, U. and Michel, H. (1997).
Structure at 2.7 Å resolution of the *Paracoccus denitrificans* two-subunit cytochrome c oxidase complexed with an antibody F_v fragment.
Proc, Natl. Acad. Sci. USA, Vol. 94, pp. 10547 - 10553.

Pourcher, T., Leclercq, S., Brandolin, G. and Leblanc, G. (1995).
Melibiose Permease of *Escherichia coli*: Large Scale Purification and Evidence That H^+, Na^+, and Li^+ Sugar Symport Is Catalyzed by a Single Polypeptide.
Biochemistry, Vol. 34, pp. 4412 - 4420.

Préhaud, C., Takehara, K., Flamand, A. and Bishop, D. H. L. (1989).
Immunogenic and Protective Properties of Rabies Virus Glycoprotein Expressed by Baculovirus Vectors.
Virology, Vol. 173, pp. 390 - 399.

Sambrook, J., Fritsch, E. F. and Maniatis, T. (1989).
Molecular Cloning
A Laboratory Manual.
Second Edition.
Cold Spring Harbor Laboratory Press, ISBN 0 87969 309 6.

Sanger, F. and Coulson, A. R. (1975).
A Rapid Method for Determining Sequences in DNA by Primed Synthesis with DNA Polymerase.
J. Mol. Biol., Vol. 94, pp. 441 - 448.

Sanger, F., Air, G. M., Barrell, B. G., Brown, N. L., Coulson, A. R., Fiddes, J. C., Hutchison III, C. A., Slocombe, P. M. and Smith, M. (1977).
Nucleotide sequence of bacteriophage ΦX174 DNA.
Nature, Vol. 265, pp. 687 - 695.

Sarkar, H. K., Thorens, B., Lodish, H. F. and Kaback, H. R. (1988).
Expression of the human erythrocyte glucose transporter in *Escherichia coli*.
Proc. Natl. Acad. Sci. USA, Vol. 85, pp. 5463 - 5467.

Schägger, H. and Von Jagow, G. (1987)
Tricine-Sodium Dodecyl Sulfate - Polyacrylamide Gel Electrophoresis for the Separation of Proteins in the Range from 1 to 100 kDa.
Analytical Biochemistry, Vol. 166, pp. 368 - 379.

Schertler, G. F. X., Bartunik, H. D., Michel, H. and Oesterhelt, D. (1993).
Orthorhombic Crystal Form of Bacteriorhodopsin Nucleated on Benzamidine Diffracting to 3.6 Å Resolution.
J. Mol. Biol., Vol. 234, pp. 156 - 164.

Shi, Y., Liu, H., Vanderburg, G., Samuel, S. J., Ismail-Beigi, F. and Jung, C. Y. (1995).
Modulation of GLUT1 Intrinsic Activity in Clone 9 Cells by Inhibition of Oxidative Phosphorylation.
The Journal of Biological Chemistry, Vol. 270, No. 37, pp. 21772 - 21778.

Simons, C. H., Weinglass, A. B. and Baldwin, S. A. (1997).
Studies on the expression of the human erythrocyte glucose transporter (GLUT1) in the yeast *Saccharomyces cerevisiae*.
Biochem. Soc. Trans., Vol. 25, p 463S.

Szkutnicka, K., Tschopp, J. F., Andrews, L. and Cirillo, V. P. (1989).
Sequence and Structure of the Yeast Galactose Transporter.
Journal of Bacteriology, Vol. 171, No. 8, pp. 4486 - 4493.

Tamori, Y., Hashiramoto, M., Clark, A. E., Mori, H., Muraoka, A., Kadowaki, T., Holman, G. D. and Kasuga, M. (1994).
Substitution at Pro^{385} of GLUT1 Perturbs the Glucose Transport Function by Reducing Conformational Flexibility.
The Journal of Biological Chemistry, Vol. 269, No. 4, pp. 2982 - 2986.

Tefft, R. E., Carruthers, A. and Melchior, D. L. (1986).
Reconstituted Human Erythrocyte Sugar Transporter Activity Is Determined by Bilayer Lipid Head Groups.
Biochemistry, Vol. 25, pp. 3709 - 3718.

Waeber, U., Buhr, A., Schunk, T. and Erni, B. (1993).
The glucose transporter of *Escherichia coli*
Purification and characterization by Ni^{+} chelate affinity chromatography of the $IIBC^{Glc}$ subunit.
FEBS Letters, Vol. 324, No. 1, pp. 109 - 112.

Walz, T., Smith, B. L., Zeidel, M. L., Engel, A. and Agre, P. (1994).
Biologically Active Two-dimensional Crystals of Aquaporin CHIP.
The Journal of Biological Chemistry, Vol. 269, No. 3, pp. 1583 - 1586.

Walz, T., Hiral, T., Murata, K., Heymann, J. B., Mitsuoka, K., Fujiyoshi, Y., Smith, B. L., Agre, P. and Engel, A. (1997).
The three-dimensional structure of aquaporin-1.
Nature, Vol. 387, pp. 624 - 627.

Weinglass, A. B. and Baldwin, S. A. (1996).
Characterisation and purification of recombinant GLUT1 expressed in insect cells.
Biochemical Society Transactions, Vol. 24, p.S. 478.

Wellner, M., Monden, I. and Keller, K. (1992).
The differential role of Cys-421 and Cys-429 of the GLUT1 glucose transporter in transport inhibition by *p*-chloromercuribenzenesulfonic acid (pCMBS) or cytochalasin B (CB).
FEBS Letters, Vol. 309, No. 3, pp. 293 - 296.

Wellner, M., Monden, I. and Keller, K. (1994).
The role of cysteine residues in glucose-transporter-GLUT1-mediated transport and transport inhibition.
Biochem. J., Vol. 299, pp. 813 - 817.

Wellner, M., Monden, I., Mueckler, M. M. and Keller, K. (1995a).
Functional consequences of proline mutations in the putative transmembrane segments 6 and 10 of the glucose transporter GLUT1.
Eur. J. Biochem., Vol. 227, pp. 454 - 458.

Wellner, M., Monden, I. and Keller, K. (1995b).
From triple cysteine mutants to the cysteine-less glucose transporter GLUT1: a functional analysis.
FEBS Letters., Vol. 370, pp. 19 - 22.

Widdas, W. F. and Baker, G. F. (1991a).
The role of the surface energy of water in the conformational changes of the human erythrocyte glucose transporter.
Cytobios, Vol. 66, pp. 179 - 204.

Widdas, W. F. and Baker, G. F. (1991b).
The polyguanidinium-ring-complex cation shield in the human red cell glucose transporter.
Cytobios, Vol. 68, pp. 71 - 76.

Widdas, W. F. and Baker, G. F. (1991c).
The polyguanidinium complex of the glucose transporter: a possible basis for bistable cationic gates and anionic channels in biology.
Cytobios, Vol. 68, pp. 131 - 152.

Wu, J., Sun, J. and Kaback, H. R. (1996).
Purification and Functional Characterization of the C-Terminal Half of the Lactose Permease of *Escherichia coli.*
Biochemistry, Vol. 35, pp. 5213 - 5219.

Yi, C., Charalambous, B. M., Emery, V. C. and Baldwin, S. A. (1992).
Characterization of functional human erythrocyte-type glucose transporter (GLUT1) expressed in insect cells using a recombinant baculovirus.
Biochem. J., Vol. 283, pp. 643 - 646.

Zinth, W., Kaiser, W. and Michel, H. (1983).
Efficient photochemical activity and strong dichroism of single crystals of reaction centers from *Rhodopseudomonas viridis*.
Biochimica et Biophysica Acta, Vol. 723, pp. 128 - 131.

Zottola, R. J., Cloherty, E. K., Coderre, P. E., Hansen, A., Hebert, D. N. and Carruthers, A. (1995).
Glucose Transporter Function Is Controlled by Transporter Oligomeric Structure. A Single, Intramolecular Disulfide Promotes GLUT1 Tetramerization.
Biochemistry, Vol. 34, pp. 9734 - 9747.